EXPLOITING RESOURCE USE EFFICIENCY AND RESILIENCE IN ANCIENT WHEAT SPECIES

Anisha Parmar

Thesis submitted to the University of Nottingham in partial fulfilment of the requirements for the degree of Doctor of Philosophy

June 2014

Division of Plants and Crop Sciences
School of Biosciences, University of Nottingham
Sutton Bonington Campus, Loughborough, LE12 5RD

Abstract

Modern bread wheat (*Triticum aestivum*) initially derived from wild progenitors which underwent hybridisation and domestication events. It is hypothesised that modern plant breeding has reduced the genetic variation among modern cultivars (Sparkes, 2010). Ancient wheat species form a conduit between wild ancient wheat and cultivated *Triticum* species, and may harbour the genetic variation required to supplement the modern bread wheat gene pool. The current work investigated a range of morphological and physiological aspects of several ancient species including several representatives of spelt, emmer and einkorn. These were compared to modern bread wheat in two field and three glasshouse experiments with the aim to investigate their resource use efficiency, where radiation use and water use formed the crux. The main components of the current work relate to 1) canopy interception characteristics 2) leaf photosynthetic capabilities and 3) water use. Spelt genotypes demonstrated increased WUE and green area longevity compared with modern bread wheat. Emmer displayed increased WUE, assessed on three scales using instantaneous transpiration efficiency (ITE), biomass to water uptake ratios, and carbon isotope discrimination ($\Delta^{13}C$). In addition, the mechanisms whereby emmer, einkorn and spelt maintained ITE appeared to differ. Emmer was observed to increase photosynthetic rates, whereas spelt maintained low transpiration as a result of low stomatal conductance. Einkorn however, maintained ITE through an intermediate of both of these mechanisms. This was further supported by species differences for maximum photosynthetic rates (A_{sat}) which, for emmer and einkorn, were comparable with modern bread wheat. Investigation of WUE through $\Delta^{13}C$ and biomass production to water uptake ratios ranked species similarly, showing emmer

and spelt to have superior WUE during grain filling. Additionally, spelt was observed to produce biomass comparable to modern bread wheat, thought to be due to enhanced RUE (observed in one field trial) or increased green area longevity rather than increased assimilation capability. In field experiments, biomass production and light interception was relatively high for einkorn species, however this was believed to derive from excessive tiller production due to poor emergence. Overall, ancient species did partition a larger proportion of assimilates toward tillers. Modern bread wheat produced fewer tillers, but directed more biomass towards the ear, and therefore had greater harvest indices (HI) compared to all ancient species. Despite this broad analysis, further investigation of the mechanisms responsible for these traits is required. This research therefore indicates that there is sufficient variation for traits, which could be used to improve radiation and water use efficiency, and therefore warrants further exploration. With further investigation, resource capture and utilisation efficiency, and the morphological traits that confer these advantages in these genotypes, genetic markers could be identified with the aim to introduce valuable traits for the production of novel modern bread wheat varieties. The differences observed between these ancient wheat species and modern bread wheat provide an opportunity through which modern wheat gene pools may be improved to stabilise yields, particularly in sub-optimal environmental conditions, thus increasing biomass production per unit resource, thereby enhancing the productivity and the efficiency of crop systems.

Acknowledgements

I would like to thank my principle supervisor, Dr. Debbie Sparkes, for the countless hours spent proofreading and discussing my research. I am extremely grateful for her constructive advice, patient guidance and support throughout the duration of this project. I would also like to thank my second supervisor, Dr. Sean Mayes. The instruction that I have received during my time at the University of Nottingham has been invaluable.

I would also like to thank all of those people at the University of Nottingham who provided support to plan and implement my experiments. Special thanks to Dr. Michael Osei Adu, Dr. Olubukola Ajigboye, John Alcock, Dr. Pedro Carvalho, Assia Hammadi, Mark Meacham, Dr. Erik Murchie, Dr. Ian Smillie, Matthew Tovey and Fiona Wilkinson.

This research would not have been possible without the financial support of the University of Nottingham and the Home Grown Cereals Authority (HGCA) in the award of a Postgraduate Research Studentship.

I would also like to extend my warmest thanks to the family and friends that have helped along the way, in particular thanks to my mum, dad and sister. Your encouragement when times were difficult was much appreciated and duly noted. Finally, thanks to Dr. Antoine Larrieu for giving me a push to get started and more importantly, finished. You have all been purveyors of encouragement, support and reason for which I am extremely grateful.

Table of contents

Abstract *i*

Acknowledgements *iii*

Table of contents *iv*

List of figures *xiii*

List of tables *xviii*

List of abbreviations *xxi*

Chapter One: Literature review 1

1.1 Global food demand in a changing climate 2

1.2 Wheat production and agriculture 3

1.3 Ancient wheat: a historical perspective 6

1.3.1 Einkorn wheat (*Triticum monococcum*) 8

1.3.2 Emmer wheat (*Triticum dicoccum*) 8

1.3.3 Spelt wheat (*Triticum spelta*) 9

1.4 Genetic progress and limitations in modern bread wheat 10

1.5 Ancient wheat species as a tool for wheat improvement 12

1.6 Increasing agricultural productivity and efficiency to meet growing demands 13

1.7 Physiological traits determining yield and resource capture 14

1.8 Conversion of radiation through photosynthesis 15

1.8.1 Photosynthetic response to atmospheric carbon dioxide 18

1.8.2 Photosynthetic response to photon flux 21

1.8.3 Stomatal behaviour during photosynthesis 22

1.9 Growth, development and radiation interception 24

1.10 Radiation Use Efficiency 26

1.11 Green area senescence and persistence 28

1.12 Water Use Efficiency 30

1.13 Measuring photosynthesis and WUE: techniques and implications 34

1.14 Objectives 37

1.15 Hypotheses 38

Chapter Two: Plant development, growth and canopy architecture 40

2.1 Introduction 41

2.1.1 Field trials (2010 and 2011) 41

2.2 Materials and Methods 43

2.2.1 Experimental sites 43

2.2.2 Seed source and plant material 43

2.2.3 Germination Assays 46

2.2.4 Plant husbandry 46

2.2.5 Trial management (2010 and 2011) 47

2.2.6 Experimental design 47

2.2.7 Field techniques (2010 and 2011) 48

2.2.7.1 Growth stage determination 48

2.2.7.2 Sampling procedure 49

2.2.7.3 Sampling of crop growth and development 49

2.2.7.4 Laboratory analysis of field samples 50

2.2.7.5 Pre-Harvest Sample analysis 52

2.2.7.6 Yield analysis 52

2.2.7.7 Leaf Development and tiller Economy 52

2.2.8 Canopy radiation attenuation 52

2.2.8.1 Plant height 52

2.2.8.2 Radiation and light interception 53

2.2.9 Radiation use efficiency (RUE) 54

2.2.10 Canopy light attenuation, distribution and extinction 54

2.2.11 Stay green assessments 55

2.3 Results 57

2.3.1 Plant growth and development 57

2.3.1.1 Establishment 57

2.3.1.2 Shoot production and tiller economy 58

2.3.1.3 Plant development 52

2.3.2 Plant morphology and architectural characterisation 63

2.3.2.1 Plant height 63

2.3.2.2 Green Area Index (GAI) 66

2.3.2.3 Green Area Index Partitioning 71

2.3.3 Distribution and capture of solar irradiance 75

2.3.3.1 Light attenuation 75

2.3.3.2 Light Extinction through the crop canopy 79

2.3.4 Resource assimilation and investment efficiency 82

2.3.4.1 Carbon assimilation 82

2.3.4.2 Assimilate partitioning 87

2.3.4.3 Pre-harvest biomass partitioning 91

2.3.4.4 Conversion efficiency of solar radiation 94

2.3.5 Canopy persistence and stay green 97

2.3.5.1 Canopy duration (2010 SPAD measurements) 97

2.3.5.2 Stay green (visual scoring in 2010) 99

2.3.5.3 Canopy duration (2011 SPAD measurements) 102

2.4 Discussion 106

2.4.1 Plant morphology, growth and development 106

2.4.1.1 Establishment 106

2.4.1.2 Shoot production and tiller economy 107

2.4.1.3 Plant development 109

2.4.2 Plant height 109

2.4.3 Green Area Index 111

2.4.3.1 Green Area Index partitioning 113

2.4.4 Distribution and capture of solar radiation 114

2.4.4.1 Light attenuation 114

2.4.4.2 Light extinction through the crop canopy 116

2.4.5 Resource assimilation and investment efficiency 118

2.4.5.1 Carbon assimilation 118

2.4.5.2 Carbon partitioning 120

2.4.5.3 Conversion efficiency of solar radiation 122

2.4.6 Chlorophyll content and canopy persistence 124

2.5 Conclusions 126

Chapter Three: Leaf level biochemical and physiological aspects of photosynthesis and water use efficiency 127

3.1 Introduction 128

3.1.1 The A/C_i response 128

3.1.2 Practical interpretation of the A/C_i response 129

3.2 Materials and methods 131

3.2.1 Experimental site 131

3.2.2 Glasshouse experiment I 131

3.2.2.1 Plant material 131

3.2.2.2 Seedling Transplanting and Husbandry 132

3.2.2.3 Experimental design and glasshouse husbandry 132

3.2.3 Assessments 132

3.2.3.1 Carbon dioxide response curves 132

3.2.4 Glasshouse Experiment II 133

3.2.4.1 Plant material 133

3.2.4.2 Seedling husbandry 134

3.2.4.3 Experimental Design 134

3.2.4.4 Column construction and irrigation 134

3.2.4.5 Glasshouse Husbandry 136

3.2.5 Glasshouse experiment II measurements 137

3.2.5.1 Gas exchange measurements 137

3.2.5.2 Flag leaf ITE measurements. 137

3.2.5.3 Light response (*A*/Q) curves 138

3.2.5.4 Plant sampling 138

3.2.6 Stay green assessments 138

3.2.7 Data analyses 139

3.3 Results 140

3.3.1 Glasshouse experiment I 140

3.3.2 Genotypic photosynthetic response to changing CO_2 concentrations 140

3.3.3 Glasshouse experiment II 150

3.3.4 Assessment of radiation use parameters using Infra-Red Gas Analysis 150

3.3.4.1 Photosynthetic response curves 150

3.3.4.2 A_{max} 153

3.3.4.3 Light saturation point 155

3.3.4.4 Quantum yield 155

3.3.4.5 CO_2 lost through respiration 156

3.3.5 Water Use Efficiency 157

3.3.5.1 ITE Measurements 157

3.3.5.2 Instantaneous photosynthesis measurements 160

3.3.5.3 Transpiration rates 161

3.3.5.4 Internal stomatal CO_2 concentrations 162

3.3.5.5 Stomatal CO_2 conductance 165

3.3.6 GH II accumulated biomass 165

3.3.7 Water extraction 167

3.3.8 Stay green traits 168

3.4 Discussion 171

3.4.1 Biochemical parameters 171

3.4.2 Biochemical parameters from A/C_i response curves 173

3.4.3 Comparisons for photosynthetic capacity 174

3.4.3.1 Light response parameters 175

3.4.4.2 Instantaneous Transpiration Efficiency 180

3.4.4.3 Biomass 182

3.5 Conclusions 185

Chapter Four: Photosynthesis and water use efficiency 187

4.1 Introduction 188

4.2 Materials and Methods 189

4.2.1 Seed preparation and germination assays 189

4.2.2 Experimental Site 189

4.2.3 Glasshouse Experiment III 189

4.2.3.1 Plant Material 190

4.2.3.2 Seedling transplanting and husbandry 191

4.2.3.3 Experimental design 191

4.2.4 Glasshouse Experiment III Measurements 191

4.2.4.1 Gas exchange measurements 191

4.2.4.2 Flag leaf ITE measurements. 192

4.2.4.3 CO_2 response curves 192

4.2.4.4 Plant growth and development analyses 192

4.2.4.5 Specific leaf area 193

4.2.4.6 Stay green assessments 193

4.2.4.7 Data analyses 193

4.3 Results 194

4.3.1 Biochemical aspects of photosynthesis pre and post anthesis 194

4.3.2 Water Use Efficiency 202

4.3.2.1 ITE Measurements 205

4.3.2.2 Photosynthesis 207

4.3.2.3 Transpiration rates 207

4.3.2.4 Internal stomatal CO_2 concentrations 208

4.3.2.5 Stomatal conductance 208

4.3.3 Specific Flag Leaf Area 210

4.3.4 Assessment of WUE using Carbon Isotope Discrimination 212

4.3.5 GH III Biomass 215

4.3.6 Green area persistence 215

4.4 Discussion 219

4.4.1 Glasshouse experiment III 219

4.4.2 Biochemical parameters from A/C_i response curves 220

4.4.3 Instantaneous Transpiration Efficiency 221

4.4.4 WUE through $\Delta^{13}C$ of the grain 223

4.4.5 Specific Leaf Area 224

4.4.6 Biomass production 224

4.5 Conclusions 227

Chapter Five: General discussion and conclusions 229

5.1 Introduction 230

5.2 Plant growth, development and canopy architecture 231

5.3 Biomass production and RUE 233

5.4 Photosynthetic radiation capture and conversion 235

5.4.1 Biochemical aspects of leaf physiology 235

5.4.2 Photosynthetic capacity 236

5.5 Water Use Efficiency 239

5.6 Green area persistence 242

5.7 Further work 243

5.8 Conclusions 245

References 247

Appendices 258

Appendix One: Field trials layout and husbandry (2010) 259

Appendix Two: Field trial layout and husbandry (2011) 262

Appendix Three: Glasshouse experiment I layout 265

Appendix Four: Glasshouse experiment I sample output 266

Appendix Five: Glasshouse experiment II layout 268

Appendix Six: Glasshouse experiment III layout 269

Appendix Seven: GH experiment chemical application information 270

List of figures

Figure 1.1: Global wheat yields and production (tonnes) from 1961 to 2007. 3

Figure 1.2: The effects of different *Rht* alleles on plant height in wheat. 5

Figure 1.3: Several ploidy alterations through chance hybridisation among *Triticum* sp. have produced modern bread wheat (*Triticum aestivum*). 7

Figure 1.4: Ear appearance of several wheat species. 7

Figure 1.5: An overview of photosynthesis showing the cooperation between light reactions and the Calvin cycle. 16

Figure 1.6: The three phases of the Calvin cycle. 17

Figure 1.7: Idealised A/C_i response. 20

Figure 1.8: Schematic A/Q (Photosynthetic rate/Quanta) response curve. 21

Figure 1.9: Schematic diagram showing gas exchange between the atmosphere and sub-stomatal leaf air spaces. 23

Figure 1.10: The relationship between total dry matter at harvest and the amount of solar radiation intercepted throughout a season. 28

Figure 1.11: Diagram showing the mechanisms by which photosynthetic rates and transpiration rates are attained in an open Infra-Red Gas Analyser. 35

Figure 1.12: The negative correlation between $^{13}C\Delta$ and transpiration efficiency in wheat. 37

Figure 2.1: Average species height (cm) for einkorn, emmer, MBW and spelt wheat during 2010 and 2011 winter field experiments. 65

Figure 2.2: Total green area index of spelt, einkorn, emmer and modern bread wheat cultivars. 67

Figure 2.3: Total green area index of spelt, einkorn, emmer and MBW species averages. 68

Figure 2.4: Species green area index of spelt, einkorn, emmer and modern bread wheat cultivars in the 2011 winter wheat field experiment. 70

Figure 2.5: Species averages for total green area index of spelt, einkorn, emmer and modern bread wheat. 71

Figure 2.6: Green area index partitioning of twelve wheat cultivars in 2010 at GS 31, 39 and 61. 73

Figure 2.7: Green area index partitioning of twelve wheat cultivars in 2011 at GS 31, 39 and GS 61. 74

Figure 2.8: Fractional interception of twelve ancient wheat cultivars (2010) showing spelt, einkorn, emmer and modern bread wheat genotypes. 76

Figure 2.9: Fractional interception of four wheat species (2010). 77

Figure 2.10: Fractional interception of twelve ancient wheat cultivars (2011). 78

Figure 2.11: Fractional interception of four species of wheat cultivars (2011). 79

Figure 2.12: Light extinction of four wheat species (2010). 81

Figure 2.13: Biomass accumulation of twelve wheat genotypes in 2010. 83

Figure 2.14: Species dry weight accumulated (g/m^2) in 2010. 84

Figure 2.15: Total biomass accumulated for spelt, einkorn, emmer and modern bread wheat cultivars (2011). 85

Figure 2.16: Species average for biomass accumulated throughout the 2011 winter wheat growing season. 86

Figure 2.17: Genotypic differences in biomass partitioning in 2010. 88

Figure 2.18: Genotypic differences for biomass partitioning. 90

Figure 2.19: Biomass partitioning in 2010 and 2011. 92

Figure 2.20: Pre-Harvest component analysis of assimilates (in 2010 and 2011). 93

Figure 2.21: SPAD values versus time for spelt, einkorn, emmer and MBW cultivars in 2010. 98

Figure 2.22: Average species SPAD values versus time in 2010 99

Figure 2.23: Visual scores versus time (DAS) for spelt, einkorn, emmer and MBW cultivars in 2010. 100

Figure 2.24: Average species visual 'greenness' scores versus time. 101

Figure 2.25: SPAD values versus visual 'greenness' scores. 102

Figure 2.26: Genotypic SPAD values throughout the 2011. 104

Figure 2.27: SPAD reading of twelve ancient wheat cultivars averaged over four species. 105

Figure 3.1: Columns constructed to grow plant material in glasshouse experiment II showing 20cm increments where theta probe measurements were taken. 136

Figure 3.2 Glasshouse experiment I setup in agronomy glasshouse. 140

Figure 3.3: Example output for genotypic responses to varying carbon dioxide concentrations. 141

Figure 3.4 (*i* and *ii*): Values determined from fitted A/C_i curves at T leaf, showing the maximum rate of carboxylation (V_{cmax}), the rate of electron transport (J_{max}), triose phosphate utilisation (TPU) limitation and the respiration rates (R_d). 143

Figure 3.5: Values determined from fitted A/C_i curves with a normalised leaf temperature of 25ºC showing the maximum rate of carboxylation (V_{cmax}), electron transport rates (J_{max}), the triose phosphate utilisation (TPU) limitation and respiration rates (R_d). 146

Figure 3.6: Values determined from fitted A/C_i curves, performed with a block temperature of 20ºC showing the maximum rate of carboxylation (V_{cmax}), the rate of electron transport (J_{max}), the triose phosphate utilisation (TPU) and respiration rates (R_d). 148

Figure 3.7: Values determined from fitted A/C_i curves, with a normalised leaf temperature of 25ºC showing the maximum rate of carboxylation (V_{cmax}), the rate of electron transport (J_{max}), triose phosphate utilisation (TPU) limitation and respiration rates (R_d). 149

Figure 3.8: RUE and Amax correlations in 2010 and 2011. 154

Figure 3.9: SPAD values throughout glasshouse experiment II (DAS). 169

Figure 3.10: SPAD values throughout glasshouse experiment II (DAS). 170

Figure 4.1 (*i* and *ii*): Values determined from fitted AC_i curves at T leaf showing the maximum rate of carboxylation (V_{cmax}), the rate of electron transport (J_{max}), the triose phosphate utilisation (TPU) limitation and respiration rates (R_d). 195

Figure 4.2 (*i* and *ii*): Values determined from fitted A/C_i curves, with a normalised leaf temperature (25°C) showing the maximum rate of carboxylation (V_{cmax}), the rate of electron transport (J_{max}), the triose phosphate utilisation (TPU) limitation and dark respiration rates (R_d). 198

Figure 4.3: Values determined from fitted A/C_i curves, performed at T leaf showing the maximum rate of carboxylation (V_{cmax}), the rate of electron transport (J_{max}), the triose phosphate utilisation (TPU) limitation, and respiration rates (R_d). 200

Figure 4.4: Values determined from fitted A/C_i (A/C_c) curves, with a normalised leaf temperature of 25ºC. A shows the maximum rate of carboxylation (Vc_{max}), B the rate of electron transport (J_{max}), C the triose phosphate utilisation (TPU), D the determined dark respiration rates (R_d). 201

Figure 4.5 (*i* and *ii*): Instantaneous transpiration use efficiency (A, D and G), photosynthetic rate (B, E and H) and transpiration rate (C, F and I) of a subset of the original ancient wheat species including all emmer (A, B and C) and spelt species (D, E and F) as well as modern bread wheat (G, H and I) for comparison from growth stage 31 onwards. 203

Figure 4.6: Instantaneous transpiration efficiency, photosynthetic rate and transpiration rate of a subset of ancient wheat species from GS 39 onwards. 206

Figure 4.7: Internal stomatal CO_2 concentration and conductance measured during ITE measurements of five ancient, and two modern bread wheat cultivars both pre and post anthesis. 209

Figure 4.8: Stomatal responses simultaneously measured during ITE measurements of three species both pre and post anthesis. 210

Figure 4.9: Specific flag leaf area for five ancient wheat cultivars and two modern bread wheat cultivars measured in gashouse experiment III. 211

Figure 4.10: Specific flag leaf area (m^2 kg^{-1}) for five ancient wheat cultivars and two modern bread wheat cultivars measured in gashouse experiment III. 212

Figure 4.11: Carbon isotope discrimination for five ancient wheat cultivars and two modern bread wheat cultivars measured in glasshouse experiment III. 213

Figure 4.12: Carbon isotope discrimination for three wheat species measured from grain in glasshouse experiment III. 214

Figure 4.13: SPAD reading of seven ancient species and two modern bread wheat species throughout glasshouse experiment III (from 154 to 208 DAS). 217

Figure 4.14: SPAD reading of four wheat species throughout glasshouse experiment III (from 154 to 208 DAS). 218

Figure A1.1: Field trial layout and husbandry (2010). 259

Figure A2.1: Experimental design and layout of field experiment (2011). 262

Figure A3.1: Experimental design and layout of glasshouse experiment I. 265

Figure A4.1: Example of A/C_i output using the model constructed by Sharkey *et al*. (2007). 266

Figure A5.1: Experimental design and layout of glasshouse experiment II. 268

Figure A6.1: Experimental design and layout of glasshouse experiment III. 269

List of tables

Table 2.1: Included genotypes in the study detailing species, genome group and general distribution. 45

Figure 2.2: Description of wheat growth stage identifiers and benchmark dates. 48

Table 2.3: Dates when key growth stages were reached and sampling took place in the 2010 and 2011 winter wheat growing season. 49

Table 2.4: Dates on which fractional interception sampling was performed. 54

Table 2.5 Average rates of emergence with the corresponding number of plants per m^2 observed in 2010 and 2011. 58

Table 2.6: Average genotype total shoot number and fertile shoot number (per m^2) according to growth stage for 2010. 59

Table 2.7: Average shoot number and fertile shoot number (per m^2) according to growth stage by species in 2010. 60

Table 2.8: Average total shoot number and fertile shoot number (per m^2) according to growth stage by species in 2011. 60

Table 2.9: Average species shoot numbers and fertile shoot numbers (per m^2) according to growth stage in 2011. 61

Table 2.10: Dates at which cultivars reached benchmark growth stages in the 2010 field experiment. 63

Table 2.11: Estimates of the parameters for light distribution fitted curves for four wheat species. 80

Table 2.12: Ear biomass, ear index, pre-anthesis radiation use efficiency and post-anthesis radiation use efficiency (PAR) for twelve wheat genotypes. 95

Table 2.13: Ear biomass, ear index, pre-anthesis RUE and post-anthesis RUE species averages (RUE calculated from intercepted PAR). 95

Table 2.14: Ear biomass, ear index, post and pre-anthesis radiation use efficiency (intercepted PAR) for twelve modern and ancient wheat cultivars from the field experiment carried out in 2011. 96

Table 2.15: Species averages for ear biomass, ear index, post and pre-anthesis radiation use efficiency (calculated from intercepted PAR) from the field experiment carried out in 2011. 97

Table 3.1: Genotypes selected for photosynthetic analysis for glasshouse experiment I. 131

Table 3.2: Plant cultivars selected for glasshouse experiment II. 134

Table 3.3: Radiation use characteristics of seven ancient wheat varieties and modern bread wheat, Xi19 for comparison. 151

Table 3.4: Radiation use characteristics of four wheat species. 152

Table 3.5: The instantaneous transpiration use efficiency, photosynthetic and transpiration rates of seven ancient wheat varieties and modern bread wheat, whilst pre and post anthesis. 158

Table 3.6: Instantaneous transpiration use efficiency, photosynthetic and transpiration rates of four wheat species both pre and post anthesis. 159

Table 3.7: Stomatal responses during ITE measurements of seven ancient wheat varieties as well as modern bread wheat, Xi19 for comparison, both pre and post anthesis. 162

Table 3.8: Parameters indicating stomatal behaviour during ITE measurements, pre and post anthesis. 163

Table 3.9: Grain harvested (m^{-2}), total above ground biomass and harvest index of seven ancient and one modern bread wheat from glasshouse experiment II where plants were grown in 1m columns. 166

Table 3.10. WUE (ratio of biomass to water extracted) (g l^{-1}) for genotypes in glasshouse experiment II. 167

Table 4.1: Genotypes selected for photosynthetic analysis in GH III. 190

Table 4.2: Grain yield, biomass and the deduced harvest index from glasshouse experiment III. 215

Table A1.1 Site details for the 2010 field experiment. 260

Table A1.2: Sowing information for field experiment, 2010. 260

Table A1.3: Details of soil cultivation for field experiment 2010. 260

Table A1.4: Details of plant growth regulator applications in the 2010 field experiment. 260

Table A1.5: Details of fertiliser application in the 2010 field experiment. 261

Table A1.6: Details of herbicide applications in the 2010 field experiment. 261

Table A1.7: Details of fungicide applications in the 2010 field experiment. 261

Table A1.8: Details of insecticide applications in the 2010 field experiment. 261

Table A2.1: Site details for experiment 2011. 263

Table A2.2: Sowing information for field experiment, 2011. 263

Table A2.3: Details of soil cultivation for field experiment 2011. 263

Table A2.4: Details of plant growth regulator applications in the 2011 field experiment. 263

Table A2.5: Details of fertiliser applications in the 2011 field experiment. 264

Table A2.6: Details of herbicide application in the 2011 field experiment. 264

Table A2.7: Details of fungicide applications in the 2011 field experiment. 264

Table A2.8: Details of insecticide application in the 2011 field experiment. 264

Table A7.1: Components of Hortimix standard 15-7-30 (fertiliser). 270

Table A7.2: Corbel information (fungicide). 270

Table A7.3: Decis information (insecticide). 271

List of abbreviations

ANOVA - Analysis of variance

A - CO_2 assimilated during photosynthesis

AGDW - Above ground dry weight

A_{sat} - Maximum photosynthetic rate when the leaf is saturated with light

AWFC - Available water at field capacity

BD - Bulk density

C_a - Partial pressure of CO_2 in the atmosphere

C_i - Partial pressure of CO_2 in the inter-cellular spaces

DAS - Days after sowing

DM - Dry mass

T - Transpiration

ET - Evapotranspiration

FC - Field capacity

GH I, II, III– Glass House Experiment I, II and III

GS - Growth stages

G_s - Stomatal conductance for CO_2

G_w - Stomatal conductance for water

HI - Harvest index

k - Resource capture coefficient

LAI - Leaf area per unit ground area

LCP - Light compensation point

LRWC - Leaf relative water content

LSP - Light saturation point

MBW – Modern bread wheat

NABIM – National Association of British & Irish Millers

NUE - Nitrogen-use efficiency

PAR - Photosynthetic active radiation

PGR – Plant growth regulator

Q - Photon flux density

Φ - Quantum yield

R_a - Molecular ratio $^{13}C/^{12}C$ in the air

R_d - Respiration

SEM - Standard error of the mean

SED - Standard error deviation

SLA - Specific leaf area

VL - Volume at layer L

W_a - Difference of partial pressure of water in the atmosphere

WHC - Water holding capacity

WU - Water-use

WUE - Water-use efficiency

Y - Grain yield

$\delta^{13}C$ - Carbon isotopic composition

$\Delta^{13}C$ - Carbon isotopic discrimination

δ_a - Deviation of the isotopic composition of the air in relation to a standard

δ_p - Deviation of the isotopic composition of the plant in relation to a standard

Chapter One:

Literature review

1.1 Global food demand in a changing climate

Recent projections indicate that global populations will grow from 6.9 billion to over 9.0 billion by 2050 (Lutz *et al.*, 2001). Provision for this growing population is heavily dependent on the agricultural sector (Peleg *et al.*, 2005) and so far, cereal productivity, has kept pace with population growth (Araus *et al.*, 2002). However, food requirements are predicted to increase from 12 to 25 teracalories d^{-1} by 2030, thought to be more critical in developing countries which incidentally also have limited capability for nutrient and water provisions (Murchie *et al.*, 2009). Water availability can be a major constraint to plant productivity (Araus *et al.*, 2002; Boyer, 1982) and one which accounts for the largest proportion of crop losses (Kramer & Turner, 1980; Peleg *et al.*, 2005). The situation is further exacerbated by unpredictable weather associated with changes in the physical global climate due tropospheric CO_2, ozone concentrations and denitrification of nitrate fertilisers (Ewert & Pleijel, 1999). Additionally, there have been significant reductions in crop-land per capita (Hoisington *et al.*, 1999) as well as soil losses (Davies *et al.*, 2009; Murchie *et al.*, 2009). Land must also be allocated to bio-energy and textile production, whilst also considering biodiversity protection as well as urbanisation (Hoisington *et al.*, 1999). Furthermore, the rise of the 'Green Revolution' has typically encouraged intensified cropping systems that deplete water and soil resources (Hardin, 2008). Therefore the current focus is geared towards 'sustainable intensification', which aims to achieve intensive production whilst minimising the environmental impacts. The agricultural sector therefore has a large undertaking; they must increase crop yields per unit area, whilst also reducing input resources such as fertiliser, water and energy (Cassman, 1999; Hoisington *et al.*, 1999). The complexity of this task creates a significant challenge to food security.

1.2 Wheat production and agriculture

Triticum aestivum (modern bread wheat) production accounts for 200 million hectares of agricultural land and 21% of caloric intake for global populations (Ortiz *et al.*, 2008). Globally, 590 million metric tonnes of wheat are produced per year, however by 2025, the requirement is estimated to be approximately 840 million tonnes (Murchie *et al.*, 2009). Wheat yields have increased remarkably throughout the past century with average gains of 250% (Calderini & Slafer, 1998) commonly attributed to the 'Green Revolution', which saw improved management practices and genetic cultivar improvement which lead to steady increments in wheat production (Figure 1.1) for enhanced yield potentials within established conditions (Calderini & Slafer, 1998; Frederick & Bauer, 1999; Hay & Porter, 2006).

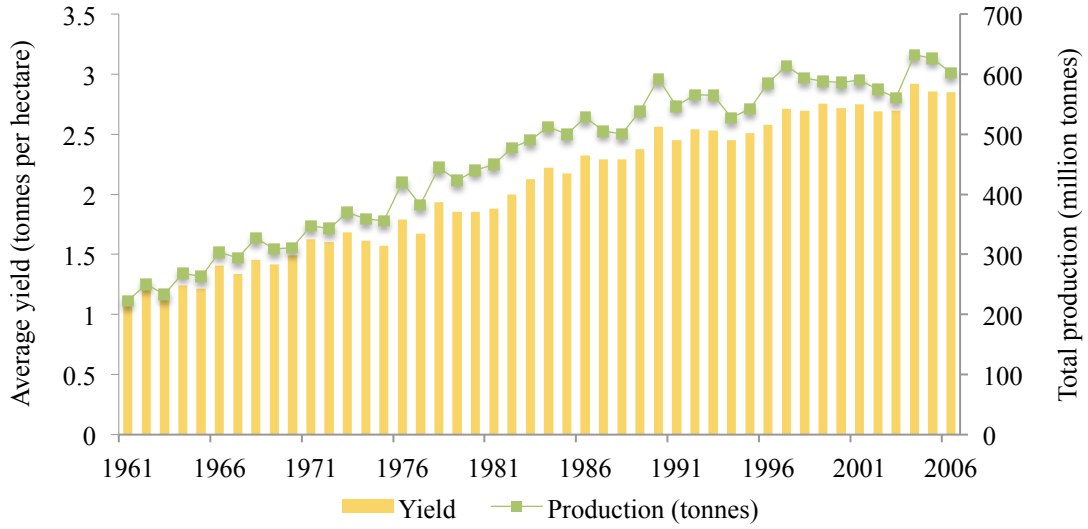


Figure 1.1: The trends in global wheat yields (tonnes/hectare) and production (million tonnes) from 1961 to 2007 (data from FAOSTAT database, 2012).

Breeding improvements have primarily focused on plant morphology such as canopy architecture which have not necessarily improved the photosynthetic capacity of plants but have rather enhanced light interception, for instance the quantity of assimilate partitioning, producing more 'stocky' plants which are less likely to lodge, reducing losses (Hardin, 2008). As a result, productivity and yield stability have improved (Araus *et al.*, 2002; Murchie *et al.*, 2009). This was most notably achieved through the manipulation of several major genes to manipulate plant height (using the *Rht* gene) (Figure 1.2), photoperiod (*Ppd)* as well as growth habit (*Vrn*) (Fischer & Edmeades, 2010; Skovmand *et al.*, 2001). Collectively these introgressions altered plant morphology by increasing partitioning to the ear and the number of grains per unit area, leading to a boost in Harvest Index (HI) (the ratio of economic yield i.e. grain to total biomass produced) (Hibberd *et al.*, 2008); furthermore these changes have increased responsiveness to agricultural inputs as well as lodging resistance, allowing greater fertiliser applications. The exact genetic gain in grain yield potential is unknown although it is likely that breeding has dramatically altered the physiological processes that impact yields (Frederick & Bauer, 1999).

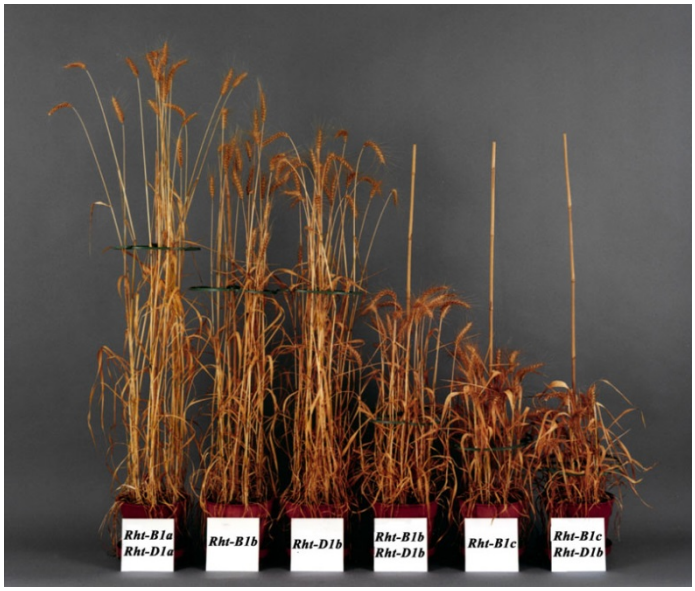


Figure 1.2: The effects of different *Rht* alleles on plant height in wheat (cv. April Bearded). The wild-type contains *Rht-B1a* and *Rht-D1a*, which are homologous (corresponding) genes on the B and D genomes. *Rht-B1c* is a more severe allele at the *Rht-B1* locus. Image origin unknown, however the wheat mutants *Rht-B1b* and *Rht-D1b* were described in Peng *et al.*, (1999).

Physiologists have adopted a reductionist approach by identifying and targeting those factors that impact yield; nutrient uptake, metabolism, photosynthesis and respiration, carbon partitioning, leaf senescence and plant water relations are but a few (Frederick & Bauer, 1999). Improvement in one or several of these will likely improve yield (Frederick & Bauer, 1999). Increasing global populations mean that victual requirements are mounting, additionally the heightened need for sustainable agriculture highlight the importance of increased production efficiencies. This relates to the transduction of externally acquired resources such as radiation, water and nutrients, into biological yields (Murchie *et al.*, 2009). Identifying and understanding how these processes interact to regulate yield will aid the selection of higher-yielding cultivars which possess an increased proficiency to mine available resources (Cassman, 1999; Frederick & Bauer, 1999).

1.3 Ancient wheat: a historical perspective

Triticum aestivum has derived from a number of progenitors with varying cytogenic classifications (from diploid to hexaploid), originating from the Fertile Crescent. The first wheat species to be successfully cultivated (a diploid) was *T. monococcum* (einkorn) (initially derived from *T. boeticum*) (Salamini *et al.*, 2002) from which the A genome originates (Campbell, 1997). Einkorn cultivation however, was abandoned for the tetraploid, *Triticum dicoccoides* (wild emmer) (AABB) later selectively bred to produce *Triticum dicoccum* (emmer) (AABB). *Triticum dicoccum* had traits that made it more suitable for larger scales of production such as free-threshing ears. Emmer was eventually replaced by *Triticum spelta* (spelt), resulting from a cross between *T. turgidum* and *Aegilops squarrosa* (Pagnotta *et al.*, 2005; van der Veen & Palmer, 1997) (Figure 1.3). Finally, following accidental crosses between *Triticum dicoccoides* (domesticated emmer) and *Aegilops tauschii* (a wild diploid species) (D), free-threshing hexaploids (*Tritcum aestivum*) (AABBDD) were produced which marginalised previously cultivated species (Figure 1.4 shows the impact of these genetic alterations made on ear appearance). Today, these form large-scale homogenous systems that produce far greater yields. It is now thought that only 3% of cultivable land accounts for landrace cultivars (Reif *et al.*, 2005). *Triticum aestivum* has no wild progenitors with hexaploid genomes (Salamini *et al.*, 2002). It is this hexaploid (*Triticum aestivum*) that forms the crux of wheat cultivation today (Salamini *et al.*, 2002).

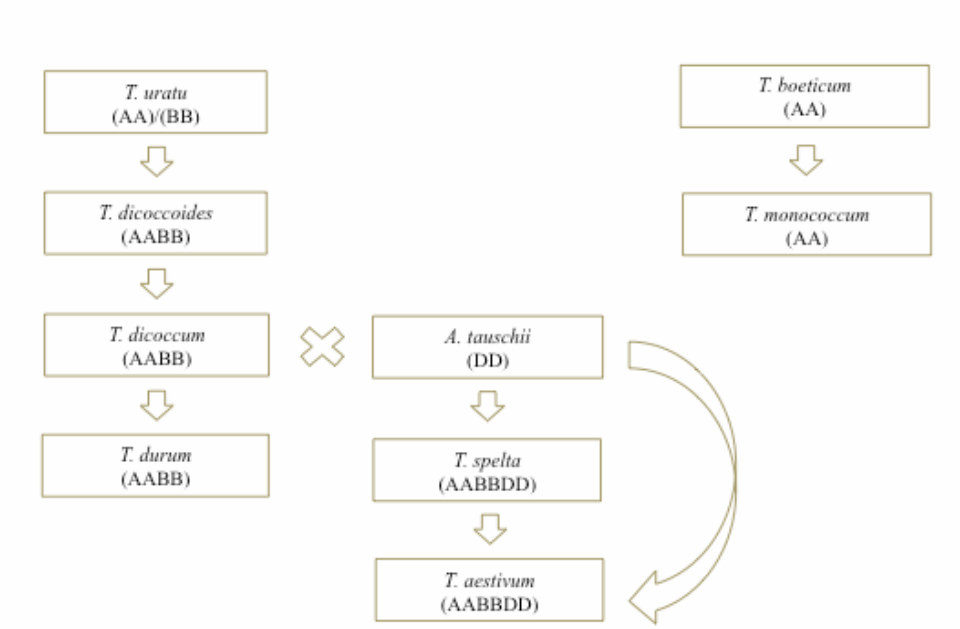


Figure 1.3: Several ploidy alterations through chance hybridisation among *Triticum* species have produced modern bread wheat (*Triticum aestivum*). These can be categorised into three distinctive cytogenic groups; Einkorn (2n), Emmer (4n) and the Vulgare (6n) group (adapted from Hancock, 2012 and Salamini *et al.*, 2002).



Figure 1.4: Ear appearance of several wheat species from left to right: *T. monococcum*, *T. boeticum*, *T. dicoccoides*, *T. dicoccum*, *T. durum*, *T. spelta*, and twice *T. aestivum*. Diploid and tetraploid species are characterised the presence of awns (image origin unknown).

Ploidy changes and selective breeding mean that modern wheat plants are hybrids formulated throughout domestication processes (Salamini *et al.*, 2002) thus many

ancient hulled wheat species (including einkorn, emmer and spelt) form an intermediary stage from wild ancient wheat species to the hulled cultivated forms of the *Triticum* species (Pagnotta *et al.*, 2005); these species are commonly referred to as 'farro' species and are still cultivated in Italy, however generally considered to be underutilised (Troccoli & Codianni, 2005). Subsequent to the early domestication processes described, wheat production proliferated due to seed transportation, which indicated plants to have the capacity to adapt to new environments (Hay & Porter, 2006). Consequently, wheat which was initially adapted to short Mediterranean winters, now produce record yields within cool climates that typically have long growing seasons of ten months (Hay & Porter, 2006).

1.3.1 Einkorn wheat *(Triticum monococcum)*

Einkorn, a diploid species, was the first wheat species to be successfully cultivated. The wild related form, *Triticum tauschii* has been used as a source of simply inherited traits, however there are relatively few reports of this diploid positively impacting yields after introgressions of genetic material although there have been observed advantages through introgression from its wild relative *T. tauschii* (Gororo *et al.*, 2002).

1.3.2 Emmer wheat *(Triticum dicoccum)*

Emmer wheat, a hulled tetraploid species, form a conduit between modern cultivated wheat (bread and durum wheat) and wild wheat species, the main difference between the two being the presence of the Q locus (a single gene on chromosome five) (Pagnotta *et al.*, 2005). Whereas einkorn cultivation is limited to marginal areas mainly within Europe, emmer wheat continues to be cultivated on an economically important scale within Ethiopia and remains a minor crop in India and Italy (Troccoli

& Codianni, 2005) and is widely distributed throughout the Near Eastern Crescent (Peleg *et al.*, 2005). Such regions are generally characterised by long, hot, dry summers with short, mild and wet winters. The emmer wheat grown in such environments have developed to possess the AABB genome, from which tetraploid and hexaploid wheat were derived (Peng *et al.*, 2000). Emmer has been observed to have a lower grain yields than durum wheat but a higher yield when compared to einkorn (Troccoli & Codianni, 2005). In addition to spelt, wild emmer is thought to be a viable source of genetic variation.

1.3.3 Spelt wheat (*Triticum spelta*)

Half way through the first millennium BC, emmer was replaced by *Triticum spelta* (spelt) as the main cultivated wheat species (van der Veen & Palmer, 1997). *Triticum spelta* is still a cultivated species throughout south-eastern Europe, most notably in Germany and Switzerland, although is still underutilised (Bertin *et al.*, 2001; Troccoli & Codianni, 2005) and is also of interest within numerous wheat breeding programmes (Winzeler *et al.*, 1993). The yields of spelt are thought to be lower than that of bread wheat and emmer however superior to those of einkorn (Troccoli & Codianni, 2005). Furthermore, spelt wheat has been described to be more robust than modern wheat during early germination and early seedling development (Burgos *et al.*, 2001) and has been seen to display more vigorous growth under adverse conditions (Bertin *et al.*, 2001). The positive impacts of the introduction of spelt genetic material (spelt cv. Oberkulmer and Rouqin) into winter wheat was reported by Winzeler *et al.*, (1993) who observed the F_1 generation to have superior yields due to heterosis improving grains per ear and single grain weight.

1.4 Genetic progress and limitations in modern bread wheat

Wheat breeders have genetically altered modern genotypes through cultivation and breeding, most notably during the 'Green Revolution' when key genes were introduced, creating plants with common characteristics. These traits altered plant morphology and increased farming capacity significantly (Davies *et al.*, 2009). Wheat has been adapted and developed through focused breeding initiatives to improve specific morphological characteristics such as Harvest Index (HI) in resulting progenies (Murchie *et al.*, 2009). These plants are also more responsive to agricultural inputs than their predecessors and have increased yield stability (Araus *et al.*, 2002; Calderini & Slafer, 1998). However, trends suggest that global wheat yields may be approaching an asymptotic threshold level (Calderini & Slafer, 1998), a situation that does not fare well in light of demands projected to increase from 2.5 to 3.5 tonnes per hectare over the next 25 years (Ortiz *et al.*, 2008).

Further genetic enhancements are now thought to be somewhat limited since focused breeding schemes and early domestication are hypothesised to have resulted in a genetic bottleneck, causing an erosion of allelic variance within modern plant breeding (Peleg *et al.*, 2005). Reif *et al.* (2005) state that 86% (excluding China) of spring wheat cultivable area was sown with CIMMYT (International Maize and Wheat Improvement Center) or CIMMYT related germplasm derived from at least one CIMMYT ancestor, illustrating the narrow genetic basis of modern hexaploid wheat today.

The limited modern bread wheat gene pool makes it increasingly difficult to select for new plant types with the capabilities to resist biotic and abiotic stresses (Sparkes, 2010) consequently reducing overall productivity through drought, salinity,

temperature and nutrient imbalances (Araus *et al.*, 2002; Trethowan & Mujeeb-Kazi, 2008). Even new plant types, bred to be high yielding, have negligible yields in harsh environments, illustrated by observed yields being inversely proportional to the environmental stresses imposed (Araus *et al.*, 2002). This is further indicated by yield increments in the United Kingdom being ten times those witnessed in Australia (Araus *et al.*, 2002). Furthermore, it is thought that the genetic uniformity of the modern bread wheat gene pool will heighten the vulnerability of wheat to disease epidemics (Gororo *et al.*, 2002; Smale, 1997). It is also often the case that those characteristics selected for throughout the rise of the 'Green Revolution' may have improved overall light interception to increase the conversion of light energy into dry matter per unit land area however, has not improved per unit leaf area (Murchie et al., 2009). In fact, several studies have shown that wheat assimilation rates have declined following domestication (Murchie et al., 2009) therefore, in some instances, these changes may need to be reversed for the production of novel wheat cultivars.

In light of increasing demands and climate change producing increasingly capricious weather conditions, as well as the necessity to reduce inputs, agricultural productivity is no longer sufficient, nor is it sustainable (Murchie *et al.*, 2009; Skovmand *et al.*, 2001). This poses a great challenge for the selection of plants with characteristics that are more amenable to adverse conditions, conditions that are commonly observed to impede production particularly where resource limitations occur (Trethowan & Mujeeb-Kazi, 2008). It is therefore imperative that the genetic variation is supplemented from external sources; these are predicted to occur from 1) synthetic hexaploid wheat, 2) genetic manipulation and 3) related species or landraces (Trethowan & Mujeeb-Kazi, 2008). The latter presents an extraordinary opportunity since most cultivated crop species display the 'founder effect'. This

states that the genetic variation within cultivated species is diminutive compared to the variation present within wild relatives of the same species (Zamir, 2001). In fact, much of the emphasis of crop research institutes is targeted towards the collection, preservation and utilisation of genetic resources (Hoisington *et al.*, 1999). Regardless of the means through which these improvements occur, it is becoming clearer that advancements are required through a multi-disciplinary assault to better establish 'sustainable intensification' (Davies *et al.*, 2009).

1.5 Ancient wheat species as a tool for wheat improvement

Previous research has indicated that ancient wheat species harbor substantial genetic variation that remains untapped (Skovmand *et al.*, 2001; Trethowan & Mujeeb-Kazi, 2008). Many of these resources include traditional varieties and non-domesticated species (Hoisington *et al.*, 1999); these are relatively underutilised and are a prospective source from which genetically variable alleles can be mined. An example of such a feat within modern breeding relates to the introgression of wild *Avena sterilis* L. germplasm being introgressed into *A. sativa* L. which increased yields by up to 30% (Gororo *et al.*, 2002).

Wild emmer has been observed to harbour a great deal of variation that may be critical for the improvement of economically valuable traits within modern bread wheat (Peleg *et al.*, 2005). Additionally, *Triticum dicoccoides* is thought to harbour many morphophysiological traits of high agronomic and economic importance (Carver & Nevo, 1990; Nevo *et al.*, 1991). Furthermore, landraces and varieties of spelt wheat could be crucial for the improvement of wheat as a result of their mutual hexaploid status increasing the chances of viable crosses (Burgos *et al.*, 2001). Peleg *et al.*, (2005) also highlights the relative ease of crossing between tetraploid emmer

and hexaploid wheat species. This is particularly appealing as it provides a promising source of genetic material that can be mined for the improvement of modern wheat through conventional breeding techniques (Peleg *et al.*, 2005), therefore great emphasis has been placed on introgression of these traits into wheat cultivars (Foulkes *et al.*, 2009). However, detailed information on physiological traits, and how they impact yield are not currently available. The combination of genetic methods and investigations of plant physiology will allow the adaptive mechanisms to be discerned to biotic and abiotic stresses that may be useful for the improvement of modern bread wheat (Peleg *et al.*, 2005).

1.6 Increasing agricultural productivity and efficiency to meet growing demands

High yielding, efficient crop systems are reliant upon optimal growth and development (Reynolds *et al.*, 2001). The efficiency of a large scale agricultural system is inherently dependent on its basic components; these include agronomic management practices, resource availability, as well as the genetic material used, as ultimately this provides the final limitation on productivity. Since productivity is commonly inefficient within many cultivated crop species, enhancement could be key. It is therefore necessary to evaluate traits within a population that has large variation; this increases the chances of identifying combinations of alleles that confer efficiency or tolerance associated traits (Hoisington *et al.*, 1999). Genetic diversity is therefore critical for production of successful, efficient and sustainable production systems. Zamir, (2001) makes the pertinent statement that: *'plant breeding is the art and science of the genetic improvement of crops to produce new varieties... [and] genetic variation is the engine that propels breeding to meet future challenges'*. As a result, much emphasis within crop breeding is directed towards improvement of

cultivars, which has the potential to ensure that yields achieved thus, far are surpassed.

1.7 Physiological traits determining yield and resource capture

The resource-capture and conversion efficiency of plants are directly related to biological yield; harvestable yield is determined by the proportion of total biomass that has been directed towards harvestable structures, most notably the grain for wheat. Plants accumulate biomass through the capture of photosynthetically active radiation (PAR) (at a wavelength of 0.4-0.7 μm); the energy contained within this frequency can be used to fix carbon by driving pigment based systems in the process of photosynthesis (Azam-Ali & Squire, 2002). In this process photons (units of radiation) are absorbed by pigment molecules such as chlorophyll, which transform atmospheric CO_2 into complex carbohydrates (Azam-Ali & Squire, 2002). An informative way of investigating genotypes is the study of the efficiency with which these external resources can be converted into biomass (Hay & Porter, 2006; Miralles & Slafer, 1997). The amount of dry matter accumulated per unit of Photosynthetically Active Radiation (PAR) that has been intercepted is termed radiation use efficiency (RUE) (Monteith & Moss, 1977). This was further described by Mitchell & Sheehy, (2006) who stated that harvestable grain yield as dry matter (Y) (g m^{-2}) can be achieved by increasing any one of the following terms; harvest index (HI), radiation conversion factor (RUE) (ε) (g MJ^{-1}), growth duration (days) (*n*) (days), Q_i is the PAR intercepted on the i^{th} day (MJ m^{-2}) and F_i is the fraction of incident PAR that is intercepted, averaged over the i^{th} day (Equation 1.1).

$$Y = HI\ \varepsilon \sum_{i}^{n} Q_i\ F_i$$

Equation 1.1

It is widely accepted that there are significant differences in biomass accumulation and resource use efficiency between and within species. It is this variation that is critical within breeding programmes (Azam-Ali & Squire, 2002; Mwale *et al.*, 2007). The details of domestication of ancient wheat species have been well documented however, very little information exists regarding the physiology, growth and development (van der Veen & Palmer, 1997). The following sections review the literature concerning biomass accumulation, canopy architecture and radiation capture.

1.8 Conversion of radiation through photosynthesis

Photosynthesis (within C_3 plants) is the process whereby plants accumulate stored chemical energy in the form of organic carbon from water and carbon dioxide (CO_2). Photosynthesis takes place in virtually all mesophyll cells and occurs through two processes; 1) light reactions and the Calvin cycle, both of which have multiple steps (Figure 1.5). In the former, photons are absorbed by chlorophyll (within chloroplast internal membranes), to generate chemical energy in the form of ATP (adenosine triphosphate) and NADPH (nicotinamide adenine dinucleotide phosphate) (Campbell & Reece, 2002). The second stage, termed the light independent reactions through the Calvin cycle (Figure 1.6), begin with 1) carbon fixation, whereby Rubisco (ribulose-1, 5-bisphosphate carboxylase) incorporates CO_2 from the air into organic molecules in the chloroplasts by conjugating it to a five carbon sugar (ribulose bisphosphate) (RuBP) (Beadle and Long, 1985; Campbell & Reece, 2002; Langdale

et al., 1988). With the addition of electrons, the products of this process then undergo a 2) Reduction phase, producing complex carbohydrates. In the final steps of the Calvin cycle, ATP is used to rearrange carbon products to 3) Regenerate the CO_2 acceptor, RuBP. It is this concluding step that enables the cycle to continue. The maximum potential for energy conversion through these processes is thought to be 4.6%, although many species rarely achieve this, particularly under natural conditions (Lawson *et al.*, 2012). This reaction can be simply described as the production of two energy rich compounds (oxygen and carbohydrate) that derive from two energy-poor compounds (CO_2 and water), in the presence of solar radiation (Campbell & Reece, 2002):

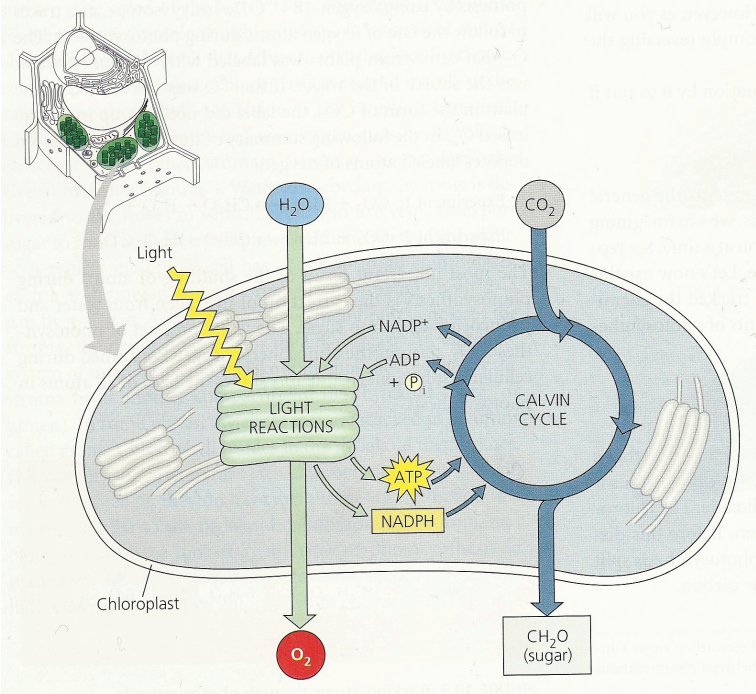


Figure 1.5: An overview of photosynthesis: cooperation of the light reactions and the Calvin cycle. In the chloroplast, the thylakoid membranes are the sites of the light reactions, whereas the Calvin cycle occurs in the stroma. The light reactions use solar energy to make ATP and NADPH, which function as chemcial energy and reducing power, respectively, in the Calvin cycle. The Calvin cycle incorperates CO_2 into organic molecules, which are converted to sugar (Campbell & Reece, 2002).

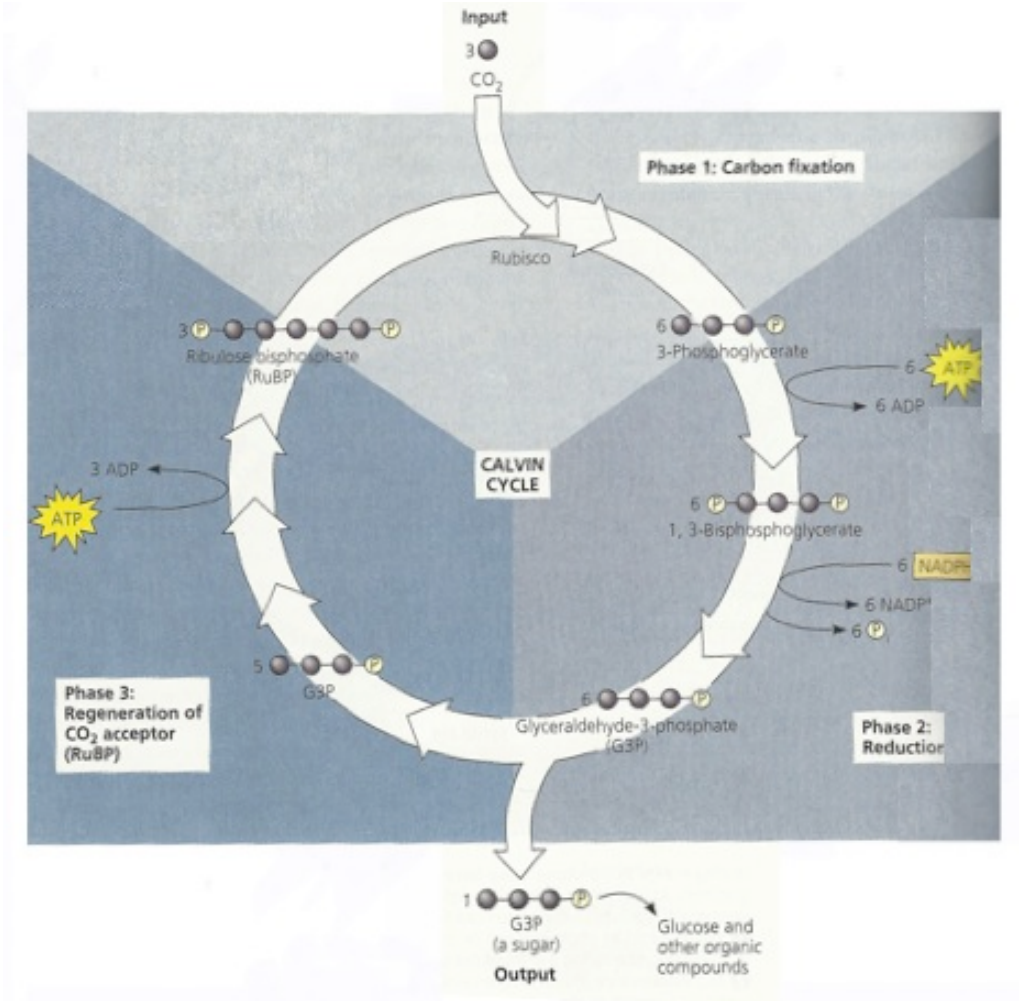


Figure 1.6: The Calvin cycle. The diagram tracks carbon atoms (grey balls) through the Calvin cycle. The three phases of the cycle correspond to the phases discussed in the text. For every three molecules of CO_2 that enter the cycle, the net output is one molecule of glyceraldehyde-3-phosphate (G3P), a three-carbon sugar. For each G3P synthesised, the cycle spends nine molecules of ATP and six molecules of NADPH. The light reactions sustain the Calvin cycle by regenerating ATP and NADPH (Campbell & Reece, 2002).

The productivity of a crop system is ultimately set by the efficiency of absorption light energy, and the efficiency of its transduction into biomass (Murchie *et al.,* 2009). This is heavily influenced by the distribution of quanta over individual elements of the crop foliage, the relationship between photosynthetic rates and irradiance for the various elements of the crop canopy as well as the corresponding rates at which CO_2 is lost (Azam-Ali & Squire, 2004). When light is saturating, the limitation is set by the rate at which atmospheric CO_2 can be fixed and reduced to

carbohydrates whereas when irradiance is low, the limitation is set by photo absorption; this linear phase provides a measure of the 'quantum efficiency' by measuring the amount of CO_2 absorbed per unit irradiance (Azam-Ali & Squire, 2002). Beyond this phase, with increasingly stronger light incidence, photosynthetic rates typically increase until they become saturated, leading to a plateau in photosynthetic rate (Azam-Ali & Squire, 2002). There has been a great deal of focus directed towards the enzyme Rubisco in order to increase CO_2 assimilation rates. This is because Rubisco is capable of catalising two distinct reactions; the first leads to the formation of phosphoglycerate, when CO_2 is the substrate, and the second produces phosophoglycollate, which is broken down to release CO_2 in a process called photorespiration (Reece & Campbell, 2002). The net photosynthetic rate of a plant is dependent on the difference between the rate that CO_2 is reduced to carbohydrates and the rates of CO_2 loss through photorespiration (not including mitochondrial respiration in this case). Photorespiration accounts for a substantial proportion of carbon losses; these are thought to occur at approximately 30% of the rate of CO_2 assimilation in temperate climates (Rawsthorne, 1992). At higher temperatures, oxygenase activity is favoured over carboxylase activity, further reducing photosynthetic efficiency (Murchie et al., 2009; Rawsthorne, 1992). This therefore imposes limitations on biomass production at the most basic level of plant productivity. Crop yields are indeterminately impacted by the inherent capacity to accumulate carbon through this mechanism since the quantities of dry matter fixed during this process are linearly related to the amount of intercepted radiation (Murchie *et al.*, 2009; Takahashi & Nakaseko, 1990).

In addition to photorespiration, all plants also undergo dark respiration (R_d), where atmospheric oxygen and carbohydrates are converted into CO_2 and water, producing energy which is used to produce even more complex molecules from the comparatively simple products of photosynthesis (Azam-Ali & Squire, 2002). Respiration, both under light and dark conditions, is a critical aspect in the carbon budget of a crop and forms an important aspect of growth. The impact of respiration varies with crop age and weight (Azam-Ali & Squire, 2002). It is the efficiency of light interception and photosynthetic reactions that set the threshold for biomass production (Beadle & Long, 1985). Since the primary determinant of yield is cumulative photosynthetic rate, enhancing photosynthesis in C_3 species has been identified as a potential avenue through which crop yields may be boosted (Lawson *et al.*, 2012).

1.8.1 Photosynthetic response to atmospheric carbon dioxide

Infra-Red Gas Analysis (IRGA) allows leaf level reactions to varying atmospheric CO_2 concentrations to be monitored. Photosynthetic and transpiration rates, as well as a defined leaf-air vapour pressure deficit (D), can be used to calculate internal CO_2 leaf concentrations (C_i) (Long & Bernacchi, 2003). A graphical representation of this response in Figure 1.7 shows three phases; 1) as C_i increases from the lowest of concentrations, the reaction is characterized by Rubisco activity which is termed the maximum ribulose 1-5 bisphosphate carboxylase/oxygenase (Rubisco) carboxylation rate (V_{cmax}) (Miao *et al.*, 2009). Phase 2) occurs during further increases in atmospheric CO_2 and is characterised by limited RuBP regeneration due to electron transport (during CO_2 saturated photosynthesis) (Long & Bernacchi, 2003). The final phase 3) is evident when *A* plateaus or decreases, even in the

presence of increasing C_i. At this point, triose-phosphate utilization (TPU) restricts any further increases in photosynthetic rates. This response allows differences in biochemical kinetic variables that determine photosynthetic capacity, to be comparatively assessed (Long & Bernacchi, 2003).

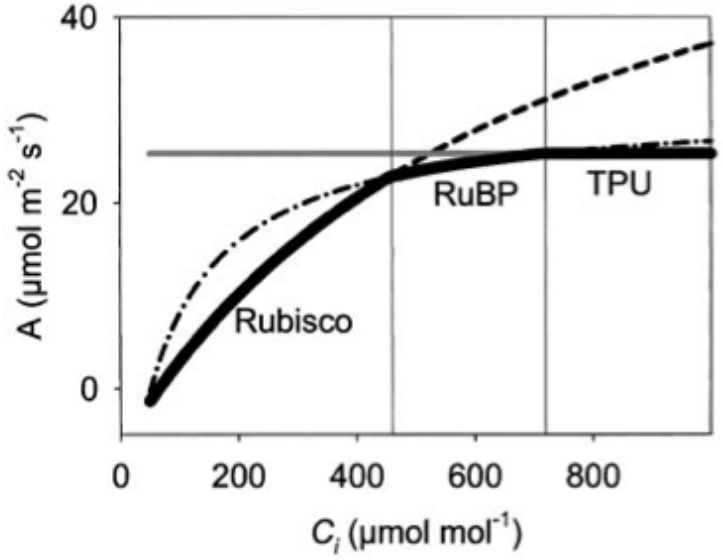


Figure 1.7: Idealised A/C_i response. The rates of photosynthesis that would be achieved are indicated when Rubisco, RuBP or TPU are limiting. The figure also shows the actual photosynthetic rates of a typical response (solid line) at any given C_i is the minimum of these three potential limitations. The parameters used were: V_{cmax} = 70 µmol m^{-2} s^{-1}, J_{max} = 130 µmol m^{-2} s^{-1}, TPU = 9.1 µmol m^{-2} s^{-1}, R_d = µmol m^{-2} s^{-1} (Long & Bernacchi, 2003).

1.8.2 Photosynthetic response to photon flux

During the reaction of photosynthetic rates to quantum flux, responses reveal differences for the underlying characteristics of photosynthesis relating to light dependent and light independent reactions. The response to light can be divided into two distinct phases; 1) initial photosynthetic rates are limited by light incidence from which quantum yields (Φ) are obtained, the second phase 2) occurs where light is saturating the leaf, therefore it is the quantity or activity of the enzyme Rubisco or primary substrate CO_2 that becomes limiting (A_{max}) (Figure 1.8). Different plant species show varying relationships between these parameters (however the overall shape is uniform), the convexity however (Θ) refers to specific points at which phases apply.

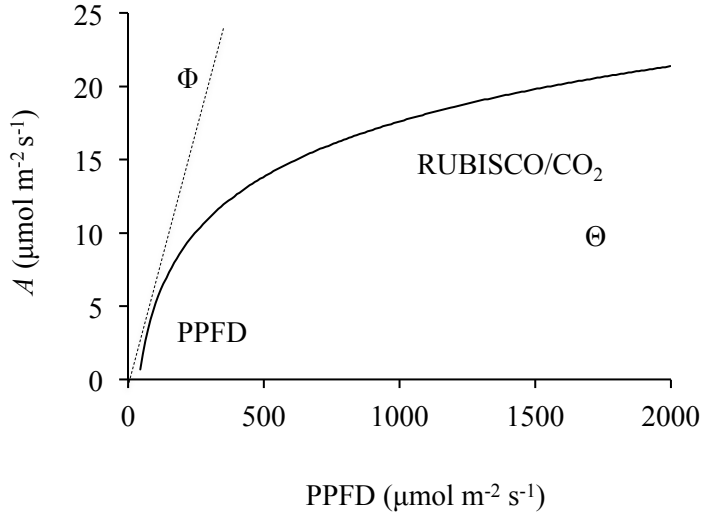


Figure 1.8: Schematic *A*/Q (Photosynthetic rate/Quanta) response curve. The rates of photosynthesis that would be achieved are indicated when PPFD and RUBISCO/CO_2 are limiting, broken line represents Quantum yield (Φ) and convexity (Θ) represents the variation between each of the phases. The solid line denotes actual photosynthetic rates at a given light intensity. The parameters derived from this response were: A_{max} = 20.40 μmol m^{-2} s^{-1}, Φ = 0.0437 μmol m^{-2} s^{-1}, Light saturation estimate = 490 and respiration = -1.03 μmol m^{-2} s^{-1}.

1.8.3 Stomatal behavior and characteristics during photosynthesis

The amounts of CO_2 reduced to carbohydrate, as well as the decay of compounds broken down to fulfill energy requirements for metabolic process, is termed the net photosynthetic rate (A) (μmol m^{-2} s^{-1}) and can be described as:

$$A = (C_a - C_i) / (r_a - r_s) \qquad \text{Equation 1.2}$$

Where C_a (g of CO_2 per m^3 of air) and C_i are the concentrations of CO_2 in the atmosphere and internal air spaces of the leaf, respectively (g of CO_2 m^{-2} s^{-1}) and r_a and r_s are the leaf boundary resistances created at the leaf surface as well as stomatal resistances (created by the behaviour and distribution of stomatal apertures at the leaf surface) (s m^{-1}) (Equation 1.2). Stomatal resistances are regulated by both physiological and environmental factors and govern CO_2 uptake as well as water loss (Lawson & Blatt, 2014). Stomatal opening is typically stimulated by exposure to PAR, low CO_2 concentrations, and high humidity, whereas stomatal closure stomata is stimulated by the reverse (Lawson & Blatt, 2014; Lawson & Morison, 2006). When closed, stomatal openings are restrictive to carbon diffusion into the leaf, this reduces carbon assimilation and will therefore limit the yields produced (Lawson & Blatt, 2014). Figure 1.9 shows the stomatal pathways which allow water and CO_2 to diffuse from the leaf to the atmosphere and *vice versa* and are subject to resistances (Condon *et al.*, 2004). Stomatal openings must allow sufficient CO_2 to enter the leaf whilst avoiding water losses that may cause dehydration and metabolic disruption (Lawson, 2009; Lawson *et al.*, 2012; Lawson & Morison, 2006). Stomatal density varies with species and can range from 0 to more than 2000 mm^{-2} (Lawson & Morison, 2006). The importance of stomata is illustrated by Lawson & Blatt, (2014) which outlines a study in which stomatal density was overexpressed in mutants

causing an increase of 2/3 greater stomatal densities, which corresponded with a 30% increase in photosynthetic rate. This was also linked with an increase in water use and a 50% reduction in water use efficiency (WUE) (Lawson & Blatt, 2014).

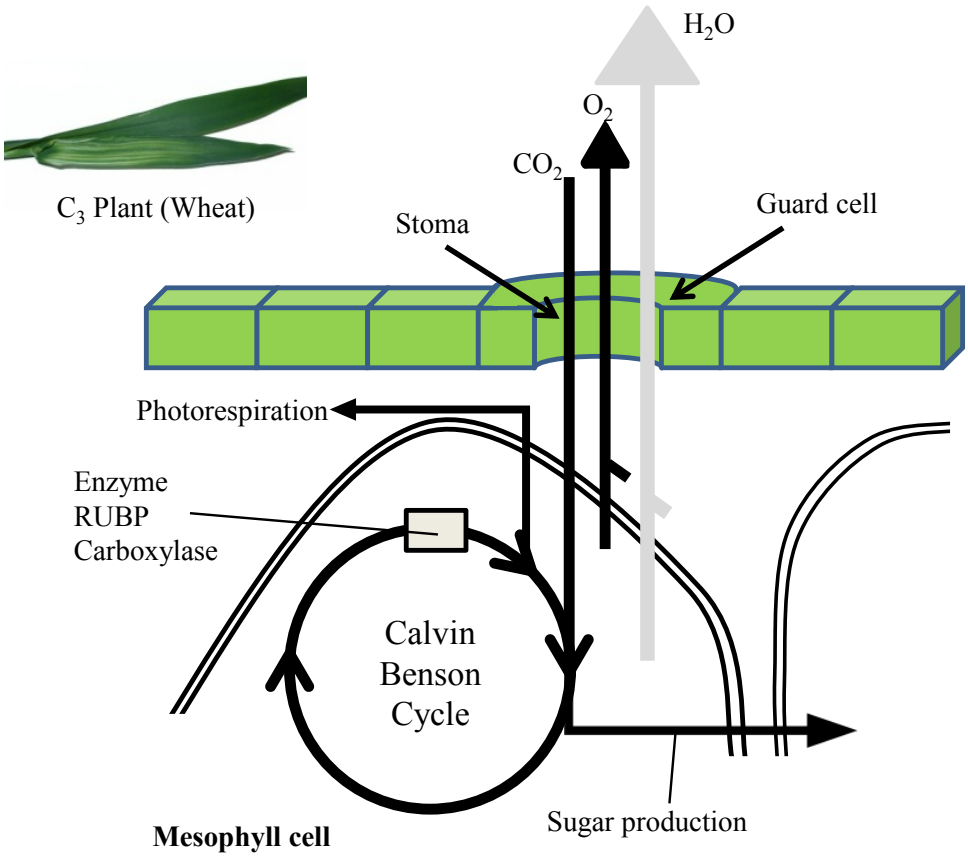


Figure 1.9: Schematic cross-section showing typical gas exchange between the atmosphere and stomatal air spaces within the leaf showing carbon dioxide entry and water vapur loss. The biochemical pathways involved in this process are also shown (adapted from Azam-Ali & Squire, 2002).

The primary biochemical reaction is consistent in all C_3 species; there is considerable variation for photosynthetic rates per unit leaf area, some of which is accounted for by differences in biochemical capacities. One particular study investigated the maximum photosynthetic responses using A/C_i curves of a number of species, under steady state conditions. Maximum photosynthetic rates varied from 29 µmol m^{-2} s^{-1} (for wheat) to 6 µmol m^{-2} s^{-1} in *Picea engelmanni* (Wullschleger, 1993).

Wullschleger, (1993) illustrated the variation for photosynthetic capacity to derive from biochemical carboxylation (which varied from 6 to 194 μmol m^{-2} s^{-1}), RuBP generation through electron transport rates (which varied from 17 to 232 μmol m^{-2} s^{-1}) and photosynthetic rate within high atmospheric CO_2. There are a range of explanations for these differences; kinetic properties and regulation of enzymes, enzyme expression levels, developmental responses to growth in different environmental conditions, as well as the plasticity of stomatal regulation which can take anything from seconds to hours (Lawson, 2009; Lawson *et al.*, 2012).

1.9 Growth, development and radiation interception

A large degree of crop architecture is determined by genetic lineage (Miralles & Slafer, 1997) however it is also influenced by light incidence. A way of assessing area is through leaf area index (LAI), which Watson, (1952) defined as the total one-sided leaf area of leaf tissues per unit ground area; this provides a scale for comparative measure of leaf coverage of a crop. The size and duration of leaf area will affect dry matter accumulation and duration (Azam-Ali & Squire, 2002).The leaf area index (LAI), as well as the angular arrangement of leaves will affect the amount of light that is distributed down the canopy (Azam-Ali & Squire, 2002).

Naturally, the canopy will experience a range of light environments throughout the day due to leaf angle and altering incoming radiation, cloud cover and overshadowing canopy cover; this means that leaves will only reach maximum photosynthetic rates for a small period of the day (Lawson *et al.*, 2012). Also of consequence is the speed at which leaves can respond (termed induction) following increments of PAR, which have the potential to impact daily radiation by as much 10%; increasing the rapidity of this response could provide significant gains in terms

of biological yields (Lawson *et al.*, 2012). This may be achieved by altering electron transport processes, Calvin cycle activation, and rates of stomatal responses, all of which affect the adjustment periods to changing light conditions (Lawson *et al.*, 2012). Additionally, partitioning towards components such as leaf area will also influence the proportion of photosynthetically active radiation that are intercepted and converted into organic carbon compounds (Azam-Ali & Squire, 2002). Canopy structure was explored by Monteith (1965) who stated that structure could be described by area, geometric position and size; this typically affects canopy light transmission. Incident light can be assessed relative to light attenuation through fractional interception (*F*) (Equation 1.3), where I denotes incident radiation, r is the reflected radiation and I_0, the Intercepted radiation:

$$F = 1 - (I + r) / I_0 \qquad \text{Equation 1.3}$$

A study by Zhang *et al*. (1998) showed that fractional interception peaked at 148 days after sowing (DAS) and was lower for modern bread wheat when rain-fed rather than when irrigated; *F* also varies with genotype, crop management, irrigation, row spacing and agronomic practices (Singels & Smit, 2002). Additionally, Rajbhandari, (2004) highlighted that leaf geometry was responsible for variation for fractional interception, that larger canopy sizes reduced PAR interception and that greater plant density was related to increased interception. Furthermore, Sparkes, (2010) found that spelt and emmer cultivars had greater fractional interception through canopy development indicating the potential variance for interception characteristics between modern and ancient wheat species. Other parameters such as the extinction coefficient for radiation (k) can also be obtained empirically using the

gradient of the Ln (I/I_0) against LAI using principles detailed in the Monsi-Saeki equation (Azam-Ali & Squire, 2002):

$$F = 1 - e^{-kLAI} \qquad \text{Equation 1.4}$$

Azam-Ali & Squire (2002), also describe the extinction of light through the canopy; this commonly impacts light distribution, growth rate, yields and radiation use efficiency (RUE). By measuring stratified leaf clippings, the vertical structure of the canopy can be characterised, referred to as the leaf area density (LAD); a measure of the leaf area within a single volume layer of canopy. Mashhadi & Zand (2004) found that light transmission was lower for Iranian winter wheat cultivars in which LAD was greater. The proportion of light intercepted showed that modern cultivars intercepted a greater proportion of light (up to 95% of PAR was intercepted) in the top layer of the canopy, although the study did not indicate whether cultivars differed in size (all being modern wheat cultivars however, it would be assumed that the variation for height would be relatively small).

1.10 Radiation Use Efficiency

Jamieson *et al.* (1998) state that RUE can be affected by many factors including nutrient imbalances (Sinclair & Horie, 1989) and temperature (Goyne *et al.*, 1993) although the extent to which the latter affects RUE depends on the leaf response to temperature (Sinclair & Muchow, 1999). The relationship between light intercepted and total crop biomass is linearly related (Kiniry *et al.*, 1989; Monteith & Moss, 1977) although little variance has been observed for RUE as a result of LAI (Sinclair & Muchow, 1999). Many researchers have explored other canopy traits of bread wheat and their influence over RUE; Calderini & Slafer, (1998) reported the morphological characteristics of old and newer wheat cultivars released from 1920-

1990; and found that pre-anthesis RUE did not differ widely, however there was variation for post anthesis RUE. Also, newer cultivars had more consistent RUE from the pre- to post-anthesis period when compared to the older cultivars which also had lower RUE and produced less biomass (Calderini & Slafer, 1998). Muurinen & Peltonen-Sainio, (2006) also found that, at lower altitudes, RUE differed between old and modern cultivars; ancient wheat species had increased RUE. Furthermore, spelt and emmer purportedly perform favourably in low-input conditions (Troccoli & Codianni, 2005) and have been observed to display increased RUE when compared to their modern counterparts (Muurinen & Peltonen-Sainio, 2006). Sparkes (2010) also investigated a range of ancient wheat characteristics and compared them to modern wheat; spelt was found to have the greatest RUE (1.81 MJ m^{-2}).

Monteith & Moss (1977) estimated that within an optimal environment, approximately 1.4g of dry biomass were accumulated per megajoule (MJ) of intercepted solar radiation. Monteith (1981) demonstrated that this is generally quite consistent across C_3 species, as shown in Figure 1.10, especially when crops are not stressed (Kiniry *et al.*, 1989). Literature commonly states that increased yields are often associated with high RUE (Han *et al.*, 2008; Li *et al.*, 2009) therefore increasing RUE may be central to the improvement of modern bread wheat yields. Furthermore, Reynolds *et al.* (2000) states that to date, breeding has not substantially improved RUE. Monteith & Moss (1977) suggested that by increasing maximum photosynthetic rates, RUE could be significantly boosted, especially where crops have resource limitations. This is further supported by Sinclair & Horie (1989) who state that leaf CO_2 assimilation rates and leaf nitrogen content are both functions of RUE; they demonstrated that RUE remained generally consistent when leaves had

high CO_2 assimilation rates but noticeably decreased when photosynthetic rates were low.

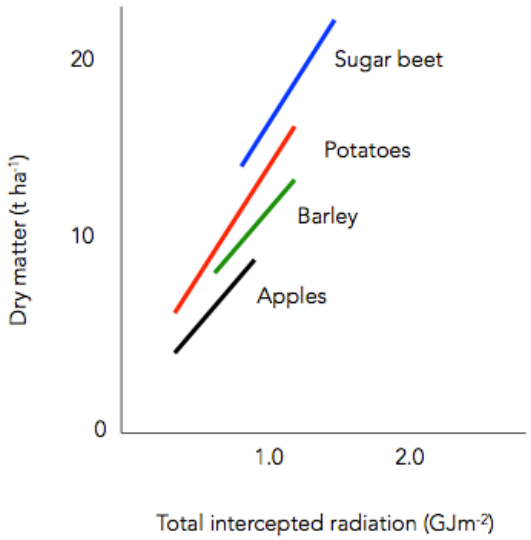


Figure 1.10: The relationship between total dry matter (t ha^{-1}) at harvest and the amount of solar radiation (GJ m^{-2}) intercepted throughout a season for apple, barley, potato and sugar beet plants (Monteith, 1981).

1.11 Green area senescence and persistence

As previously stated, photosynthetic activity, leaf area and green leaf duration are imperative to crop productivity. Senescence is a natural ageing process, whereby chlorophyll, proteins, lipids and nucleic acids degrade (Falqueto *et al.*, 2009). Falqueto *et al*. (2009) also states that photosynthetic efficiency is largely reduced as a result of senescence; the associated chlorophyll catabolism leads to disassembly of photosynthetic apparatus, the timing of which could affect overall efficiency of carbon assimilation. Greater biomass production and yield are associated with functional stay-green traits (Gregersen *et al.*, 2008; Takahashi & Nakaseko, 1990). Information collated about mutant stay-greens indicates that true stay green may be caused by a specific defect in the chlorophyll catabolism pathway (Thomas *et al.*,

2002). Delayed senescence would potentially increase the duration of CO_2 assimilation. However, it may be the case that extended duration is offset by lower overall photosynthetic capacity. During photosynthesis, highly reactive oxygen species (ROS) are produced when light absorbance exceeds the rate at which the carbon accumulated can be utilised, the accumulation of which can interfere with the electron transport chain to reduce photosynthetic efficiency (Chaves & Oliveira, 2004; Lawson *et al.*, 2012). Increased adaptation to respond to these rapid changes may lead to prolonged survival (Lawson *et al.*, 2012), potentially a factor within green area persistence. Senescence timing is likely to affect the remobilisation of nutrients; a process whereby resources are translocated from old to newer organs, particularly towards the flag leaf, which contributes the largest proportion of assimilates to grain yield (Gregersen *et al.*, 2008). Delayed senescence may also delay remobilisation, potentially leading to reduced grain weight (Gregersen *et al.*, 2008).

The stay green persistence trait has been highlighted in the literature to be particularly advantageous when plants are exposed to abiotic stresses. Many authors have reported genetic variation for senescence as a response to water or heat stresses in durum wheat; (Falqueto *et al.*, 2009; Hafsi *et al.*, 2007; Srivalli & Khanna-Chopra, 2009). Green area persistence has most often been associated with drought tolerance where the ability to maintain CO_2 assimilation is associated with increased yields, particularly when drought was imposed post-anthesis (Borrell & Hammer, 2000; Christopher *et al.*, 2008; Hafsi *et al.*, 2007). Many other studies have correlated senescence and drought tolerance with yield (Gelang *et al.*, 2000; Gregersen *et al.*, 2008; Verma *et al.*, 2004). Sparkes (2010) suggested that emmer and spelt may harbour stay green traits.

1.12 Water Use Efficiency

Although 80% of the world's allocatable water resource is directed towards agriculture, water availability is still a commonly limiting factor within many crop systems (Condon *et al.*, 2004). Crop plants routinely undergo periods where soil and atmospheric water is in deficit (Chaves *et al.*, 2002). It has been well established that reduced water availability typically reduces plant transpiration rates (Weir & Barraclough, 1986), which also reduce leaf carbon fixation (*A*) as a result of stomatal closure (Chaves & Oliveira, 2004; Lawson & Blatt, 2014) both of which are conducive to reduced biological yields (Murchie *et al.*, 2009). Weir & Barraclough, (1986) illustrate that when soil surface water is very low, transpiration reduces. In this instance, the root density at the soil surface obstructs the rate of transpiration therefore, the plant can only transpire at the rate established by the atmospheric demand, even if the soil surface is well supplied with water (Weir & Barraclough, 1986). Furthermore, severe drought has also been observed to reduce Rubisco activity and RuBP (Chaves & Oliveira, 2004). The production of drought tolerant varieties has been limited due to the sheer complexity of water use efficiency (WUE) traits since these are entwined with morphological and physiological characteristics; there is also difficulty in assessing these traits since methods are time consuming and often destructive (Chaves & Oliveira, 2004; McAusland *et al.*, 2013). Literature however does state that there is genetic variation for the underlying traits that alter WUE, which can be used to improve crop species (Condon *et al.*, 2004). An example of which is the development of new Australian wheat cultivars 'Drysdale' and 'Reese' which both exhibit WUE (Condon *et al*., 2004). WUE involves a measure of water in exchange for a unit of production (Condon *et al.*, 2004) although there is no definitive description, and it often depends on the specialism in which it is being

considered. That which forms the basis for farming and productivity and is perhaps of the most consequence within crop breeding is the agronomists' interpretation of WUE, relating carbon gain to cumulative transpiration (Steduto & Albrizio, 2005):

Yield = ET x T / ET x W x HI Equation 1.5

These principles have been used previously to assess WUE of ancient wheat species in a glasshouse study, where plants were grown in columns maintained at 80% water holding capacity (WHC) (considered to be irrigated) and 50% WHC (considered to be under drought). Results indicated that spelt and emmer had potential WUE traits. Furthermore, emmer displayed yield stability, showing an 18% reduction in yield compared to 37, 36 and 62% for einkorn, spelt and modern bread wheat, respectively from irrigated to drought conditions (Diaz-Alves, 2008).

Equation 1.5 considers yield to be a function of the volume of water utilised by the crop (evapotranspiration) (ET), the fraction of water that was actively transpired by the plant (T / ET), the efficiency term relating to the volume of water utilised relative to the amount of biomass produced (W) and finally how efficient the plant is at translocating this water into the harvestable product (Condon *et al.*, 2004; Passioura, 1977).

Alternatively, at the leaf level, WUE can be defined as a function of photosynthesis (number of moles of carbon gained) relative to water transpired (T) (see equation 1.6). This provides an instantaneous measurement of WUE that may be identified through leaf Infra-Red Gas Analysis (IRGA) (Kramer & Boyer, 1995; Larcher, 2003).

ITE mol mol^{-1} = *A* (μmol CO_2 m^{-2} s^{-1})/ T (mmol H_20 m^{-2} s^{-1}) Equation 1.6

There are a number of factors that affect ITE. Photosynthesis (*A*) is directly influenced by stomatal conductance ($G_{s\ CO2}$) for CO_2 set by the concentration gradient of CO_2 between the surrounding air and the internal leaf (C_i). Generally, reduced stomatal conductance denotes higher WUE, although this is usually observed in conjunction with a reduction in assimilation rates (*A*) as well as slower growth rates (Lawson, 2009; Lawson & Blatt, 2014). There is therefore a trade-off between water loss and carbon assimilation; however stomatal behavior and the relationship between these factors can be manipulated to reduce water loss (Chaves & Oliveira, 2004).

Stomatal response is typically much slower than photosynthetic response, creating a disparity (Lawson & Morison, 2006); the removal of stomatal limitation could increase photosynthetic rates by 20% in C_3 species; it is therefore a possibility that identifying plants with rapid sensory and or signaling mechanisms that infer rapid, tuned stomatal control, has the potential to enhance CO_2 gain and water use throughout plant growth and development (Lawson *et al.*, 2012) since slow response when stomata are required to close, or keeping stomata open to maintain photosynthetic rates, may lead to an unnecessary loss of excess water (Lawson *et al.*, 2012). The relationship between C_i and C_a remains relatively consistent with changing concentrations, indicating the linear relationship between *A* and stomatal conductance (G_s) (Condon *et al.*, 2002). Other factions of the equation are affected similarly; T is also influenced by stomatal conductance and the water vapour concentration gradients within the leaf (W_i) and in the surrounding atmosphere (W_a) (Condon *et al.*, 2002):

a) $A = G_{s\,C02}\,(C_a - C_i)$ Equation 1.7

b) $T = G_{s\,H20}\,(W_i - W_a)$ Equation 1.8

W_i is typically greater than W_a and the converse is true of CO_2 concentrations (C_i and C_a) (Condon *et al.*, 2002). There is an expanse of recent research that is geared towards stomatal metabolism. It is thought that this area of research might hold the key in the production of drought tolerant plants (Lawson, 2009; Nilson & Assmann, 2007). All of these physiological principles culminate to form the basis from which instantaneous WUE can be derived:

$$ITE = A / T = [G_{s\,CO2}\,(C_a - C_i)\,] \;/\; [G_{s\,H20}\,(W_i - W_a)\,] \quad \text{Equation 1.9}$$

Farquhar & Richards (1984) purport significant amounts of variation for ITE between genotypes. Equation 1.9 shows that there are two avenues through which leaf level transpiration efficiencies may be altered; 1) the ratio of C_i/C_a may be increased, 2) alternatively or in conjunction with reductions in the value of $W_i - W_a$. Both avenues reduce the concentration gradient between the atmospheric air and the leaf internal cavity to lower water loss (Condon *et al.*, 2004), although the latter states that manipulation of the W_i-W_a gradient remains the most straightforward where genetic variation may be used through breeding to increase the ratio of *A* to T; the quest to understand the effects of stomatal control over photosynthesis and water relations is increasingly important in light of more erratic environments (Chaves & Oliveira, 2004; Lawson, 2009). For instance, Lawson & Blatt (2014) state that by manipulation of stomatal densities, gaseous conductance can be modified accordingly. Furthermore, knowledge of stomatal function is critical to determine plant responses to environmental stresses, particularly reduced water availability, and is necessary to identify plants with decreased water use that are capable of high

yields (Lawson, 2009). Stomata have the capacity to alter mechanisms of response depending on environmental conditions, and further respond to temporal factors (Lawson, 2009). Stomatal responses are also variable by species which further complicates WUE traits at the leaf level (Lawson, 2009). Condon *et al.*, (2004) states that both of these definitions will be required in order to improve of WUE in wheat.

Progress has previously come from experiments that empirically selected for tolerance to drought stress: current genetic progress however is based on the additive variance for yield under drought within current wheat gene pools (Trethowan & Mujeeb-Kazi, 2008). The prospect of increasing the WUE of crops species seems more probable as a result of relatively new genetic methods which when combined with classical plant physiology, will allow investigation of available germplasm for improvement of cultivated plants (Peleg *et al.*, 2005). Additionally, such analyses will facilitate an understanding of plant adaptive mechanisms and their genetic basis in response to water stress (Peleg *et al.*, 2005; Trethowan & Mujeeb-Kazi, 2008).

1.13 Measuring photosynthesis and WUE: techniques and implications

The principles discussed so far have related to plant physiology, which address the metabolic processes that typically affect yields. Historically these have been integrated into crop species through breeding. However, it is increasingly evident that yield gains and resource use efficiency will not be achieved by simply using one tool or trait as efficiency traits are, by their very nature, highly complex. Physiological research therefore must utilise a wide range of tools to assess a number of traits.

Infra-Red Gas Analysis measurements allow biochemical and biophysical aspects of carbon assimilation to be assessed, particularly the limitations that are imposed on

the leaf photosynthetic capacity (Long & Bernacchi, 2003). Using gas exchange it is possible to observe parameters such as CO_2 uptake (*A*), transpiration (T), leaf conductance (G_s) as well as intercellular CO_2 mole fraction (C_i), in real-time. These can be manipulated to determine a far wider range of characteristics such as photosynthetic efficiencies, capacities, and compensation values *in vivo* (Parsons *et al.*, 1998). Using principles initially outlined by Farquhar *et al.* (1982) gas exchange measurements allow greater insight into the stomatal and biochemical aspects of carbon assimilation and WUE (Long & Bernacchi, 2003) (Figure 1.11). IRGA measurements are also indicative of the biochemical activity occurring within the leaf (Long & Bernacchi, 2003).

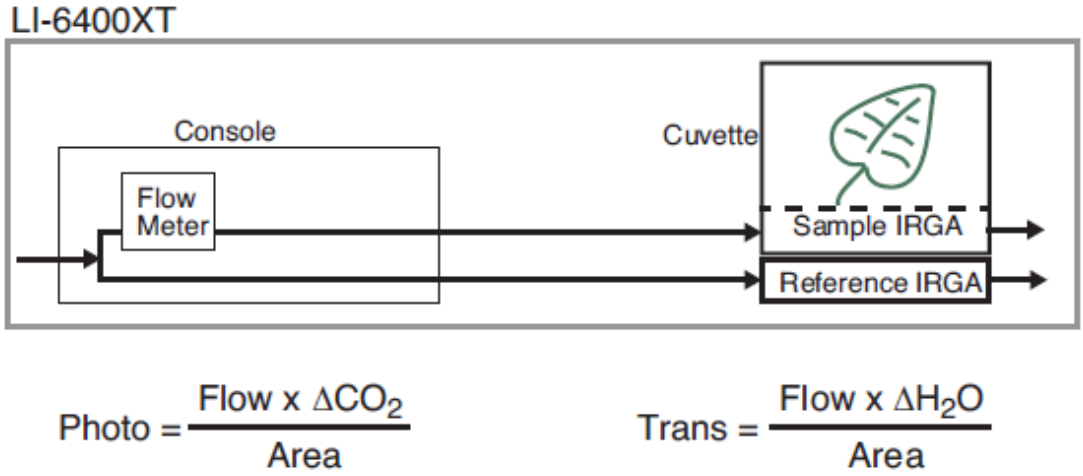


Figure 1.11: Diagram showing the mechanisms by which photosynthetic rates and transpiration rates are attained in an open Infra-Red Gas Analyser. IRGAs typically use the differential carbon dioxide and water vapour concentrations in the chamber (sample line) compared to the reference line in which no photosynthetic activity occurs (Li-Cor Manual, 2004).

Carbon isotope discrimination ($\Delta\ ^{13}C$) can also be used as a means to assess genetic variation for WUE throughout the lifetime of the plant, since it is a highly heritable trait (Condon *et al.*, 1993; Condon *et al.*, 2004). Like gas exchange, carbon isotope discrimination ($\Delta\ ^{13}C$) provides an indication of the gradients between C_i/C_a. These

are inferred by determining the ^{13}C content of plant dry matter by assuming that Rubisco will discriminate against ^{13}C, which only constitutes for 1.1% of atmospheric CO_2, and for ^{12}C which accounts for 98.9% (Farquhar *et al.*, 1989). The biochemical discrimination derives from the significantly reduced affinity of the primary carboxylating enzyme, ribulose-1, 5-bisphosphate carboxylase against ^{13}C (Condon *et al.*, 2004; Farquhar *et al.*, 1982). $\Delta^{13}C$ refers to the ratio of $^{13}C/^{12}C$ in plant material relative to the ratio of these within atmospheric air (Farquhar & Richards, 1984). Principles of $\Delta^{13}C$ are summarised in Equation 1.10 where δ_p is the $\delta^{13}C$ of the plant material, δ_a is the $\delta^{13}C$ of atmospheric CO_2, taken as -8‰ (Hancock, 2012):

$$\Delta\ (‰) = [(\delta_a - \delta_p)/(1+ \delta_p)] \times 1000 \qquad \text{Equation 1.10}$$

Farquhar & Richards, (1984) illustrated that $\Delta^{13}C$ is positively related to C_i/C_a; with the knowledge that A/T is negatively related to C_i/C_a, then $\Delta^{13}C$ should be negatively related to A/T (Condon *et al.*, 2004) (Figure 1.12) although the ^{13}C discrimination method itself does not provide an indication of whether differences in WUE derive from CO_2 assimilation (A) or water loss (T) (Farquhar *et al.*, 1989; McAusland *et al.*, 2013).

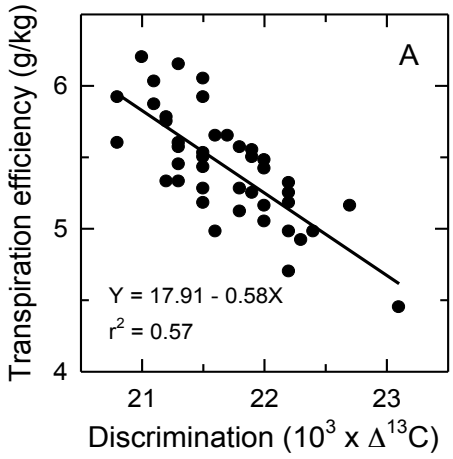


Figure 1.12: The negative correlation between $^{13}C\Delta$ and transpiration efficiency in wheat (Farquhar and Richards, 1984).

$\Delta^{13}C$ is proven to be a robust means of quantifying WUE (Condon *et al.*, 2004). It has been established that there is variation for $^{13}C\Delta$ between species, a prominent example of its use are the production of relatively new wheat cultivars, 'Reese' and 'Drysdale' developed for differing environments in Australia (Condon *et al.*, 2004). Furthermore, it is closely related to variation seen among plants in C_i/C_a. Indicative measurements of the $\Delta^{13}C$ of one einkorn, emmer, spelt species, as well as modern bread wheat for comparison was performed by Sparkes (2010). The field experiment suggested that emmer had the greatest WUE (indicated by $\Delta^{13}C$ of grain). This was further corroborated by Isaaks (2009) using ITE, $\Delta^{13}C$ and biomass production per unit water uptake, who found that emmer had the greatest WUE at each level.

1.14 Objectives

The primary focus of the current project was to characterise several cultivars for variation of a range of above-ground physiological traits. The study covered a broad spectrum of resource capture and use traits which related to radiation and water utilisation. Genotypes were grown under conventionally managed conditions with

judicious fertiliser applications so that canopy development was optimised. The data derives from a mixture of rain-fed field experiments and glasshouse experiments where plants were kept without limitation (with the exception of one glasshouse experiment) in order to compare modern bread wheat (MBW) with ancient wheat genotypes. The overall objectives of this work were to:

1) Identify and compare developmental differences, canopy growth, and potential biological yields for modern bread wheat as well as a variety of einkorn, emmer and spelt cultivars.
2) Characterise resource acquisition (of radiation and water) in einkorn, emmer, as well as spelt, and compare these to those of modern bread wheat cultivars under limited and non-limited conditions.
3) Identify the basis of the physiological traits that endow enhanced capture and conversion of resources, scaling from the leaf to the canopy level.

1.15 Hypotheses

The specific hypotheses tested in this experiment were:

H_1) The quantities of biomass that einkorn, emmer and spelt accumulate will be comparable to those of modern bread wheat.

H_2) Modern bread wheat will produce fewer tillers and partition fewer assimilates towards tillers than all investigated ancient wheat species.

H_3) Spelt species will display the ‘stay green’ trait through increased green area duration compared to other genotypes.

H_4) Modern bread wheat will partition more carbon towards the ear than ancient species and hence have greater Harvest Index (HI).

H_5) Spelt germplasm will have greater RUE compared to all other genotypes.

H_6) Photosynthetic capacity will not differ between ancient wheat and modern bread wheat.

H_7) Ancient wheat varieties originating from the dry, rain-fed fertile crescent will have increased WUE deriving from lower transpiration rates and stomatal conductance.

Chapter Two:

Plant development, growth and canopy architecture

2.1 Introduction

Germplasm characterisation has become increasingly important within agriculture. With erosion of allelic variation, specialised gene banks have been created to conserve the genetics of plants. Through efficient, accurate and systematic evaluation of germplasm, economically important traits can be identified to the advantage of plant breeding.

The current study aims to report the physiological and genetic analyses of bread wheat and a number of ancient wheat species in order to characterise their resource capture and resource use efficiency. These parameters were investigated and recorded throughout the growing season in order to gain an overview of plant phenological, physiological, development and growth for the included genotypes, which have not been reported previously. Data allowed timelines to be formulated, which were then related to the results from further aspects of the study. Furthermore, the differences between these species were used to establish the underlying traits that related to these characteristics.

2.1.1 Field trials (2010 and 2011)

The first phase of the experiment assessed a relatively broad but fundamental spectrum of resource use in modern bread wheat as well as their wild progenitors for comparisons within and between species. Morphological parameters were related to growth, development and radiation acquisition to allow a comprehensive characterisation of the plants within the study. This survey aims to shed light on key traits in the determination of resource use efficiency, providing breeding objectives for new wheat types as well as identification of the potential sources. Such analyses will also emphasise the genetic variation within these wheat lines and will therefore

give an indication of the extent allelic variation within genotypes. The overall objective for the project relates therefore to the exploration of the potential genetic resources that are relatively easily introgressed into cultivars that are widely distributed today.

2.2 Materials and Methods

2.2.1 Experimental sites

Two field trials, located at The University of Nottingham, Sutton Bonington Campus, south west Nottinghamshire, England (52°49'53.55"N, 1°15'1.32"W) were established over the 2010 and 2011 winter wheat growing season. In 2010 and 2011, the experiments were established at two different sites, both of which were managed conventionally, and established as part of a crop rotation on a sandy loam soil (the Dunnington Heath Series).

2.2.2 Seed source and plant material

In the current study it was important to include genotypes that represented all cytological groups. The grain used in the current project was acquired from the seed stores at the University of Nottingham in 2009. Table 2.1 outlines the name of each genotype however, these were given to each genotype so that they could be distinguished from one another rather than because the name represents any true detail about the lineage or origins of the cultivars. Table 2.1 also outlines the species, genome group and the typical distribution (although the latter is again, not necessarily specific to these genotypes). Also included in Table 2.1 are any additional details about the seeds, which were provided by the archeological department at the University of Oxford, from which the seeds came in 2007. Since having been acquired, all grain was stored in a seed storage facility, in cool and dark conditions, within air-tight containers. Table 2.1 also includes a range of modern bread wheat cultivars, which were chosen from the Home Grown Cereals Authority (HGCA) recommended list, released in 2008/2009. One modern bread wheat cultivar was chosen from each NABIM group, which represents a classification term used by

millers which imply the grain quality produced by the cultivar. This indicated the use for which it is suitable. These modern wheat cultivars were bought from seed companies, without treatment to mirror the conditions of ancient wheat seed.

Once acquired, seeds were then bulked in the glasshouse. These bulked seeds were used in the 2010 field experiment whereas for the 2012 field experiment, seeds originated from the previous harvest (in 2011). In 2011 grain underwent germination tests prior to drilling.

Table 2.1: Included genotypes in the study detailing species, genome group and general distribution. The table also outlines specific cultivars information when possible.

Variety	Species	Genome Group	Distribution	Details*
Emmer	*T. dicoccum*	4n (AABB)	Italy, Ethiopia, India, Fertile crescent	Asturias, North Spain
Emmer SB	*T. dicoccum*	4n (AABB)	Italy, Ethiopia, India, Fertile crescent	
Spelt SB	*T. spelta*	6n (AABBDD)	Italy	
Spelt Tauro	*T. spelta*	6n (AABBDD)	Italy	West stow, UK
Spelt Oberkulmer	*T. spelta*	6n (AABBDD)	Italy	
Einkorn	*T. monococcum*	2n (AA/BB)	Marginal areas in Europe	Kastamonu, Turkey
Einkorn SB	*T. monococcum*	2n (AA/BB)	Marginal areas in Europe	
Einkorn Hungarian	*T. monococcum*	2n (AA/BB)	Marginal areas in Europe	Szazhalombatta, Hungary
Einstein	*T. aestivum*	6n (AABBDD)	UK	
Claire	*T. aestivum*	6n (AABBDD)	UK	
Xi19	*T. aestivum*	6n (AABBDD)	UK	
JB Diego	*T. aestivum*	6n (AABBDD)	UK	

*Details: Information was provided by Dr. Amy Bogaard, School of Archaeology, University of Oxford who initially provided these four genotypes.

2.2.3 Germination Assays

In 2011, germination assays were performed to assess seed viability (due to low germination observed in 2010) whereby 50 seeds were imbibed. These seeds were placed on filter paper dampened with distilled water and subsequently sealed with paraffin film (Paraffin M, Alcan Packaging, UK) to reduce water-loss. Additional water was added every 12 hours. Plates were then placed in a growth room with a 12 hour day and night at 19°C. The germination index (GI) was then calculated according to Equation 2.1 (below) where n is the number of seedlings emerging on day 'd' and d corresponds to the day number after planting. The GI for each consecutive day of testing was accumulated and the seed lot with the greatest germination index was considered to have the greatest vigour (Gupta, 1993).

$$\text{Germination Index} = n / d \qquad \text{Equation 2.1}$$

Seeds were considered viable when it was established that the germination index was 85% or greater. Modern wheat did not undergo these tests as seed was sourced from Limagrain UK Ltd. (Angus, UK) and Senova Ltd. (Cambridge, UK).

2.2.4 Plant husbandry

In 2010, a winter wheat field experiment was established (52d 50' N, 1d15' W) where the previous crop had been winter oats. Twelve genotypes (outlined in Table 2.1) were drilled on 27/10/2009 at a rate of 300 seeds m^{-2}, having been ploughed and power harrowed prior to this. The soil type was a sandy loam with soil indices of P: 3, K: 3, Mg: 4 and a pH of 6.9, with a nitrogen (N) content (measured on 12 November, 2009) of 174.1 kg ha^{-1}, to a depth of 90cm (12 November, 2009). The

2010 winter wheat growing season had a mean daily maximum temperature of 13°C, total average rainfall of 713mm with 1060 total sunshine hours.

In the 2011 experiment, the field site, previously cropped with winter oats, was drilled on 13 October 2010, at 300 seeds m^{-2} using a Wintersteiger drill with a 12.5cm row width. Prior to this, the field was ploughed (16 September 2010) and harrowed (11 September 2010). Soil was rolled after drilling on 14 October 2010. The soil was a sandy loam with soil indices of P:4, K:3, Mg:4, a pH of 7.2 and a N content of 32.9kg ha^{-1}, measured to 90cm on 9 September, 2010 (further field experiment details are outlined in Appendices One and Two). The 2011 winter wheat growing season had a mean maximum daily temperature of 7°C, 874mm total average rainfall and 1470 total hours of sunshine. Additionally, the start of the 2011 winter wheat growing season was characterised by prolonged frosts likely to have impacted emergence rates.

2.2.5 Trial management (2010 and 2011)

The 2010 and 2011 field experiments were conventionally managed using best farm practice to minimise weeds, pests and diseases. The experiments were rain-fed, without additional irrigation.

2.2.6 Experimental design

The experiment was set up in a randomised complete block design with four replicates, each of which was surrounded by discard plots of Claire and Duxford (in 2010 and 2011, respectively) (Figures A1.1 and A2.1 in Appendices One and Two) with an equal seed rate of 300m^{-2}. In both years, the plots allocated, measured 24m

by 1.63m. These were split into northern and southern sections (measuring 12m by 1.63m) which were categorised to be either destructive or non-destructive.

2.2.7 Field techniques (2010 and 2011)

2.2.7.1 Growth stage determination

Growth stages were assessed fortnightly and then daily closer to key growth stages during visits to field sites in both seasons. In 2010, decisions regarding when sampling took place were based on the point at which ~80% of plants within the whole trial had reached a specific growth stage, as adapted from Ewert and Pleijel (1999). This meant that the growth stages of plant material, when sampled, differed between genotypes, albeit marginally and as a result, this method was altered in 2011 where genotypes were sampled individually, once they had reached specific growth stages. For growth stage determination, 5-10 plants were assessed according to the HGCA's benchmarks for UK wheat growth (Table 2.2). Data was then pooled to allow dates at which key growth stages were reached for each plot and for each genotype. By performing these analyses at intervals throughout the season, crop growth, development and biomass accumulation over time was assessed.

Table 2.2: Descriptions of wheat growth stage identifiers and benchmarks dates for general reference (HGCA, 2009).

Growth stage	Identifier of GS	Benchmark date
GS 31	First node detectable, stem extension starting	10 April
GS 39	Flag leaf blasé all visible, no further leaves emerge	19 May
GS 61	Start of flowering, little further extension of height occurs	11 June

Table 2.3: Dates when key growth stages were reached and sampling took place in the 2010 and 2011 winter wheat growing season. Dates stated for 2011 provide averages dates across the range of genotypes.

Growth analyses	Sampling date in 2010	Sampling date in 2011
GS 31 (~)	16 May, 2010	18 April, 2011
GS 39 (~)	9 June, 2010	14 May, 2011
GS 61 (~)	28 June, 2010	8 June, 2011

2.2.7.2 Sampling procedure

Leaf area index and biomass accumulation were determined using 0.72 m^2 quadrats, which were randomly placed within the central strip of the plots. Leaf area index (LAI) was measured destructively by sampling all plant material within the specified area. In the laboratory, each sample component was separated and run through an electronic leaf area meter. Plant material was collected on three sampling dates throughout the season, these coincided with growth stages 31, 39 and 61 (Table 2.3).

2.2.7.3 Sampling throughout crop growth and development

Quadrats used for sampling measured 1.2 x 0.6 m^2, covering an area of 0.72 m^2. Larger quadrats were used to limit the amount of variation observed within the data. Within the plots, destructive samples were taken from the southern section. Sampling was randomised within the central strip of the plots (thus minimising edge effects). This left sufficient area for yield assessments at crop maturity using the combine harvester. The first sampling date occurred at growth stage 31 where all plant material was cut at ground level and collected in labeled plastic bags. These were then placed into storage in a cold room within 5 hours of collection. Samples were then maintained at 4°C for no more than seven days before processing.

2.2.7.4 Laboratory analysis of field samples

Prior to analysis, plant material was washed and dried to remove any soil debris from the field. The total fresh weight of each sample was recorded, and an approximate sub-sample (25%) was taken. In both years, where samples were small due to establishment, a larger percentage of the sample was processed. Sub-samples were categorised into three groups of shoots. These categories were:

1) Potentially fertile shoots, deemed to be so due to a lack of dying tissue on or at the tips of the youngest leaves (therefore contributing to the photosynthetic capacity of the whole plant).

2) Dying or potentially infertile shoots, classified when the youngest leaf was senescing/yellowing to a large extent (50% yellow or greater).

3) Dead shoots (no green material present).

The fresh weight and number of shoots in each group was recorded. Potentially infertile and dead shoots were then dried at 80°C for 48 hours, and the dry weights recorded. Subsequently, each photosynthetically active component (green lamina, shoots and ears) were processed by separating the potentially fertile shoots into:

1.1) Green lamina.

1.2) Green true stem including the leaf sheath.

1.3) Dead lamina.

Whole leaves were considered to be dead when they had senesced by 50% or more. With leaves that were less than 50% yellow, yellowing regions were 'pinched off' and placed in with dead laminar and green area was added to green lamina.

Remaining shoots were placed with the green true stem plus leaf sheath components after which, the fresh weight of the green lamina, green shoot plus sheath and dead lamina was recorded. The area of green lamina and green shoot plus sheath was measured using a Licor 3100 electronic area meter (LI-3100 Area Meter, Li-COR, Lincoln, Nebraska, USA) ensuring that the leaf material did not overlap or fold. Each of these components were then oven dried at 80°C until they reached a constant weight. Dry weights were then weighed and recorded. Leaf area increments were analysed over time (days after sowing).

These analyses were performed at growth stages 31 and 39. At growth stage 61, sample mass was much greater and because of space and time limitations, the total sample weight was recorded after which two sub-samples were taken. The first, was a ~20% sub-sample 1 (SS1), which was analysed in detail (as above). A ~10% sub-sample was also taken and oven dried. The remaining 70% of the sample was discarded. This allowed total dry weight per m^2 to be calculated on the basis of the SS1 (10% sub-sample). Additionally, at growth stage 61, ear material was separated from fertile shoots. Each ear was clipped at the peduncle, the number and weight recorded and area taken. These were then dried at 80°C and re-weighed.

The growth stage analyses within field trials and glasshouse trials followed this protocol where growth analysis has been performed. Variations to the methods have been stated in further chapters, where appropriate.

2.2.7.5 Pre-Harvest Sample analyses

In addition to the samples collected throughout the growth and development outlined in section 2.2.7.4, samples were also collected directly before harvest when the crop was fully mature and had senesced completely. Quadrats (measuring 0.72m^2) were randomly placed and all above ground plant material was collected. Analyses were performed as in previous growth stage analyses, where fertile and infertile shoots were separated; samples had fully senesced, therefore were considered to be fertile when they had produced an ear. Infertile shoots were considered to be so when no ear was present. From fertile shoots, leaf straw and ear components were further separated which were then weighed and oven dried at 80°C until the weights were constant.

2.2.7.6 Yield analysis

From pre-harvest samples, ear material was separated and subsequently threshed to determine the grain yield per area sampled. In addition, the southern sections of plots were combined.

2.2.7.7 Leaf development and tiller economy

As stated in section 2.2.7.3, tiller numbers were recorded as part of the growth analysis and were assessed on a tiller number per unit area basis.

2.2.8 Canopy radiation and light attenuation

2.2.8.1 Plant height

The *in situ* height of the canopy was measured non-destructively using a metre rule in randomly selected positions among the central strip of plots in order to minimise

edge effects. Measurements were taken at 10 different positions along the length of the plot on a number of dates.

2.2.8.2 Radiation interception

Throughout both growing seasons, roughly on a bi-weekly basis, the fraction of PAR that was intercepted by the crop (*F*) was measured using a SunScan Canopy Analysis System (Delta-T Devices, Cambridge, UK) with Beam Fraction Sensor (BFS) (sampling dates are provided in Table 2.4). The BFS allows the measurements of incident PAR (above the canopy) to be measured as well as transmitted PAR (below the canopy) to be recorded as the SunScan probe is lowered into the canopy and maintained at 90° to the ground. The BFS increases measurement accuracy as it allows direct and diffuse fractions of incident radiation to be separated (Delta T Devices, 2002). Ten measurements, made two hours either side of mid-day, were made below each canopy while simultaneously logging direct and diffuse light above the canopy. The average fraction of light intercepted by the canopy was then calculated where:

$$F = I_0 - I / I_0 \qquad \text{Equation 2.2}$$

Where I_0 is the radiation above the crop canopy and I is the radiation below the canopy. These measurements were performed as often and as close to key growth stages as possible.

Table 2.4: Dates on which fractional interception sampling was performed.

Sampling date no.	2010	DAS	2011	DAS
1	24 April 2010	179	25 April 2011	195
2	15 May 2010	200	20 May 2011	219
3	5 June 2010	222	21 June 2011	251
4	23 June 2010	240	30 June 2011	260
5	21 July 2010	268	12 July 2011	272

2.2.9 Radiation use efficiency (RUE)

Fractional interception measurements (*F*) and total daily total of incident radiation (I_0) gained through sequential measurements above and below the crop were used to calculate the cumulative PAR intercepted for each genotype throughout the growing season using incident radiation measurements from the nearby weather station. These data, coupled with dry matter production data from growth stage analyses, quantified by destructive sampling, were used to calculate the conversion efficiency (ε) of incident PAR (IPAR) to biomass to be calculated (Equation 2.3):

$$\text{DW Biomass} = \varepsilon F I_0 \qquad \text{Equation 2.3}$$

This calculation allowed the quantities of radiation energy per unit area received and intercepted by the crop to be calculated, providing an indication of productivity relative to light energy flux received.

2.2.10 Canopy light attenuation, distribution and extinction

In the 2010 growing season, light distribution through the canopy was measured to assess the light attenuation traits of the different genotypes. Irradiance was measured at various levels within the canopy; the exponential decay of radiation was then

calculated. Measurements were performed on 22 June, 2010 using the SunScan Canopy Analysis System (Delta-T Devices, Cambridge, UK) crop analayser with Beam Fraction Sensor (BFS). Canopies were fully mature, with no indication of senescence or lodging. Distribution curves were obtained by measuring PAR in three random positions along the length of each plot. SunScan probe measurements began at ground level (0cm), and were repeated at every 10cm interval, moving up the canopy. The average light transmitted through the canopy was calculated at each horizontal height interval, whereby the measured PAR for positions within the canopy was subtracted from the incident radiation. Comparison of regressions were used to determine differences in light distribution.

2.2.11 Stay green assessments

During the 2010 growing season, post-anthesis leaf senescence was assessed using two different methods. Visual scores of flag leaves were performed when plants within the canopies had fully expanded flag leaves.

Each plot was scored twice a week from late grain filling onwards (7 July, 2010) until leaves had fully senesced (29 July, 2010). Each plot was attributed an average score, obtained from ten plants which were randomly selected and scored on a scale of 0 to 10. Leaves were scored on the basis of proportion of leaf photosynthetic area lost to senescence. The scoring chart attributed scores by dividing the percentage of the estimated total area that had senesced by 10 where a score of 0, indicated no leaf area loss to senescence at all, 1 indicated 10% of the leaf had senesced, 2 signified that 20% of the leaf area had been lost to senescence and so on, the maximum score of 10 indicated that the entire leaf area had senesced.

Additionally, the presence of the 'stay-green' traits was also assessed in genotypes by measuring the total leaf chlorophyll content of flag leaves using a Minolta Chlorophyll Meter SPAD-502 (Minolta Camera Company Limited). SPAD measurements were taken of ten randomly placed plants at three different positions on the flag leaf. These measurements were taken at the flag leaf base, mid-section and leaf tip and the average of these was recorded. The average per plot was then calculated to assess which genotypes displayed green area longevity and therefore potentially photosynthetically active leaf area.

2.3 Results

Data from 2010 and 2011 harvests provided an expanse of information regarding the morpho-physiological traits of investigated ancient wheat species, highlighting the variation present for some of these traits. The data set includes investigation of radiation capture, radiation use efficiency, and canopy persistence as well as developmental information, examined comparatively between the 2010 and 2011 field seasons. The following chapter, where possible, presents these results side by side in order to compare seasons.

2.3.1 Plant growth and development

2.3.1.1 Establishment

Rates of emergence differed between cultivars across both growing seasons but were more variable in 2011 than 2010 (Table 2.5). Einkorn genotypes established reasonably well in 2010, showing emergence rates of 48% or higher. In 2011 however, emergence for these same genotypes was very low, where einkorn SB established only 3.5%. Emergence was variable within spelt genotypes ranging from 18.5% (spelt Oberkulmer) to 57.79% (spelt SB) in 2010 and 6.63% (spelt SB) to 23.89% (spelt Tauro) in 2011. All MBW cultivars established well in 2010 and 2011, showing emergence rates of 70 % and 53% or greater, respectively. MBW cultivars had average emergence rates of 77.5 and 54.1%, in 2010 and 2011 respectively, whereas spelt, emmer and einkorn had significantly lower emergence rates in both years (34.0, 63.3 and 58.6 in 2010 and 15.3, 43.0 and 16.7% in 2011, respectively).

As several genotypes had poor emergence (such as spelt Oberkulmer and Tauro), results stated here may not be truly indicative of a closed crop canopy. Further, the low establishment meant that weeds became more invasive, introducing a competitive factor to resource acquisition, potentially hampering the growth of some genotypes.

Table 2.5 Average rates of emergence with the corresponding number of plants per m^2 observed in 2010 and 2011.

	2010		2011	
Cultivar	Emergence (%)	Plants m^{-2}	Emergence (%)	Plants m^{-2}
Claire	88.1	264.2	54.9	164.7
Einstein	70.0	210.1	55.2	164.5
JB Diego	72.7	218.0	53.5	160.0
Xi19	79.3	237.9	52.8	158.4
Einkorn	69.5	208.6	19.0	57.0
Einkorn hungarian	57.8	173.4	27.5	82.6
Einkorn SB	48.5	145.6	3.5	10.5
Emmer	64.9	194.7	34.2	102.4
Emmer SB	61.7	185.0	51.7	155.0
Spelt Oberkulmer	18.5	55.5	15.4	46.2
Spelt SB	57.8	173.4	6.6	19.9
Spelt Tauro	25.9	77.7	23.9	71.7
P	< 0.001	< 0.001	<0.001	<0.001
SED (33 DF)	4.56	13.69	3.0	9.0

Species averages for emergence in 2010 show MBW to have the highest emergence rates, followed by emmer, einkorn and spelt. In 2011, although species ranked similarly, average emergence was not consistently reduced by the same genotypes.

2.3.1.2 Shoot production and tiller economy

Total shoot production varied markedly between cultivars in 2010, being particularly low for spelt Oberkulmer and spelt Tauro (Table 2.6). Total and fertile tiller

production was significantly different at all growth stages (P <0.001). Overall, einkorn produced the largest number of fertile shoots per m^2 although establishment data must also be considered. Total and fertile shoot number followed a similar pattern among all cultivars; fertile shoots initially peaked at growth stage 31, reduced around growth stage 39 and then plateaued by growth stage 61 (except for einkorn, for which shoot number increased for growth stage 39 to 69).

Table 2.6: Average genotype total shoot number and fertile shoot number (per m^2) according to growth stage (including SED) for 2010.

	Total Shoot Number (m^{-2})			Fertile Shoot Number (m^{-2})		
	Growth Stage			Growth Stage (approx.)		
Genotype	31	39	61	31	39	61
Claire	937.0	762.5	686.1	908.0	550.3	518.2
Einkorn	1826.0	1624.6	1789.3	1812.0	1160.0	1294.9
Einkorn hungarian	1170.0	936.1	1250.0	1096.0	644.1	923.9
Einkorn SB	1990.0	1474.1	1874.9	1935.0	956.1	995.0
Einstein	901.0	744.8	762.7	876.0	377.8	514.6
Emmer	1059.0	709.3	1017.8	1052.0	445.3	668.9
Emmer SB	1050.0	845.4	593.9	1050.0	579.6	414.6
JB Diego	1182.0	849.9	1042.5	1119.0	612.6	674.0
Spelt Oberkulmer	572.0	663.6	659.9	542.0	446.1	491.7
Spelt SB	1094.0	880.5	827.5	946.0	689.3	542.0
Spelt Tauro	760.0	624.3	458.0	746.0	511.9	372.1
Xi19	1071.0	686.0	746.7	1029.0	535.6	544.8
P (Genotype)	<0.001	<0.001	<0.001	<0.001	<0.001	<0.001
SED (33 DF)	190.52	156.20	221.95	190.52	179.71	114.46

When assessed by species, differences between total and fertile tiller numbers were highly significant at all growth stages (P <0.001) (Table 2.7). Species averages, showed fertile tiller numbers to be greatest at growth stage 31, after which production of fertile tillers reduced. Spelt species carried the largest proportion of

shoots carried through to maturity (growth stage 61 or later) whereas einkorn carried the least (72.45 and 65.39, respectively).

Table 2.7: Average shoot number and fertile shoot number (per m^2) according to growth stage by species (including SED) in 2010.

	Total Shoot Number (m^{-2})			Fertile Shoot Number (m^{-2})		
	Growth Stage (approx.)			Growth Stage (approx.)		
Species	31	39	61	31	39	61
Einkorn	1661.8	1344.9	1638.1	1614.1	920.1	1071.3
Emmer	1054.6	777.3	805.9	1051.1	512.4	541.7
Spelt	808.5	722.8	648.5	744.6	549.1	468.6
MBW	1023.0	760.8	809.5	982.9	519.1	562.9
P	<0.001	<0.001	<0.001	<0.001	<0.001	<0.001
SED (44 DF)	146.03	115.22	152.80	139.48	99.30	80.96

Table 2.8: Average total shoot number and fertile shoot number (per m^2) according to growth stage by species (including SED) in 2011.

	Total Shoot Number (m^{-2})			Fertile Shoot Number (m^{-2})		
	Growth Stage (approx.)			Growth Stage (approx.)		
Genotype	31	39	61	31	39	61
Claire	771.3	490.0	530.1	587.4	200.6	352.5
Einkorn	904.4	1016.0	817.4	822.9	451.1	748.0
Einkorn hungarian	728.6	322.0	328.5	584.1	221.6	257.3
Einkorn SB	125.0	291.0	477.4	117.4	112.0	399.2
Einstein	1017.6	933.7	438.9	709.0	449.0	356.5
Emmer	1022.7	264.8	182.1	879.1	110.4	86.8
Emmer SB	915.5	338.9	765.3	714.0	139.7	584
JB Diego	1030.6	489.7	497.2	914.3	112.5	354.2
Spelt Oberkulmer	435.5	377.4	392.6	322.4	207.2	250.7
Spelt SB	167.9	309.4	400.9	158.5	236.2	252.8
Spelt Tauro	563.8	262.2	347.6	472.1	81.1	280.2
Xi19	690.3	534.9	554.8	588.4	296.5	380.0
P	<0.001	<0.001	<0.001	<0.001	0.025	<0.001
SED (33 DF)	91.0	139.3	108.9	71.6	114.3	53.2

In 2011, total and fertile shoot production varied markedly between cultivars at all growth stages (P <0.001 on all dates except at growth stage 39 where P = 0.025) (Table 2.8). Einkorn SB and Spelt SB had particularly low total (and therefore also fertile shoot) numbers per unit area, potentially a result of low establishment observed for these genotypes. Emmer and modern bread wheat, Einstein and JB Diego had the greatest number of total shoots per unit area. The total shoot production over key growth stages followed no particular trend, however the majority of ancient species tended to have large total shoot numbers at growth stage 31, which then declined between growth stages 39 and 61, which was consistent with data from 2010. Also noteworthy is the large disparity between total shoot number and fertile shoot number at growth stage 39, where generally no more than 50% of shoots were fertile, however the cause of this was unknown. Xi19 had the least variable number of total shoots across growth stage (approximately 600 total shoots throughout). Differences between genotypes for fertile shoot number production, were significantly different at all key growth stages (Table 2.9). Einkorn, einkorn SB, Einstein and spelt Tauro had the highest rate of tiller survival.

Table 2.9: Average species shoot numbers and fertile shoot numbers (per m^2) according to growth stage (including SED) in 2011.

	Total Shoot Number (m^{-2})			Fertile Shoot Number (m^{-2})		
	Growth Stage (approx.)			Growth Stage (approx.)		
Species	31	39	61	31	39	61
Einkorn	586	543.2	541.1	508.1	261.6	468.2
Emmer	969.1	301.8	473.7	796.6	125.0	335.4
MBW	877.5	612.1	505.2	699.8	264.7	360.8
Spelt	389.1	316.3	380.4	317.7	174.8	261.2
P	<0.001	0.017	0.326	<0.001	0.243	0.042
SED (44 DF)	108.9	121.3	95.7	93.3	80.2	73.9

In 2011, shoot numbers, analysed according to species averages, showed no particular trend for shoot number per unit area (Table 2.9). All spelt and einkorn genotypes peaked in terms of fertile shoots present at growth stage 61, however the numbers of shoots produced did not vary significantly. Modern bread wheat, on average produced some of the highest total shoot and fertile shoot numbers, 70.8% of which were carried through to create productive tillers. Fertile shoot numbers varied significantly between species at growth stage 31 and 61 ($P < 0.001$ and 0.042, respectively), indicating large differences in early canopy expansion. Overall, the number of fertile shoots reduced from growth stage 31 to 39 and increased from growth stage 39 to 61. At growth stage 61, einkorn had the highest number of fertile shoots per unit area ($468.2m^{-2}$) compared to spelt which had the lowest number of fertile shoots ($261.2m^{-2}$), potentially a result of the low emergence observed for spelt in 2011. Einkorn and spelt species had the highest and lowest tiller survival, respectively. In contrast to data from 2010, these results suggest that tiller production reduced from growth stage 31 to 39 and then increased from growth stage 39 to 61, which may have been indicative of the increased vegetative period for ancient species.

2.3.1.3 Plant development

Table 2.10 shows the dates at which genotypes reached key growth stages. Ancient species were seen to develop at a slower pace than MBW varieties in 2010 and 2011.

Table 2.10: Dates at which cultivars reached benchmark growth stages in the 2010 field experiment.

	2010			2011		
Cultivar	GS 31	GS 39	GS 61	GS 31	GS 39	GS 61
Einkorn	02/06	10/06	23/06	21/04	22/05	13/06
Einkorn hungarian	30/04	10/06	12/07	27/04	25/04	11/06
Einkorn SB	02/06	10/06	12/07	24/04	29/05	14/06
Einstein	27/04	02/06	23/06	15/04	12/05	03/06
Claire	27/04	02/06	23/06	18/04	13/05	05/06
JB Diego	27/04	02/06	23/06	15/04	13/05	05/06
Xi19	30/04	10/06	23/06	16/04	15/05	10/06
Emmer	02/06	10/06	12/07	18/04	22/05	10/06
Emmer SB	27/04	10/06	12/07	13/04	15/05	10/06
Spelt Oberkulmer	30/04	10/06	23/07	17/04	26/04	10/06
Spelt SB	27/04	02/06	23/06	17/04	19/05	07/06
Spelt Tauro	27/04	02/06	12/07	19/04	16/05	07/06

2.3.2 Plant morphology and architectural characterisation

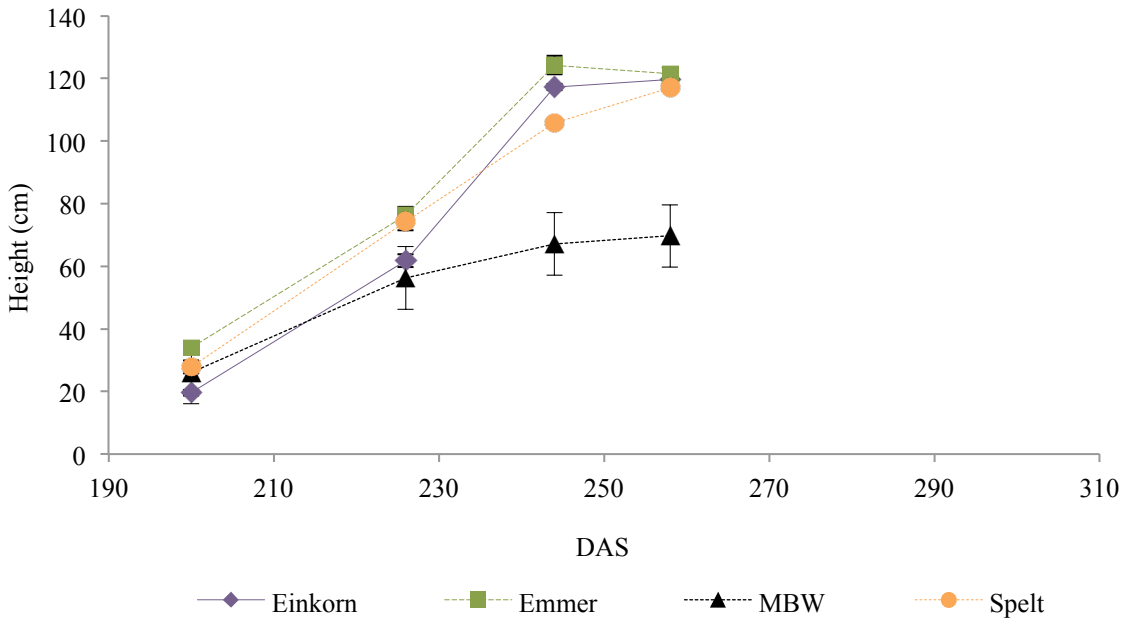
2.3.2.1 Plant height

Height differed significantly between all genotypes on every sampling date in the 2010 experiment ($P < 0.001$) (Figure 2.1). Ancient species were taller than all modern bread wheat varieties grown. Although ancient wheat varieties were generally taller later in the season, measurements taken on the first sampling date (200 DAS), showed MBW cultivars (except for Xi19), to be taller than ancient species. The variance for the heights of MBW cultivars was also seen to be much greater compared to other genotypes in 2010. Generally however, emmer species were consistently taller throughout development. In 2010, lodging, particularly for emmer and einkorn did occur late in the season, after height measurements were performed.

In both field experiments, plant growth regulators were applied as a measure to prevent the partial lodging witnessed for some of the ancient genotypes in 2010, this did not seem to reduce plant height in either year (Figure 2.1). As observed in 2010, standing height was similar among all genotypes at 195 and 221 DAS which corresponded to growth stages 31 and 39. Plant height later became significantly different beyond 242 DAS. Canopy standing height was lowest in modern bread wheat cultivars throughout the season. Ancient wheat genotypes had greater standing heights compared to modern bread wheat cultivars. The height of each species peaked at 242 DAS, corresponding with growth stage 61.

In 2010 and 2011, canopy height peaked at 244 and 242 DAS, respectively, which corresponded to the onset of anthesis. Species were not ranked similarly, however as expected, modern bread wheat cultivars did consistently have the lowest canopy heights beyond 240 DAS in both years.

A



B

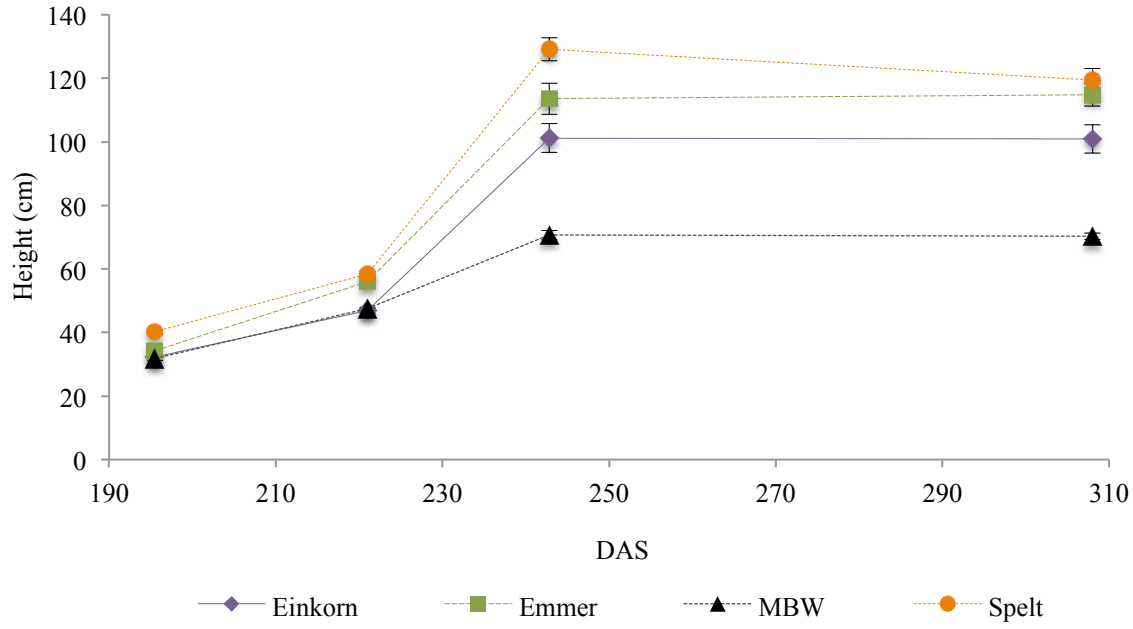


Figure 2.1: Average species height (cm) for einkorn, emmer, MBW and spelt wheat throughout A) 2010 winter wheat field experiment (P<0.001, 173 DF, SED = 2.37) and B) 2011 winter wheat field experiment (P<0.001, 173 DF, SED = 3.664) (error bars show species SEM).

2.3.2.2 Green Area Index (GAI)

In 2010, green area index (GAI) increased from 203 DAS to 227 DAS (which corresponded to growth stages 31 and 39, respectively) after which each genotype either plateaued or reduced in terms of GAI, except for JB Diego (Figure 2.2). The majority of genotypes followed this trend except Emmer SB, Xi19 and Claire where GAI seemingly decreases drastically after 227 DAS. JB Diego had the highest recorded GAI (5.5) of the varieties throughout the season. Spelt Oberkulmer exhibited the lowest GAI (2.7) throughout the season. Interestingly, spelt Oberkulmer and einkorn hungarian, although displaying the lowest GAI on the first measurement date, 'caught up' with other genotypes by 246 DAS, therefore at 227 DAS to 246 DAS, GAI continued to increase at a rate greater than many other genotypes. Total green area index (GAI) was significantly different between genotypes on all harvest dates ($P < 0.001$, $P < 0.001$ and $P < 0.002$ for 203, 227 and 244 DAS, respectively) but when averaged across species, no significant differences were found (Figure 2.3). Species averages showed that GAI increased for all genotypes from growth stage 203 to 227, after which all genotypes plateaued except for einkorn for which GAI continued to increase.

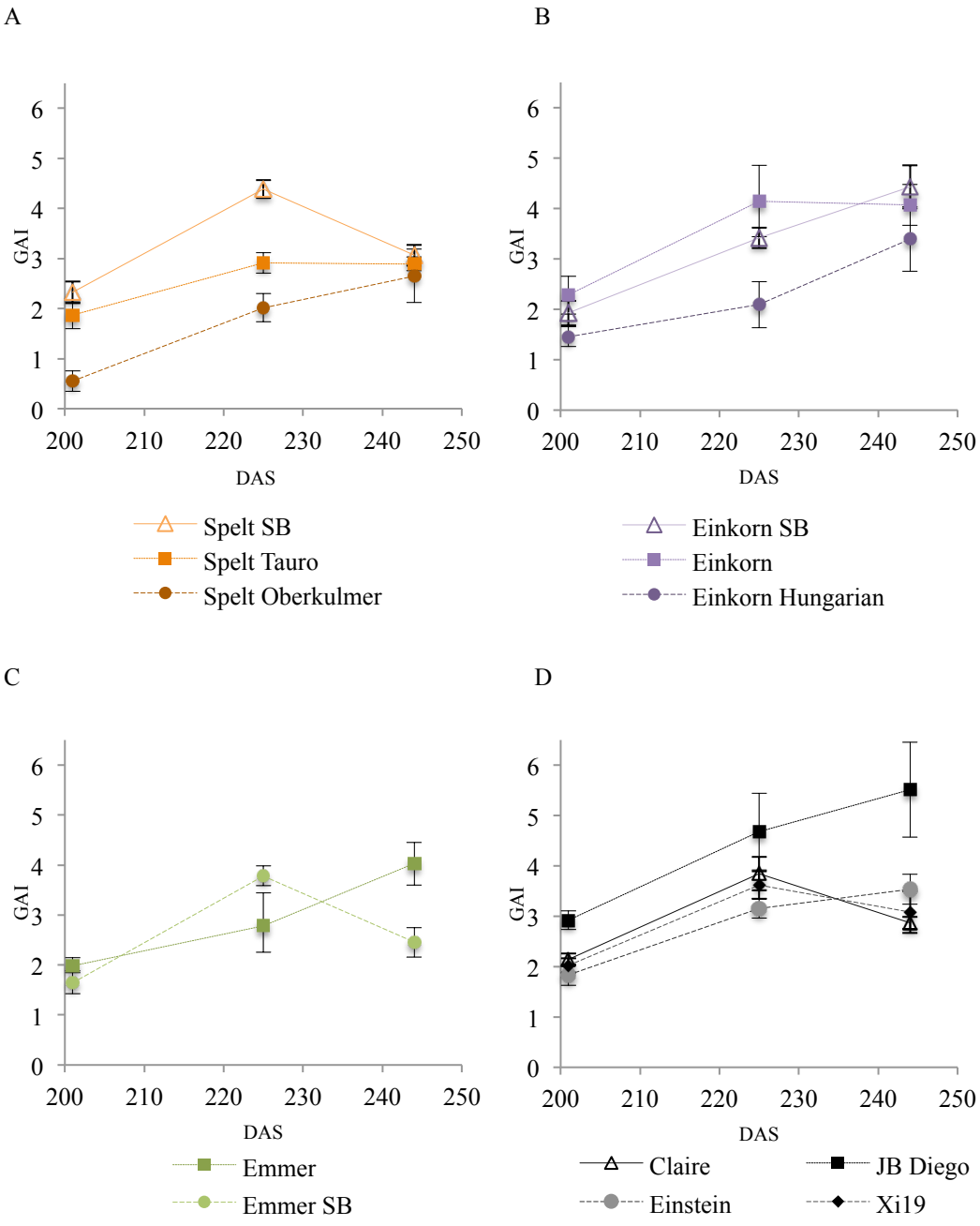


Figure 2.2: Total green area index of A) spelt B) einkorn C) emmer and D) modern bread wheat cultivars (P = 0.02, 105 DF, SED = 0.6169) (error bars represent species SEM).

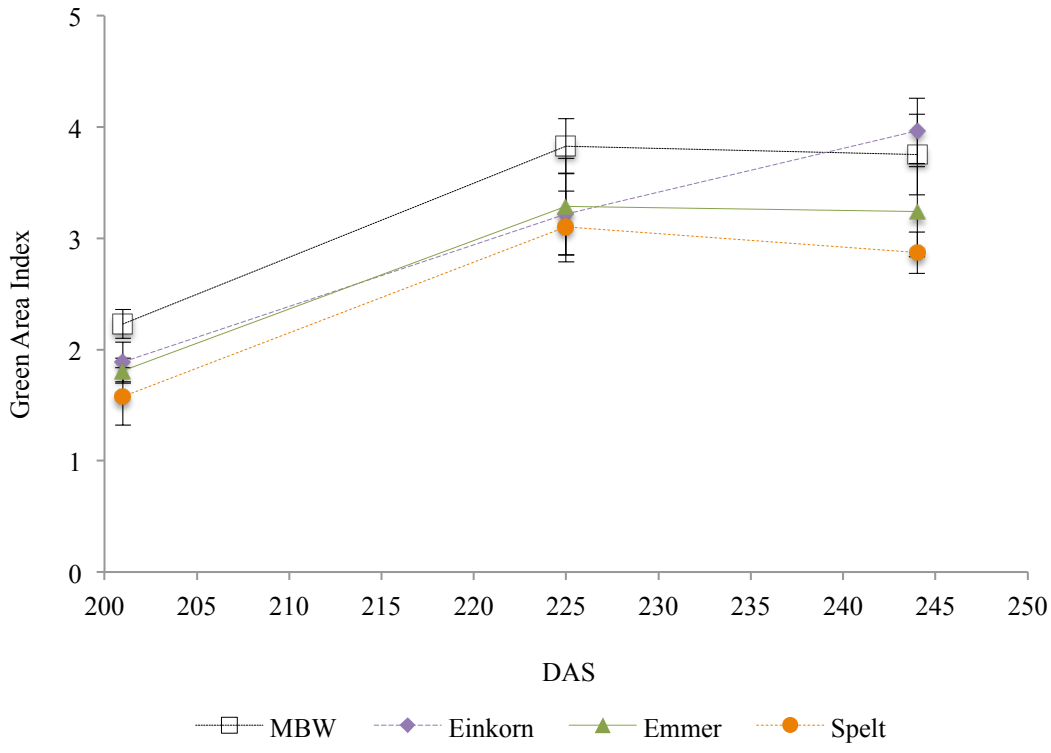


Figure 2.3: Total green area index of spelt, einkorn, emmer and modern bread wheat species averages in 2010 (P = 0.67, 129 DF, SED = 0.4341) (including species SEM).

In 2011, green area index (GAI) increased from 194 DAS to ~221 DAS (approximate since different genotypes were sampled on different dates) after which GAI either plateaued or reduced from 194 to 221 DAS for all genotypes except for spelt SB. MBW cultivars showed the most dramatic reduction in GAI from growth stage 216 to 237 DAS. Trends observed in 2011 were consistent with those observed for GAI in 2010. Differences were significantly different on all sampling dates, which coincided with growth stage 31, 39 and 61 (where P <0.001, P = 0.008 and P <0.001, respectively). Also consistent with data from 2010, spelt Oberkulmer and einkorn Hungarian had the lowest recorded GAI throughout the season. However, spelt Oberkulmer was seen to 'catch up' in terms of GAI. The consistency across the field experiments may be indicative of a lower capacity to generate green area for these genotypes.

Differences between species (Figure 2.4) were also significant on the first two sampling dates ($P < 0.001$ and $P = 0.002$, respectively) but not on the final sampling date. Modern bread wheat had the greatest GAI at 194 and 216 DAS, (corresponding to growth stage 31 and 39) when compared to all ancient wheat species. Figure 2.5 shows that modern bread wheat cultivars reached growth stage 61 first, followed by spelt, emmer and then einkorn. Genotypes sampled on the first and second sampling dates, corresponding to growth stages 31 and 39, were ranked similarly in both 2010 and 2011. Furthermore, in both years, ancient wheat species (einkorn and emmer in 2010, spelt in 2011) 'overtook' modern bread wheat for GAI on the final sampling date.

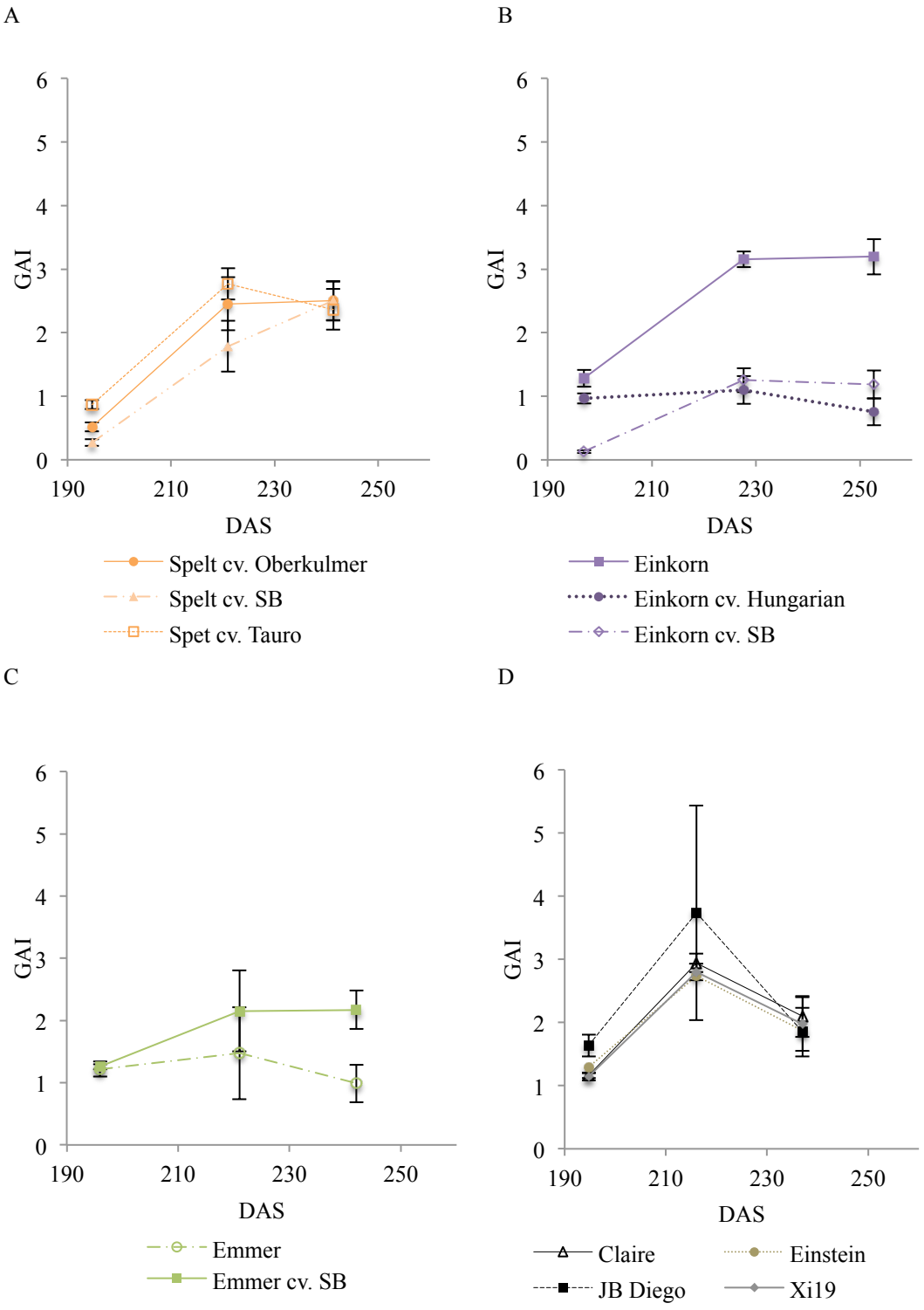


Figure 2.4: Green area index of A) spelt B) einkorn C) emmer and D) modern bread wheat cultivars in the 2011 winter wheat field experiment (error bars show cultivar SEM) (33 DF).

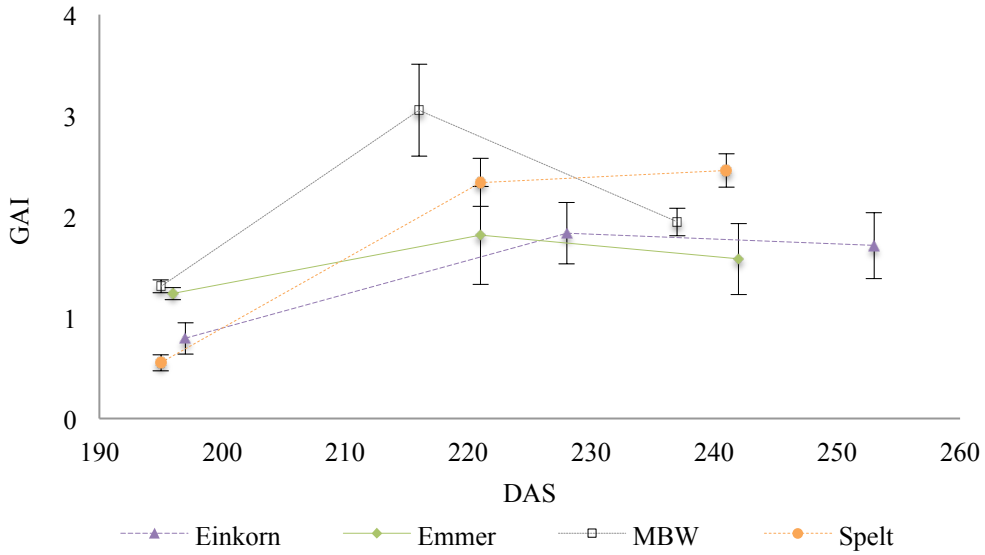


Figure 2.5: Species averages for total green area index of spelt, einkorn, emmer and modern bread wheat (error bars represent species SEM).

2.3.2.3 Green Area Index Partitioning

Accumulated dry weight in 2010, when separated into components, showed that cultivars partitioned varying amounts of carbon toward differing green area components. Differences between genotypes, across growth stages, for the partitioning of green leaf area and sheath area index were significant ($P < 0.001$ and $P = 0.004$, respectively), however were not for ear area index.

Generally, all genotypes showed a large proportion of assimilates partitioned towards green area in the initial phase of development (GS 31 and prior), beyond which the green lamina index declined (Figure 2.6). From GS 31 to GS 61, all genotypes generally increased partitioning to shoot and leaf. Emmer partitioned more biomass toward the ear than all other genotypes. The amounts of dry matter partitioned towards different components were significantly different between cultivars for biomass accumulated in lamina ($P < 0.001$, SED =13.20, DF = 33) ($P <$

0.514, SED = 25.81, DF = 33), shoot (P <0.001, SED = 20.39, DF = 33) (P <0.001, SED = 80.4, DF =33) for growth stages 31 and 39, respectively. The accumulation of biomass within canopy lamina was higher at growth stage 31 than 39; during the initial phase of the season plants were establishing green area after which leaf matter senesced.

Green area indices were also analysed in 2011 (Figure 2.7). Similarly, genotypes directed differing levels of carbon towards flag leaf (P = 0.005), green lamina (P <0.001), shoot (P <0.001) and ear indices (P <0.001). Modern bread wheat, JB Diego had higher area partitioning towards green area and flag leaf when compared to other genotypes. Consistent with 2010 observations, plants generally acquired more green area in green lamina at early developmental stages, the proportion of which reduced at growth stage 61 when area was allocated towards shoot and ear area.

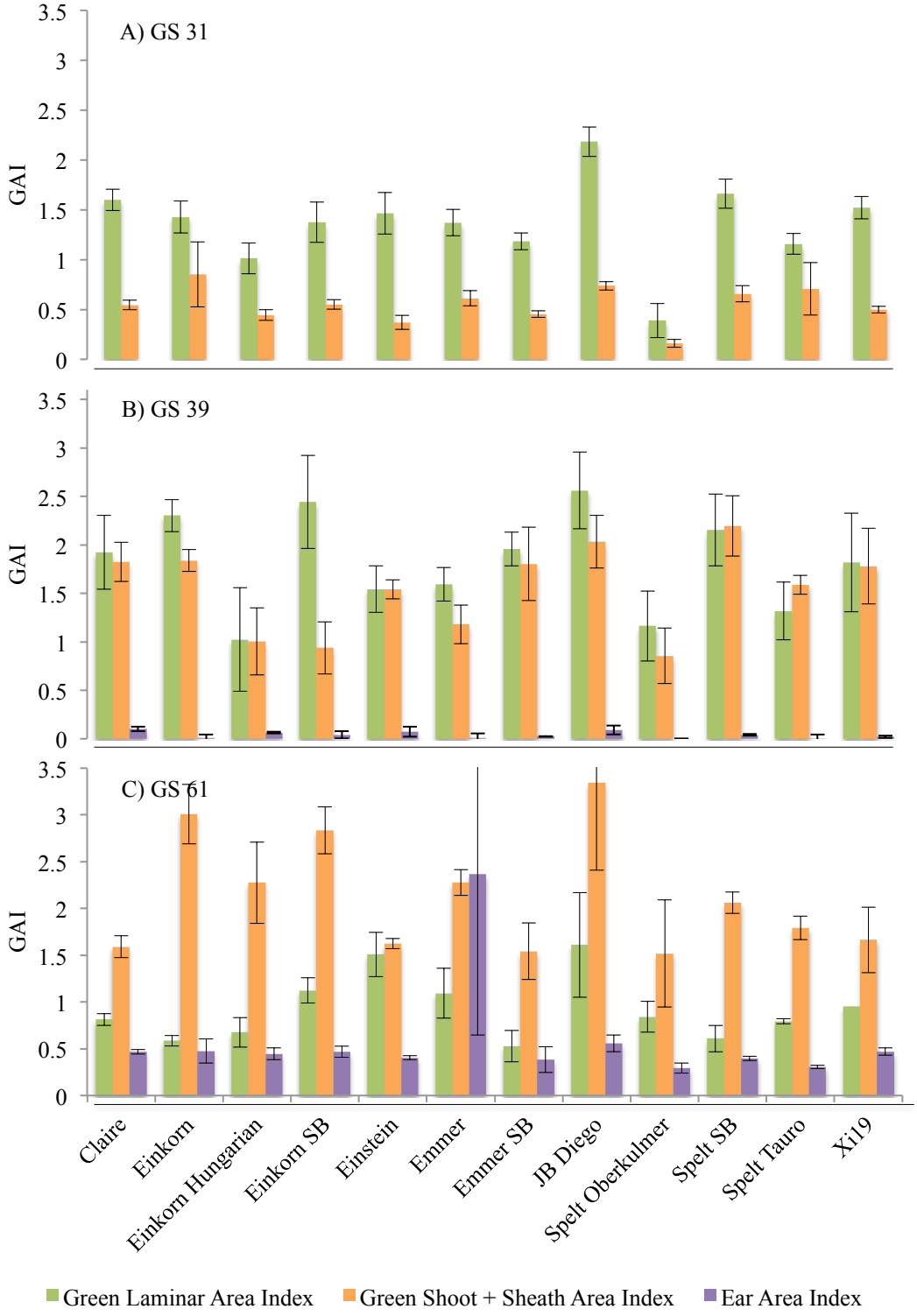


Figure 2.6: Green area index partitioning of twelve wheat cultivars in 2010 at A) GS 31, B) GS 39 and C) GS 61. Each figure shows green lamina area index (P = 0.01, SED = 0.311), green shoot area index (P = 0.004, SED = 0.386) and green ear index (P = 0.245, SED = 0.504), where present (error bars denote SEM).

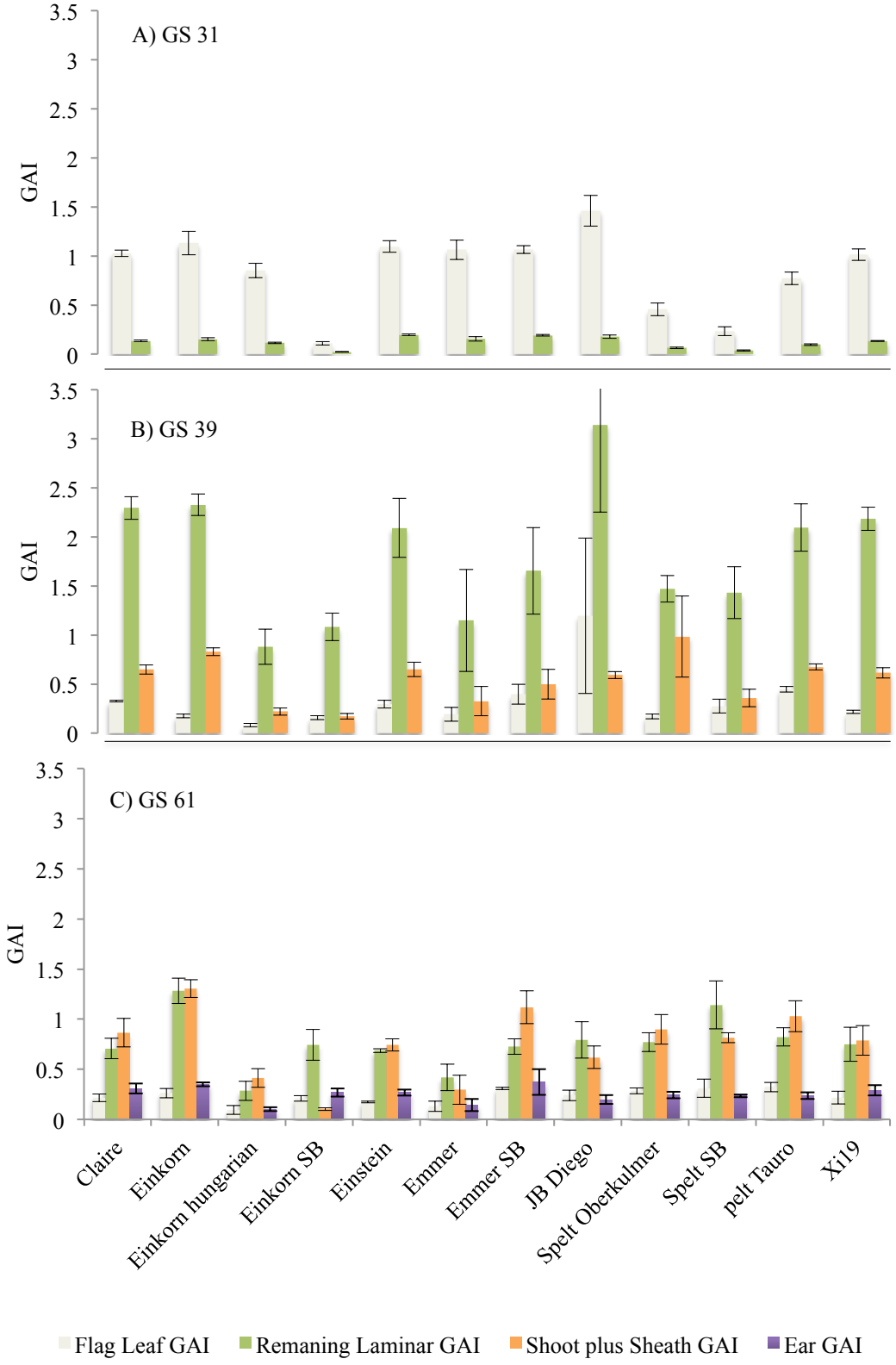


Figure 2.7: Green area index partitioning of twelve wheat cultivars in 2011 at (a) GS 31, (b) GS 39 and c) GS 61 showing flag leaf area index (P = 0.005, 36 DF, SED = 0.1367), green lamina area index (P <0.001, 105 DF, SED = 0.3230), green shoot plus leaf sheath area index (P = <0.001, 105 DF, SED = 0.1534) and ear area index (P <0.001, 72 DF, SED = 0.07470) (error bars represent SEM).

2.3.3 Distribution and capture of solar irradiance

2.3.3.1 Light attenuation

During the 2010 growing season, the proportion of incident radiation intercepted by canopies differed significantly by genotype ($P < 0.001$) (Figure 2.8). All genotypes followed the same trend whereby fractional interception (*F*) increased from 179 DAS to 240 DAS, at which point *F* began to decline. Although einkorn SB also followed this trend, the irradiance fraction intercepted at the start of the season was lower than for other genotypes, however it did increase at a faster rate as the season progressed. This may be a result of canopy expansion occurring later in the season indicating slower development rates. On the final SunScan sampling date however, einkorn SB recorded the largest *F* value, which may have been a result of the onset of lodging. Overall, spelt SB and emmer SB genotypes had increased *F* compared to all other genotypes. Spelt Oberkulmer consistently recorded the lowest *F* throughout the season, potentially a result of the low establishment.

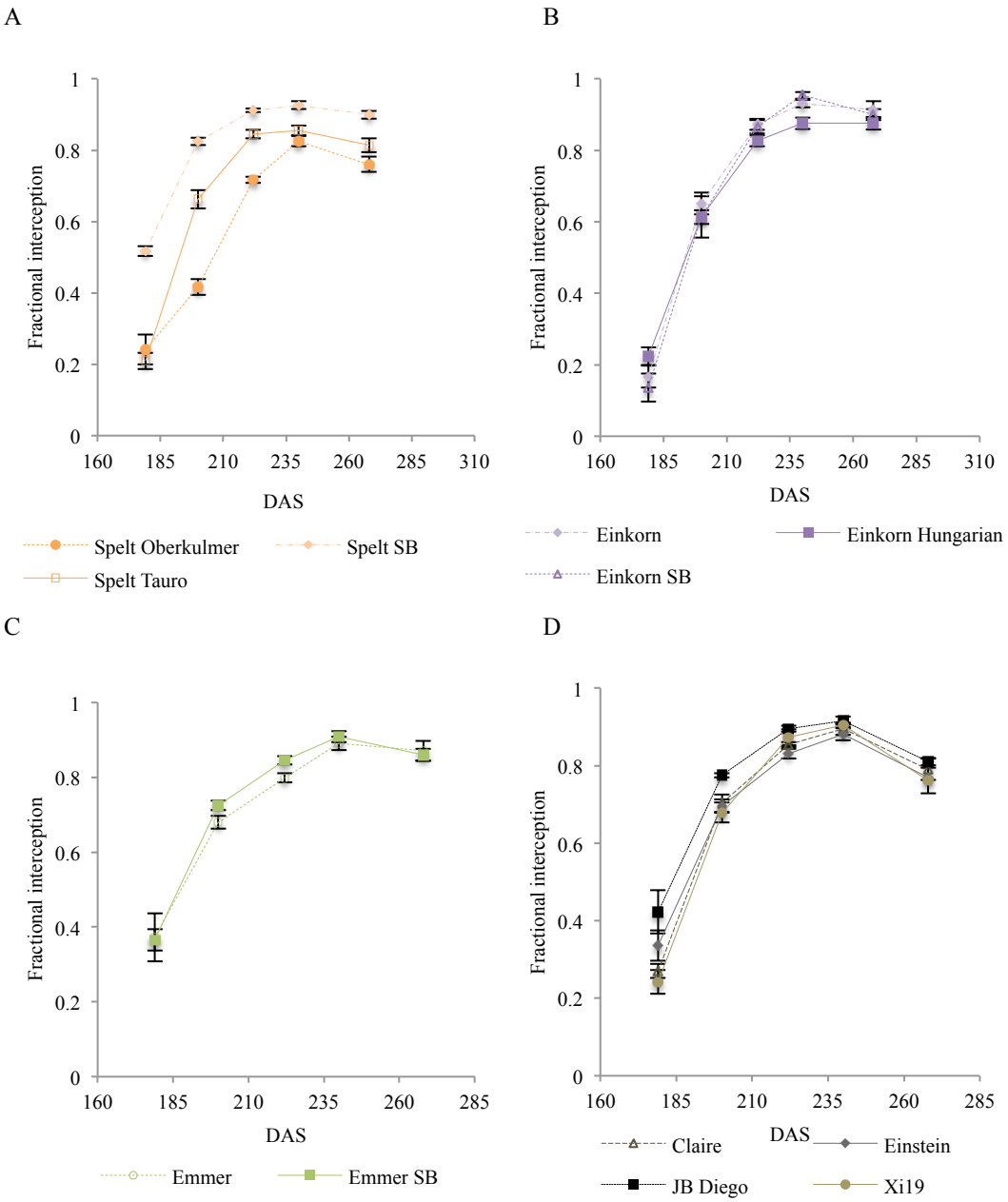


Figure 2.8: Fractional interception of twelve ancient wheat cultivars in 2010, showing A) spelt B) einkorn C) emmer and D) modern bread wheat genotypes (P <0.001, 177 DF, SED = 0.05228) (error bars represent SEM).

Further simplification of the data collates values for *F* by species (Figure 2.9). Differences were found to be significant (P = 0.002) on all sampling dates. Generally, einkorn had low *F* at the start of measurements but had the highest *F* towards the end of the season. MBW showed the fastest decline in fractional interception after 240 DAS.

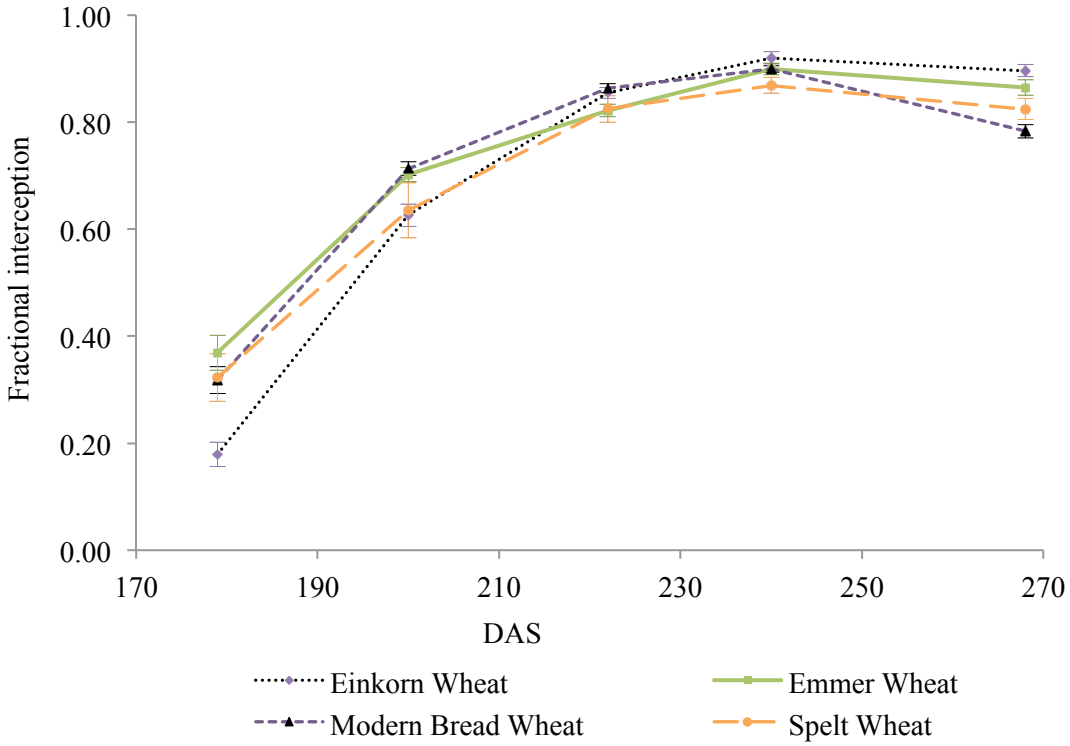


Figure 2.9: Fractional interception of twelve wheat cultivars in 2010 assessed by species (P = 0.002, 217 DF, SED = 0.05085) (error bars show SEM).

SunScan measurements were also collected during the 2011 field experiment. The field trial was maintained conventionally as in 2010. Graphical representation of overall trends in 2011 showed more variable results than the previous year (Figure 2.10). All modern bread wheat maintained a general trend whereby *F* increased (albeit at a slow rate) and then reduced (also at a slow rate) after 251 DAS. In 2011, Claire showed the highest *F* whereas once again, einkorn SB captured the lowest fraction of incident light when compared to other genotypes, as seen in the previous season. At 218 DAS most genotypes were intercepting a large fraction of light (around 0.9) except for einkorn SB and spelt SB, also observed in the last growing season. Although these genotypes did not increase with other genotypes as they had done previously. Later in the season differences between the genotypes were also

statistically significant (P <0.003 at 251 DAS), (P <0.001 at 260 DAS) and (P <0.001 at 272 DAS).

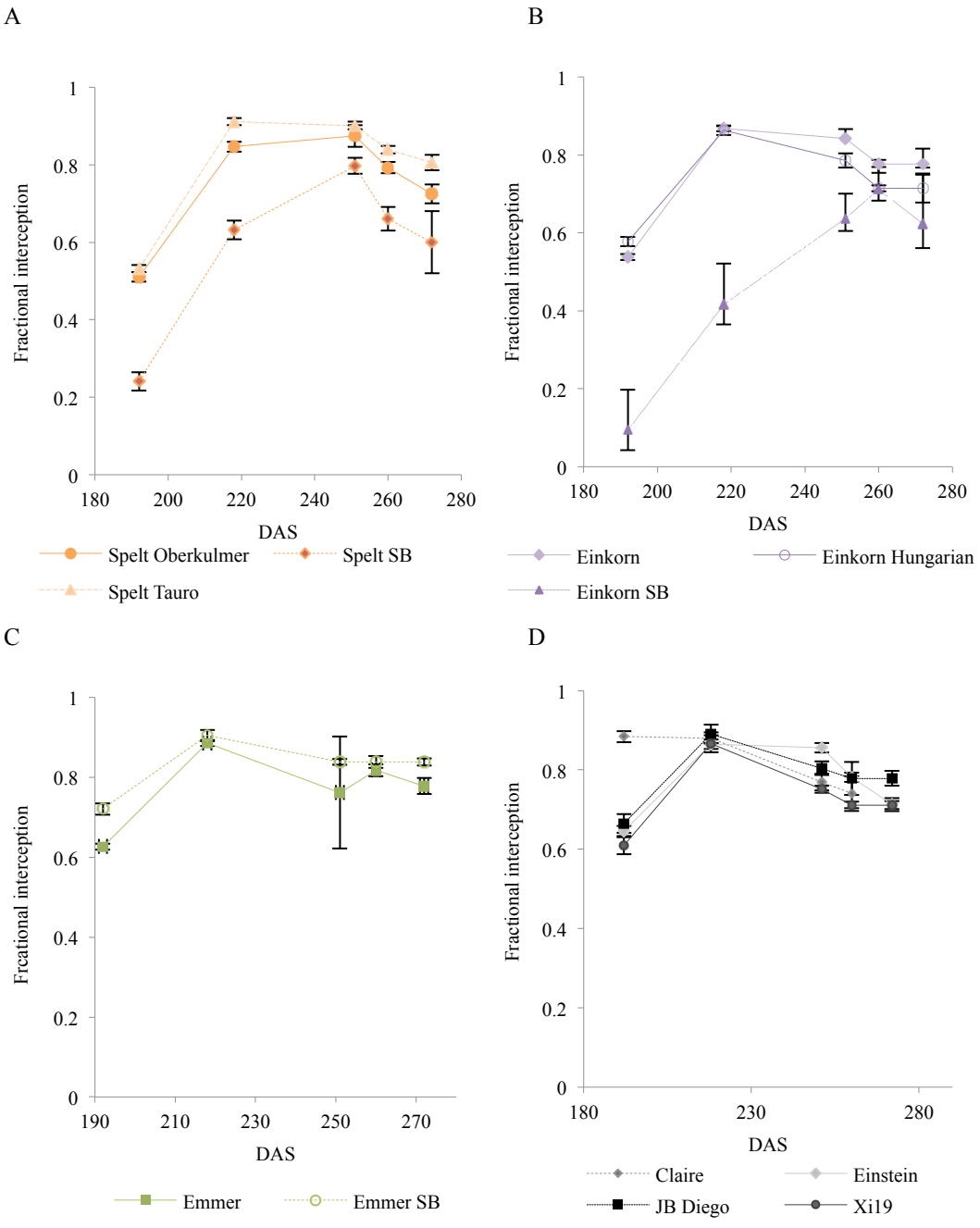


Figure 2.10: Fractional interception of twelve ancient wheat cultivars in 2011 showing A) spelt B) einkorn C) emmer and D) modern bread wheat genotypes (P<0.001, 177 DF, SED = 0.034) (error bars show SEM).

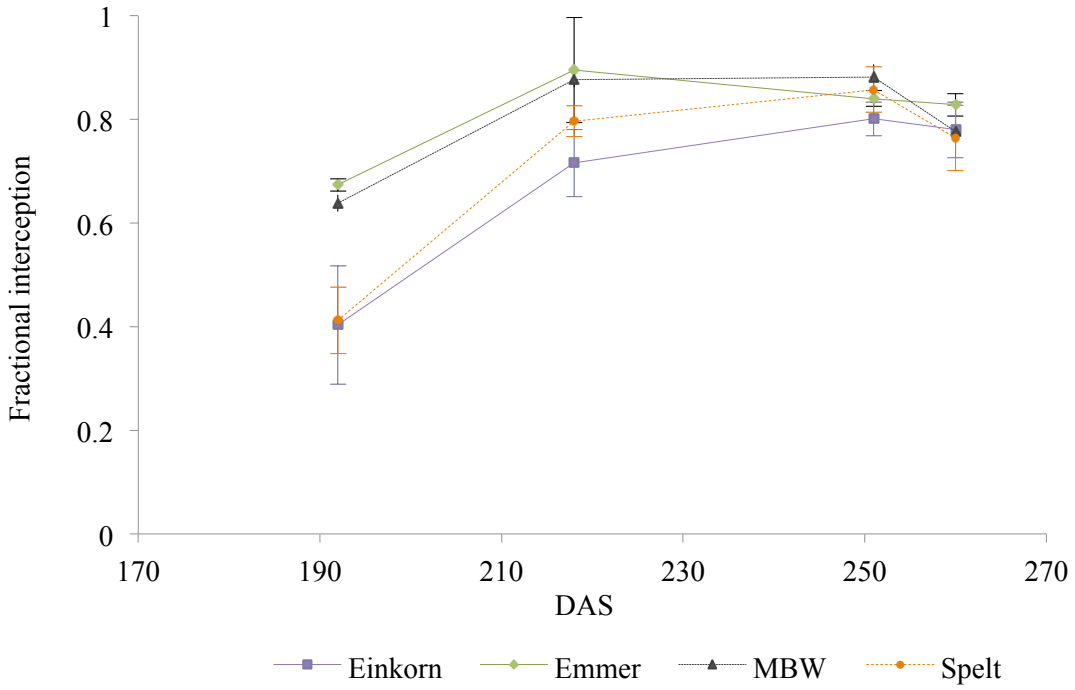


Figure 2.11: Fractional interception of four species of wheat at 218, 251, 260 and 272 DAS (2011) (P <0.001, 217 DF, SED = 0.033) (error bars show SEM).

Fractional interception, collated by species, is shown in Figure 2.11. None of the species displayed the expected trend, as fractional interception values generally remain consistent throughout the sampling period, although there was a slight increase in *F*, followed by a stabilisation phase, and a decline, the differences between these phases were however, marginal. Differences were significant (P <0.001) with emmer having the highest *F* (0.9 and 0.8) and einkorn species (0.7 and 0.7) having the lowest *F* both on 218 and 272 DAS, respectively. As observed in 2010, modern bread wheat had rapid decline of fractional interception however spelt and einkorn did not. Emmer maintained generally consistent fractional interception values throughout the season and maintained the greatest *F* on the final sampling date.

2.3.3.2 Light Extinction through the crop canopy

Regression analyses illustrated significant differences ($P < 0.001$) between the light extinction through the crop canopies among different genotypes. The proportion of light transmitted at differing intervals allowed the light extinction going down the canopy to be ascertained (Figure 2.12). Light transmission for all assessed genotypes were found to fit a logistic curve which described 93% of the variation observed; non-linear regression was used to determine a fitted model for each of the cultivars after which, fitted curves were plotted using the Gaussian equation:

$$A + C\,(1+e^{(-B\,(X-M))}) \qquad \text{Equation 2.4}$$

The equation states X to be the height at which the SunScan probe was inserted into the canopy. Predicted curves were attained using parameter estimates from regression analyses (outlined in Table 2.11).

Table2.11: Estimates of parameters for light distribution fitted curves for four wheat species.

Species	B	M	C	A
Einkorn	0.04960	47.11	1.0060	-0.0140
Emmer	0.04794	52.53	0.9810	-0.0110
MBW	0.06450	36.18	1.0430	-0.0019
Spelt	0.05165	52.87	0.8797	0.0821

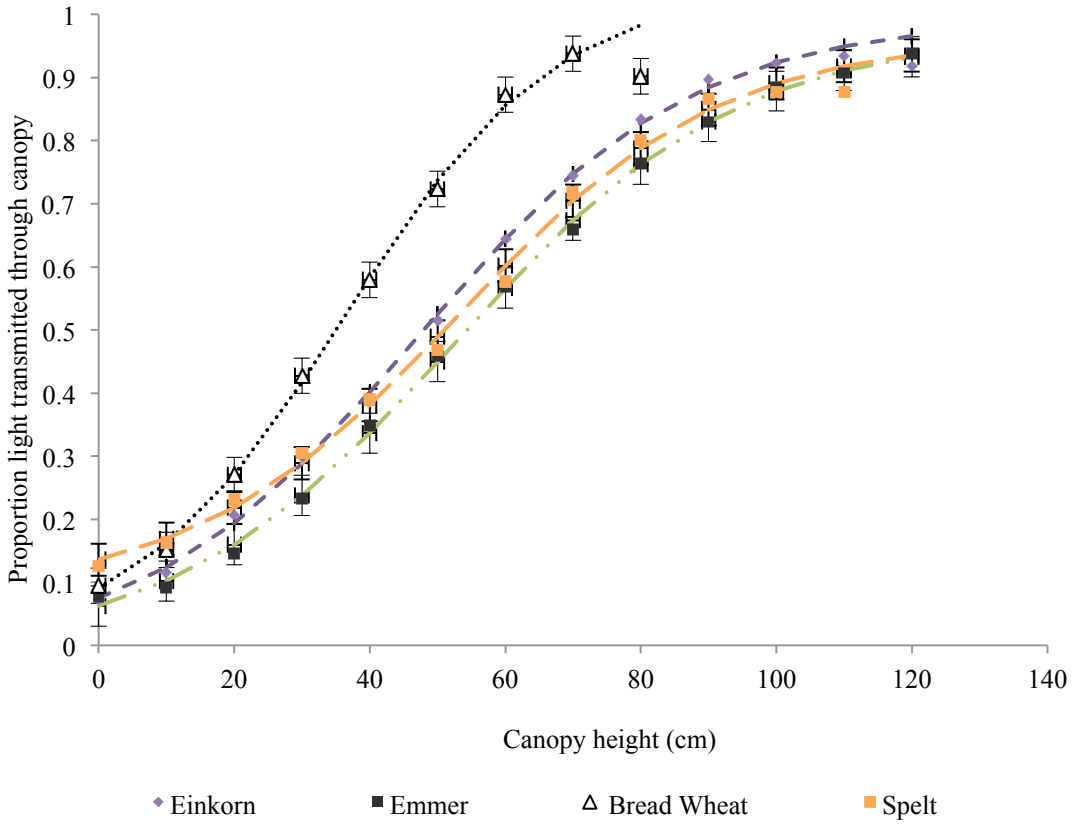


Figure 2.12: Light extinction of four wheat species in 2010 (P <0.001, SED = 0.00315, DF = 15) showing MBW, einkorn, emmer and spelt species averages.

Investigation of this data showed significant differences between genotypes (P <0.001, SED = 0.0803, 47 DF) and also by species (P <0.001) for the light transmission at intervals through the crop canopy. Modern bread wheat had the steepest decline, therefore indicating that the largest proportion of light was intercepted per 10cm leaf layer. Einkorn intercepted greatest proportion of light per unit leaf layer of ancient wheat species, followed by spelt and finally emmer although in graphical representation, ancient species looked similar. The proportion of light transmitted through the crop canopy per unit height (every 10cm) was lower for modern bread wheat species, which reduced the amount of light that was transmitted to lower canopy layers. However, modern bread wheat cultivars were also much shorter therefore interception started at a lower level. Greater interception

of PAR through modern bread wheat canopies compared to ancient species indicated that the extinction of light was more staggered for ancient species, allowing leaves further down the canopy to intercept ambient light. From observational comparisons of the two canopy types in the field, modern bread wheat had a 'denser' canopy structure overall, therefore leaves and ears were more condensed within the area that the canopy occupied, compared to ancient wheat canopies within which, leaves and ears were much more spaced. However, a confounding factor within this data are the relative differences in height between ancient and modern bread wheat species.

2.3.4 Resource assimilation and investment efficiency

2.3.4.1 Carbon assimilation

Growth stage analyses showed that the quantities of dry matter per m^2 increased with each sampling date at least until growth stage 61 (Figure 2.13). Overall, JB Diego produced the most biomass at GS 31 and 39 (308.0g m^{-2} and 765.00g m^{-2}, respectively). Spelt SB and emmer SB produced the largest amount of biomass per m^{-2} at growth stage 61 (1250 and 1264g m^{-2}, respectively). At GS 31, 39 and 61, spelt Oberkulmer produced the least biomass (64.50, 332.00 and 884.0g m^{-2} respectively) potentially a result of the poor emergence observed. After growth stage 61, biomass accumulation plateaued for the majority of genotypes, however all spelt genotypes displayed increased biomass from growth stage 61 to pre-harvest sampling. The effect of genotype was statistically significant ($P < 0.001$), so too was that of growth stage ($P < 0.001$), however the interaction between these factors were not.

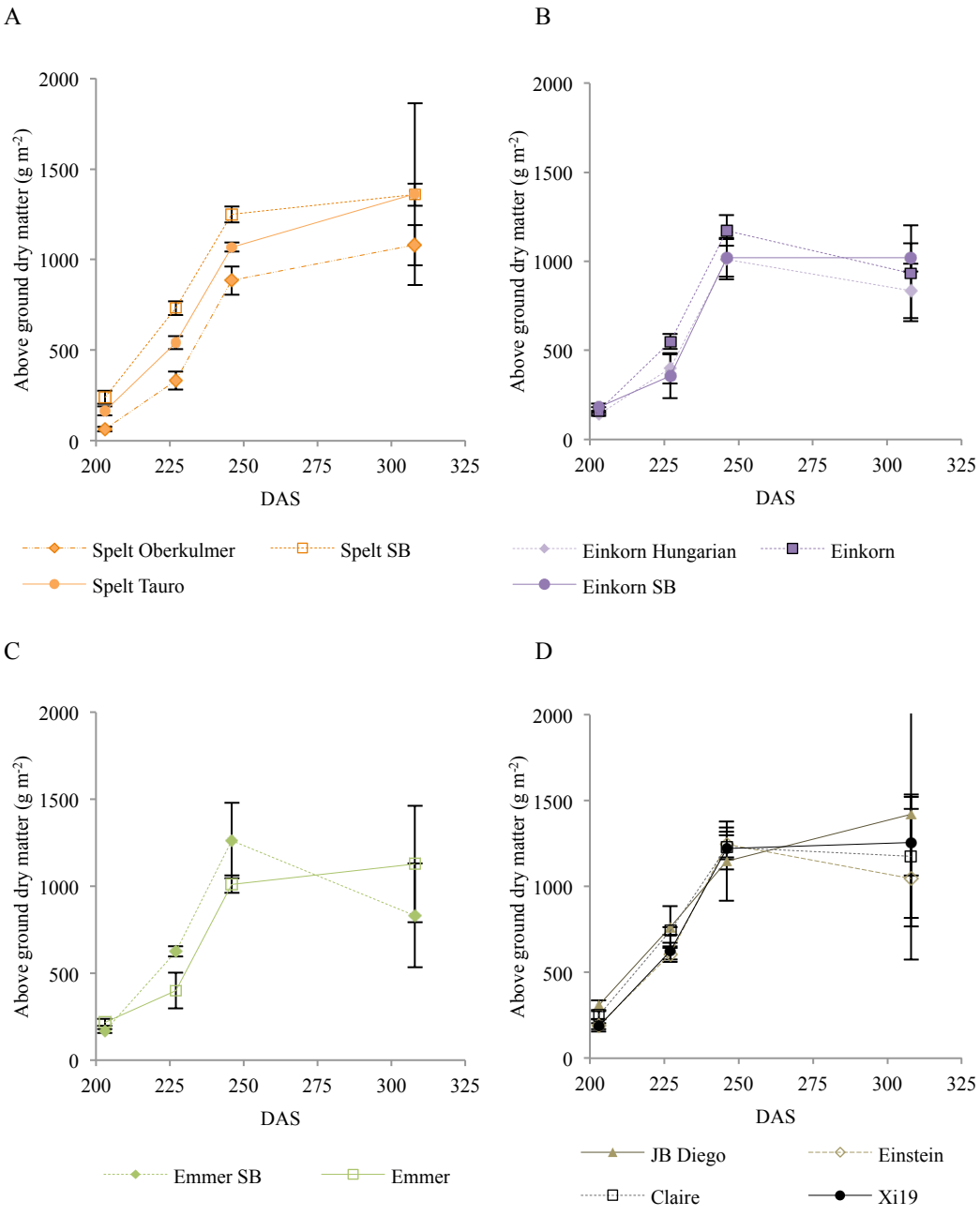


Figure 2.13: Biomass accumulation of twelve wheat genotypes in 2010 (P = 0.401, 141 DF, SED = 150.6) (error bars show genotype SEM).

When analysed by species, bread wheat cultivars produced the most biomass on all sampling dates except for pre-harvest, at which spelt species produced the greatest biomass (1267g m^{-2}) (Figure 2.14). Differences between species and growth stage were significant (P <0.001) however, the combined effects of these factors were not.

Although relationships were not significant, it is noteworthy that spelt species had increased biomass accumulation late in the growing season when compared to other species, which either declined or plateaued beyond growth stage 61.

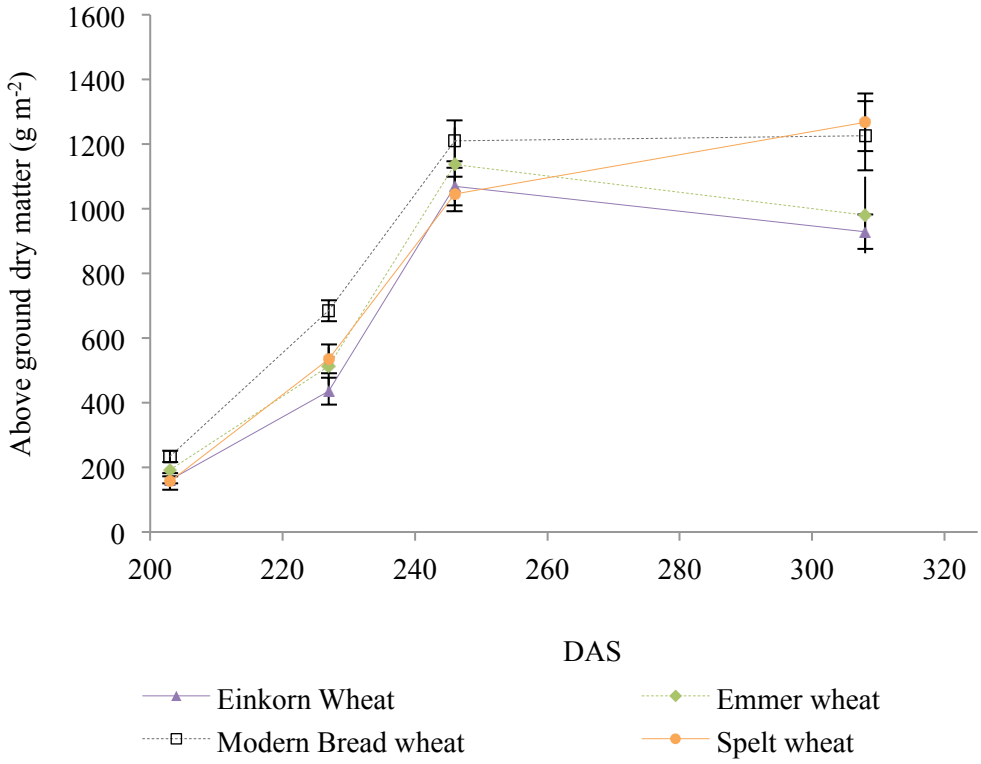


Figure 2.14: Species dry weight accumulated (g/m^2) in 2010 (P = 0.13, 173 DF, SED = 94.9).

In 2011, modern bread wheat cultivars produced the most biomass at GS 31 (ranging from 127.04 to 182.22g m^{-2}) (Figure 2.15). Differences were observed across growth stages and genotypes (P <0.001). Modern bread wheat and spelt genotypes tended to show similar patterns of biomass accumulation (as was the case in 2010); however, more variation was observed within einkorn and emmer genotypes, potentially a result of the highly variable emergence rates observed. Spelt genotypes produced the greatest amounts of biomass after modern bread wheat across the season. Spelt

genotypes were also observed to have the lowest emergence rates recorded for genotypes in 2011.

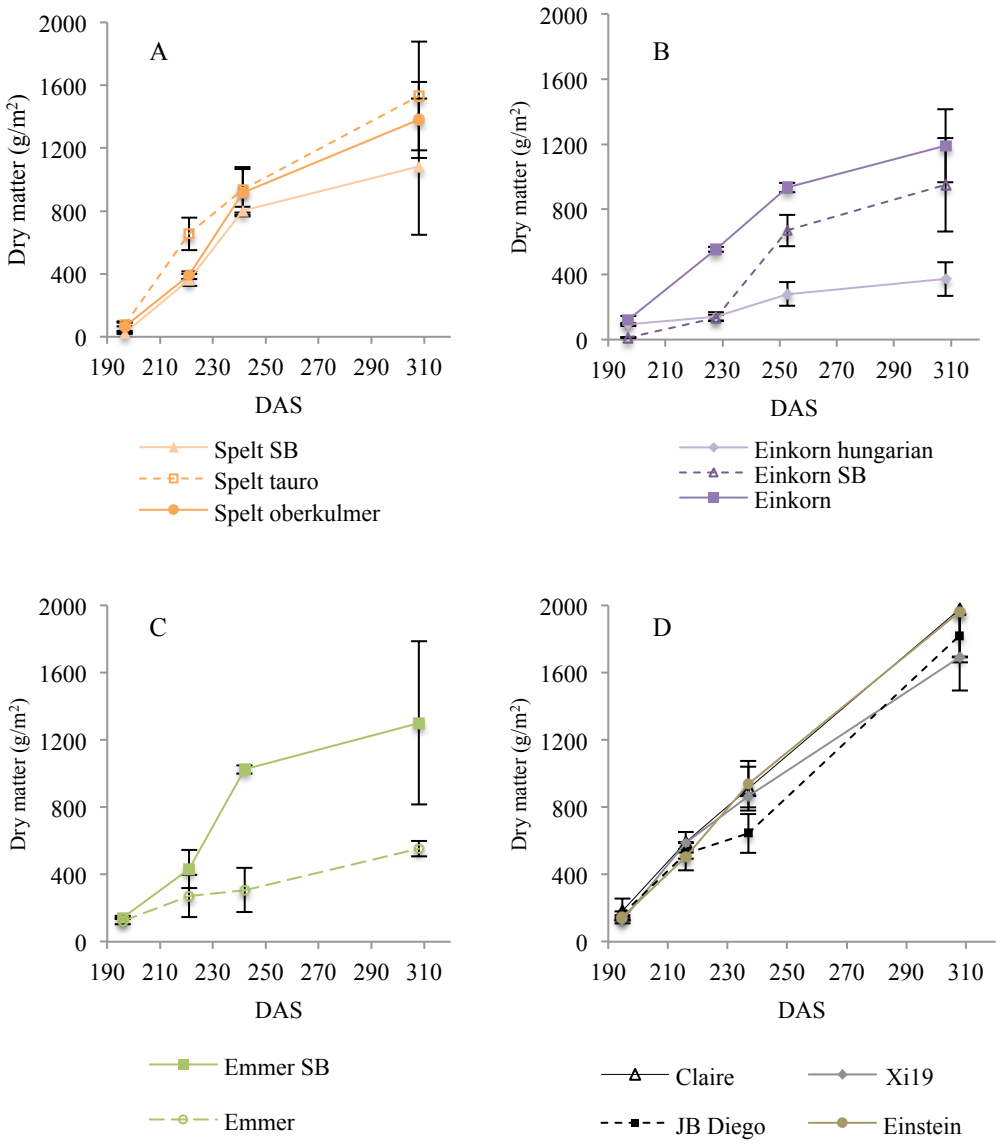


Figure 2.15: Total biomass accumulated for A) spelt, B) einkorn, C) emmer and D) modern bread wheat cultivars in 2011 (including SEM by genotype) (P <0.001, 141 DF, SED = 224.7).

Modern bread wheat accumulated the greatest amount of above ground biomass compared to all other species on all sampling dates except at 242 DAS where spelt species accumulated an average of 884.26g m^{-2} (compared to 839.74g m^{-2} for modern bread wheat varieties) (Figure 2.16). Differences were significantly different by growth stage ($P < 0.001$). Overall, einkorn species produced the least biomass at growth stages 39, 61 and pre-harvest.

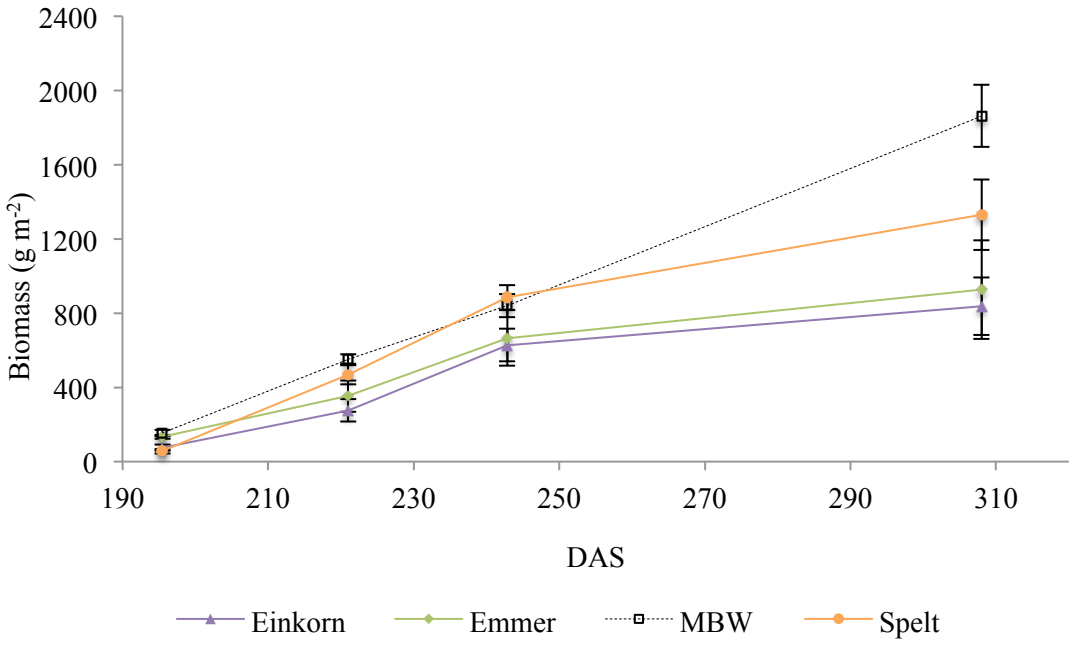


Figure 2.16: Species average for biomass accumulated throughout the 2011 winter wheat growing season (error bars indicate SEM by species) ($P < 0.001$, DF 173, SED = 148.5).

2.3.4.2 Assimilate partitioning

Assessment of the partitioning of biomass in 2010 showed that most genotypes directed assimilates toward shoot plus sheath at growth stages 31 and 39 (Figure 2.17). The quantities of biomass directed towards green lamina were significantly variable by genotype ($P < 0.001$), with JB Diego producing the most at all growth stages (107.8) and spelt Oberkulmer directing the least (47.5g m^{-2}) to green lamina. Biomass directed towards shoot plus sheath was highly significant ($P < 0.004$) for genotypes throughout the key growth stages where spelt SB directed the greatest quantity of biomass m^{-2} towards shoot plus sheath (382.0 g m^{-2} overall), and spelt Oberkulmer, the least (205.9g m^{-2}). At growth stage 61, a greater quantity of biomass was directed towards the ear for all genotypes where significant differences were observed ($P < 0.001$). Claire and JB Diego (231.8 and 239 g m^{-2}, respectively), both modern bread wheat cultivars, produced the greatest ear biomass compared to ancient wheat genotypes spelt Oberkulmer and einkorn SB which produced the least (72.1 and 80.9 g m^{-2}, respectively).

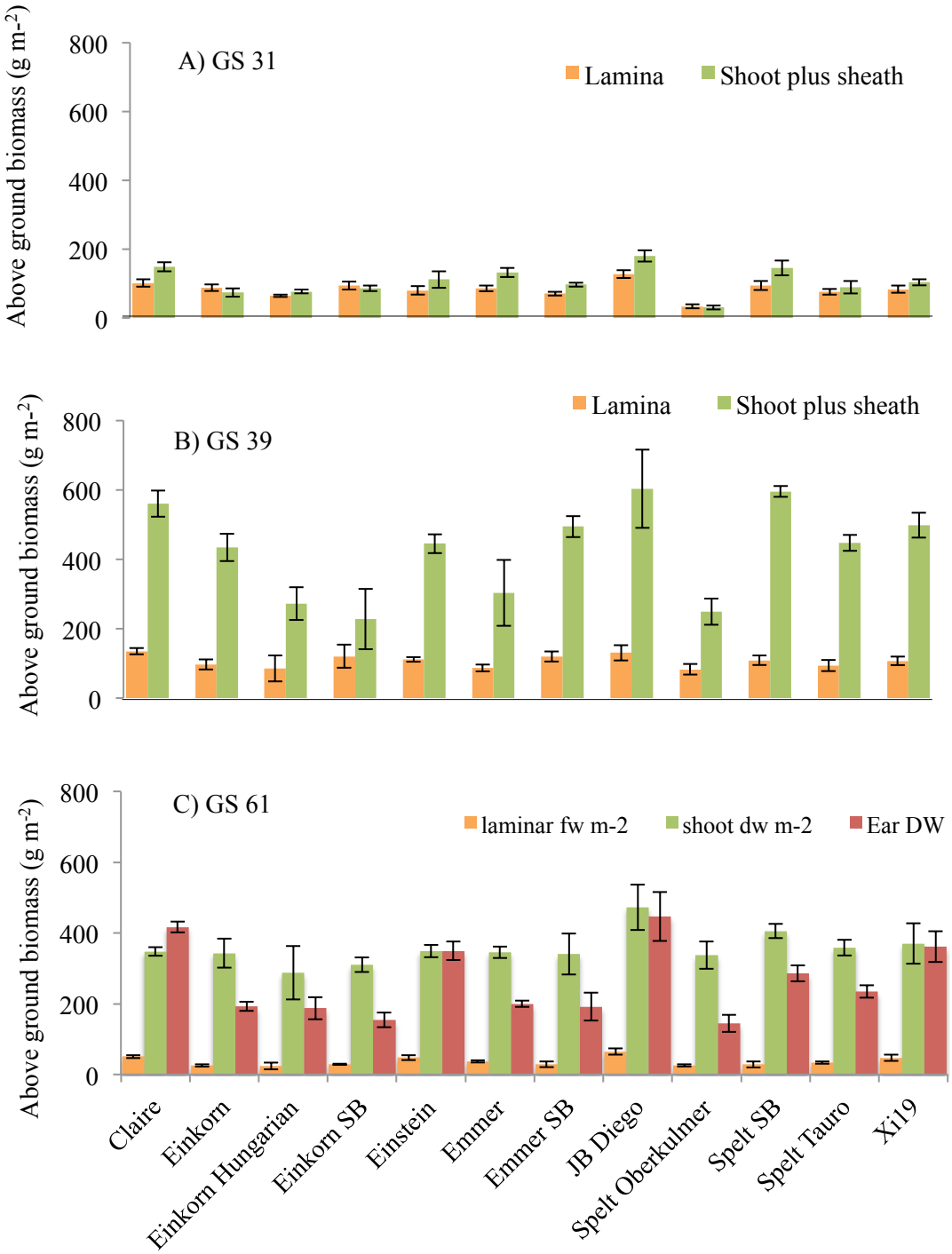


Figure 2.17: Genotypic differences in biomass partitioning in 2010 for A) GS31 (P=0.759, 105 DF, SED = 17.82) B) GS 39 (P=0.004, 105 DF, SED = 59.94) and C) GS 61 (P<0.001, 105 DF, SED = 35.87) (error bars show SEM).

Biomass partitioning was also assessed by species (data not shown). Differences between species and growth stage for lamina and shoot plus sheath biomass were significant ($P < 0.001$), however the interactions were not. There were significant differences between ear biomass produced ($P < 0.001$). Modern bread wheat cultivars produced the most ear biomass (393.7g m^{-2}) followed by spelt (221.4g m^{-2}), emmer (195.7g m^{-2}) and einkorn species (178.3g m^{-2}).

In 2011, assimilate partitioning showed that early in the season, at growth stage 31, most genotypes except for Claire and einkorn, partitioned roughly equal amounts of assimilates towards green lamina and shoot and sheath (Figure 2.18). Differences for lamina biomass assimilated between genotypes and growth stages were highly significant ($P < 0.001$). Overall, spelt tauro produced the greatest lamina biomass (132.97) compared to einkorn hungarian which produced the least (44.01). Results also showed that there were significant differences between the genotypes and growth stages for biomass directed towards shoot plus sheath ($P < 0.001$). In contrast to 2010, where ancient species were observed to partition more biomass towards shoots compared to the significantly shorter modern bread wheat cultivars, at growth stages 39 and 61 modern bread wheat species partitioned more biomass towards shoots and sheath. Also analysed was the amount of biomass directed towards the ear. Differences were signifcantly different ($P < 0.001$); Claire, Xi19 and Einstein paritioned the most biomass toawards the ear compared to emmer and einkorn hungarian which partitioned the least.

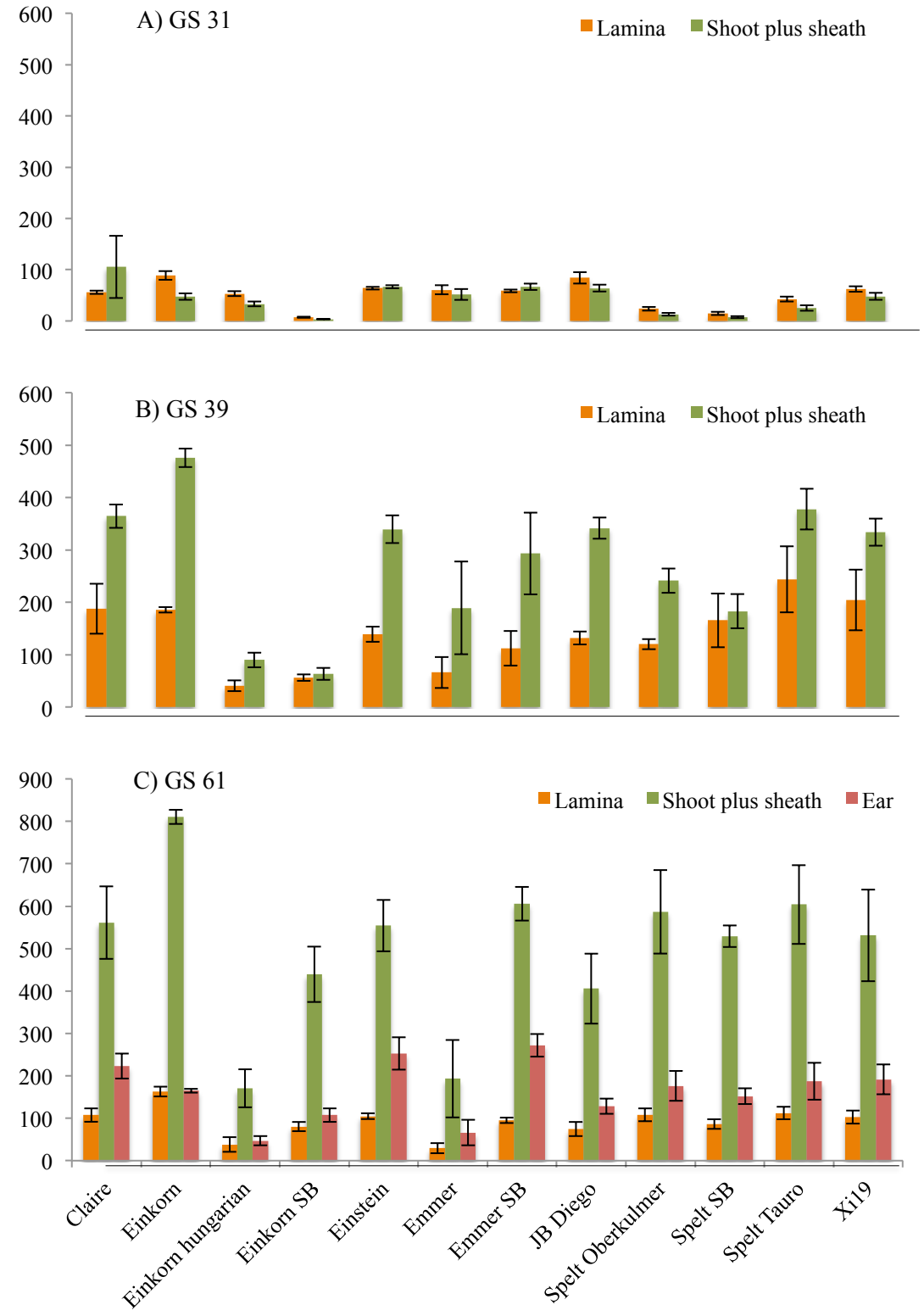


Figure 2.18: Genotypic differences for biomass partitioned at A) GS 31 B) GS 39 and GS) 61 towards green laminar (P <0.001, 105 DF, SED = 30.23), shoot plus sheath (P <0.001, 105 DF, SED = 69.14) and ear in 2011 (P <0.001, 33 DF, SED = 38.45) (error bars show SEM).

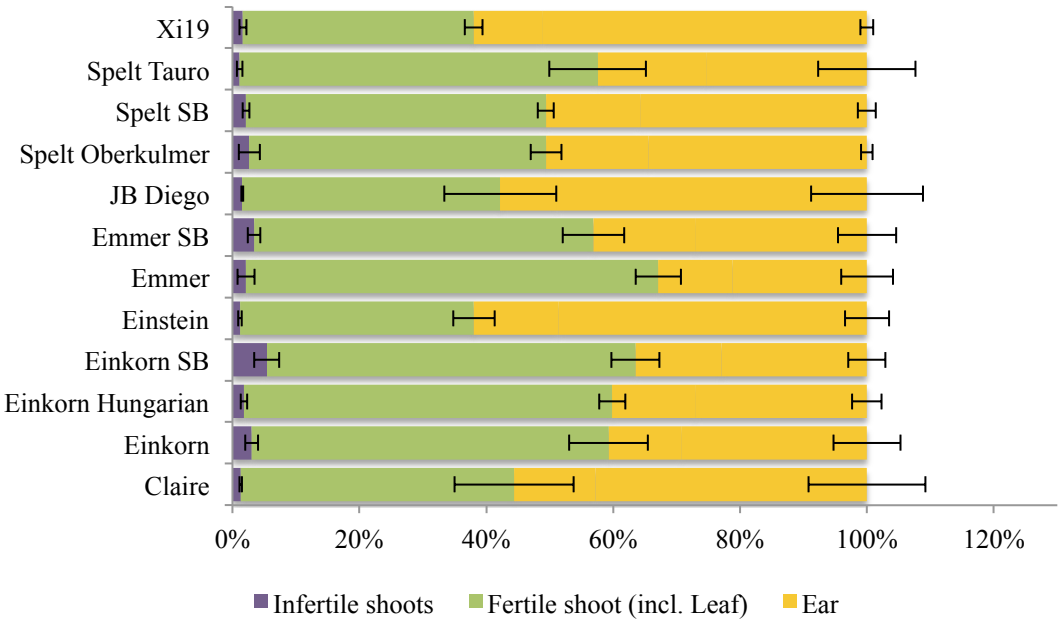
In 2011, when assessed by species (data not shown), there were significant differences between the amounts of biomass directed to lamina and ear ($P < 0.001$) but not for shoot plus sheath. Rather unsurprisingly, MBW produced the greatest lamina biomass at growth stage 31 and 39 however at growth stage 61 spelt had the greatest amount of lamina biomass, potentially indicating that where the lamina of other species was senescing, spelt lamina was being maintained for a longer period. Unsurprisingly, modern bread wheat cultivars on average produced the most ear biomass followed by spelt, emmer and finally einkorn species.

2.3.4.3 Pre-harvest biomass partitioning

In 2010 infertile shoots, ear and straw were separated and assessed according to dry weight. All modern bread wheat cultivars partitioned a larger proportion of assimilates towards the ear compared to the ancient wheat species. Spelt SB and Oberkulmer also directed a larger proportion of total biomass towards the ear (Figure 2.19, A). Differences for biomass partitioned towards the ear were highly significant ($P < 0.001$). Generally emmer and einkorn SB partitioned a larger proportion of assimilates toward shoots and lamina (fertile shoots) ($P < 0.001$). The differences in biomass directed towards infertile shoots however were insignificant.

In 2011, a similar pattern was observed in the partitioning of biomass (Figure 2.19, B). As in 2010, Einstein, Claire, JB Diego and Xi19 partitioned the highest proportion of biomass towards the ear followed by spelt Oberkulmer and SB, as was also the case in 2010 ($P < 0.001$). Differences between leaf, shoot and infertile shoot biomass weight per m^{-2} were also significant ($P < 0.001$, 0.002 and < 0.001, respectively).

A



B

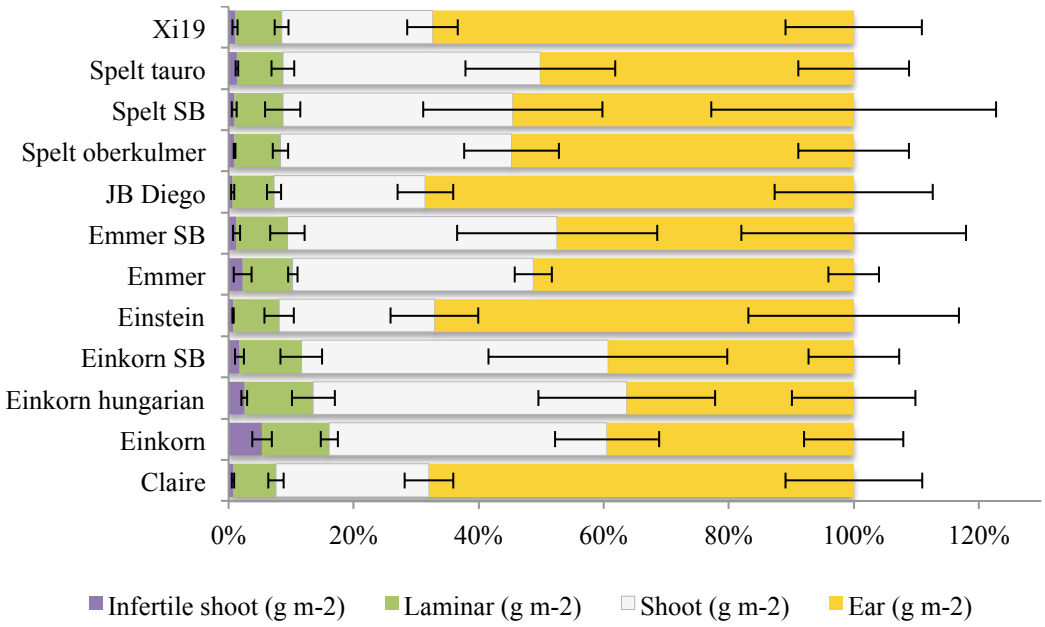


Figure 2.19: Biomass partitioning, pre-harvest A) in 2010 showing infertile shoots (P = 0.16, SED = 1.39) fertile shoots (P <0.001, SED = 5.65) and ear (P <0.001, SED = 5.69). B) Pre-harvest biomass partitioning in 2011 where infertile shoots (P <0.001, SED = 9.57), leaf material (P <0.001, SED = 19.61), shoot material (P = 0.002, SED = 95.7) and ear material (P <0.001, SED = 150.1) were separated, all of which had 33 DF (error bars show SEM).

When analysed by species, modern bread wheat cultivars partitioned a larger proportion of assimilates overall, towards the ear (P <0.001) whereas ancient wheat species, particularly einkorn, were observed to invest more assimilates in fertile shoots as leaf and shoot material (Figure 2.20, A). This trend was observed in 2011 also, indicating that modern bread wheat generally partitioned more assimilate towards the ear (P <0.001) whereas ancient genotypes directed the large proportion to shoots (although insignificant) and leaves (P = 0.002) (Figure 2.20, B).

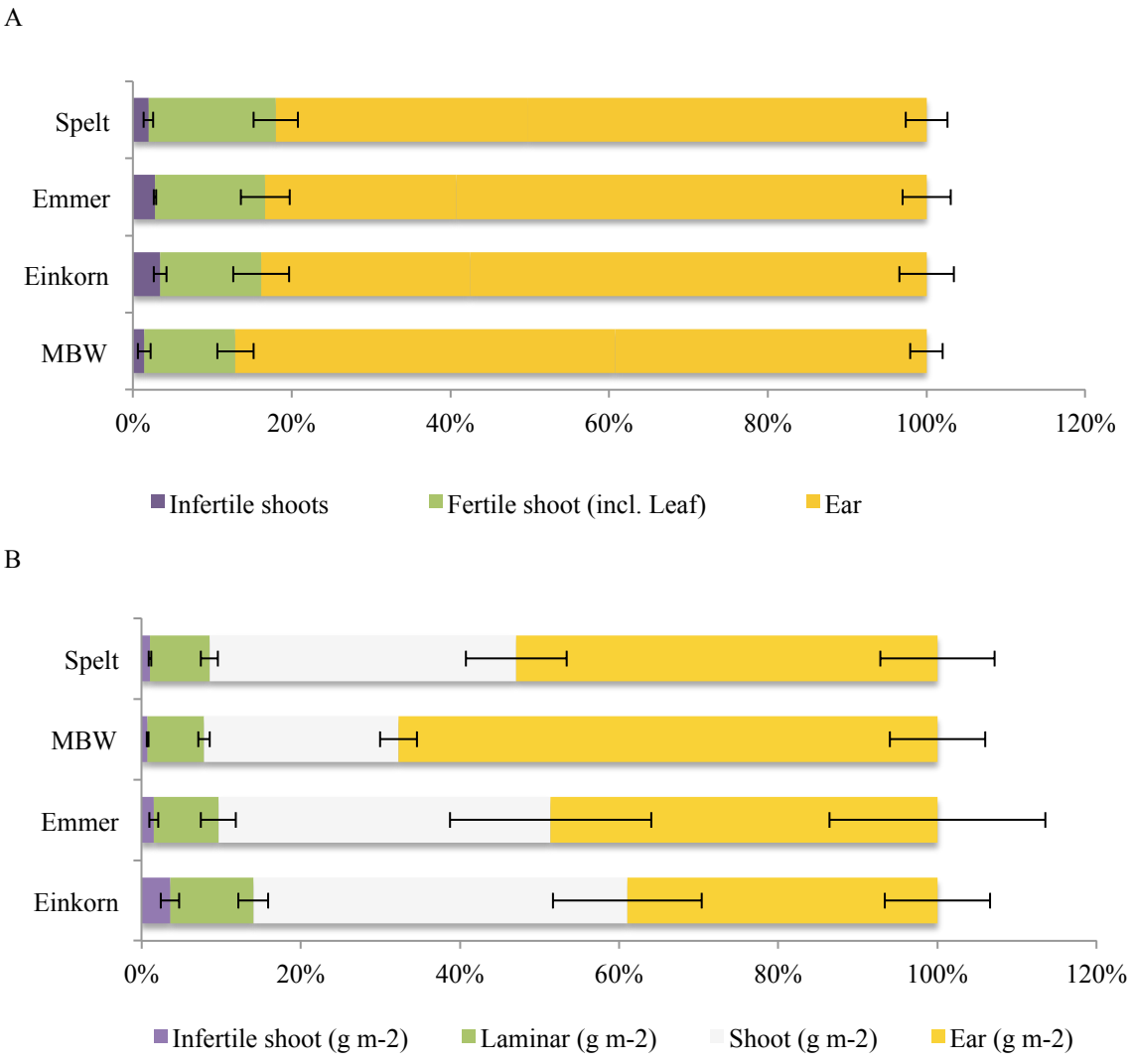


Figure 2.20: Pre-Harvest component analysis of assimilates partitioned toward A) infertile shoots (P = 0.06, SED = 0.86) ears (P <0.001, SED = 3.50) and fertile shoots (including leaf and straw) (P <0.001, SED = 3.54) in 2010. B) Pre-harvest partitioning of species towards infertile shoots (P = 0.1, SED= 7.81), lamina (P = 0.002,SED =15.3), shoots (P = 0.297, SED = 75.3) and ear (P <0.001, SED = 98.6) all of which had 41 DF.

2.3.4.4 Conversion efficiency of solar radiation

As previously discussed, radiation is crucial for the production of biomass. The ratio between the amount of radiation intercepted and the chemical energy actually converted into biomass provides an overall radiation use efficiency. This was performed using fraction of incident light intercepted estimated for a set time period and biomass production for the same period ($\delta W/\delta t$). This can be expressed as:

$$\frac{\delta W}{\delta t} = \varepsilon_s f I_0 \qquad \text{Equation 2.5}$$

where fI_0 (MJ m^{-2}) is the amount of light intercepted by the crop (the product of the fractional interception (F), and the daily total incident radiation I_0) and ε_s (g MJ^{-1}) is the efficiency which the crop uses light to produce dry matter (Azam-Ali and Squire, 2004).

RUE was calculated both pre-anthesis and post-anthesis. Surprisingly, einkorn and einkorn SB showed the greatest RUE of all genotypes followed by Claire, Einstein and Xi19 (Table 2.12). Spelt Oberkulmer had the lowest pre-anthesis RUE (1.19g MJ^{-1}) followed by JB Diego (1.20g MJ^{-1}). Other modern bread wheat cultivars investigated had RUE ranging from 1.49 to 1.43g MJ^{-1} among the highest recorded, except for einkorn (1.61g MJ^{-1}).

Table 2.12: Ear biomass, ear index, pre-anthesis radiation use efficiency and post-anthesis radiation use efficiency (PAR) for twelve wheat genotypes. Field experiment, 2010.

Genotype	Ear biomass (g/m^2)	Ear Index	ε_{PAR} (pre-anthesis) ($g\ MJ^{-1}$)	ε_{PAR} (post-anthesis) ($g\ MJ^{-1}$)
Claire	703.5	0.56	1.49	1.00
Einkorn	360.7	0.41	1.61	1.09
Einkorn Hungarian	331.1	0.40	1.30	1.28
Einkorn SB	374.0	0.36	1.63	1.00
Einstein	672.3	0.62	1.43	1.12
Emmer	387.6	0.33	1.22	1.00
Emmer SB	376.4	0.43	1.38	1.00
JB Diego	873.6	0.58	1.20	1.36
Spelt Oberkulmer	547.0	0.51	1.19	0.73
Spelt SB	689.2	0.51	1.21	0.73
Spelt Tauro	631.4	0.42	1.41	0.85
Xi19	779.7	0.62	1.49	0.94
P	0.006	<0.001	0.147	0.013
SED (33 DF)	152.6	0.06	0.19	0.15

Overall RUE values were lower than expected and by calculating species averages, RUE did not differ significantly pre-anthesis (Table 2.13). Differences did however differ significantly post-anthesis (P = 0.012) ranging from 0.84 (spelt) to 1.12 (for einkorn). Overall, einkorn and modern bread wheat displayed the highest RUE.

Table 2.13: Ear biomass, ear index, pre-anthesis RUE and post-anthesis RUE species averages (RUE calculated from intercepted PAR). Field experiment 2010.

Genotype	Ear Biomass (g/m^2)	Ear Index	ε_{PAR} (pre-anthesis) ($g\ MJ^{-1}$)	ε_{PAR} (post-anthesis) ($g\ MJ^{-1}$)
Einkorn	355.3	0.39	1.39	1.12
Emmer	382.0	0.38	1.42	1.06
MBW	757.3	0.59	1.46	1.10
Spelt	622.5	0.48	1.23	0.84
P	<0.001	<0.001	0.215	0.012
SED (41 DF)	87.6	0.04	0.12	0.10

In 2011, ear index was highest for einkorn Hungarian and Xi19 and lowest in Spelt tauro, although differences here were not significant (Table 2.14). Pre-anthesis radiation use efficiency varied significantly ranging from 0.20g MJ $^{-1}$ recorded for emmer to 1.78g MJ^{-1} (einkorn SB). Most modern bread wheat cultivars had among the highest RUEs recorded, except for JB Diego (1.04g MJ^{-1}). Consistent with 2010, einkorn and einkorn SB showed comparatively high RUE and high ear indices. All spelt cultivars had high RUE pre-anthesis (1.55, 1.76 and 1.72g MJ^{-1} for Spelt Oberkulmer, SB and tauro, respectively). Radiation use efficiency for all genotypes reduced from pre to post anthesis, except for emmer and JB Diego. Interestingly however, all spelt genotypes maintain relatively high RUE even post-anthesis, this was also true of modern bread wheat Claire, Xi19 and Einstein highlighting a potential to utilise radiation intercepted after anthesis when irradiance levels are likely to be highest in the UK winter wheat growing season.

Table 2.14: Ear biomass, ear index, post and pre-anthesis radiation use efficiency (intercepted PAR) for twelve modern and ancient wheat cultivars from the field experiment carried out in 2011.

Genotype	Ear biomass (g/m^2)	Ear Index	ε_{PAR} (pre-anthesis) (g MJ^{-1})	ε_{PAR} (post-anthesis) (g MJ^{-1})
Claire	634.1	0.52	1.45	1.42
Einkorn	519.2	0.54	1.57	1.26
Einkorn hungarian	752.7	0.57	0.41	0.39
Einkorn SB	767.7	0.56	1.78	1.44
Einstein	601.5	0.56	1.54	1.48
Emmer	373.5	0.52	0.20	0.22
Emmer SB	1123.9	0.54	1.55	1.23
JB Diego	1259.2	0.52	1.04	1.13
Spelt Oberkulmer	1253.7	0.52	1.55	1.31
Spelt SB	438.6	0.49	1.76	1.42
Spelt Tauro	617.5	0.51	1.72	1.46
Xi19	697.0	0.57	1.48	1.37
P	0.298	0.999	<0.002	<0.001
SED (33 DF)	354.3	0.10	0.28	0.18

Species averages showed Spelt genotypes overall to have the highest pre-anthesis RUE and Emmer to have the least (P = 0.033) (Table 2.15). Species maintained the same ranking post-anthesis although overall, modern bread wheat generally declined in terms of RUE by a much lower degree than other genotypes.

Table 2.15: Species averages for ear biomass, ear index, post and pre-anthesis radiation use efficiency (calculated from intercepted PAR) from the field experiment carried out in 2011.

Genotype	Ear Biomass (g/m^2)	Ear Index	ε_{PAR} (pre-anthesis) ($g\ MJ^{-1}$)	ε_{PAR} (post-anthesis) ($g\ MJ^{-1}$)
Einkorn	679.8	0.56	1.26	1.01
Emmer	748.7	0.53	0.87	0.73
MBW	798.0	0.54	1.38	1.35
Spelt	769.5	0.51	1.68	1.40
P	0.952	0.762	0.033	0.003
SED (41 DF)	236.1	0.05	0.25	0.18

2.3.5 Canopy persistence and stay green

2.3.5.1 Canopy duration (2010 SPAD measurements)

In 2010, flag leaf persistence was assessed using SPAD measurements over time. Significant differences were observed among cultivars 255 DAS (P <0.001) (Figure 2.21). After the initial screening of flag leaf chlorophyll concentration however, SPAD values reduced rapidly, particularly in modern bread wheat. Spelt Oberkulmer had the highest SPAD readings (30.55) (P <0.001). Differences on subsequent sampling dates (270 and 277 DAS) were also statistically significant (P <0.001). At the close of measurements, spelt Oberkulmer and spelt Tauro had the highest SPAD readings (10.22-16.07) compared to all other genotypes.

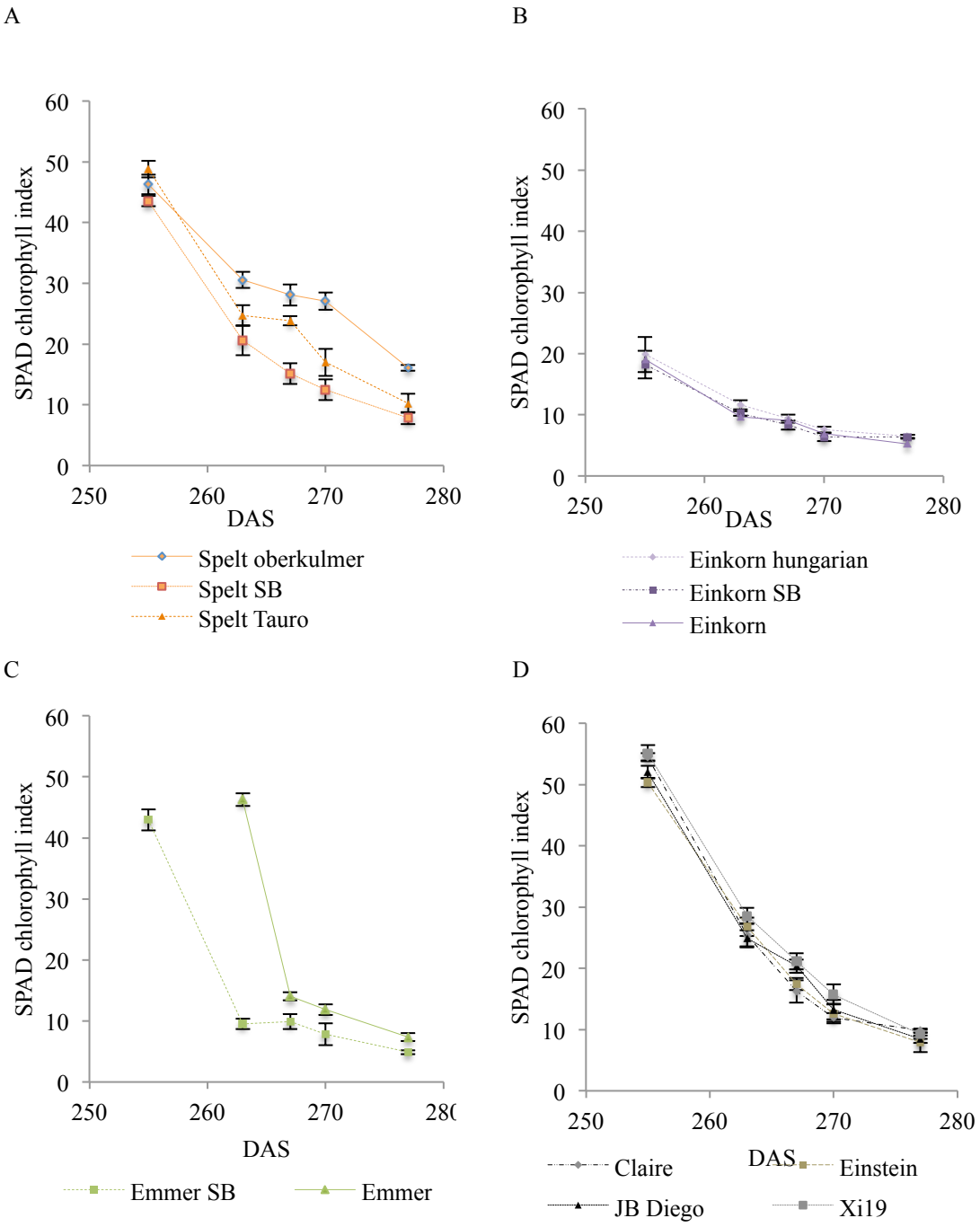


Figure 2.21: SPAD values versus time for A) spelt B) einkorn C) emmer and D) MBW cultivars in 2010 (P <0.001, 177 DF, SED = 1.777) (error bars denote SEM).

SPAD values by species (Figure 2.22) showed significant differences between species and sampling dates (P <0.001) where modern bread wheat had increased chlorophyll content within the flag leaf compared to ancient species, however this declined beyond that for spelt species on the final three sampling dates.

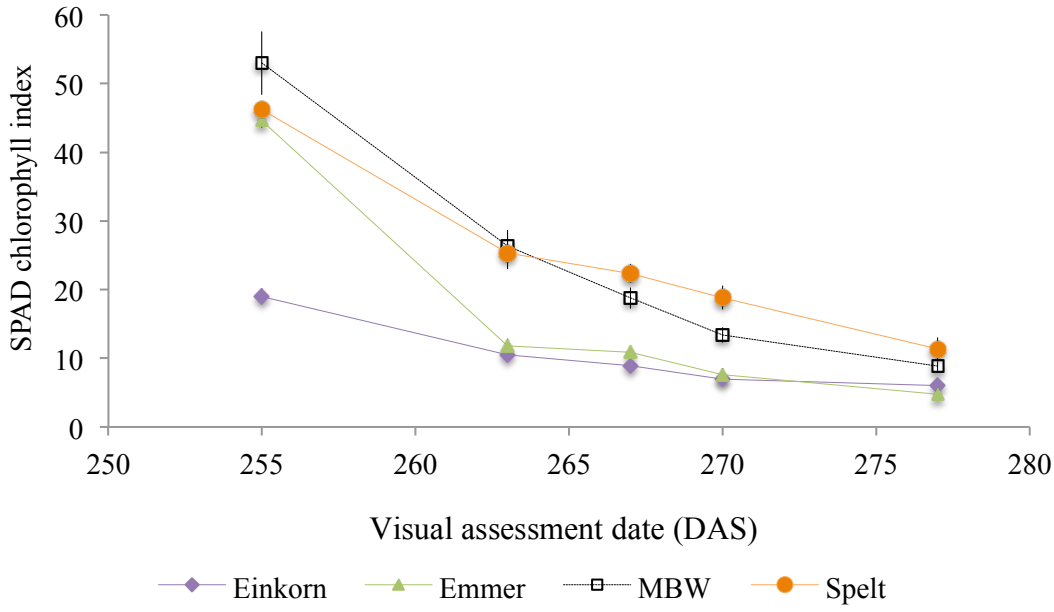


Figure 2.22: Average species SPAD values versus time (2010) (P <0.001, 217 DF, SED = 1.500) (error bars denote SEM) (beginning of DAS axis denotes the onset of anthesis).

2.3.5.2 Stay green (visual scoring in 2010)

All cultivars showed consistent decline of flag leaf 'greenness' over time, which was measured as per section 2.2.11. Analysis of visual scores between cultivars showed that there were significant differences (P <0.001) on all sampling dates (Figure 2.23). Spelt Oberkulmer and Tauro performed particularly well, showing the slowest decline in leaf greenness throughout the sampling period. Spelt Oberkulmer had the lowest overall score (across all sampling dates) of 3.78 when compared to other genotypes. Einkorn and einkorn Hungarian however had comparatively high visual scores on all dates, indicating that these genotypes had senesced to a large degree, even before the onset of sampling. The variation between ancient wheat cultivars was observed to be higher than that of modern bread wheat cultivars.

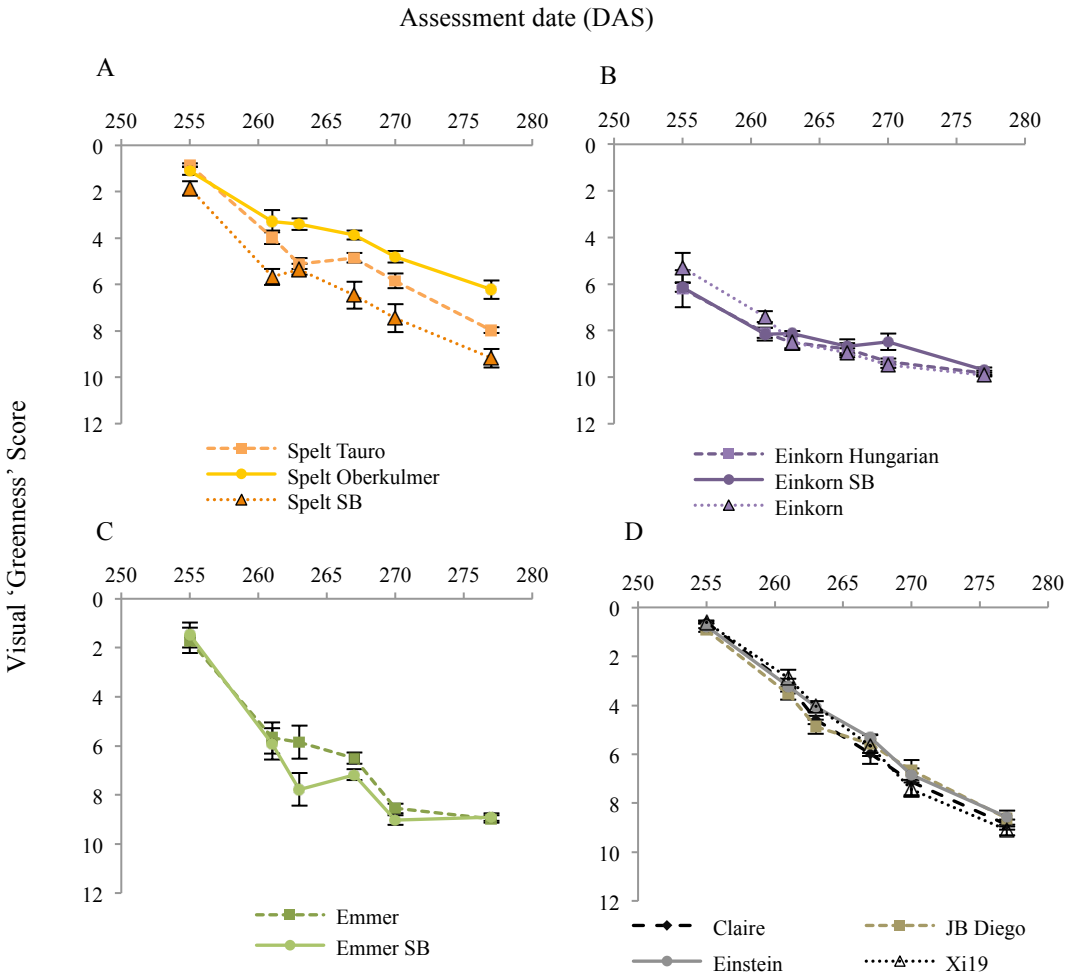


Figure 2.23: Visual scores versus time (DAS) for A) spelt B) einkorn C) emmer and D) MBW cultivars in 2010 (P <0.001, 213 DF, SED = 0.4695) (error bars denote SEM). The scores indicate degree of senescence, therefore the greater the visual 'greenness' score, the higher the proportion of the flag leaf that had senesced.

Differences were also highly significant between species and sampling date (P <0.001) (Figure 2.24). Modern bread wheat initially had low recordings, indicating a high proportion of greenness in the flag leaf however this declined with time more rapidly when compared to other species. Overall, spelt had prolonged flag leaf 'greenness' when compared to other species.

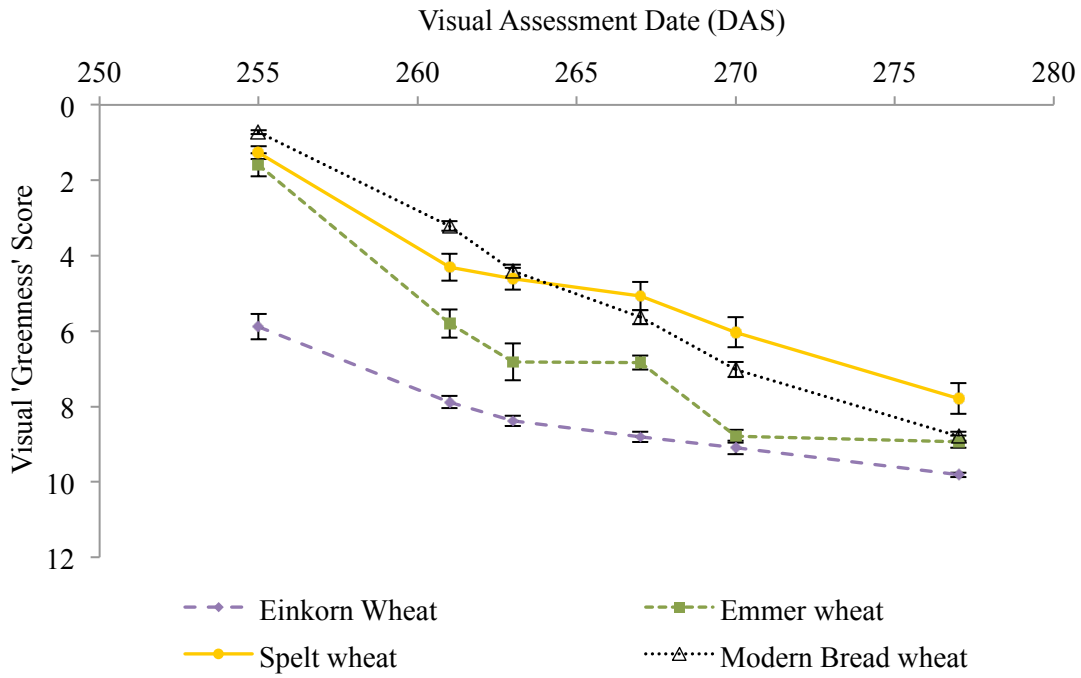


Figure 2.24: Average species visual 'greenness' scores versus time (DAS) (P<0.001, 261 DoF, SED = 0.3641) (error bars denote SED).

Linear regression was used to assess the relationship between SPAD scores and visual ratings for the four species. For each species, there was a strong, linear relationship between visual score and SPAD value (P <0.001) but the slope of the relationship varied between species (Figure 2.25).

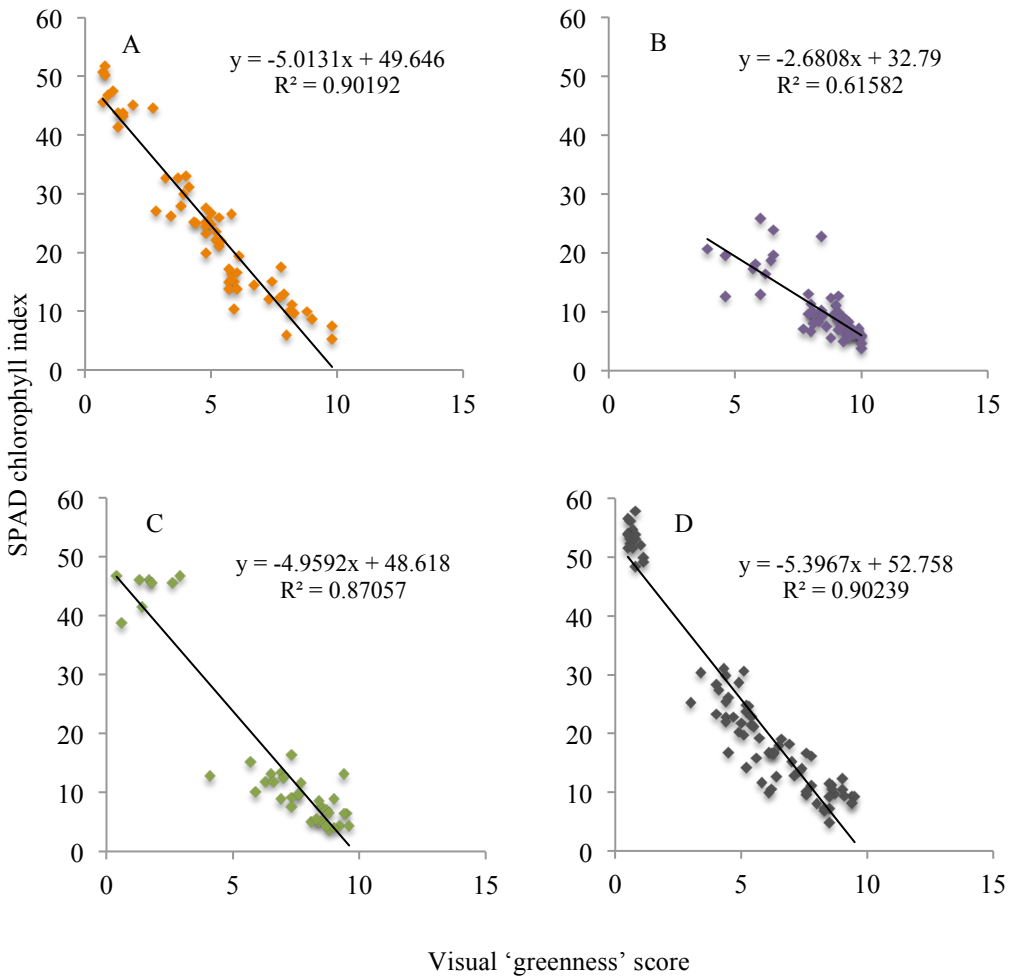


Figure 2.25: SPAD values versus visual 'greenness' scores for A) spelt, B) einkorn, C) emmer and D) MBW. SPAD and DAS were linearly related for all species. ($P < 0.001$, $R^2 = 90.2\%$).

2.3.5.3 Canopy duration (2011 SPAD measurements)

Collation of these data by species showed measurements taken 255 DAS to be significantly different ($P < 0.001$), showing MBW to have the highest flag leaf chlorophyll content, followed by spelt, emmer and einkorn (Figure 2.26). After this initial measurement however, SPAD readings declined in MBW. At 263 DAS SPAD readings showed the 'greenness' of MBW flag leaves to reduce significantly, at which point spelt wheat had higher chlorophyll content than all other genotypes. Although values reduced drastically in all genotypes, spelt maintained an increased SPAD value until the final measurement date. Einkorn showed the lowest SPAD values on all sampling dates except for 277 DAS.

SPAD readings were seen to be significantly different between genotypes on all dates ($P < 0.014 - 0.001$) except for 240 DAS (Figure 2.26). All genotypes tended to have high SPAD values at the start of sampling which corresponded with the average date at which genotypes reached anthesis, after which flag leaf chlorophyll content then began to decline. Modern bread wheat, Xi19 had the highest chlorophyll content at 240 DAS (59.54). Einkorn SB, once again showed the lowest flag leaf chlorophyll content of all genotypes (46.32) at the onset of measurements however, towards the end of the season, SPAD remained comparatively higher than all einkorn genotypes as well as all emmer and modern bread wheat genotypes. Although all modern wheat cultivars had high SPAD readings at the outset of sampling, their decline was seen to be more abrupt than ancient species, particularly spelt which was observed to senesce at a slower rate, consistent with results from the 2010 experiment.

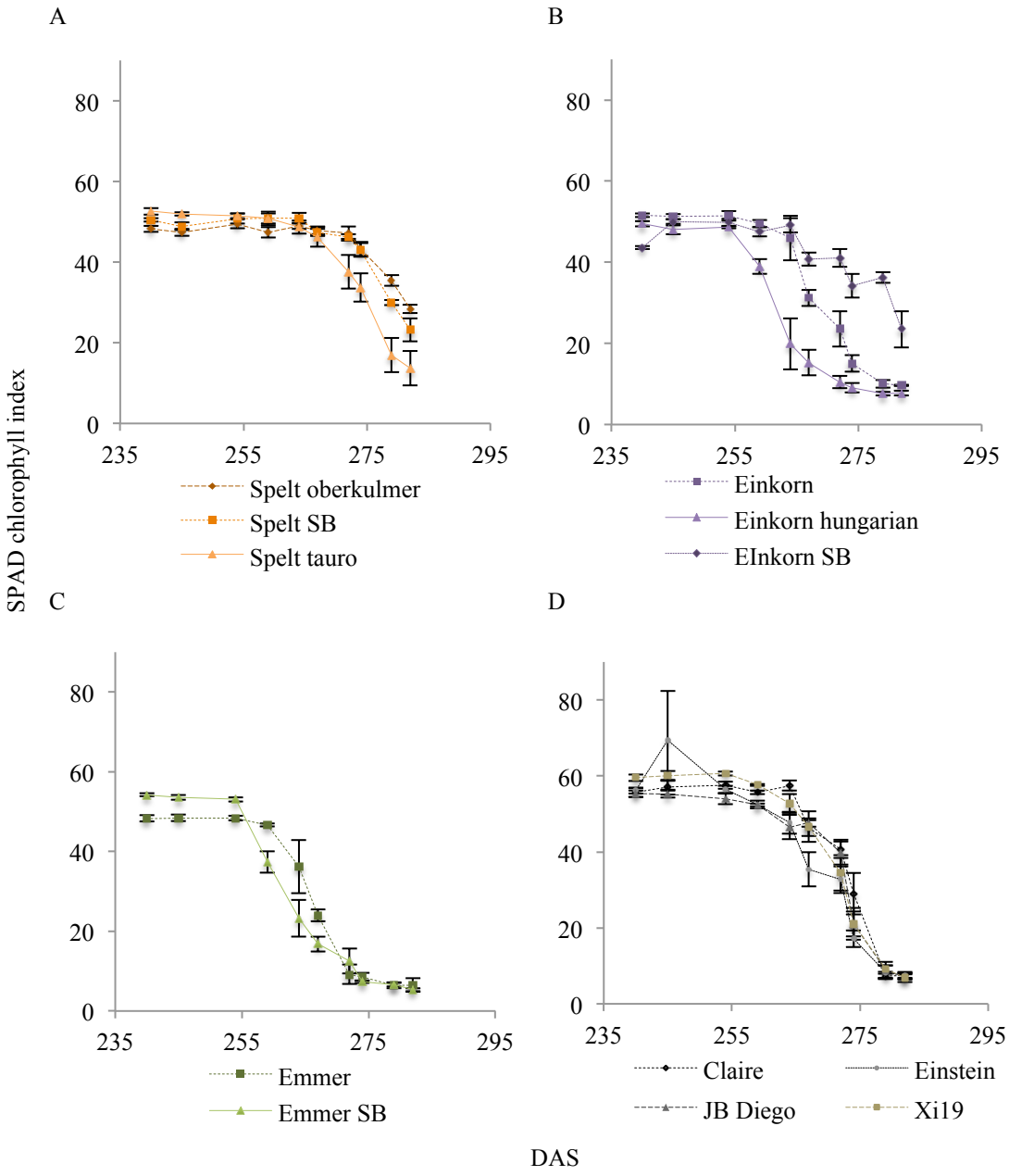


Figure 2.26: Genotypic SPAD chlorophyll index values throughout the 2011 season, A) spelt, B) einkorn, C) emmer and D) MBW cultivars (P <0.001, 357 DF, SED = 3.468) (error bars represent SEM).

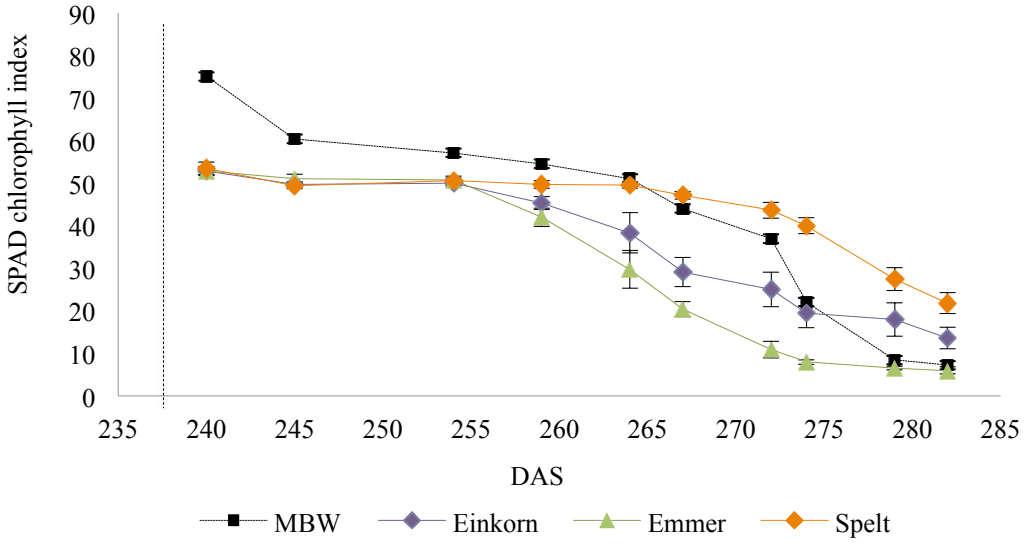


Figure 2.27: SPAD reading of twelve ancient wheat cultivars averaged over four species (spelt, modern bread wheat, emmer and einkorn) against days after sowing in the 2011 field experiments (P <0.001, 437 DF, SED = 3.118) (showing SEM by species). Vertical dotted line represents the average date of anthesis.

When analysed by species, there were significant differences on all dates (except for 240 DAS) (P <0.001) (Figure 2.27). MBW generally showed a sharper decline than ancient species, which maintained green area for a longer period of time. At the close of sampling, spelt species were seen to have the highest SPAD chlorophyll index (21.78) followed by einkorn (13.59), modern bread wheat (7.23) and finally emmer (5.92).

2.4 Discussion

The success of any cropping system is highly dependent on its environment; optimal conditions allow leaf area expansion which ultimately impact growth and development (Hay & Porter, 2006). Essentially, it is the ability of a crop canopy to intercept photosynthetically active radiation that influences the biological yields produced; it is widely acknowledged that the two are linearly related. However, leaf area is also a result of a number of other factors including emergence date, development rates, tiller production and survival, as well as leaf senescence. All of these factors are impacted by genetic, environmental and agronomic factors (Hay & Porter, 2006), which in turn affect seasonal leaf distribution, thus influencing leaf arrangement and therefore canopy architecture (Azam-Ali & Squire, 2002). This highlights the importance of crop growth and development processes in yield formation (Wang & Engel, 1998). The following section aims to interpret the data presented in section 2.2, so as to discuss the differences between the genotypes investigated including developmental, morphological and physiological aspects for wide ranging characterisation of genotypes.

2.4.1 Plant morphology, growth and development

2.4.1.1 Establishment

Both ancient and modern wheat seeds alike were untreated which may be an important factor first as to why emergence was significantly different in both experimental years, as well as for the potential growth and development of the canopies. Seed treatments are primarily used to limit seed-borne diseases but can also be an effective control for foliar diseases such as bunt and *Fusarium* seedling blight (Paveley *et al.*, 2000). Potential pathogens known to affect emergence include

fungi, *Microdochium nivale*, *Fusarium graminearum* or *Septoria nodorum,* all three of which cause seedling blight or thinning of the plant stand, often to reduce plant establishment (Clark *et al*., 2004). Furthermore, these seedling diseases tend to be more severe if poor quality seed is used or if conditions at planting are not favourable for quick germination and establishment, for instance in 2011 the winter was particularly cold and seeds were exposed to prolonged frosts; all of which could have been instructive of the low establishment observed. Another factor was that drilling ancient species was problematic due to the difficulty in removing the glume and awns without damaging the seed, occasionally causing blockages during drilling. This was particularly the case for einkorn but all ancient species had non-threshing ears.

2.4.1.2 Shoot production and tiller economy

In 2010 total shoot numbers peaked at GS 31 and subsequently declined. This was expected as at later growth stages, shoots often die or production slows (Sparkes *et al.*, 2006). This initial spike in total shoot numbers was also observed in 2011 for all genotypes except for einkorn, einkorn SB and spelt SB. However, the large tiller production for these genotypes could be a result of the low establishment recorded (19, 3.5 and 6.6%, respectively). It is thought that the period in which tiller initiation occurred was extended as a result of low population density (Sparkes *et al.*, 2006). Shoot production varied between years; in 2010 ancient species generally produced greater numbers of tillers compared to modern wheat, however the converse was true in 2011. MBW was expected to have the fewest fertile shoots, which would be attributed to lower shoot number with greater resource partitioned to each shoot however, this was not the case. In both years MBW cultivars had greater emergence

rates with larger numbers of shoots; these were probably attributed to greater plant populations. Higher establishment rates would have introduced a higher degree of competition for resources between adjacent plants, therefore initiating tiller death, often genetic differences in shoot production may be masked by the effects of high plant population density (Hay & Porter, 2006). Modern bread wheat cultivars and emmer SB had among the highest emergence rates; tiller production peaked at GS 31 and declined thereafter, a pattern that is often seen in typical commercial plant densities. The described data however is highly limited by establishment that may have skewed the results of ancient species. Spelt had the lowest number of fertile shoots at each growth stage when compared to other species, spelt also had the lowest emergence rate of assessed species.

Although in 2010, ancient species generally had low emergence, some ancient genotypes, for instance spelt Tauro, and Oberkulmer as well as all einkorn cultivars produced the largest number of fertile shoots per m^2; therefore compensating for low plant population by producing large numbers of shoots per plant (Sparkes *et al.*, 2006). Furthermore, in 2010 einkorn also had the lowest rate of tiller survival meaning that although tiller production was high, this did not necessarily translate into harvestable yield. This is corroborated by ear biomass in 2010 for einkorn being among the lowest of all investigated genotypes. Surprisingly, einkorn also had high GAI, probably a result of increased tiller numbers. From these observations, it can be theorised that biomass partitioned toward tillers reduced overall productivity by investing carbon into infertile shoot production. Conversely, spelt genotypes had the highest rate of tiller survival (72.26) and produced among the highest amount of ear biomass, similar to that of some modern bread wheat cultivars. Modern bread wheat produced among the least number of total and fertile shoots. As stated earlier, this

could be due to increased numbers of plants m^{-2} which may have imposed space limitations or alternatively due to faster development, reducing vegetative phase length. Critchley (2001) stated that with a reduced vegetative period, the time frame in which tiller production may occur is also reduced, possibly the case for modern cultivars for which development was faster.

2.4.1.3 Plant development

Plant development also differed. Observational data of development dates indicate that all modern bread wheat cultivars developed faster than ancient species. This meant that as well as having varying numbers of plants per metre square, respective plots within the experiment reached varying developmental stages in disparate environmental conditions. Although many of the physiological aspects discussed here are comparatively assessed, it is important to note these factors as they may have implications for findings in the following discussions.

2.4.2 Plant height

Plant height was analysed to assess its effect on light interception through other parameters such as biomass accumulation, to provide an indication of the effect of height on light interception and efficiency. In both years, ancient species were significantly taller than modern bread wheat varieties during later growth phases (GS 39 and 61). Early in the 2010 season however, modern bread wheat (MBW) (with the exception of Xi19), were taller than ancient species. In both years, taller species had lower green area index (GAI) and total biomass production than modern bread wheat. The much shorter modern genotypes also achieved the greatest ear indices

and overall ear biomass, indicating that light interception for economic yield was favourable in shorter species.

Experiments across both years indicated that cultivars with greater height did not have increased green area expansion. In fact, the shorter stature of modern bread wheat was associated with comparatively high GAI, generally maintained throughout the experiments (with the exception of growth stage 61 in 2011). This may have been due to the onset of senescence, reducing the amount of green area present, expected towards the end of the season and further supported by senescence measurements. Early in 2010 however, modern bread wheat genotypes were significantly taller than ancient species. This was associated with their faster development, allowing faster leaf area and canopy expansion (indicated by significantly greater GAI), potentially increasing early fractional interception. Increased expansion early in the season would also limit the establishment of weeds and maximise interception of limited radiation levels in the UK winter wheat growing season. Furthermore, aboveground biomass was also observed to be greater for modern bread wheat species indicating that greater height is not necessarily instructive of ancient wheat species, and does not increase the overall ability of the canopy to intercept light. This was also stated by Miralles & Slafer (1997) who found that genetic reductions in the height of wheat canopies would not adversely affect light interception, where plants were under optimal environmental conditions.

One of the most important factors contributing to increased wheat yields has been the introduction of semi-dwarfing genes *Rht1* and *Rht2* which are associated with reduced plant height as well as reduced lodging risk (Miralles & Slafer, 1997). These genes also influence carbon partitioning towards the ear rather than the culm to

further increase grain production (Bognár *et al.*, 2007; Toyota *et al.*, 2010). Additionally, Toyota *et al*. (2010) suggested greater radiation use efficiency (RUE) could be linked to lower culm length in shorter wheat cultivars. In the experiments, particularly in 2010, a degree of lodging occurred with taller ancient wheat genotypes. This was mainly due to adverse weather conditions towards the end of the season, and only occurred after full canopy senescence, therefore did not reduce light interception or photosynthetic ability of the canopy drastically, however it did reduce the yields collected by the combine harvester.

2.4.3 Green Area Index

Leaf area for wheat undergoes seasonal development patterns; initially low temperatures suppress leaf area. As temperatures increase, leaf area also increases to after which it then began to decline due to senescence (Hay & Porter, 2006). Genotypes in 2010 generally followed this pattern; green area index increased until GS 61, except in spelt, which declined for GAI from GS 39 onwards. The reduction of GAI at this point would potentially limit yield; the reduction of photosynthetically active green area could be purported to decrease the capacity of the canopy to accumulate carbon assimilates when grain filling occurs.

This conflicted with SPAD and stay green scoring results, however observing data by genotype, the decline in GAI is attributed to spelt SB; spelt Oberkulmer and tauro increase or at least maintain GAI from GS 39 to 61. Furthermore, low GAI for spelt genotypes were thought to be a result of poor establishment rather than the onset of senescence.

In 2010, increased GAI was seen, unsurprisingly, to affect fractional interception as spelt had low interception at the start of the season. JB Diego displayed the highest GAI of all assessed cultivars. Hay and Porter (2006) state that interception will be low where plant density is low because the canopy has not yet had time to adjust, once more mature, ancient wheat canopies, particularly those with low establishment such as spelt Oberkulmer, compensated by increasing shoot production. At later growth stages, increases in green area associated with increased shoot production (observed in spelt SB) were associated with increases in *F* to a similar extent as those genotypes that established well and, although fractional interception was observed to increase from GS 39 to 61, these were not necessarily associated with increased biological yields (as biomass production for spelt was low). The lower GAI of ancient species, in particular einkorn, were associated with low biological yields where reduced green area was thought to limit the capacity of the canopy to accumulate carbon assimilates. Consequently all ancient species produced lower quantities of biomass. JB Diego had the highest recorded GAI of the varieties at crop maturity and averaged throughout the season (5.5), which translated to increased biomass accumulation also.

Once again, the experiment in 2011 showed MBW cultivars to have increased GAI compared to ancient species. Emmer and einkorn SB had the lowest GAI, corresponding with low emergence rates observed in 2011. However, despite having lower GAI, emmer and einkorn produced larger amounts of biomass than spelt species, probably due to the low emergence observed for spelt cultivars. Emmer was not observed to increase shoot production later in the season, however einkorn SB total shoot production proliferated, increasing over two fold from GS 31 to 39 and doubling again by GS 61. This is indicated at GS 61 where GAI remains constant

from GS 39 to 61 for einkorn SB. Biomass production and fractional interception also increased over this period indicating the associations between these traits. Furthermore, in 2011, spelt species had the lowest GAI at GS 31 which was also reflected by low biomass accumulation for spelt genotypes, however these must also be due in part to low population densities.

GAI was significantly different between cultivars in 2010, however no significant differences were observed between species. Noteworthy however, is that modern bread wheat and spelt followed the expected trend whereby GAI increased, plateaued and declined at the end of the season. However, GAI for einkorn and emmer continued to increase, suggesting that, as genotypes reached GS 61, GAI was still expanding. Lunagaria & Shekh, 2006 suggest that GAI is regulated according to growth stages and therefore the onset of GS provides a threshold as to when a crop will, for instance, begin to senesce or remobilise nitrogen from leaves. As mentioned earlier, ancient wheat tended to develop more slowly than modern bread wheat, therefore the differences in phase transitions for GAI observed in 2010 could be due to crop phenology, as sampling was performed by date rather than by growth stage. In 2011 however, sampling was performed on the basis of GS to increase consistency.

2.4.3.1 Green Area Index partitioning

At different growth stages, cultivars partitioned varying amounts of green area toward different components in both years. For both years, during the initial development phase (up to GS 31) the majority of green area was accounted for by lamina (75% or greater) except in spelt Tauro (in 2010) where approximately 40% of green area was lamina. At GS 39, the majority of green area was accounted for by

green lamina, although to a lesser degree than at growth stage 31 (accounting for 40% and 60% or more of the total green area in 2010 and 2011, respectively), expected as internode extension would have meant that more biomass was directed toward the stem and leaf sheath (Hay and Porter, 2006). In 2010, einkorn SB attributed 80% of green area to lamina, this was not reflected in the quantities of biomass partitioned to leaf and shoot material. This sample however also showed the presence of ears, indicating that growth stages were variable within the plot and between genotypes. At GS 61, lamina area accounted for approximately 40% of total green area and shoot and ear area accounted for the remainder. In 2011, 20% of total green area was accounted for by lamina and shoots with the remainder being attributed to ear area however, this was not reflected in the amount of ear biomass produced. The proportion of area attributed to differing components did not show a clear trend by genotype or by species, which was also the case for biomass partitioning however these differences would certainly impact the ability of the crop canopy to intercept light. In order to assess whether there are differences between the genotypes or species, it would be necessary to explore such traits in a closed crop stand where emergence rates were not a significant artifact.

2.4.4 Distribution and capture of solar radiation

2.4.4.1 Light attenuation

In 2010, fractional interception was significantly different between cultivars. Data presented in the previous section shows that cultivars emmer SB and spelt SB intercepted a larger proportion of irradiance at several points over the season compared to other genotypes. This may be associated with high biomass production for spelt SB, this was not the case for emmer SB in 2010 (although differences for

total biomass production were not significant). *F* was more variable among spelt species in 2010 than other species. Additionally, *F* varied between species to a larger degree at the start and end of the season (at GS 31 and 61). MBW cultivars intercepted larger amounts of radiation from 170 to 200 DAS which may have been due to increased development rates. In 2011, Claire showed the highest *F*. Once again, einkorn SB captured the lowest fraction of incident light compared to other genotypes. Einkorn SB had low *F* at the beginning of sampling but then increased, thought to be due to increased tiller production, also identified in GAI results. The low emergence rates observed for einkorn SB however, may have skewed the proportion of photosynthetically active radiation intercepted.

In both years, *F* followed a general seasonal trend where it increased from 179 DAS; this was characterised as a linear exponential phase followed by a climactic phase. *F* then began to decline as a result of leaf maturation and senescence. In 2011, einkorn SB also followed this trend, although *F* was much lower than other genotypes however, did increase at a faster rate as the season progressed, and had the greatest *F* on the final sampling date. This may have been a result of canopy expansion 'catching up' by compensating for low emergence (Sparkes *et al*., 2006). This may also be indicative of slower development rates as has been previously observed for ancient species. In 2010, spelt SB and emmer SB genotypes had increased fractional interception when compared to all other genotypes, which may be a result of increased ground cover attributed to comparatively high tiller production (Reynolds & Trethowan, 2007).

In both years einkorn had low *F* at the start of the season but 'caught up' with other genotypes. Also in both experimental years, modern bread wheat cultivars

intercepted a large fraction of light throughout the season, possibly due to increased canopy size. Other components of the study corroborated this as GAI and biomass production was generally greater for modern bread wheat. Einkorn senesced first however, in both years, MBW showed a rapid rate of decline in *F* which may be attributed to leaf death and therefore a reduction in green area. O'Connell *et al.* (2004) reported that seasonal factors had a large impact on *F* in wheat, the differences for *F* over the course of the season in these experiments supports this, furthermore differences also indicated that differences between exist between the genotypes investigated.

2.4.4.2 Light extinction through the crop canopy

The proportion of light transmitted down the canopy at differing intervals allowed light extinction to be assessed. There were genotypic differences between the light extinction through canopies. Overall, MBW allowed the smallest fraction of light to be transmitted per unit height to the canopy below, followed by einkorn, spelt and emmer. The proportion of light transmitted through the crop canopy per unit height (every 10cm) was higher in ancient species, which increased the amount of light that was transmitted to lower canopy layers, potentially indicating that lower leaf levels were ultimately more productive due to increased PAR availability and therefore interception (positively impacting with carbon accumulation). Light transmission through modern bread wheat canopy per unit height was increased compared to ancient species indicating that the extinction of light was much 'faster' at heights equidistant from ground level. Modern wheat species showed a steep reduction in light moving down the canopy, therefore intercepted more ambient light in the upper canopy layers. This data highlights the importance of crop architecture and

corroborates Muurinen and Peltonen-Sainio (2006) statement that canopy height influences radiation spread within the canopy; height influenced the fraction of light intercepted, radiation use efficiencies as well as the biomass accumulation, in turn impacting GAI. These findings also support that the *Rht* allele introgression reduces height to impact light distribution; the interception of MBW at the uppermost leaf layers, most notably the highly productive flag leaves, intercepted the greatest proportions of light, allowing for an efficient distribution use of radiation, given the spatial arrangement of flag leaves in particular. Reduced height therefore means that middle and bottom layers of the canopy received a smaller proportion of PAR. Mashhadi and Zand (2004) state that the leaf area density is an important factor in light attenuation and distribution through the canopy; leaf area density is inversely related to light penetration. When considering these data, it is also pertinent to note the stark differences between the heights of the two canopy types (ancient and modern). This variation meant that, although modern bread wheat intercepted more light, per leaf layer, light interception started 'later' because the modern bread wheat canopies were significantly shorter.

Initially, this component of the project aimed assess leaf density within canopies using stratified samples at varying levels down the canopy, however this was not feasible due to time constraints and the difficulty of the task, particularly in the field. The principle behind this analysis however could prove to be very useful for investigation of ancient wheat species. Three-dimensional arrangement of leaf matter could unearth many of the fundamental differences between modern and ancient wheat genotypes. In particular, a three dimensional representation of the canopy could allow *in situ* canopy arrangement and further produce valuable information about the canopy throughout the season using investigation of heliotropism and

phyllotaxis (Hay and Porter, 2006), although in such a project the issue of uneven emergence would need to be resolved.

2.4.5 Resource assimilation and investment efficiency

2.4.5.1 Carbon assimilation

Since the green area of a crop canopy positively correlates with carbon accumulation, the increased GAI of modern bread wheat cultivars explains the observed high biological yields when compared to ancient species. Generally, MBW varieties produced the most biomass on all sampling dates before harvest in 2010. Einkorn, emmer and spelt had gradual biological yield accumulation between GS 31 and GS 39, after which production for these genotypes increased. Although differences were not significant, spelt SB and emmer SB produced the largest amount of biomass per m^2 at growth stage 61. Additionally, despite low emergence rates, spelt species generally produced more biomass than einkorn and emmer, indicating that this species may have traits that allow greater biomass production. The trends observed in 2010 corroborate that GAI is instructive of carbon accumulation, which highlights that intensively bred MBW has an enhanced canopy architecture that increases the efficiency of PAR acquisition, especially when compared to ancient progenitors.

In both experimental years, dry matter accumulation for MBW cultivars followed a linear trend, increasing from GS 31 to 39 and then from GS 39 to 61, in keeping with common assumptions about seasonal canopy leaf expansion, primarily due to increased temperatures at this time of year. In both years, ancient wheat cultivars also followed this trend however, carbon accumulation occurred at a slower rate from GS 31 to GS 39. From growth stage 39 onwards, particularly for einkorn and

emmer genotypes, the rate at which biomass was being assimilated (against time) increased at a faster rate, implying that green area was still being accumulated, however this is only evident from GAI results in 2010. As of growth stage 61 however, species results from 2010 and 2011 differ. In 2010, MBW stopped producing biomass at GS 61. This corresponds to the onset of anthesis when leaf senescence was taking place (also shown by stay green measurements), indicating that photosynthetic area within the canopy was in decline. Unexpectedly, einkorn and emmer however showed a reduction in biomass from GS 61 to harvest. This may be a result of a number of factors, for instance the lower and more variable emergence rates within plots and hence, difficulty in representative sampling. Further still, emmer and einkorn species also underwent a degree of lodging (although sampling attempted to refrain from using parts of the canopy that were severely affected). It is therefore proposed that the reduction in biomass from growth stage 61 to harvest was observed as a result of within plot variation, and that the expected trend would behave as modern bread had. Spelt genotypes showed an increase in the accumulation of biomass from growth stage 61 to pre-harvest. The rate of biomass accumulation was similar to that observed early in the season. This could be purported to be due to the exponential growth rate or relative growth rate (RGR). This relates to the densities at which spelt genotypes were growing (lower than other genotypes as a result of poor emergence, particularly for spelt Oberkulmer and spelt Tauro). In a study conducted by Karimi & Siddique (1991), modern wheat was characterised to have higher RGR, which, during the vegetative period of plant development, lead to increased grain yields. Furthermore, Whaley *et al.* (2000) stated that the exponential growth rate of a less populated crop may be higher due to increased radiation use efficiency (RUE). Spelt cultivars (particularly Oberkulmer

and Tauro), had low plant densities in 2010 and were also recorded to have high pre-anthesis (1.55 and 1.72 gMJ^{-1}, respectively) and post-anthesis (1.31 and 1.46g MJ^{-1} respectively) RUE. It could also be suggested that the increase in biomass after GS 61 was due to increased green area longevity. Stay green scoring and SPAD measurements also confirmed this, indicating that the maintained green area is photosynthetically active and therefore contributes to biomass accumulation.

Results gained from the 2011 experiment however, differ; MBW appears to continue producing biomass beyond growth stage 61, showing no sign of biomass production slowing although all genotypes continued to produce biomass from growth stage 61 to pre-harvest, (except einkorn Hungarian). Once again, einkorn and emmer species showed a reduction in RGR from GS 61 to pre-harvest, probably a result of the onset of senescence, although accumulation of biomass was still occurring (in contrast to the previous 2010 field experiment). Spelt species had increased biomass production from GS 61 to pre-harvest sampling however, not to the extent observed in 2010. In 2011, the RGR of bread wheat cultivars was greater than those of spelt species. All ancient wheat species had significantly lower plant populations than modern bread wheat cultivars, which could have increased radiation use efficiency as Whaley *et al*. (2000) found higher RUE at lower plant densities.

2.4.5.2 Carbon partitioning

By observing where above ground biomass was partitioned in 2010 and 2011, it can be seen that at growth stage 31 and 39, most genotypes partitioned the majority of biomass towards shoots (except at GS 31 in 2011, where the largest fraction of biomass was generally partitioned towards lamina). Overall, when observed by species, taller genotypes did not have more biomass partitioned towards shoots

indicating that the shoots produced by these taller ancient wheat was more likely to be have a lower assimilates per unit area shoot, which may be the reason that ancient wheat lodged and were more difficult to collect, pre-harvest (owing to lesser straw strength). However, this might also be due to climatic factors as all genotypes were affected.

The majority of GAI was allocated toward leaf area at GS 31, 39 and 61 in both years. Data from both years also shows that overall, the proportion of GAI accounted for by lamina, when compared to shoot plus sheath was higher at GS 39 compared to growth stage 31. After growth stage 39, this partitioning, potentially a result of the transition of vegetative phase, meant that a larger proportion of carbon was directed toward shoot and leaf sheath. This was expected as earlier in the season, the canopy would be much smaller, and potentially by GS 39, tiller production would slow. This was consistent at GS 39 and 61; the increased production of green shoot area rather than leaf lamina may be one factor contributing to overall lower carbon assimilation (compared to MBW) as shoot GAI may make a smaller contribution to biological yield production than lamina area. Assessment of biomass partitioned to the harvestable yield (ear) show emmer species to direct the largest proportion of biomass toward the ear although JB Diego still achieved the highest harvest index (HI), suggesting that emmer has more structural material within the ear that will end up as chaff. The investigations performed in 2010 and 2011 could not identify a clear trend in dry biomass partitioning by genotypes or by species, however Takahasi & Nakaseno (1990) suggested that biomass partitioning typically influences the extinction coefficient of a crop, and therefore will also impact the fraction of irradiance that the canopy is able to intercept and thus will indirectly impact the amounts of biomass accumulated.

2.4.5.3 Conversion efficiency of solar radiation

Radiation use efficiency was calculated using the linear relationship observed in 2010 and 2011 between above ground dry matter and cumulative intercepted radiation. RUE for all species ranged from 0.87 to 1.68 MJ^{-1} across both years which was below that which was expected; according to a study performed by O'Connell *et al.* (2004), RUE for modern bread wheat ranged between 1.20 - 2.93g MJ^{-1}. Low RUE observed within the current experiments may have been brought about by assumptions made for the period of time leading up to growth stage 31, which were assumed to be 50% of that measured at GS 31 (the first SunScan sampling date). Furthermore, particularly in 2010, there was some weed contamination within ancient wheat plots that could have skewed fractional interception readings taken (although the utmost was done to limit the impact of this through continuous rouging). Although conclusions based on this data are by no means clear cut, the use of cumulative efficiency, rather than dry matter versus intercepted PAR do provide a more reliable means to assess RUE (Kanton & Dennett, 2008). Therefore, it is reasonable that these data would provide an indication of the true RUE. In the current experiments, root matter was not assessed as a result of time limitation however this is likely to influence RUE also (O'Connell *et al*., 2004).

Overall species RUE showed significant differences for post-anthesis RUE in 2010 and significant differences between pre and post anthesis in 2011. In both years, RUE reduced from pre to post-anthesis, expected as after anthesis green area is likely to rapidly senesce. In 2010, post-anthesis RUE was highest for einkorn Hungarian and lowest in spelt Oberkulmer and SB, perhaps a result of the low *F* reported. Surprisingly, einkorn SB had the greatest pre-anthesis RUE, potentially a result of

low emergence which Whaley *et al*. (2001) state may have been due to greater tiller expansion, indirectly increasing the efficiency of the canopy. High pre and post-anthesis RUE however did not necessarily equate to high harvestable product, einkorn SB had among the lowest ear index of all genotypes in 2010.

In 2010 MBW had the highest pre-anthesis RUE (1.46g MJ-1). This corresponds with Siddique *et al.* (1989) who found MBW to have greater RUE compared to older wheat genotypes. Modern bread wheat cultivars however did have comparatively high ear index compared to other genotypes. In 2011, the highest observed RUE was for einkorn SB and spelt Tauro, both pre and post-anthesis. Post anthesis RUE was highest for einkorn species, potentially due to the low establishment observed; this meant that individual plants could expand into the space without resource limitation or space restraints. This was also reflected by fractional interception for einkorn species, which was similar to those genotypes that had more dense canopies (in terms of plant population), despite low emergence for these cultivars however, biomass production was comparable with other genotypes. MBW had the greatest RUE and high ear index; MBW also produced among the greatest total biomass of all genotypes indicating it was the most efficient in terms of radiation resource use efficiency in 2010.

In contrast with 2010, spelt species had the highest pre-anthesis and post-anthesis RUE in 2011, despite particularly low fractional interception (particularly for spelt SB) and comparatively low biomass production. Results did however coincide with previously reported data from preliminary glasshouse experiments (Sparkes, 2010) where spelt RUE was 1.81g MJ^{-2} compared to 1.68g MJ^{-2} in 2011. Modern bread wheat also had comparatively high RUE, as observed in the 2010 field experiment. Emmer had the lowest RUE of all the species, pre and post-anthesis. Species

followed the same ranking in terms of total biomass production in 2010 and 2011, where MBW also produced the highest ear biomass and therefore had the highest ear index in both years.

2.4.6 Chlorophyll content and canopy persistence

Green area persistence is greater in certain genotypes thus increasing the potential photosynthetic capability by allowing greater light interception for biological yield production. It is thought that increased flag leaf duration correlates with yield (Gregerson *et al*., 2008; Hafsi *et al*., 2007) since longer crop seasons have been identified to positively correlate with yield (Takahashi & Nakaseko, 1990), therefore increasing productivity. Additionally, it is thought that plants with a capacity to stay green for longer have an increased yield capability and potential proficiency to resist drought in certain environmental conditions (Christopher *et al.*, 2008; Borrell & Hammer, 2000).

In 2010, SPAD reduced by the largest degree in all cultivars of MBW (ranging from 24.70 - 28.52). At the end of sampling, spelt Oberkulmer and spelt Tauro had the highest SPAD readings (10.22 - 16.07) compared to all other genotypes, perhaps indicating the capacity of this species green flag leaf area to remain green for longer. Einkorn had the lowest readings throughout the season however the decline in leaf 'greenness' occurred at a reduced rate compared to other genotypes, potentially a result of slower developmental rates. Modern bread wheat had the highest flag leaf SPAD readings, followed by spelt, emmer then einkorn. After the first SPAD sampling date however, readings declined. The consecutive measurement dates showed the 'greenness' of modern bread wheat leaves to reduce significantly, at which point spelt species had the greatest SPAD readings. Spelt maintained

increased SPAD values (compared to other genotypes) until the end of sampling. Generally, einkorn showed the lowest SPAD chlorophyll index in both experiments. Concurrently, as SPAD measurements were being performed, so too were visual inspections of flag leaves in order to score the 'greenness' of each genotype. It was found that visual scoring and SPAD chlorophyll indices correlated, furthermore the same assumptions were made about the visual scoring data than were made about SPAD chlorophyll readings, therefore either can be used to assess say green in flag leaves, the advantage of visual scoring being that no equipment is required except for a comparison chart although (Xu *et al.*, 2000) have stated this methods to be subjective and should therefore be performed by the same individual throughout the experiment (as was done here).

Differences between SPAD values between trials were observed; SPAD chlorophyll indices in 2011 were generally higher than those of 2010, particularly at the beginning of the season. Different SPAD meters were used in 2011 than in 2010, which might be why SPAD values were higher in the latter. However for future investigations it was ensured that the same equipment was used and that all equipment was calibrated before each use.

Data gained from 2010 and 2011 is consistent, observed trends indicate that the flag leaf chlorophyll content of modern cultivars may be intrinsically higher than those of ancient species; therefore these cultivars may have an increased photosynthetic capability early in the season however this was not maintained post anthesis. So, whereas spelt began with lower chlorophyll content, the species 'compensated' by maintaining the flag leaf for longer. The trends observed here are similar to those observed for GAI where bread wheat initially had larger GAI, which decreased

drastically before GS 61. Spelt however maintained green area, corroborating the observation that spelt has higher canopy persistence (Sparkes, 2010). Larbi & Mekliche (2004) state that genotypes reported to have green area persistence during grain filling may be the key to securing wheat yields in semi-arid regions.

2.5 Conclusions

The field trials highlighted a number of differences between the modern and ancient wheat species. The ancient wheat species produced greater numbers of tillers than modern genotypes in 2010 only, however, they did consistently partition larger proportions of biomass towards shoot production, probably due to differences in developmental rates. MBW produced the greatest yields, and consistently had greater HI. The chapter highlighted that it is the proficiency of ancient wheat species to produce comparable biological yields rather than harvestable yields that may be useful in the improvement of MBW (even with highly variable establishment between modern and ancient species). This proficiency to produce biological yield may well be due to green area persistence, consistently observed in spelt, furthermore, this is potentially where the observed high RUE for several ancient species derived. Results therefore indicate that ancient species warrant further investigation particularly in regards to green area persistence, RUE and biomass accumulation.

Chapter Three:

Leaf level biochemical and physiological aspects of photosynthesis and water use efficiency

3.1 Introduction

The investigations recorded in Chapter Two were performed to identify genotypes that had significantly different physiology and resource use traits, compared to modern bread wheat cultivars. Among those traits was the potentially superior RUE for genotypes einkorn, einkorn SB, spelt Tauro and spelt SB however, while the data set indicated improved RUE, the physiological basis of this was not clear. In 2011, a glasshouse experiment was established to investigate the physiological traits, at the leaf level, that are responsible for improved RUE.

Biophysical and biochemical processes have various effects on photosynthetic rates and observing these properties can be used as a tool to predict how environmental and genetic influences affect photosynthetic rates (Sharkey *et al*., 2007). Furthermore, they are also indicative of leaf physiology and plant productivity (Sharkey *et al*., 2007). A/C_i response curves were performed using Infra-Red Gas Analysis (IRGA) to provide gauge potential biochemical and biophysical limitations on photosynthesis in vivo and therefore supplement the anatomical characterisation of genotypes, in particular aim to understand previously measured differences in RUE.

3.1.1 The A/C_i response

Exposure of a leaf to varying atmospheric CO_2 concentrations (C_a) will affect photosynthetic rates and the intercellular CO_2 mole fraction (C_i) within a leaf. The relationship between these parameters is not linear and therefore provides a means by which the biochemical and stomatal limitations on photosynthesis may be assessed quantitatively (Long & Bernacchi, 2003). A to C_a can not provide a means to assess the leaf since gas exchange is subject to boundary layers, stomatal and

mesophyll processes; on the other hand, by modeling the response of A to C_i, the boundary layers and stomatal influences may be removed, leaving the impact imposed by mesophyll processes (Long & Bernacchi, 2003). Typical leaf responses can be modeled assuming that A is 100% of the lowest rate allowed by each of these biochemical conditions (Sharkey *et al*., 2007). As conditions change, A will vary as predicted by the limiting process until another aspect becomes limiting (Sharkey *et al*., 2007), investigated here by exposing the leaf to varying CO_2 concentrations.

3.1.2 Practical interpretation of the A/C_i response

Farquhar *et al.*, (1980) detailed that the biochemical reactions of the leaf are generally in one of two distinct steady states; in the first 1) A can be predicted based on the properties of ribulose 1, 5-bisphosphate carboxylase (Rubisco) when there is a saturating supply of the substrate, RuBP. This is termed the Rubisco-limited state of photosynthesis and typically occurs when atmospheric CO_2 concentrations are low (Sharkey *et al*., 2007). This component of the response is linear and can be described by the *in vivo* apparent Rubisco activity (V_{cmax}). In the second state 2) A is predicted assuming that RuBP is being utilised at a constant rate and is therefore limiting. This is termed RuBP regeneration-limited photosynthesis, and typically occurs at higher CO_2 concentrations where A will increase due to increased CO_2 availability, saturating Rubisco active sites. This is only reversible by regeneration of RuBP through the Calvin cycle, which will be influenced by the maximum rate of electron transport for the regeneration of RuBP (J_{max}) (Long & Bernacchi, 2003). The limitation of A by RuBP increases as CO_2 concentrations increase because carboxylation is favoured at the expense of oxygenation. This also means that CO_2 loss through photorespiration is much reduced (Sharkey *et al*., 2007). These two phases are the main component processes of the CO_2 response curve, there is

however a third state, which occurs at saturating CO_2 concentrations. Here, photosynthetic rate gains are no longer possible, the production of photosynthetic metabolites during chloroplast reactions, namely (but not exclusively) triose phosphate, inhibits further reactions (Sharkey *et al*., 2007). This state is termed triose phosphate utilisation (TPU) and is the final limitation phase of the A/C_i response and can also be indicative of the maximum rate of photosynthesis possible by the leaf (Sharkey *et al*., 2007).

The following chapter outlines various biochemical capacities (primarily for V_{cmax}, J_{max} and TPU) investigated in order to observe whether there are fundamental differences for carbon assimilation between genotypes. The second component of the current chapter relates to a glasshouse experiment in which analyses were widened to include leaf level water use efficiencies under controlled water conditions (GHII). This experiment focused on IRGA measurements that were performed *in situ*.

3.2 Materials and methods

The following chapter outlines two glasshouse experiments that included the genotypes previously grown in the field in order to investigate leaf level photosynthetic traits.

3.2.1 Experimental site

The following experiments were performed in a glasshouse located on-site at the University of Nottingham, Sutton Bonington Campus, Loughborough (latitude 52° 49'56.04"N, 1d 56.86"W) in 2011.

3.2.2 Glasshouse experiment I

3.2.2.1 Plant material

Cultivars used in experiment I are outlined in Table 3.1.

Table 3.1: Genotypes selected for photosynthetic analysis for glasshouse experiment I. The selection includes representatives of each cytological classification and including three modern bread wheat cultivars.

Genotype	Species group
Claire	MBW
Einkorn	Einkorn
Einkorn SB	Einkorn
Einkorn Hungarian	Einkorn
Einstein	MBW
Emmer	Emmer
Emmer SB	Emmer
Spelt SB	Spelt
Spelt Tauro	Spelt
Spelt Oberkulmer	Spelt
JB Diego	MBW

3.2.2.2 Seedling Transplanting and Husbandry

Seeds of the listed genotypes were sown into 14 x 20 module trays using John Innes No. 3, high fertility potting compost mix on 12 January 2011. Plants were vernalised in a cool glasshouse maintained so at 6°C for 58 days. Seedlings were transplanted into 5 litre pots containing John Innes Potting Compost No. 3 on 15 February 2011 for the duration of the experiment.

3.2.2.3 Experimental design and glasshouse husbandry

The experiment was arranged as a randomised complete block design, divided into three blocks (Appendix Three). All plants were maintained within a glasshouse, without temperature or light controls and with non-limiting irrigation and nutrients. Disease and pest controls were applied as necessary (for details see Appendix Six). In addition, weeds were removed accordingly to limit resource competition. These measures were maintained throughout the experiment.

3.2.3 Assessments

3.2.3.1 Carbon dioxide response curves

Plants were transferred to a laboratory where gas exchange measurements were performed. Measurements took place between 29 June and 14 July 2011 using an Open Licor 6400 portable photosynthesis system (Licor Lincoln Nebraska, NE, USA) Infra-Red Gas Analyser between the hours of 10am and 3pm in order to reduce variation imposed by stomatal behaviour. Carbon dioxide response curves (4 per genotype) were obtained by monitoring gas exchange responses of the photosynthetic activity in leaves to intercellular CO_2 mole fraction (C_i). This was performed using the programming functions of the Licor 6400-40 during which the

section of leaf encapsulated in the chamber was exposed to 1000 μmol m^{-2} s^{-1} as standard and humidity was maintained between 50 and 60%. Leaf temperature ranged from 18 - 28°C, and averaged 23°C across all measurements. The leaf was exposed to a series of ambient CO_2 concentrations: 385, 250, 100, 80, 60, 40, 400, 600, 800 and 1200. The programme ensured that the leaf section was exposed to these concentrations for a minimum period of 3 minutes with additional time added should CO_2 levels fail to stabilise. The Licor 6400-40 automatically logged measurements using inbuilt programming functions. Analysis of stomatal CO_2 concentrations alongside measurements of photosynthesis rates, V_{cmax} and J_{max} were obtained providing information about the photosynthetic efficiency of the different genotypes.

3.2.4 Glasshouse experiment II

Glasshouse experiment II was performed to assess instantaneous transpiration use efficiency (ITE) and photosynthetic rates of all genotypes to establish any differences in resource use efficiency between genotypes.

3.2.4.1 Plant material

Cultivars used in glasshouse experiment II were those carried forward from previous experiments although einkorn Hungarian was omitted due to poor establishment and slow development. Furthermore, because of the time consuming nature of gas exchange measurements, one modern bread wheat cultivar, Xi19, which was observed to perform well in previous experiments, was used for comparison. The cultivars grown in glasshouse experiment II are outlined in Table 3.2.

Table 3.2: Plant cultivars selected for glasshouse experiment II.

Genotype	Species group
Claire	MBW
Einkorn	Einkorn
Einkorn SB	Einkorn
Einstein	MBW
Emmer	Emmer
Emmer SB	Emmer
JB Diego	MBW
Spelt SB	Spelt
Spelt Oberkulmer	Spelt
Spelt Tauro	Spelt
Xi19	MBW

3.2.4.2 Seedling husbandry

Seeds of all listed genotypes were sown in 14 x 20 module trays using John Innes No. 3, high-fertility potting mix on 15 February 2012. Modules were half filled, one seed placed per module and subsequently covered with soil. Plant material was transferred to a cold room with an air temperature of 6°C and a 12/12 hour light/dark photoperiod. These were left to vernalise for 54 days after which they were placed in a cool glasshouse. Seedlings were checked on a daily basis and watered accordingly.

3.2.4.3 Experimental Design

The experiment was arranged as a randomised complete block design with 3 blocks. Within each block there were 5 columns for each genotype, arranged in a strip (Appendix Four).

3.2.4.4 Column construction and irrigation

Plant material was grown in polyvinyl chloride (PVC) columns that allowed a maximum rooting depth of 1m. These were constructed using PVC pipe, cut lengthways. Holes with a 5cm diameter were drilled at 20cm intervals into one half of the pipe (Figure 3.1). These holes were covered with gortex. Both components of

the PVC pipe were then reassembled using duct tape, producing columns with a 15cm diameter. The underside of each column was also sealed with gortex fabric.

A total of 120 columns were constructed and filled with a 60/40% soil and sand mixture. These were then irrigated to saturation and left so that water could drain out. Upon return to columns the soil levels had reduced therefore more soil was added to each column. This process was repeated twice, at which point no more soil consolidation occurred. This step allowed for compaction within the columns, which was more representative of natural conditions in the field. Columns were considered to be at full water holding capacity (WHC) after 48 hours of drainage. By measuring the fresh and dry weights of known volumes of soil and performing theta probe measurements (using the Theta Probe Soil Moisture Sensor ML2 with data logger (Delta-T Devices, Cambridge) at each soil level (20, 40, 60, 80 and 100cm), it was possible to determine the volumetric soil moisture content of the entire column. This was used as an indicator of the 'water holding capacity' for the purpose of this experiment. The average soil moisture content of soil at 100% WHC was 0.655 m^3 m^{-3}. The first column of each strip (5 columns per genotype) was used to measure soil moisture content, after which each column within that strip was restored to 80% WHC pre anthesis, and 50% WHC post-anthesis. Soil moisture measurements were then made approximately every 4 days at which time the columns were irrigated accordingly.

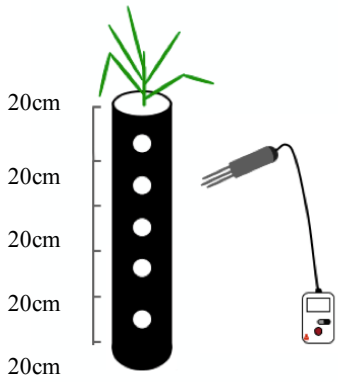


Figure 3.1: Columns constructed to grow plant material in glasshouse experiment II showing 20cm increments where theta probe measurements were taken.

3.2.4.5 Glasshouse Husbandry

Seedlings were transplanted into columns on 24 April 2012, with a seed rate equivalent to 200 seeds per m^2 (3 plants per column). Plants were maintained without nutrient limitation. Plants were irrigated with Hortimix nutrient solution (N:P:K at 15:7:30) (Hortifeeds Ltd, UK). Diseases and pests were controlled as necessary (Appendix Six). Additionally, weeds were removed to limit resource competition. These husbandry measures were maintained throughout the experiment.

3.2.5 Glasshouse experiment II measurements

3.2.5.1 Gas exchange measurements

Gas exchange measurements were performed *in situ* using an Open Licor 6400 portable photosynthesis system (Licor Lincoln Nebraska, NE, USA) infrared gas analyser between the hours of 10am and 3pm to limit variation imposed by stomatal behaviour. All gas exchange measurements were made at ambient humidity (50-60%) on the mid-end section of the main stem flag leaf. Leaf temperature during measurements ranged from 16 - 35°C, with an average leaf temperature of 26°C. The width of each leaf was measured and input into Licor software to adjust gas fluctuations for specific leaf areas. Block temperature and humidity levels were maintained at 20°C and 50-60%, respectively in order to increase uniformity of results.

3.2.5.2 Flag leaf ITE measurements.

ITE (mol mol^{-1}) was derived using the measured rate of photosynthesis and transpiration measured at a given point in time giving a ratio indicating the accumulation of carbon to water lost through stomata (where n was 3) (detailed in Chapter One). Leaf photosynthesis, stomatal conductance and transpiration rates were measured simultaneously for all genotypes at growth stages 39 and 61 (+ ~10 days) for pre and post-anthesis characterisation of genotypes. Measurements were made over 2 to 3 days. Leaves were exposed to a constant photon flux rate of 2000 μmol m^{-2} s^{-1} and 400 μmol^{-1} CO_2.

3.2.5.3 Light response (*A*/Q) curves

Photosynthetic rate and water loss were monitored through exposure of sampled leaves to quantum flux (μmol m^{-2} s^{-1}). Light curves were formulated using the inbuilt programming functions of the Licor 6400-40. Flag leaves were exposed to a sequence of differing levels of quantum flux (1500, 2000, 1500, 1000, 750, 500, 250, 100, 50 and 0 μmol m^{-2} s^{-1}) ranging from high to low in order to reduce the amount of time the leaf spends acclimating and the effects of high light intensities on stomata. Carbon dioxide levels were maintained at 400 μmol m^{-1} throughout. Leaf temperature ranged from 32 - 17°C, the average being 24°C. A large amount of data had to be discarded due to machinery malfunctions, and as a result light curve data was analysed using an unbalanced ANOVA. To ascertain quantum yield, photosynthetic response of leaves exposed to quanta below 200 μmol m^{-2} s^{-1} and under were plotted using linear regression in GraphPad Prism 6 (GraphPad software Inc. CA, USA).

3.2.5.4 Plant sampling

Destructive sampling methods were used where biomass was assessed at key growth stages, sampling one column per growth stage per genotype. Plants were cut at soil level where all above ground biomass was collected and transported to the laboratory. Storage and analysis was carried out as per Section 2.2.7.3. The final two columns remaining at full senescence were used as harvest samples.

3.2.6 Stay green assessments

Stay green persistence of the canopy was measured using a Minolta Chlorophyll Meter SPAD-502 (Minolta Camera Company Limited). SPAD measurements were

performed on each plant at 3 points on the flag leaf, recording the average of these. At the start of the experiment, there were 15 plants per genotype, which, with each consecutive sampling date, reduced by 3. Measurements began as soon as the flag leaf emerged for each genotype and continued approximately every week until senescence of the flag leaf was complete.

3.2.7 Data analyses

All data was stored using Microsoft Excel 2010 for Mac or GraphPad Prism 6 for Windows. Analyses of variance were performed to determine the significance of differences for parameters between genotypes using GenStat (16th Edition, VSN International Ltd.) for Windows (XP).

3.3 Results

3.3.1 Glasshouse experiment I

Plants were maintained in crop stands where they interacted with one another in order to provide some degree of mutual shading, although the canopy was not characterised (Figure 3.2).

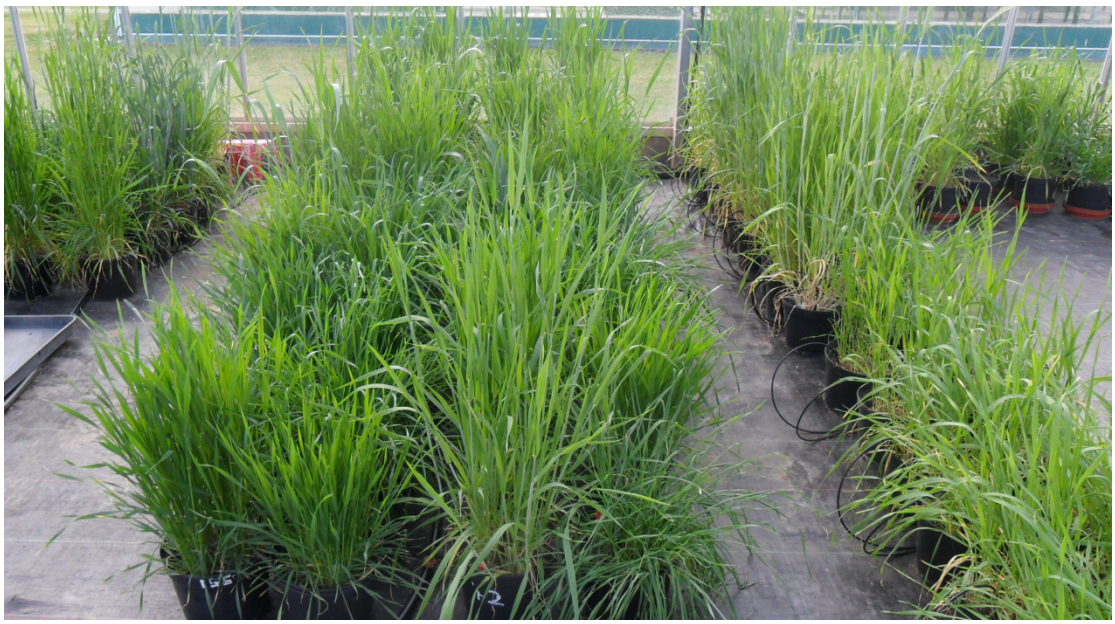


Figure 3.2 The experiment was carried out in an agronomy glasshouse without temperature or light controls, plants were grown in 3 litre pots and were drip fed using an irrigation system, without limitation.

3.3.2 Genotypic photosynthetic response to changing CO_2 concentrations

By plotting the effect of varying CO_2 concentrations on the photosynthetic rate, the three phases of the leaf can be visualised (idealised A/C_i curve, Chapter One). The response is also shown in Figure 3.4: A-E which show the output from the curve-fitting tool constructed by Sharkey *et al*. (2007) (an example of which is shown in Figure 3.3 and further examples are shown in Appendix Four). The initial slope, known as the maximum ribulose 1-5 bisphosphate carboxylase/oxygenase (Rubisco)

carboxylation rate can be determined using the leaf response to CO_2 concentrations below that of ambient, atmospheric CO_2 (Miao *et al*., 2009; Long & Bernacchi, 2003). This provides a measure of the active Rubisco, offering an indication of the extent to which photosynthesis is limited by Rubisco, indicated in Figure 3.3 by the red curve. The second phase relates to RuBP-regeneration indicating the maximum rate of electron transport observed during the exposure to CO_2 concentrations (Bernacchi & Long, 2003) and is represented by the green curve in Figure 3.3. The final phase occurs when the ambient CO_2 concentrations are saturating; the leaf is no longer able to utilise increments in CO_2 concentrations as the products from photosynthesis cannot be consumed at a fast enough rate. The leaf, when encapsulated in high ambient CO_2 concentrations, becomes limited by the intrinsic machinery, this is known as the Triose Phosphate Limitation (TPU) (Sharkey *et al*., 2007).

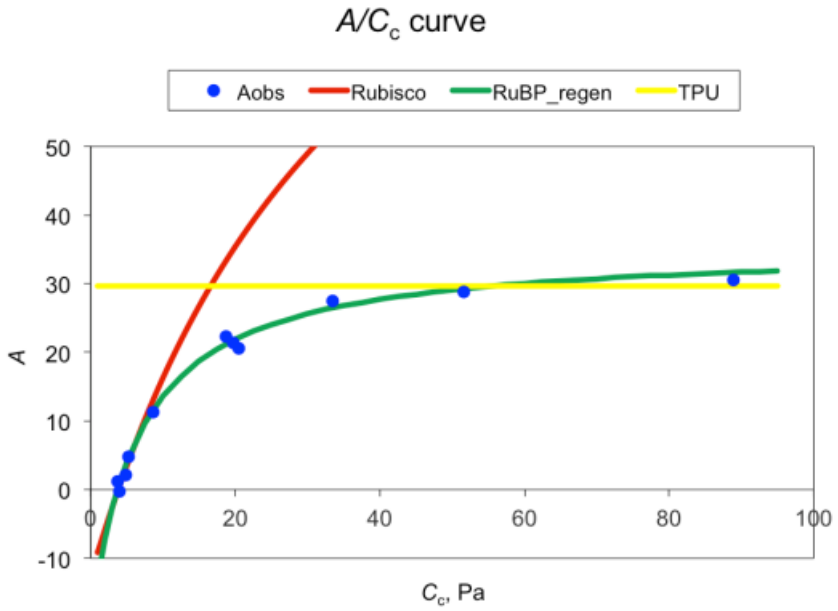


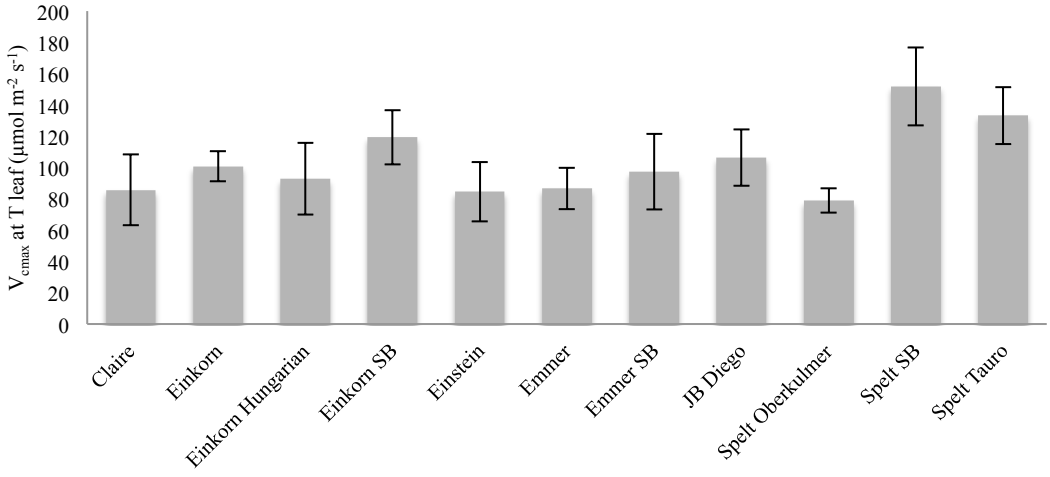
Figure 3.3: Example genotypic responses of exposure to varying carbon dioxide concentrations within the leaf chamber. Using the model constructed by Sharkey *et al*. (2007), C_i was converted into C_c (chloroplast CO_2) plotted against the net photosynthesis for the 8 genotypes; Figure shown demonstrates this for MBW, JB Diego. Blue circles (A_{obs}) denote the observed photosynthetic rate at known C_c. The red line represents the part of the photosynthetic CO_2 response that is limited by Rubisco. The green line corresponds to the RuBP-regeneration state and the yellow boundary symbolises the TPU state.

The investigated cultivars displayed a range of responses to varying atmospheric CO_2 concentrations (Figure 3.4) however triose phosphate utilisation (TPU) and respiration rates were the only significant differences ($P < 0.001$ and $P = 0.02$, respectively). Spelt Tauro and emmer SB had the highest TPU of all genotypes (13.25 and 11.69 μmol m^{-2} s^{-1}, respectively), whereas einkorn hungarian had the lowest. R_d was quite variable ranging from 2.16 to 12.05 μmol m^{-2} s^{-1} (einkorn hungarian and JB Diego, respectively).

V_{cmax} ranged from 78.9 to 151.8 μmol m^{-2} s^{-1} with spelt Tauro, spelt SB and einkorn SB displaying the greatest V_{cmax} indicating a high photosynthetic efficiency (Murchie *et al*., 2009). This may be a result of the high radiation use efficiency observed for those three genotypes in previous field experiments (section 2.3.4.4, 2011 field experiment, Chapter Two). Although V_{cmax} varied between genotypes, standard errors were relatively large and therefore differences were not statistically significant.

Other determined parameters (J_{max}) did not show significant differences between cultivars. J_{max} relates to the maximum rate of electron transport (Miao *et al*., 2009) which ranged from 78.9 to 151.8 μmol m^{-2} s^{-1}. J_{max} was greatest in spelt Tauro and emmer SB, however as a result of low variation between genotypes and relatively large error bars, conclusions cannot be made. These measurements were based on gas exchange in the laboratory, when only the leaf chamber temperature was regulated (to 20°C) therefore the enzyme kinetics involved in photochemistry may have been impacted. This may have had some bearing on the variation observed, thus the curve fitting tool allows the measurements taken to be adjusted to a leaf temperature of 25°C in order to facilitate comparisons.

A



B

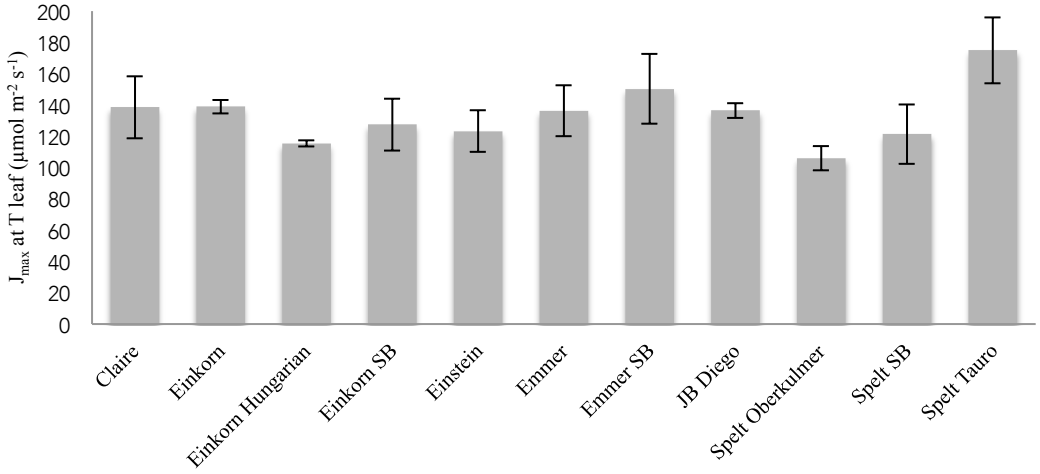
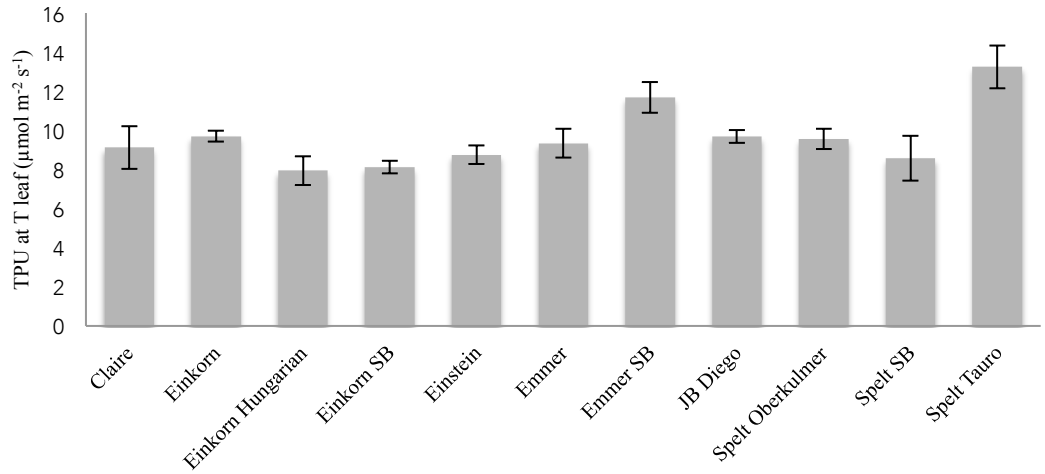


Figure 3.4 *i*: Values determined from fitted A/C_i curves at T leaf. A) shows the maximum rate of carboxylation (V_{cmax}). B) shows the rate of electron transport (J_{max}). Bars represent the standard error of the mean (where n equals 4) of each of the investigated genotypes.

C



D

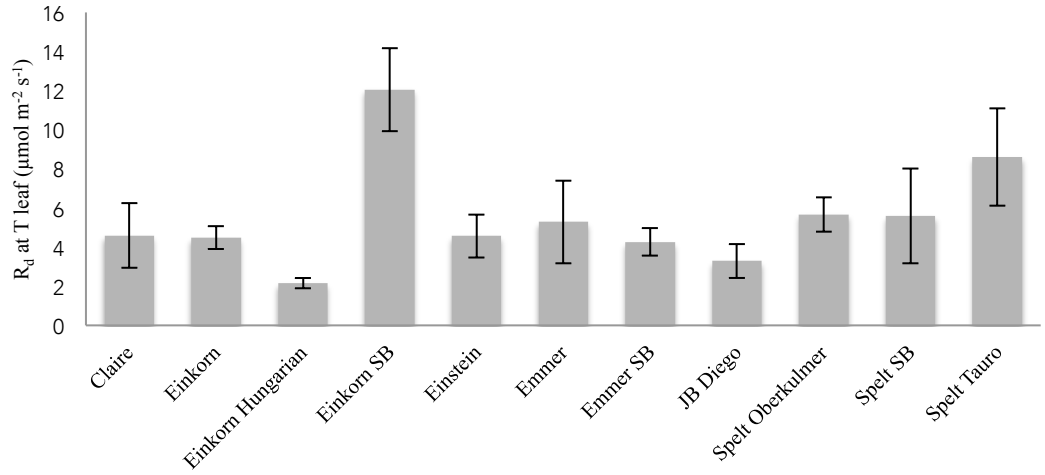


Figure 3.4 *ii*: Values determined from fitted A/C_i curves at T leaf. C) shows the triose phosphate utilisation (TPU). D) shows the determined respiration rates (R_d). Bars represent the standard error of the mean (where n equals 4) of each of the investigated genotypes.

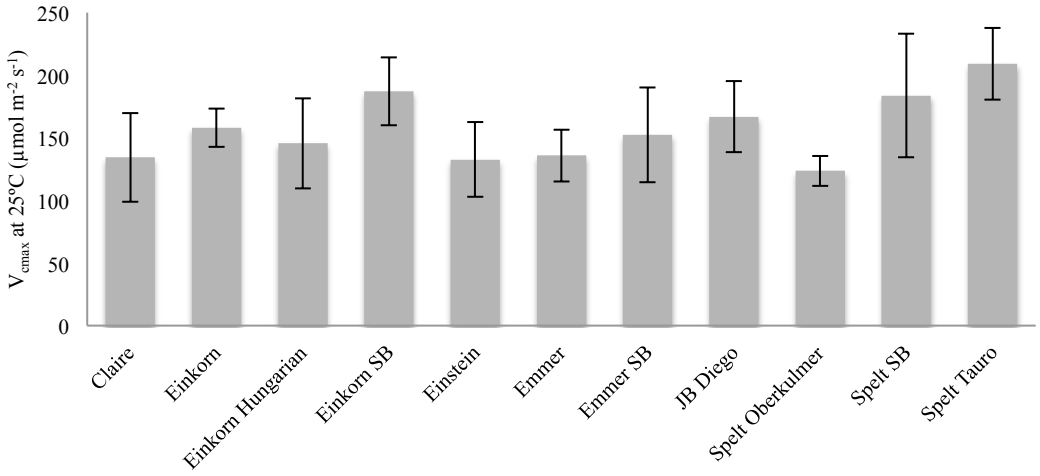
The variance observed (Figure 3.4) for each of the measured parameters was much like that observed without normalisation for leaf temperature. Genotypes were ranked similarly indicating that the variance between observed temperatures may not have had a large bearing on the results gained from the previous analysis. However, as in the previous analysis at observed leaf temperature, significant variation was only observed for TPU and R_d between the cultivars (where P was <0.001 and 0.023 respectively). Significant differences amongst triose phosphate show that spelt Tauro

and emmer SB had high TPU and were therefore genotypes to show the least limitation to increasing atmospheric carbon dioxide concentration when compared to other genotypes. Both of these genotypes have been found to have high RUE in the previously reported field trials in 2010 and 2011 (Chapter Two).

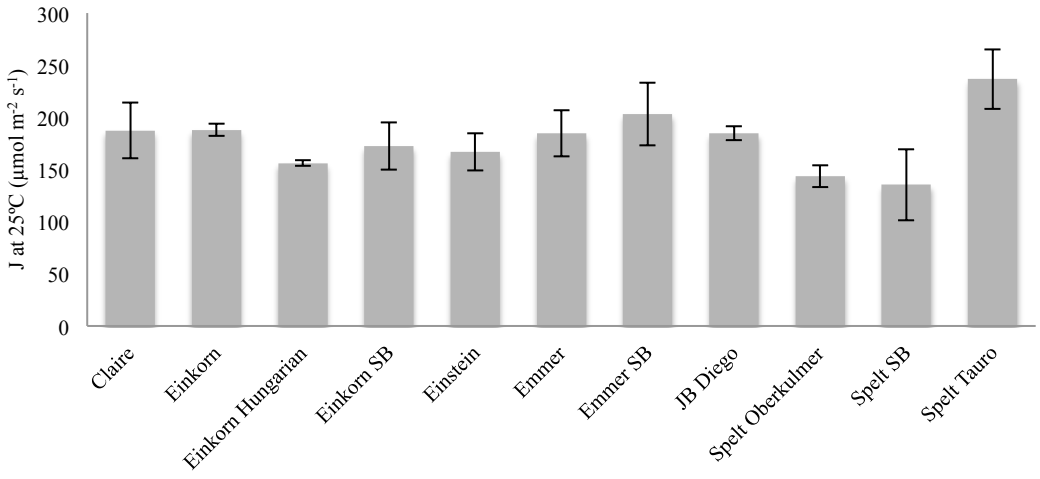
Spelt Tauro, spelt SB and einkorn SB had the greatest maximum rate of carboxylation whereas spelt Oberkulmer had the lowest V_{cmax}, potentially a result of reduced Rubisco concentrations, activity and/or specificity, or due to an increased affinity of Rubisco with oxygen, therefore reducing the efficiency of photosynthesis by the counter process, whereby CO_2 is lost through photorespiration. Einkorn SB and spelt Tauro displayed greater respiration rates compared to other genotypes. Einkorn hungarian had the lowest. Interestingly, modern bread wheat cultivars maintained a respiration rates between 6.2 and 4.5 μmol m^{-2} s^{-1}. This implies that cultivars may have had altered mitochondrial activity or different numbers of mitochondria. Electron transport rates were not significantly different.

Figure 3.4 is based on gas exchange at T leaf where block temperature was controlled however, there may have been some variation for leaf temperature thought to impact enzyme kinetics. Hence, the results were re-analysed and adjusted for a leaf temperature of 25°C to facilitate comparisons.

A



B



C

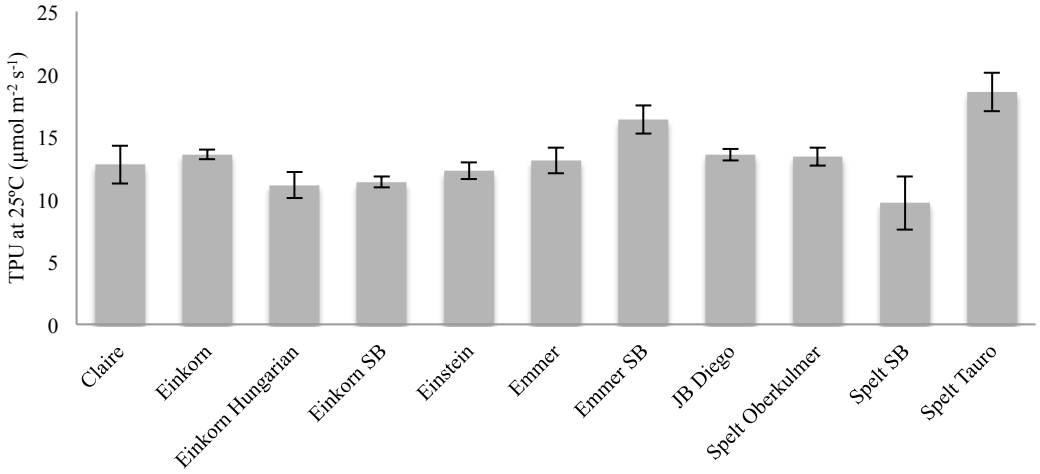


Figure 3.5 i: Values determined from fitted A/C_i curves with a normalised leaf temperature of 25ºC. A) shows the maximum rate of carboxylation (V_{cmax}). B) shows the rate of electron transport (J_{max}). C) shows the triose phosphate utilisation (TPU).

D

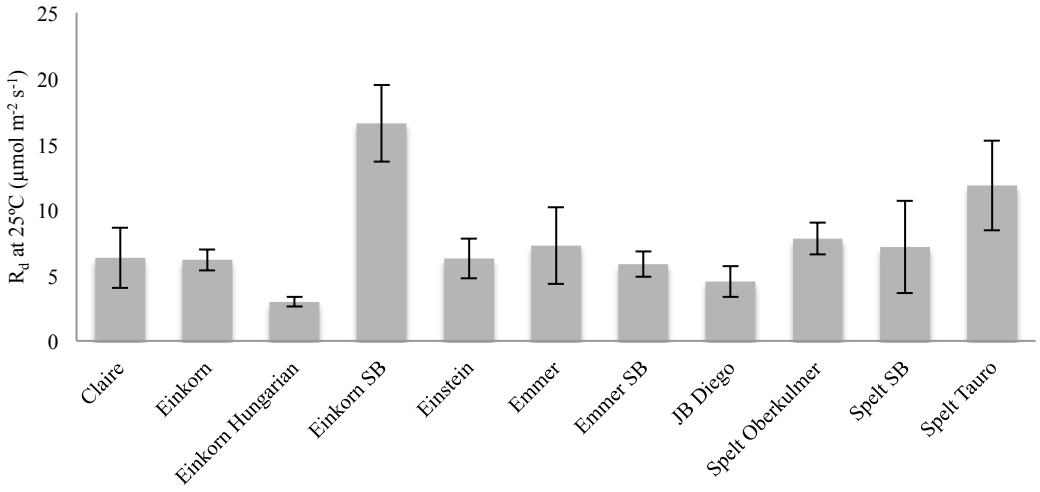


Figure 3.5 ii: Values determined from fitted A/C_i curves with a normalised leaf temperature of 25ºC. D) shows the determined respiration rates (R_d). Bars represent the standard error of the mean (where n equals 4) of each of the investigated genotypes.

The variance observed (Figure 3.5) for each of the measured paramteters was much like that observed without normalisation for leaf temoerature generally, genotypes were ranked similarly indicating that the variance between observed temperatures may not have had a large bearing on the results gained from the previous analysis. However, as observed in the previous analysis at T leaf, significant variation was only observed for TPU and R_d between the cultivars (P was <0.001 and 0.023, respectively). Significant differences amongst triose phosphate limitation show that spelt Tauro and emmer SB had the greatest TPU indicating a lesser degree of limitation imposed by the products of photosynthesis (namely triose phosphate but not exclusively). Both of these genotypes have been found to have high RUE in the previously reported field trials of 2010 and 2011 (Chapter Two).

As found observed in Figure 3.4, Spelt Tauro, spelt SB and einkorn SB had the greatest maximum rate of carboxylation whereas spelt Oberkulmer had the lowest V_{cmax}, potentially a result of reduced Rubisco concentrations, activity and/or

specificity, or due to an increased affinity of Rubisco with oxygen, therefore reducing the efficiency of photosynthesis by the counter process, photorespiration. Einkorn SB and spelt Tauro displayed greater respiration rates when compared to other genotypes where einkorn hungarian had the lowest R_d.

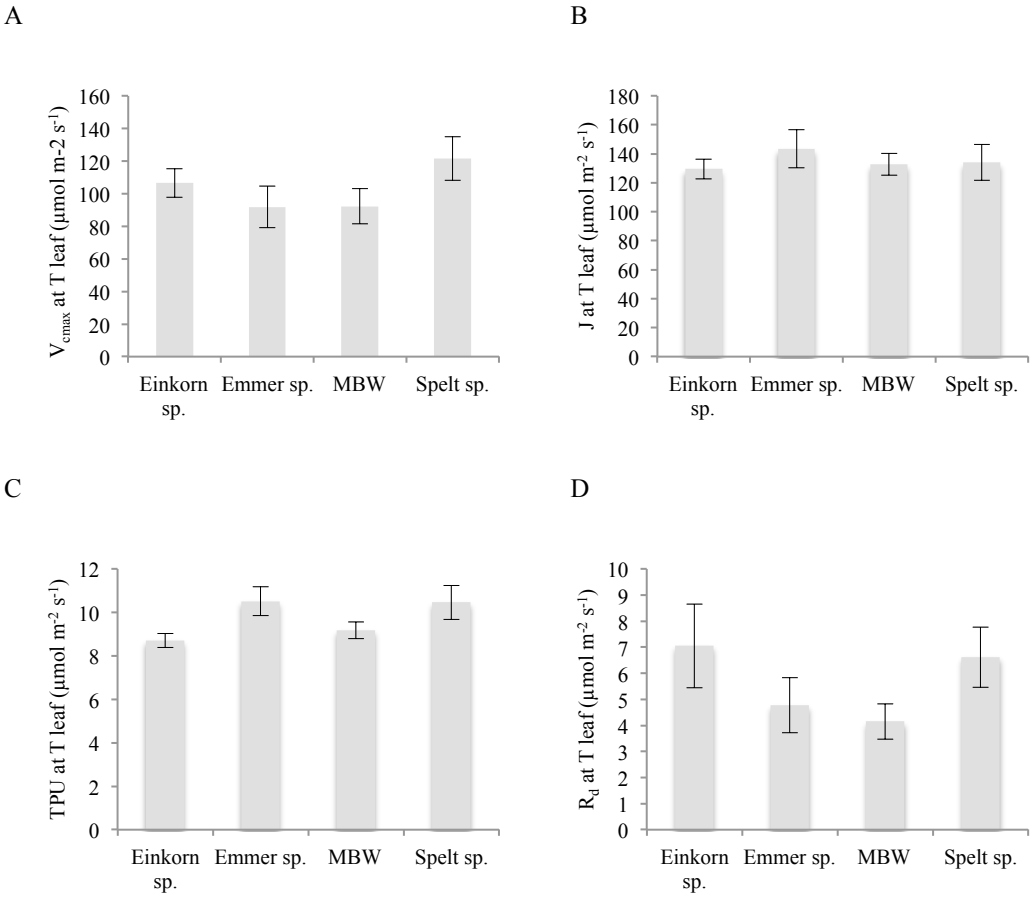


Figure 3.6: Values determined from fitted A/C_i (A/C_c) curves, performed with a block temperature of 20°C. A) shows the maximum rate of carboxylation (V_{cmax}), B) the rate of electron transport (J_{max}), C) the triose phosphate utilisation (TPU) and D) the determined respiration rates (R_d) for each of the investigated species. The bars represent the standard error of the mean.

When analysed by species, V_{cmax}, J and R_d were not significantly different (Figure 3.6). Triose phosphate utilisation was highest for spelt and emmer species, although narrowly missed being significant (P = 0.086) (Figure 3.6).

Once again, measurements were based on gas exchange at leaf temperatures and do not account for differences in temperature between the leaf chamber and the leaf. Hence, the results were re-analysed and adjusted for a leaf temperature of 25°C to facilitate comparisons.

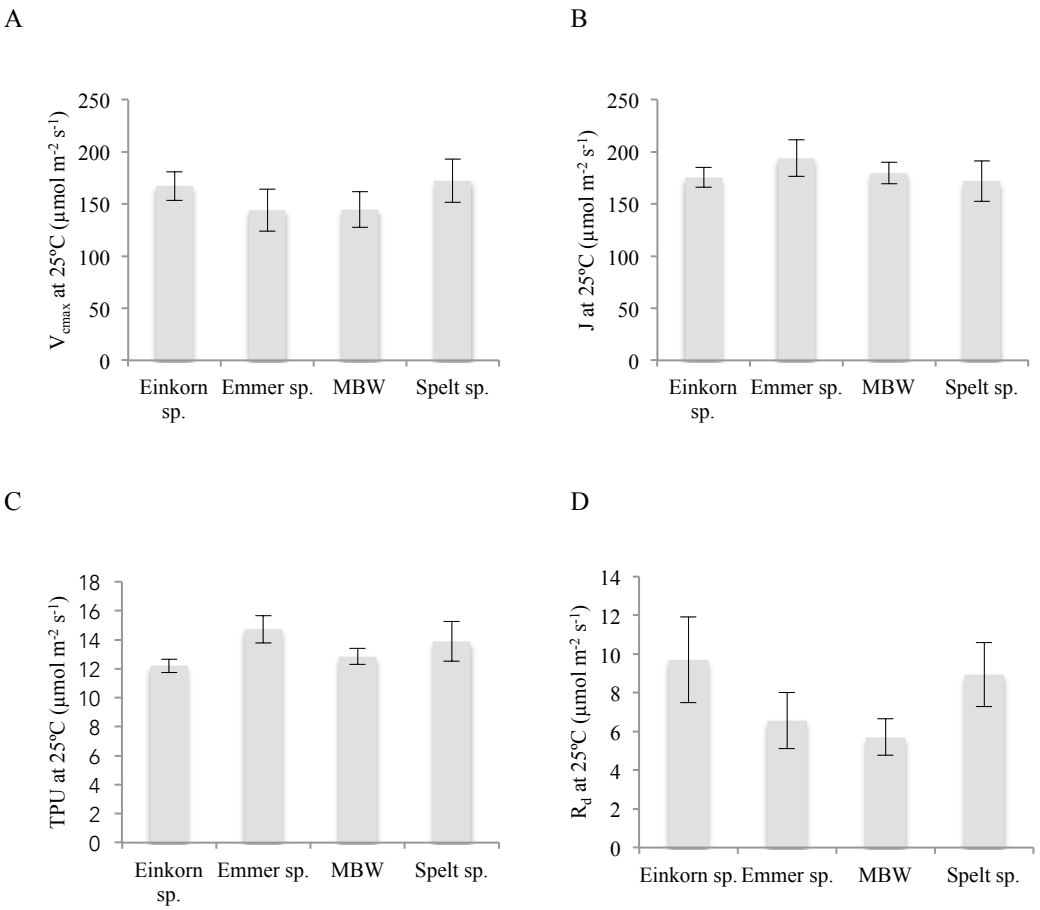


Figure 3.7: Values determined from fitted A/C_i (A/C_c) curves, with a normalised leaf temperature of 25ºC. A) shows the maximum rate of carboxylation (Vc_{max}), B) the rate of electron transport (J), C) the triose phosphate utilisation (TPU) and D) the determined respiration rates (R_d) The bars represent the standard error of the mean.

When analysed by species at 25ºC, V_{cmax}, J and R_d and TPU were not significantly different (Figure 3.7). Triose phosphate utilisation was highest for spelt and emmer species, although differences were not significant (Figure 3.7).

3.3.3 Glasshouse experiment II

In this experiment, some spelt genotypes remained in a vegetative state, either failing to reach anthesis or producing fertile shoots among many vegetative, prostrate tillers. This was observed late in the experiment, therefore these plants could not be replaced; growth analysis was continued however for the purposes of IRGA measurements, these particular plants were omitted from sampling.

3.3.4 Assessment of radiation use parameters using Infra-Red Gas Analysis

3.3.4.1 Photosynthetic light response curves

Radiation use parameters were derived from leaf responses to varying light levels. The response of all genotypes to changing light intensity was a logarithmic response curve in which initial photosynthetic rates were light limited producing a linear slope from which maximum quantum yields (Φ) were obtained. A_{sat} was also derived from the phase whereby the photosynthetic reaction was limited by Rubisco or CO_2. This was the point at which no significant increase in photosynthetic activity occurred as the leaf became light saturated. All genotypes displayed this trend although there was some variation for these parameters (shown in Table 3.3). Table 3.4 also shows species differences between these assessed traits.

Table 3.3: Radiation use characteristics of seven ancient wheat varieties and modern bread wheat, Xi19 for comparison. Parameters reported include the maximum rate of photosynthesis in saturating light (A_{sat}), the saturation at which leaves became saturated with light, quantum yields (Φ), light compensation point and respiration (R_d) for pre and post anthesis periods.

Genotype	A_{sat} (μmol m^{-2} s^{-1})		Quantum Yield (μmol m^{-2} s^{-1})		Light saturation (μmol quanta m^{-2} s^{-1})		Respiration (μmol m^{-2} s^{-1})	
	Pre-Anth	Post-Anth	Pre-Anth	Post-Anth	Pre-Anth	Post-Anth	Pre-Anth	Post-Anth
Einkorn	19.88	17.91	0.0423	0.0404	411.40	*	-0.35	*
Einkorn SB	28.22	17.65	0.0542	0.0373	445.00	473.30	-0.50	-0.84
Emmer	27.12	21.42	0.0489	0.0509	551.80	391.20	-0.84	-0.89
Emmer SB	21.40	19.18	0.0413	0.0493	499.60	364.50	-0.79	-0.95
Spelt Oberkulmer	16.59	16.53	0.0373	0.0388	472.50	393.00	-0.78	-1.41
Spelt SB	17.50	17.73	0.0355	0.0436	443.00	354.30	-1.17	-1.29
Spelt Tauro	16.54	18.68	0.0384	0.0405	416.90	470.20	-1.68	-2.04
Xi19	25.01	26.55	0.0505	0.0527	475.20	435.50	-0.37	-1.02
Mean	21.44	18.96	0.0436	0.0442	463.43	411.71	-0.81	-1.21
P Genotype		< 0.001		0.017		0.728		0.01
P GS		0.485		0.215		0.095		0.148
P Interaction		0.539		0.559		0.599		0.986
SED (DF)		2.838 (49)		0.00672 (47)		91.31 (47)		0.6597 (42)

* Denotes missing results

Table 3.4: Radiation use characteristics of four wheat species. Parameters reported include the maximum rate of photosynthesis in saturating light (A_{sat}), the quantity of light that saturates the leaf, quantum yields (QY), and respiration (R_d) for pre and post anthesis periods.

Genotype	A_{sat} (μmol m^{-2} s^{-1})		Quantum Yield (μmol m^{-2} s^{-1})		Light saturation (μmol quanta m^{-2} s^{-1})		Respiration (μmol m^{-2} s^{-1})	
	Pre-Anth	Post-Anth	Pre-Anth	Post-Anth	Pre-Anth	Post-Anth	Pre-Anth	Post-Anth
Einkorn sp.	21.35	17.75	0.0443	0.0385	417.00	473.30	-0.38	-0.84
Emmer sp.	23.31	20.67	0.0439	0.0504	517.00	382.30	-0.81	-0.91
MBW sp.	25.01	26.55	0.0505	0.0527	475.20	435.50	-0.37	-1.02
Spelt sp.	16.78	17.47	0.0375	0.0404	432.70	409.10	-1.42	-1.60
Mean	21.44	18.96	0.04	0.05	460.48	425.05	-0.74	-1.09
Genotype		< 0.001		0.002		0.402		0.001
GS		0.650		0.149		0.134		0.215
Interaction		0.640		0.269		0.256		0.821
SED (DF)		1.933 (57)		0.00472 (55)		62.59 (54)		0.4716 (49)

3.3.4.2 A_{sat}

The nature of the leaf level response to increasing light intensities is asymptotic. Therefore, A_{sat}, was considered to be the greatest reading of *A* at the end of the non-rectangular hyperbola response curve. There was significant variation among the different genotypes ($P < 0.001$), however differences between pre and post-anthesis were not significant and neither was the combination between factors (Table 3.3). Generally, A_{sat} decreased from pre-anthesis (21.44 μmol m^{-2} s^{-1}) to post-anthesis (18.96 μmol m^{-2} s^{-1}). At growth stage 39, einkorn SB, emmer and Xi19 showed higher than average flag leaf A_{sat}. All other genotypes were observed to have quite similar A_{sat} values, these ranged from 16.59 to 21.40 μmol m^{-2} s^{-1} (for spelt oberkulmer and emmer SB, respectively). Using A_{sat} as a means to assess overall photosynthetic capability, spelt Tauro performed poorly compared to other genotypes (16.54 μmol m^{-2} s^{-1}). Post-anthesis, Xi19 had the highest A_{sat} (26.55 μmol m^{-2} s^{-1}) although emmer and emmer SB (21.42 and 19.18 μmol m^{-2} s^{-1}) also had maximum photosynthetic rates that were greater than average.

Results indicated that photosynthetic capability reduced with flag leaf age, suggesting that the flag leaf may contribute to carbon accumulation to a greater extent pre-anthesis rather than post-anthesis. All genotypes followed this trend and reduced by an average of 12% except Xi19 and spelt Tauro and spelt SB for which A_{sat} increased from pre to post anthesis. Pre-anthesis, einkorn SB and emmer performed above average however, the extent to which these species 'lost' photosynthetic capability over the life of the flag leaf was comparably high (there was a 37 and 21% reduction in photosynthetic capability, respectively). The photosynthetic capability of spelt SB and spelt Tauro increased, although this was

only marginal (altering maximum photosynthetic rates by -1 and -2%, respectively). A_{sat} of spelt Oberkulmer was maintained from pre to post anthesis. Results indicate that although overall, spelt species may have low photosynthetic capabilities; these capabilities are much more conserved throughout the life of the flag leaf.

Assessment of A_{sat} by species showed significant species differences ($P < 0.001$) (Table 3.4). Emmer and MBW species had the greatest A_{sat} observed (23.31 and 25.01 µmol m^{-2} s^{-1}) compared to spelt species which displayed the lowest photosynthetic capacity (16.87 µmol m^{-2} s^{-1}) pre-anthesis and emmer displayed the greatest A_{sat} of all ancient species post-anthesis although differences were not significant between growth stages and species.

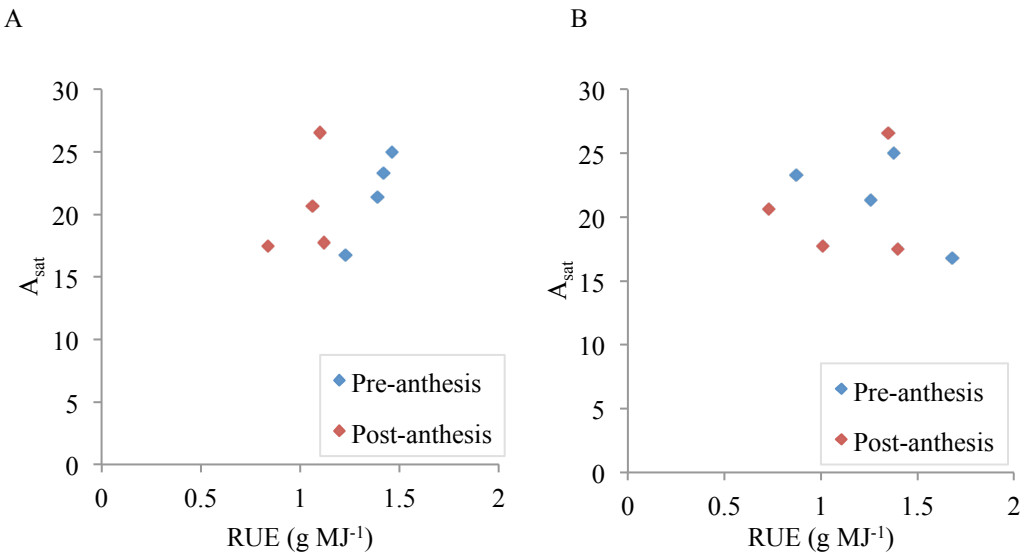


Figure 3.8: RUE and A_{sat} correlations. A) 2010 species pre and post-anthesis RUE against species pre- and post anthesis GH II A_{sat} ($r = 0.0232$). B) 2011 species pre and post-anthesis RUE against species pre and post-anthesis GH II A_{sat} ($r = -0.0822$).

Additionally, 2010 and 2011 RUE values were plotted for those genotypes where A_{sat} was obtained in GH II. When RUE and A_{sat} for pre and post anthesis were correlated (where pre and post anthesis values were plotted separately), none were

significant except for pre anthesis A_{sat} against pre anthesis RUE in 2010 (P = 0.0116). A positive relationship between pre and post anthesis A_{sat} and RUE however was observed in both years (Figure 3.8).

3.3.4.3 Light saturation point

The light intensity at which leaves were saturated was defined as the point at which increments in light intensity no longer impacted photosynthetic rates. At this stage, ATP and NADPH is produced in surplus where light independent reactions fix CO_2, therefore ambient CO_2 concentrations become limiting. Pre-anthesis point of light saturation ranged from 411.40 - 551.80 μmol m^{-2} s^{-1} (einkorn and emmer, respectively) (Table 3.3). Results showed that emmer, emmer SB and Xi19 had the highest light saturation point (expected due to the high A_{sat} observed). Post-anthesis light saturation showed that einkorn SB, spelt Tauro and Xi19 had light saturation points that were above average (411.71 μmol m^{-2} s^{-1}). The light saturation points of einkorn SB and spelt Tauro increased from growth stage 39 to 61 (increments of 6 and 13 % respectively), despite the consistent A_{sat} observed at these growth stages in spelt Tauro and the much reduced A_{sat} from growth stage 39 to 61 in einkorn SB. Generally, flag leaf light saturation reduced from growth stage 39 to 61 in all genotypes, except for einkorn SB and spelt Tauro, however genotypic differences and growth stage differences, as well as the interaction between these factors, were insignificant. Assessed by species also, there were no significant differences for light saturation point.

3.3.4.4 Quantum yield

Quantum yield is a measure of photosynthetic efficiency expressed in moles of photons absorbed per mole of CO_2 gained. Quantum yield (Φ) was derived from the

initial linear slope of the light response curve. The variation for Φ was measured in four species under which light intensities were photosynthetically limiting and atmospheric conditions were normal (400 μmol). The Φ of the genotypes assessed showed significant genotypic variation (P = 0.017). Pre-anthesis, average Φ was 0.0436 μmol m^{-2} s^{-1}. Einkorn SB, emmer and Xi19 had high Φ (0.05417, 0.0489, 0.05052 μmol m^{-2} s^{-1}), which was also the case for emmer and Xi19 post-anthesis (0.05094 and 0.05267 μmol m^{-2} s^{-1}, respectively). Large quantum yields indicate that initial photosynthetic rates, at low light intensities, are high, implying that initial increments in light intensity are better utilised. This may be a result of lower limitation on Rubisco by CO_2 concentrations (C_i). The general trend showed that Φ increased from growth stage 39 to 61 in all genotypes bar both einkorn species. Differences between the two growth stages were not significant and neither was the effect of growth stage and genotype combined.

When Φ was assessed by species, there were significant differences (P = 0.002) (Table 3.4); MBW had the highest Φ both pre and post-anthesis followed by emmer and einkorn. Spelt had the lowest quantum yield at both stages.

3.3.4.5 CO_2 loss through respiration

Respiration was empirically determined using the curve-fitting tool, Photosyn Assist (Dundee Scientific, Dundee UK). R_d infers the extent to which carbon assimilates are lost through mitochondrial respiration. There was significant variation for respiration rates among genotypes (P = 0.01) (Table 3.3). The average respiration rate was -0.81. Einkorn, einkorn SB and Xi19 had the least negative R_d. This implies that that einkorn, einkorn SB and Xi19 may possess increased photosynthetic efficiency simply by limiting respiration processes within the leaf. The largest deviation from

the mean was observed in spelt SB and spelt Tauro (-1.17 and -1.68, respectively). Post-anthesis, the average respiration rate reduced to -1.20. Einkorn SB and emmer had the highest R_d (-0.84 and -0.89, respectively). Spelt genotypes all had comparably lower R_d than other genotypes (-2.04, -1.41 and -1.21 for spelt Tauro, spelt Oberkulmer and SB, respectively). There was no significance of genotype or growth stage. Respiration rates were not significantly different by species and growth stage (Table 3.4).

3.3.5 Water Use Efficiency

3.3.5.1 ITE measurements

Instantaneous measurements allowed the relative water use efficiency at the leaf level to be determined which also assessed photosynthetic ability and transpiration rates of each genotype. Table 3.5 shows results for the genotypic assessments, whereas Table 3.6 shows the assessment of species.

Table 3.5: The instantaneous transpiration use efficiency, photosynthetic and transpiration rates of seven ancient wheat varieties and modern bread wheat, Xi19 for comparison whilst pre and post anthesis.

	ITE (mmol mol^{-1})		Photosynthetic rate (μmol m^{-2} s^{-1})		Transpiration rate (mmol m^{-2} s^{-1})	
	Pre-anth.	Post-anth.	Pre-anth.	Post-anth.	Pre-anth.	Post-anth.
Einkorn	7.30	7.18	22.81	16.10	3.40	2.49
Einkorn SB	6.67	5.90	20.94	13.82	3.46	2.24
Emmer	8.39	6.83	24.19	20.15	3.27	3.45
Emmer SB	8.05	3.87	18.54	15.04	2.41	4.18
Spelt Oberkulmer	6.65	7.52	13.34	14.30	2.07	2.08
Spelt SB	7.11	6.66	17.53	13.08	2.69	1.96
Spelt Tauro	6.28	6.64	15.98	13.97	2.62	2.52
Xi19	7.02	6.03	23.46	17.06	3.38	3.38
Mean	7.40	6.50	19.44	14.82	2.82	2.58
P Genotype		0.150		<0.001		<0.001
P GS		0.001		<0.001		0.649
P Interaction		<0.001		0.079		<0.001
SED (DF)		0.8388 (291)		2.052 (291)		0.4652 (291)

Emmer, emmer SB and spelt SB had high ITE (8.39, 8.05 and 7.11 mol mol^{-1}, respectively). MBW (Xi19) and einkorn (7.02 and 7.30 mol mol^{-1}) performed better than einkorn SB, spelt Oberkulmer and spelt Tauro (6.67, 6.65 and 6.28 mol mol^{-1} respectively) for ITE although genotypic differences were not significant. On average, ITE reduced over time from 7.40 mol mol^{-1} at growth stage 39 to 6.50 mol mol^{-1}, measured at growth stage 61 and these differences were significant (P = 0.001). This trend indicates that the younger leaves were generally more efficient although the opposite was true for einkorn and spelt Tauro which had increased ITE, post-anthesis. As well as being less efficient, post-anthesis ITE also showed much more variation, ranging from 3.87 - 7.52 mol mol^{-1}. Post-anthesis spelt Tauro had the highest ITE compared to einkorn, emmer and spelt Oberkulmer which also had ITEs that were above average. Although Xi19 had high ITE pre-anthesis, at later growth stages the efficiency of water use at the leaf level declined below average, when

compared to the other genotypes. The interaction between genotype and growth stage was highly significant (P <0.001).

Table 3.6: Instantaneous transpiration use efficiency, photosynthetic and transpiration rates of four wheat species both pre and post anthesis.

	ITE (mmol mol^{-1})		Photosynthetic rate (µmol m^{-2} s^{-1})		Transpiration rate (mmol m^{-2} s^{-1})	
	Pre-anth.	Post-anth.	Pre-anth.	Post-anth.	Pre-anth.	Post-anth.
Einkorn sp.	7.15	6.44	22.37	14.79	3.42	2.35
Emmer sp.	8.22	5.57	21.37	17.98	2.38	3.76
MBW	7.02	6.032	23.46	17.06	3.38	3.38
Spelt sp.	6.68	6.82	15.71	13.68	2.48	2.21
Mean	7.40	6.50	20.77	15.88	2.82	2.58
P Genotype		0.499		<0.001		<0.001
P GS		<0.001		<0.001		0.725
P Interaction		<0.001		0.029		<0.001
SED (DF)		0.6767 (299)		1.69 (299)		0.3742 (299)

When assessed by species, emmer had the highest water use efficiency pre-anthesis in terms of ITE followed by einkorn, modern bread wheat and spelt (P <0.001) (Table 3.6). Collated by species, spelt displayed increased ITE (by a small margin) from growth stage 39 to 61 whereas all other species declined (as observed when these results were analysed by genotype) however this is primarily owing to spelt Oberkulmer and spelt Tauro (spelt SB did not show a percentage increase in ITE over time). This indicates that whereas the other wheat species lost efficiency over time, generally spelt species have the capacity to maintain water use efficiency in the later stages of the growing season, a potentially useful trait where temperatures and radiation are high and water availability is low.

3.3.5.2 Instantaneous photosynthesis measurements

Measurements of photosynthesis and transpiration, those figures from which ITE was derived, were also analysed. Average photosynthetic rate, pre-anthesis was 19.04 mmol m^{-2} s^{-1}. Emmer, Xi19, einkorn and einkorn SB had higher than average rates of photosynthesis whereas spelt Oberkulmer and spelt Tauro had the lowest rates overall (Table 3.5). Genotypic differences were highly significant ($P < 0.001$) and so too were the differences between growth stage ($P < 0.001$). Photosynthetic rates reduced over time to 14.82 mmol m^{-2} s^{-1}. The lowest percentage decline in photosynthetic activity over time occurred for spelt Tauro, emmer and emmer SB (12.58, 16.70 and 18.88 %), interesting as these genotypes have been previously been observed to have superior radiation use efficiencies in field trials. Einkorn, einkorn SB and Xi19 reduced by the largest degree (29.41 and 34.00 and 27.28%). This reduction in photosynthetic rate from growth flag leaf emergence to after anthesis was characteristic of all genotypes except for spelt Oberkulmer which showed a pre to post-anthesis increase of 7.2%. Emmer species displayed high ITE pre-anthesis, which may have derived from high pre-anthesis photosynthetic rates. Modern bread wheat, Xi19 also displayed high pre-anthesis photosynthetic rates (23.46 mmol m^{-2} s^{-1}), which reduced by 27.28% post-anthesis. Spelt SB, also observed to have high ITE pre-anthesis however had photosynthetic rates that were lower than the average. The interaction between genotype and growth stage was not statistically significant.

Although photosynthetic rate was not significant by genotype, differences were statistically different by species ($P = 0.029$) (Table 3.6). Spelt had the lowest photosynthetic rate (15.71 mmol m^{-2} s^{-1}) pre-anthesis whereas einkorn, modern bread

wheat and emmer had comparably high photosynthetic rates (23.46, 22.37 and 21.37mmol m^{-2} s^{-1}). Post-anthesis, emmer and modern bread wheat maintained their high photosynthetic rate whereas einkorn and spelt photosynthetic rates decline substantially.

3.3.5.3 Transpiration rates

Transpiration rates ranged from 2.07 - 3.40 mmol m^{-2} s^{-1} pre-anthesis and from 1.96-4.18 mmol m^{-2} s^{-1} post-anthesis (Table 3.5). Average transpiration remained constant from pre to post anthesis and there was no clear trend; differences between growth stages were not significant. Spelt species had comparably low transpiration rates pre and post-anthesis whereas the highest transpiration rates were displayed by einkorn species and Xi19 pre-anthesis, and emmer SB, emmer SB and Xi19 post-anthesis (4.18, 3.45 and 3.38mmol m^{-2} s^{-1}, respectively). Differences between genotypes were significant ($P < 0.001$) and so too was the genotypic interaction with growth stage ($P < 0.001$).

Assessed according to species, transpiration rates were highly significant ($P < 0.001$) (Table 3.6). Emmer and spelt species had similar pre-anthesis transpiration rates, both lower than average, whereas those of einkorn and modern bread wheat were comparably high. Post-anthesis, emmer and MBW had the greatest transpiration rates and conversely spelt had very low transpiration rates. This is indicative of the differing mechanisms whereby ITE is maintained, thought to be maintained in spelt with low transpiration rates contrasting with emmer species which have greater photosynthetic rates.

3.3.5.4 Internal stomatal CO_2 concentrations

During measurements to assess photosynthesis and transpiration in investigated genotypes, stomatal response data was also collected. Table 3.7 shows results for the genotypic assessments, whereas Table 3.8 shows average across species.

Table 3.7: Stomatal responses during ITE measurements of seven ancient wheat varieties as well as modern bread wheat, Xi19 for comparison, both pre and post anthesis. Table includes internal stomatal CO_2 concentrations, the ratio between internal internal stomatal CO_2 concentrations and atmospheric CO_2 concentrations, stomatal conductance as well as intrinsic water use efficiency.

	Internal stomatal CO_2 concentrations (C_i) (μ mol mol^{-1})		Internal stomatal/atmospheric [CO_2] (C_i/C_a) (μ mol mol^{-1})		Conductance (G_s) (μ mol mol m^{-2} s^{-1})	
Genotype	Pre-anth.	Post-anth	Pre-anth	Post-anth	Pre-anth	Post-anth
Einkorn	201.6	200.8	0.5127	0.5084	0.2216	0.1746
Einkorn SB	191.8	225.3	0.4882	0.5691	0.1887	0.1391
Emmer	229.9	285.2	0.5896	0.7280	0.3493	0.4963
Emmer SB	273.8	301.5	0.6971	0.7663	0.3048	0.4540
Spelt Oberkulmer	134.1	153.8	0.3403	0.3900	0.0964	0.1064
Spelt SB	182.9	172.5	0.4651	0.4365	0.1488	0.1005
Spelt Tauro	196.6	233.8	0.5171	0.5304	0.1520	0.1334
Xi19	265.1	332.7	0.6783	0.8458	0.3977	0.5150
Mean	214.40	222.80	0.5491	0.5499	0.2409	0.2106
P Genotype		<0.001		<0.001		<0.001
P GS		0.07		0.019		0.168
P Inter.		0.607		0.062		0.010
SED (DF)		32.95 (291)		0.05225 (291)		0.06188 (291)

Table 3.8: Parameters indicating stomatal behaviour during ITE measurements both pre and post anthesis. Table includes internal stomatal CO_2 concentrations, the ratio between internal internal stomatal concentrations and atmospheric CO_2 concentrations, stomatal conductance as well as intrinsic water use efficiency.

	Internal stomatal CO_2 concentrations (C_i) (μ mol mol^{-1})		Internal stomatal/atmospheric [CO_2] (C_i/C_a) (μ mol mol^{-1})		Conductance (G_s) (μ mol mol^{-1})	
Genotype	Pre-anth.	Post-anth	Pre-anth	Post-anth	Pre-anth	Post-anth
Einkorn sp.	199.3	215	0.5069	0.5434	0.2139	0.1541
Emmer sp.	251.8	292.1	0.6433	0.7443	0.327	0.4784
MBW	265.1	332.7	0.6783	0.8458	0.3977	0.515
Spelt sp.	172.7	193.3	0.4449	0.4648	0.1338	0.1148
Mean	222.23	258.28	0.56835	0.649575	0.2681	0.315575
P Genotype		<0.001		<0.001		<0.001
P GS		0.018		0.003		0.162
P Inter.		0.668		0.035		<0.001
SED (DF)		27.13 (291)		0.04382 (299)		0.04897 (299)

ITE has been determined using measurements of instantaneous photosynthetic rate and transpiration rate however, the dynamic nature of these measurements mean that the observed values can be analysed further. This analysis relates to stomatal behaviour of which conductance and internal stomatal versus atmospheric carbon dioxide concentration can be informative of the way in which plants utilise water and CO_2 because photosynthesis and water loss through transpiration are interdependent processes. The influx and outflow of these gases underlies the plants' capacity to acquire CO_2 and the efficiency with which it does this.

The current experiment assessed the variability for the internal stomatal CO_2 concentration for each of the genotypes (Table 3.7). C_i averaged 214.40 pre-anthesis

and 222.80 μmol mol^{-1} post-anthesis, there was no significant difference in C_i between growth stages. C_i was highest in emmer, emmer SB and MBW, Xi19 (229.9, 273.8 and 265.1 μmol mol^{-1}) and lowest for spelt Oberkulmer and SB (134.1 and 182.9 μmol mol^{-1}) pre-anthesis, although einkorn species also had lower than average internal stomatal CO_2 concentrations. Genotypic differences were highly significant ($P < 0.001$) although the interaction was not. Genotypic differences were also mirrored post-anthesis with emmer, emmer SB and Xi19 having the greatest internal concentrations of CO_2. As would be expected, where photosynthetic rates were reported to be high in Table 3.7, C_i was also high for the same genotypes indicating that the internal concentrations of CO_2 could have a bearing on photosynthetic activity. Species differences were not statistically significant (Table 3.8).

Assessment of the ratio between internal and atmospheric CO_2 concentration showed emmer, emmer SB and Xi19 to have a high ratio between internal and external CO_2 concentrations where these genotypes had greater C_i/C_a than the pre-anthesis average (0.5491 μmol mol^{-1}). This was also the case post-anthesis where emmer, emmer SB and Xi19 had the greatest ratio of internal stomatal to atmospheric CO_2 concentrations (0.7280, 0.7663 and 0.8458 μmol mol^{-1}) expected as measurements were carried out in a fixed atmospheric CO_2 concentration. As was the case of C_i assessment, C_i/C_a was significantly affected by growth stage ($P = 0.019$) and by genotype ($P < 0.001$) however the interaction between the two was not ($P = 0.062$).

When assessed by species, C_i/C_a was significant ($P = 0.035$) (Table 3.8). Results mirrored the genotypic assessment of data where emmer and MBW had comparably

high internal stomatal CO_2 to atmospheric CO_2 concentrations, both pre and post anthesis when compared to einkorn and spelt species.

3.3.5.5 Stomatal conductance for CO_2

Conductance was higher in genotypes with higher photosynthesis (Table 3.7). Stomatal conductance was highest in emmer, emmer SB and Xi19, whereas spelt species had the lowest conductance observed pre-anthesis. This genotypic ranking was also mirrored post-anthesis. Genotypic differences were significantly different ($P < 0.001$) as was the interaction between genotype and growth stage ($P = 0.010$). Differences among species were also highly significant and reflected that observed when this trait was analysed by species; emmer and MBW had much greater conductance compared to einkorn and spelt species (Table 3.8).

3.3.6 GH II accumulated biomass

In glasshouse experiment II, component analyses were performed to determine how much carbon was being assimilated and to where it was being accumulated (data not shown). Also through growth analysis, harvestable yield, the total amounts of biomass accumulated (provided in m^{-2}) as well as Harvest Index were calculated (Table 3.9).

Table 3.9: Grain harvested (m^{-2}), total above ground biomass and harvest index of seven ancient and one modern bread wheat from glasshouse experiment II where plants were grown in 1m columns.

Genotype	Grain yield (m^2)	Total biomass (g m^{2-1})	Harvest Index
Einkorn	469.8	1222	0.38
Einkorn SB	447.6	1413	0.32
Emmer	493.5	1634	0.30
Emmer SB	448.7	1578	0.30
Spelt Oberkulmer	202.8	2978	0.13
Spelt SB	41.5	1989	0.07
Spelt Tauro	183.5	1875	0.17
Xi19	775.0	1269	0.61
P	<0.001	<0.084	<0.001
SED (37 DF)	98	291	0.04

Spelt SB produced the least grain m^2 however this was thought to be a result of poor development, as many spelt SB plants produced prostrate tillers which did not develop to produced grain or had few shoots which did develop to grain filling. Unsurprisingly, modern bread wheat produced the greatest grain yield per m^2 (775g m^2). Emmer and einkorn also had comparatively high grain yield also. Differences between genotypes were highly significant ($P < 0.001$).

Spelt Oberkulmer and spelt SB produced among the largest amounts of dry biomass (2978 and 2989 g m^{-2}) however this may have been due to several of the spelt plants included in the experiment not developing as expected. Plants produced lots of tillers with few shoots actually setting grain, which may have been a result of incomplete vernalisation. It is interesting to note, that although Xi19 produced among the least total biomass, grain yield was significantly better, a trait common in modern wheat through breeding.

Biomass and harvestable yield in glasshouse experiment II did not appear to mirror ITE results. Simplified, it would be expected that those genotypes where photosynthetic rates were highest, may have the greatest biomass production or grain

yield. For genotypes such as Xi19, einkorn and emmer, this was not the case. However this might be an oversimplification as spelt Oberkulmer, shown in Table 3.9 to produce the most biomass, was observed to have the most consistent photosynthetic rates from pre to post anthesis (Table 3.5).

3.3.7 Water Extraction

From theta probe data, it was possible to calculate the quantities of water extracted per column soil layer as well that extracted by the plants per column (data not shown). Cumulative water uptake data was used to quantify overall WUE (derived from the quantity of biomass relative to the accumulated water extracted from the soil profile). Table 3.10 shows the average WUE for genotypes where emmer and spelt Oberkulmer had the greatest WUE observed (3.93 and 4.51) ($P < 0.001$). Spelt Tauro and einkorn also had comparably high WUE. Spelt SB and MBW, Xi19 were the least efficient in terms of biomass produced to water utilised.

Table 3.10. WUE (ratio of biomass to cumulative water extracted) (g l^{-1}) for genotypes in glasshouse experiment II.

Genotypes	WUE (g l^{-1})
Einkorn	3.45
Einkorn SB	2.73
Emmer	3.93
Emmer SB	2.97
Spelt Oberkulmer	4.51
Spelt SB	1.87
Spelt Tauro	3.23
Xi19	2.82
Genotype	0.22
GS	<0.001
Interaction	<0.001
SED (DF)	1.209 (46)

3.3.8 Stay green traits

Green area persistence was observed in glasshouse experiment II. Genotypic differences were significantly different ($P < 0.001$) (Figure 3.9). As observed in previous experiments, plants generally followed the same trend, by maintaining flag leaf 'greenness' until approximately 160 DAS except for spelt Oberkulmer, Tauro and SB. These genotypes maintained green area with high SPAD values observed even beyond sampling indicating the presence of stay green. This was observed to a greater extent in the current results compared to previous field trials, potentially a result of the drought imposed (80% pre-anthesis and 50% post-anthesis) causing these genotypes to exhibit a stress response. Alternatively, green persistence may be observed due to the abnormal development witnessed for some spelt plants.

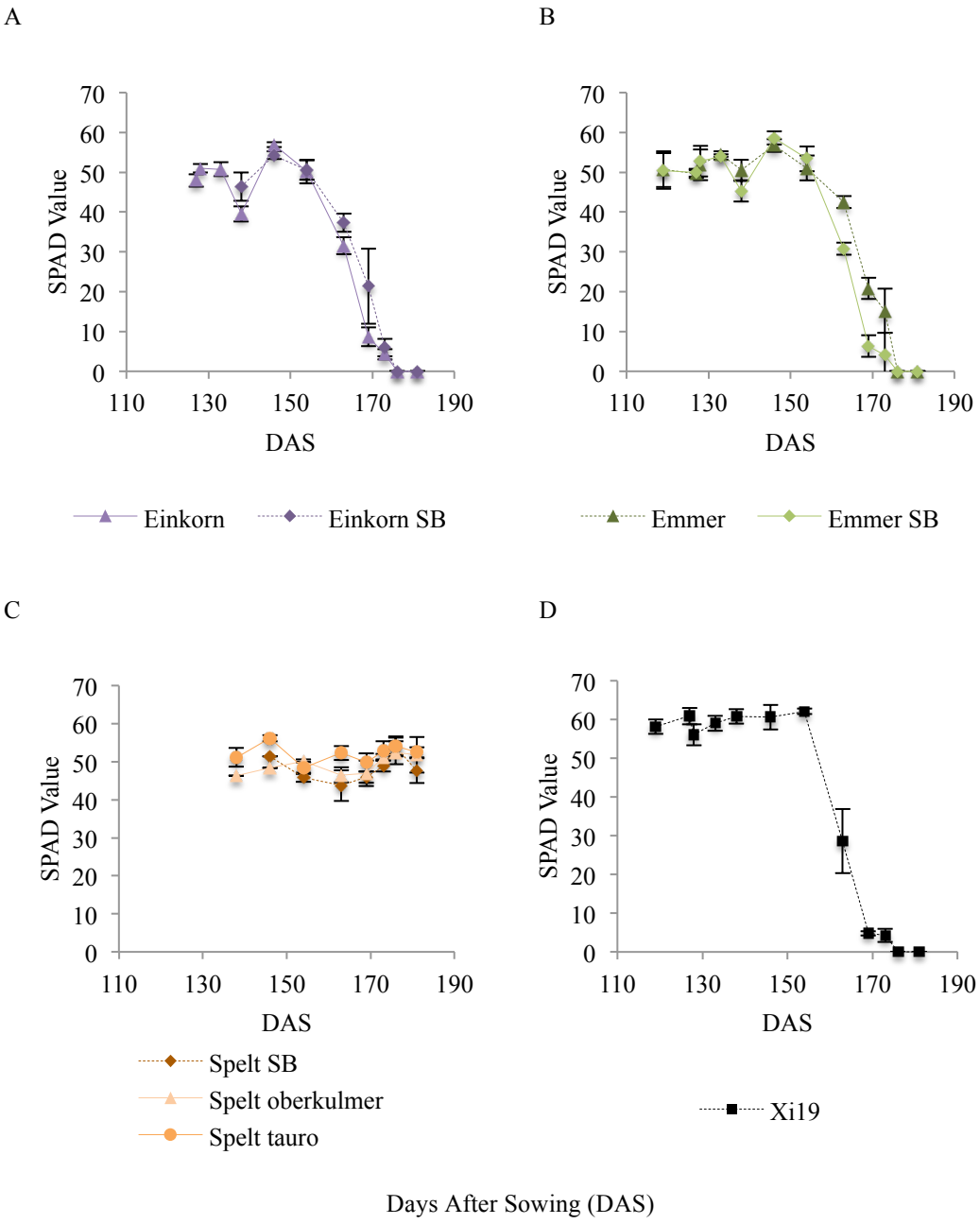


Figure 3.9: SPAD values throughout glasshouse experiment II (DAS) for A) spelt, B) einkorn, c0 spelt and D) MBW cultivars (error bars denote SEM).

Analysis by species also showed significant differences where MBW, emmer and einkorn species all declined to 0 (SPAD value) at ~180 DAS ($P < 0.001$) (Figure 3.10). Spelt had a comparatively lower SPAD value at the start of the season however, maintained this for longer.

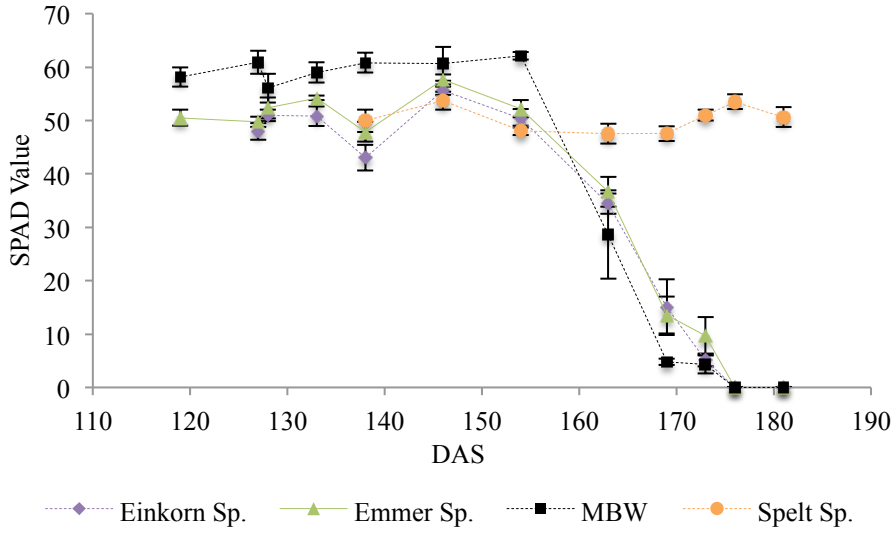


Figure 3.10: SPAD values throughout glasshouse experiment II (DAS) for all four investigated species (error bars denote SEM).

These data show the potential presence of green area persistence in spelt species however it is also important to consider the difference for developmental rates between species as this may confound the observed results. When interpreting these results it is therefore necessary to take note of the disparity between species, particularly for developmental rates. Although results do indicate that whereas MBW tended to have significantly higher SPAD values at the beginning of the season, this was not maintained and SPAD values indicated that chlorophyll content reduced at a much faster rate than it did for spelt species.

3.4 Discussion

The previous chapter indicated that there may be some resource utilisation differences between the genotypes. This chapter aims to widen the scope to look for characteristics that may discern where this variation comes from by scaling analyses down to the leaf level. Wullschleger (1993) found that there were differences in the biochemical reactions that regulated gas exchange between species (although no differences were found among agricultural crops). The current work intends to observe a small number of parameters to see whether these ancient wheat species differ in their capacity to assimilate CO_2 interpreted from A/C_i response curves.

3.4.1 Biochemical parameters

Based on the analysis, the maximum rate of carboxylation, V_{cmax} ranged from 85.6 for modern bread wheat, Claire to 151.8 μmol m^{-2} s^{-1} for spelt SB, and after normalising the data for temperature, from 132.7 and 209.1 μmol m^{-2} s^{-1} (Einstein and spelt Tauro, respectively). It would be expected that an increase in maximum rate of carboxylation would be fundamental to superior RUE. Although differences between both leaf temperature data sets showed no statistical significance, interestingly einkorn and spelt Tauro, already observed to have high RUE in field trials (2010 and 2011, respectively) displayed superior V_{cmax}. Pre-anthesis RUE was not statistically significant in 2010 but was in 2011. This may be indicative of greater V_{cmax} which could be due to an increased level of Rubisco enzyme, increased oxygenation activity Rubisco, or increased active site numbers (Long & Bernacchi, 2003). It may be purported that these genotypes have superior RUE. Further analysis may potentially look further into the leaf level traits, for instance assessment of Rubisco or nitrogen levels per leaf area (Sage, 2002). Results among modern bread

wheat generally had a consistent V_{cmax} across all cultivars with species average of 144.6 μmol m^{-2} s^{-1}, whereas between cultivars of other species there was a wider spread. Einkorn and spelt species generally had the greatest V_{cmax} compared to other genotypes although the current results showed that V_{cmax} was not significantly different between the species.

Spelt Tauro and emmer SB, were seen to have the greatest electron transport rates (J_{max}), indicating potentially increased regeneration rates for Ribulose 1-5 bisphosphate (RuBP), although results were not statistically significant. Increased J_{max} indicates a more efficient electron transport system, which would advantage genotypes. This could be potentially indicative of superior assimilation capacity. Such an advantage could be instructive of the high biomass production and RUE observed for spelt Tauro in the 2011 field trial (Chapter Two).

Spelt Tauro, observed to possess a high TPU may potentially have a high photosynthetic capacity. Furthermore, the limitation imposed by the triose phosphate utilisation (TPU) phase of the carbon dioxide response differed among genotypes at both T leaf and 25°C leaf. Spelt Tauro was observed to have the highest rate of triose phosphate utilisation, reducing the potential inhibition of carbon assimilation following on from the accumulation of chloroplast products such as triose phosphate. At this point, the leaf is saturated as it cannot increase assimilate production; it will not respond to increasing CO_2 nor is it impeded by increased oxygen levels (Sharkey *et al*., 2007). This limit provides some indication of the boundaries of the leaf, in terms of the light saturated photosynthetic rate, A_{sat} (Sharkey *et al*., 2007). Results indicated emmer SB and einkorn to potentially have advantageous TPU (analysis when the leaf temperature was 25°C).

The data here also show that R_d was different among the genotypes. R_d represents the CO_2 lost through respiration. Although far from the bounds of the current project, it may be informative to investigate leaf physiology in order to see whether the leaf machinery differs among genotypes, which would typically be expected to affect photosynthetic capacity. Analysed by species, the differences were still present with einkorn species displaying high and modern bread wheat, low day respiration rates.

In this study the photosynthetic parameters such as V_{cmax}, J, and TPU for flag leaves of plants were estimated and the response characteristics of leaf-level photosynthesis were investigated. These results show that there is a wide range of estimates for the biochemical capacities that regulate CO_2 assimilation for R_d and TPU only, although it was observed that V_{cmax} and J_{max} were highest for genotypes shown to perform well in terms of RUE. However, due to a small sample size, there is a lack of statistical significance. Furthermore, the data gained from the current experiment was noisy with large standard errors, potentially a result of the high variance observed when curve fitting using the model constructed by Sharkey *et al*., (2007). When interpreting CO_2 response curves, it can be difficult to identify the limitation phase, which is usually the TPU. However, any of these phases may be absent or unapparent in any data set (Long & Bernacchi, 2007) therefore estimation problems can be significant. This highlights the subjectivity present when fitting curves, which shows that although assumptions can be made, these are simply indicative.

3.4.2 Biochemical parameters from A/C_i response curves

The data from this component of the project does not explain the differences in productivity between genotypes observed in previous field trials. Although measures were taken to ensure the best possible results, for instance maintaining a sampling

window of three hours either side of noon to reduce the stomatal regulation, the results might also have been skewed by the sampling procedure. For practicality, measurements were made in the laboratory and plants were therefore transported from the glasshouse into a room with a lower incident light, although light exposure to the leaf sampled was maintained at 1000 μmol m^{-2} s^{-1} across to simulate normal light conditions. However, this may have altered the photosynthetic behaviour of the plants as they were transferred from normal ambient light conditions, into an environment with reduced ambient light. It is a possibility that plants may have adjusted photosynthesis levels in accordance with ambient light conditions prior to measurement, potentially reducing their photosynthetic efficacy.

A comparative experiment such as this one would benefit from analyses of leaf morphological traits with the aim to link these back to traits such as increased V_{cmax} and J_{max}. Although differences were not significant, the data outlined in this chapter is consistent with findings from field experiments indicating that spelt Tauro, spelt SB, einkorn and einkorn SB may have favourable characteristics that allow them to better use radiation. These findings warrant further investigation so that any true differences may be discerned.

3.4.3 Genotypic comparisons of photosynthetic efficiency from A/C_i responses

The experiments performed in Chapter Two assessed a wide variety of traits in the field. Results indicated that some of these ancient wheat genotypes harboured resource use efficiency traits, although it was not clear as to where these differences originated. To explore this further, a glasshouse experiment investigating the photochemical processes involved in photosynthesis, was established. It assessed a range of leaf level traits. No significant variation was observed however, results

indicated that certain genotypes may possess favourable characteristics, potentially making them better able to utilise radiation. For this reason, the following experiment was constructed with the aim to further explore these genotypes within a wider context of radiation capture and water utilisation at the leaf level and to observe a wide range of parameters related to CO_2 assimilation and water utilisation in a sub-set of modern and ancient wheat cultivars.

3.4.3.1 Light response parameters

There is no discrete sensor for photosynthesis, however photosynthetic rates can be calculated from recorded gas flow measurements (Pearcy *et al.*, 1989). By doing so, A_{sat} can be described. A_{sat} is defined as the maximal rate of photosynthesis under light saturated conditions in atmospheric CO_2 conditions. A_{sat} ranged from 16.54 to 28.22 μmol m^{-2} s^{-1} pre-anthesis and 16.53 to 26.55 μmol m^{-2} s^{-1} post-anthesis. Generally A_{sat} reduced between pre-anthesis and post-anthesis indicating that photosynthetic ability of the flag leaf reduced with age, except in spelt SB and Tauro (also observed in spelt genotypes in the previous data set). A_{sat} also increased with leaf age in modern bread wheat, Xi19. Superior A_{sat} was observed in emmer, emmer SB and einkorn SB pre-anthesis, indicating that these genotypes had an enhanced ability to assimilate carbon at saturating irradiances. Interestingly, these genotypes also had a greater ability to assimilate carbon in light limited conditions, indicated from their high quantum yields.

An increased ability to assimilate carbon, perhaps due to reduced Rubisco limitation, or alternatively increased Rubisco concentration and activity, has been previously reported to correlate with increased A_{sat} (Evans, 1996; Terashima *et al.*, 2011). In glasshouse experiment II, emmer and Xi19 had greater than average post anthesis

A_{sat}, which was in contrast to previous field results showing that emmer had low post-anthesis RUE in 2010 (1.00g MJ^{-1}) and 2011 (0.22g MJ^{-1}) although RUE was observed to be particularly low in the latter year, thus the conclusions based on these data were not entirely clear. Interestingly, einkorn SB, observed to have high pre-anthesis A_{sat}, was also observed to have higher RUE compared to other genotypes across both field trial years. Results generated from the light curve response data also highlighted that spelt SB and Oberkulmer had comparatively low A_{sat}, corresponding with low RUE in the 2010 field trial. This data was also inconsistent with RUEs observed in 2011 where spelt Oberkulmer and SB had comparatively high RUE. Despite being low, the A_{sat} for spelt genotypes were fairly consistent from pre to post anthesis and actually increased with leaf age for spelt SB and Tauro. This stability for carbon accumulation could indicate that the stay green trait suggested by SPAD measurements and visual scoring (Chapter Two) was 'functional', i.e. was still photosynthesising and therefore contributing to carbon assimilation. Thus, although other genotypes may well have an enhanced ability to assimilate carbon at limited and saturating light intensities, spelt Tauro and SB may maintain A_{sat}, providing a basis for the high RUE previously reported.

Results suggest that there are genotypic differences for photosynthetic capability. These may be indicative of chloroplast function linked to the photochemical processes of Rubisco (Beadle & Long, 1985) since Rubisco catalyses the reaction that fixes CO_2 to accumulate carbon in photosynthesis and O_2 readily competes to reverse this reaction, the amount of *in vivo* Rubisco can be rate limiting in carbon assimilation (Murchie *et al.*, 2009). Alternatively, differences may derive from biochemical or mechanistic variances between genotypes. Theoretically, it may be possible to increase light photosynthetic rates by increasing the photosynthetic

machinery per unit area leaf, (although there are limitations on accumulated protein per chloroplast and numbers of chloroplasts per mesophyll cell (Murchie *et al*., 2009). It is therefore possible that the variance observed for A_{sat} in the current experiment is due to differences in leaf architecture between genotypes. Another suggestion relates to biological variation for Rubisco specificity to CO_2 (Murchie *et al*., 2009). Where greater specificity has been reported, catalytic carboxylation rates have been observed to reduce (Zhu & Spreitzer, 1996; Murchie *et al*., 2009).

Quantum yields are commonly reported to be higher within C_4 plant species due to the modified carbon accumulation mechanisms which reduces CO_2 limitations and increases internal resistances (Aggarwal & Sinha, 1983). However, variation for Φ in C_3 genotypes may also indicate differential C_i or increased internal resistances enhancing photosynthetic efficiency at low light levels. Although those genotypes that displayed high A_{sat} were also observed to have high Φ (einkorn SB, emmer and Xi19) there were no significant differences. Interestingly however, all genotypes except for einkorn and einkorn SB had increased Φ post-anthesis, potentially an adaptation that increases flag leaf productivity during periods when irradiance is typically higher (in the UK winter wheat growing season). A similar trend was observed for pre and post anthesis A_{sat} also (although einkorn SB and both emmer genotypes were not greater post-anthesis). Φ was relatively consistent across the two time periods, which supports Ehrlinger & Bjorkman (1977) who stated that generally Φ is stable within C_3 species. Positive associations were observed between RUE and Φ in 2010 and 2011 (data was not shown). Φ observed in glasshouse experiment II ranged from 0.036 to 0.053, which are consistent with the findings of Ehleringer & Pearcy (1983) for the average Φ of a C_3 grass species (0.053 μmol m^{-2} s^{-1}). Ehleringer & Pearcy (1983) state that variation for Φ is commonly a result of

differences between the initial light requirements for energy conversion as well as CO_2 escape (which eventually reduces Φ), this may account for some of the differences observed.

A_{sat} was highest for MBW then emmer, einkorn and spelt. Post anthesis, emmer and einkorn reduced in photosynthetic ability whereas MBW, Xi19 and spelt species increased. This may be a result of the increased green area longevity previously observed in spelt genotypes, potentially increasing the duration of crop growth therefore making best use of high irradiance, post anthesis. Such differences are thought to stem from the chloroplast function and be linked to photochemical process or alternatively may be due to the differences in developmental rates observed.

The light response curves showed a varied reaction to light where some plants were better able to utilise available PAR; as discussed above, this may be a result of a number of biochemical or mechanistic characteristics of the leaf, which will inevitably affect the convexity of the response. Leverenz (1994) developed an equation that can be used to describe convexity, which relates to the progressive rate of bending between the linear gradient and maximum photosynthetic values using the light response curve. This may allow assumptions to be made regarding photosynthetic productivity (Leverenz & Jarvis, 1979) and a less subjective and more quantitative analysis of the leaf response to light. This, however, was outside the scope of the current work although data was transformed and curves fitted using some of the fundamental themes described by Leverenz (1994).

Results indicate that einkorn SB and emmer have high A_{sat} rates although this was not reflected in RUE from the 2010 and 2011 field trials. It would be expected that

increased maximum photosynthetic ability would denote highly efficient use of radiation (therefore high RUE), although it is also pertinent that carbon assimilation involves a large array of integrated reactions and processes. Snaydon (1991) states that increased A_{sat} does not necessarily denote an enhanced ability to produce biological yield, particularly under typical environmental conditions, which are often less than optimal. As a result, many studies have shown that the A_{sat} is rarely achieved (Murchie *et al*., 2009). This makes it particularly difficult to describe carbon assimilation in any way that is meaningful for agricultural purposes. However, Dempster (2013) and Ngyuen (2014) did find a relationship between glasshouse measured A_{sat} and field measured RUE.

Research has shown respiration processes to have protective and metabolic roles in plant growth and development, particularly whilst under environmental stresses. However, the process also has significantly deleterious effects. Respiration processes whilst plants are in lit conditions refer to CO_2 production from mitochondria and accounts for significant proportions of carbon lost by plants (Miao *et al*., 2009). This has been highlighted when doubling the CO_2 concentrations, biological yield production increases for a range of crops (Murchie *et al.,* 2009). Furthermore, there are theoretical models that suggest that under favourable conditions, removal of respiration could enhance yields considerably (Murchie *et al*., 2009).

Light response curves were fitted to data using the statistical analysis program Photosyn Assistant (Dundee Scientific, Scotland) which quantified respiration rates due to mitochondrial activity. Light respiration ranged from -2.04 to -0.35 μmol m^{-2} s^{-1}. Spelt SB, Tauro and Oberkulmer had lower respiration rates pre and post-anthesis however there were no significant differences for assimilation under light

respiration conditions for genotypes and growth stage. Respiration for einkorn, emmer and modern bread wheat genotypes was typically much higher inferring that these genotypes had reduced respiratory processes, potentially making them more efficient. During the life of a crop, the relative contributions of respiration to growth and maintenance alters with age and weight of the crop (Azam-Ali & Squire, 2003) and although respiration was observed to reduce between pre and post-anthesis, indicating that more assimilates were lost due to respiration, no differences were observed between growth stage or growth stage and genotype combined.

3.4.4.2 Instantaneous Transpiration Efficiency

Carbon gain and water loss in plants are intricately related, the ratio between net photosynthetic rate and transpiration rate are coupled through stomatal regulation (Jianlin *et al*., 2008; Haefele *et al*., 2008). As discussed in Chapter One, water use efficiency, defined in the current study as instantaneous transpiration use efficiency (ITE) in simplified terms can be enhanced by 1) increasing photosynthetic rates or by 2) reducing transpiration losses (Peleg *et al*. 2005). The ratio between the two is highly dependent on stomatal conductance (Hirasawa & Hsiao, 1999). IRGA measurements indicated that emmer and emmer SB had the greatest ITE pre-anthesis, although spelt SB and einkorn also displayed high ITE. ITE was measured across two dates, assessing pre and post anthesis ITE. ITE in emmer and all spelt cultivars were relatively conserved from pre to post-anthesis. IRGA assessments also indicated that emmer had the greatest photosynthetic rates on both dates. In contrast, spelt had considerably lower photosynthetic rates although this was offset by lower than average transpiration rates. Whereas emmer had maintained ITE through high photosynthetic rates, spelt cultivars, particularly spelt Oberkulmer which actually

increased ITE from pre to post anthesis, had amongst the lowest transpiration rates observed indicating that the mechanism by which ITE is controlled may well differ. Furthermore, although emmer and emmer SB both had high ITE pre anthesis, increased photosynthetic capacity of the leaf was only observed in emmer. Emmer SB did not show a conserved ITE across sampling dates indicating that this trait may be characteristic of emmer rather than of the emmer species in general. The differences between the mechanisms for ITE between spelt and emmer corroborate preliminary studies (Isaaks, 2009).

Photosynthetic measurements comprise a large number of integrated reactions and processes. Whilst measuring photosynthesis and transpiration rates, stomatal characteristics were also monitored. It is thought that reduced water losses may be achieved by reducing the concentration gradients between the atmosphere and internal stomatal CO_2 concentrations (Condon *et al*., 2004). However the C_i/C_a ratios were observed to be highest for emmer, emmer SB pre-anthesis, as well as emmer post anthesis, all of which showed high ITE. Collating pre and post anthesis C_i/C_a and ITE showed no significant correlations.

High transpiration efficiency in wheat is usually associated with lower stomatal conductance and photosynthetic rates (Fischer, 2011) which occurs when CO_2 diffusion into the leaves and diffusion of water vapour out is largely shared, therefore when stomatal control reduces the amount of water lost, photosynthesis also reduces. All spelt cultivars displayed low stomatal conductance (G_s) ranging from 0.096 – 0.149 μmol m^{-2} s^{-1} (pre and post anthesis) and displayed low photosynthetic rates and increased ITE. In contrast, emmer had among the highest conductance rates observed which may have enabled higher photosynthetic rates to

be achieved. This would likely make the crop more 'conservative' of water, which could increase overall WUE of these plants.

Also noteworthy was einkorn which, despite performing having poor emergence in previous field trials in addition to high RUE, did show high ITE. ITE was also relatively conserved between pre and post anthesis. Although for the most part data analysis has been directed towards emmer and spelt cultivars in particular, high RUE (Chapter Two) and the seemingly consistent ITE does show that this genotype may warrant further investigation. Interestingly, whereas the emmer genotype and spelt cultivars displayed either high photosynthetic rates or low transpiration rates, einkorn had high photosynthetic rate pre anthesis for high ITE and low transpiration post-anthesis and therefore seemingly uses both mechanisms to conserve ITE. Stomatal conductance for einkorn does also seem to be intermediate of those of the emmer cultivars and spelt cultivars.

3.4.4.3 Biomass

In glasshouse experiment II, the greatest biomass yield was produced by spelt Oberkulmer. Although spelt cultivars did generally produce the greatest biomass, this did not translate through to yield. Spelt Oberkulmer, Tauro and SB produced the lowest yields observed. This was a reflection of the generally quite poor development observed for spelt genotypes, particularly spelt SB. However, it was interesting to note that when assessed using IRGA, spelt genotypes, particularly Oberkulmer consistently displayed low transpiration rates coupled with moderate photosynthetic rates. The large quantities of biomass produced however suggest that the trade-off for lower photosynthetic rate and transpiration rate, leading to high ITE which paid dividends in terms of biological yield production.

Modern bread wheat, Xi19 produced the greatest yield although total biomass production was among the lowest observed (although differences were not significantly different). MBW yields therefore were thought to be due to genetic improvements for partitioning rather than increases in biomass. This is reflected in the harvest indices for glasshouse experiment II. Modern bread wheat, Xi19 had a HI similar to theoretical upper limit (Araus *et al*., 2002) whereas ancient species had significantly lower HI. Spelt SB had the lowest HI of all genotypes observed. Harvest results highlight that the largest difference between these ancient wheat genotypes and modern bread wheat cultivars, at least from an agricultural perspective seems to be the partitioning of resources (and potentially irregular development potentially due to inadequate vernalisation). Spelt cultivars and to a lesser degree emmer and einkorn cultivars, do have the capacity to assimilate and accumulate carbon however, it is the partitioning of this biomass that means that production is not economically viable.

Since the theoretical limit for HI in MBW is being approached (0.62) (Austin *et al*., 1980), genotypes like spelt Oberkulmer may provide genetic variation for increased biomass to boost yields. In the glasshouse experiment, WUE was also assessed throughout the life of the plant. These analyses indicated that cultivar emmer and spelt Tauro display a more efficient use of water; this corroborates that observed in the ITE component this experiment. The increased WUE observed for emmer may support ITE results showing that this genotype maintained a constant ITE both pre and post-anthesis. Furthermore, emmer also had comparably high photosynthetic rates. Spelt Oberkulmer increased from pre to post-anthesis for ITE indicating that high ITE is necessary for high WUE over the entire life of the plant. Emmer SB did not show increased ITE which is also consistent with the results observed for

biomass/water uptake ratio calculation of WUE indicating that this WUE might be a characteristic of the emmer genotype rather than of the species. Also interesting was that einkorn, observed to have high ITE, showed increased WUE over the entire life of the plant corroborating that, despite poor emergence and biomass accumulation, this genotype may still be of interest. However, the comparatively high HI observed, particularly for both einkorn cultivars, contradicts the literature as well as the findings of previous experiments and it is not clear where this proficiency for yield derives in the current experiment.

The final aspect of this project related to the 'stay green' trait which was observed to a large extent in all spelt cultivars where 'stay green' was greater post-anthesis when compared to all other genotypes. Christopher *et al*. (2008) states that increased flag leaf duration may afford plant the propensity to resist drought in certain environmental conditions. It could therefore be purported that spelt species, particularly spelt Oberkulmer, was able to maintain a high WUE (indicated through ITE measurements and biomass/water uptake ratios) as a result of the 'stay green' trait, particularly under drought. The extent to which spelt species stayed 'green' in this experiment surpassed that observed in any of the previous experiments and could be purported to be a result of the drought conditions imposed which might may have led to the expression of a tolerance trait however the 'stay green' trait may also have been observed to this extent as a result of the abnormal development, potentially a result of inadequate vernalisation. Further analysis should assess whether this persistent green area is photosynthetically active and whether it therefore contributes to drought tolerance.

3.5 Conclusions

Many of the ancient species, notably einkorn SB and emmer, displayed comparable photosynthetic rates when compared to modern bread wheat. Results also indicated that those genotypes that had previously displayed high RUE, also displayed greater A_{sat}, implying that the increased RUE observed, may have derived from this high photosynthetic capability.

The chapter also highlighted that several ancient wheat species, thought to originally derive from dry rain-fed environments, possessed increased ITE (namely emmer and spelt SB) as well as biomass/water uptake ratios where, for the former, mechanisms whereby ITE was maintained, were different between the emmer and spelt species (either through high photosynthetic rates or low transpiration rates, respectively).

Biomass data corroborated that several ancient wheat species had comparable proficiency to produce yield when compared to modern bread wheat, inferring that spelt genotypes in particular, made a trade-off between moderate photosynthetic rates and comparably lower transpiration rates which were observed to benefit biological yield production. Additionally, increased canopy duration, shown to be particularly distinct during post-anthesis drought imposed in glasshouse experiment II, was observed and therefore also thought to contribute to biomass production that was comparable to modern bread wheat, although, as previously observed, this did not translate to harvestable yield.

This chapter highlighted that the value of these ancient wheat species may not derive from yield production but from a proficiency to produce biological yield, potentially a result of increased growth duration through delayed senescence and more

conservative use of water resource, both of which are traits that could be useful in producing novel plant types for the production of more efficient wheat production.

Chapter Four:

Photosynthesis and water use efficiency

4.1 Introduction

Chapter Two indicated that resource utilisation differences might exist between genotypes. To discern the origin of these differences, Chapter Three explored leaf level CO_2 assimilation characteristics, for which there was some variation. Among genotypes there was found to be a wide range of biochemical capacities that regulated CO_2 assimilation, respiration rates and Triose Phosphate Utilisation. This however, was not the case for the maximum rate of carboxylation or observed rates of electron transport (although the latter was highest in those genotypes that had high RUE in Chapter Two). The small sample size and noisy data set however, did not allow for firm conclusions to be made regarding each of the genotypes or species. The following chapter therefore outlines an experiment in which some of these aspects were investigated again with greater control of growing conditions and where measurements were performed *in situ*. The analyses were also widened to include instantaneous water use efficiency over time, where plants were fully irrigated. The most prominent component of the experiment utilised Infra-Red Gas Analysis (IRGA). In addition however, other techniques were also employed including carbon isotope discrimination for assessment of water use efficiency, providing more detailed information for the characterisation of genotypes.

This could provide an understanding of the differences between genotypes on yield formation. Prior to glasshouse experiment III, poor biomass accumulation and poor emergence meant that einkorn species were not chosen to carry into the next experiment. Therefore, a smaller subset of the cultivars were assessed which included emmer and spelt species as well as a modern bread wheat cultivar for comparison.

4.2 Materials and Methods

The following chapter outlines glasshouse experiment III that included a subset of the genotypes previously grown in the field in order to perform measurements of traits at the leaf level.

4.2.1 Seed preparation and germination assays

Seed for the following experiments were obtained from the 2010 field harvest. After which, grain was stored in cool and dark environment in airtight containers. Germination assays were performed prior to sowing. Initially, dormancy was broken by placing seeds in petri dishes containing wet filter paper sheets. Petri dishes were then sealed and placed in a 19°C growth room with a 12 hour photoperiod. The numbers of seeds that germinated each day over the following week were recorded. Germination indices were calculated according to details outlined in Chapter Two. If seeds had an average germination index above 90% within the initial 36 hours, they were considered viable for use in the experiment.

4.2.2 Experimental Site

The following experiments were performed in a glasshouse (for location details refer to Chapter Three, section 3.2.1).

4.2.3 Glasshouse Experiment III

In 2013, a glasshouse experiment was established to measure a range of parameters on a sub-set of those ancient wheat displaying favourable characteristics in previous investigations, under non-limited irrigation conditions.

4.2.3.1 Plant Material

Previous work at included 12 genotypes (which include four MBW, two emmer, three spelt and three einkorn genotypes). Due to space, equipment and time limitations, it was not possible to include all ancient lines therefore einkorn hungarian plants, seen to generally perform quite poorly in terms of light attenuation, biomass production and emergence were excluded. Table 4.1 lists the genotypes that were included.

Table 4.1: Genotypes selected for photosynthetic analysis in Glasshouse Experiment III including representatives of each cytological classification and including two modern bread wheat cultivars.

Genotype	Species group
Einkorn *	Einkorn
Einkorn SB *	Einkorn
Einkorn Hungarian *	Einkorn
Emmer	Emmer
Emmer SB	Emmer
Spelt SB	Spelt
Spelt Tauro	Spelt
Spelt Oberkulmer	Spelt
Xi19	MBW
JB Diego	MBW

* Genotypes that were analysed for SLA, biomass and SPAD only.

4.2.3.2 Seedling transplanting and husbandry

Seeds of the listed genotypes were sown into 2.54cm compartments within 14 x 20 module trays using John Innes No. 3, high fertility potting compost mix on 7 December 2012. Plants were vernalised in a glasshouse as cool glasshouse for 62 days. Seedlings were transplanted into individual pots on 13 February 2013 and were checked and irrigated when necessary. Conditions were generally uniform within the glasshouse and plants were watered without limitation using a drip irrigation system.

4.2.3.3 Experimental design

The experiment followed a randomised complete block design with three blocks. Each block contained three pots per genotype (Appendix Five).

4.2.4 Glasshouse experiment III measurements

4.2.4.1 Gas exchange measurements

Gas exchange measurements were performed *in situ*, using an Open Licor 6400 portable photosynthesis system (Licor Lincoln Nebraska, NE, USA) infrared gas analyser between the hours of 10am and 3pm to limit variation imposed by stomatal behaviour. All gas exchange measurements were made at ambient humidity (50-60%) on the mid-end section of the main stem flag leaf. The width of each leaf was measured and input into Licor software to adjust gas fluctuations for specific leaf areas. Measurements were performed at growth stages 39 and 61 according to HGCA benchmark growth stages for estimation of parameters, pre and post anthesis, to observe any variation due to developmental stage. Block temperature and light levels were maintained at 20ºC in order to increase uniformity of results.

4.2.4.2 Flag leaf ITE measurements.

In the experiments, water use efficiency was derived using the measured rate of photosynthesis and transpiration measured at a given point in time giving a ratio indicating the accumulation of carbon to water lost through stomata.

In glasshouse experiment III, flag leaf ITE measurements were made at bi-weekly intervals beginning before anthesis, continuing until after anthesis. Measurements were made over 2 to 3 days on 3 separate occasions. Leaves were exposed to a constant photon flux rate of 2000 μmol m^{-2} s^{-1} and 385 μmol m^{-1} CO_2. Flag leaf temperature ranged from 20 - 29°C, with an average temperature throughout measurements of 24°C.

4.2.4.3 CO_2 response curves

Carbon dioxide response curves were obtained by monitoring gas exchange responses of the photosynthetic activity in leaves to intercellular CO_2 mole fraction (C_i) as per Chapter Three, the only differences being that these were performed *in situ*. Flag leaf temperatures ranged from 20 - 25°C, with average leaf temperatures of 23°C.

4.2.4.4 Plant growth and development analyses

Destructive analyses were carried out once plants reached maturity and had undergone full canopy senescence; as a result, methods did not include measurement of green area of components or include analysis of infertile shoot numbers.

4.2.4.5 Specific Leaf Area

Fully expanded, mature flag leaves without any obvious symptoms of pathogen attack were collected. In order to reduce measurement errors, several flag leaves were collected per genotype. The flag leaf areas were measured and recorded after which they were oven dried at 80°C until a constant weight was achieved.

4.2.4.6 Stay green assessments

The stay green persistence of the canopy was measured using a Minolta Chlorophyll Meter SPAD-502 (Minolta Camera Company Limited). SPAD measurements were performed on each plant at 3 points on the flag leaf, recording the average of these. Measurements began as soon as the flag leaf emerged for each genotype and continued approximately every 4 days until senescence of the flag leaf was complete.

4.2.4.7 Data analyses

All data was stored using Microsoft Excel 2010 for Mac or GraphPad Prism 6 for Windows. ANOVAs were used to determine the significance of differences for parameters between genotypes using GenStat (16^{th} Edition, VSN International Ltd.) for Windows (XP).

4.3 Results

4.3.1 Biochemical aspects of photosynthesis pre and post anthesis

Results gained in chapter three showed some variation between genotypes in CO_2 response curves however experimental conditions and sampling procedure may have impacted results, therefore this component of the experiment was performed once again in glasshouse III. Figure 3.3 (Chapter Three, section 3.3.2) show typical responses of each of the genotypes when exposed to varying CO_2 concentrations, generated by a curve fitting tool (Sharkey *et al*., 2007) from which values in Figure 4.1 and 4.2 derive.

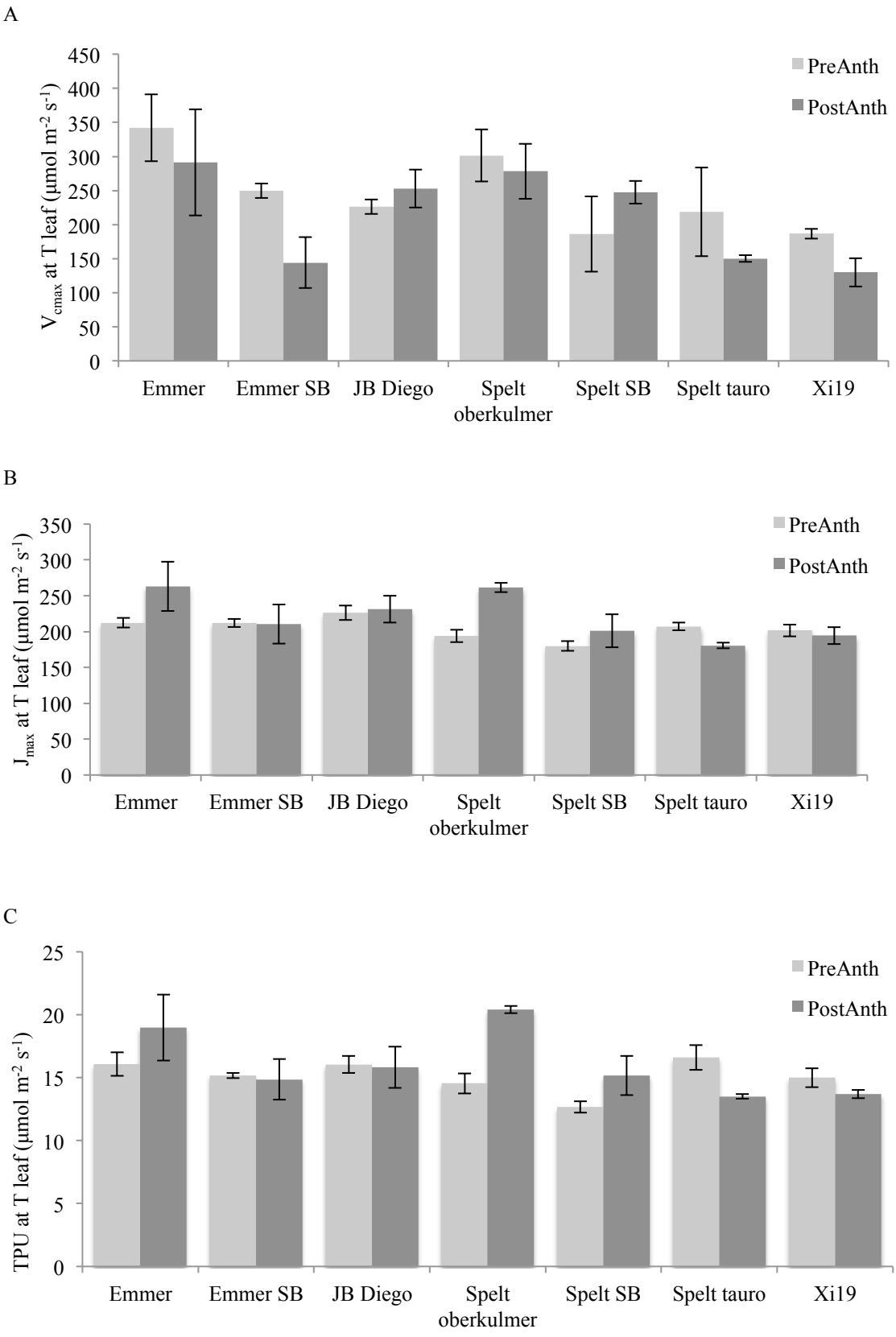


Figure 4.1 *i*: Values determined from fitted A/C_i curves at T leaf (where block temperature was set to 20 °C). A shows the maximum rate of carboxylation (V_{cmax}), B the rate of electron transport (J_{max}) and C the triose phosphate utilisation (TPU) limitation. Bars represent the standard error of the mean (where n is 3).

D

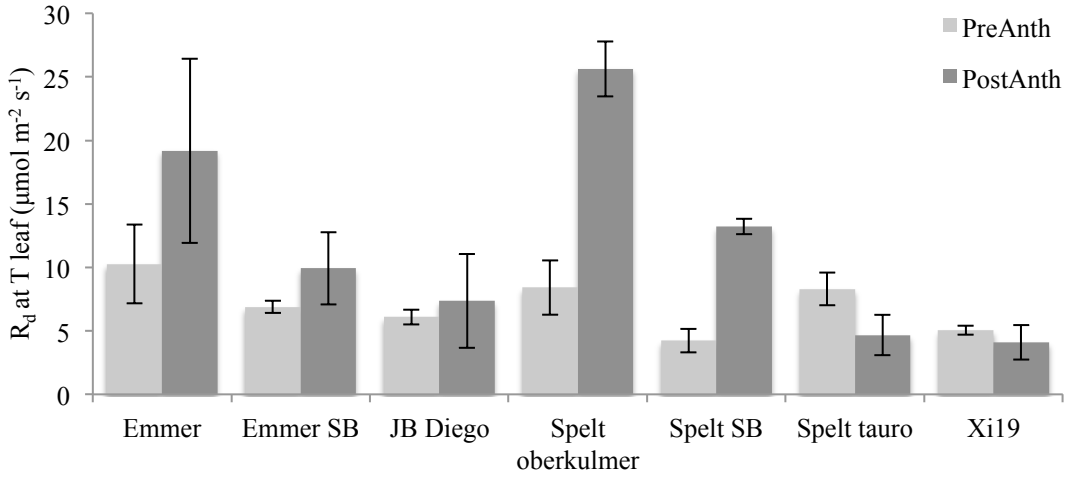


Figure 4.1 *ii*: Values determined from fitted A/C_i (A/C_c) curves at T leaf (where block temperature was set to 20 °C). D shows the determined respiration (R_d) of each of the investigated genotypes. The bars represent the standard error of the mean (where n is 3).

Figure 4.1 shows that cultivars investigated displayed a range of different responses to CO_2 atmospheric concentrations however differences were not significant except for Triose Phosphate Limitation (P = 0.015) and respiration (P = 0.012). TPU ranged from 4.32 to 10.26 µmol m^{-2} s^{-1} (Spelt SB and emmer, respectively) pre anthesis and from 4.11 to 25.63 µmol m^{-2} s^{-1} post-anthesis (Xi19 and spelt Oberkulmer). TPU generally tended to be higher in ancient wheat cultivars compared to modern bread wheat, Xi19 and JB Diego. Respiration was also significantly different between genotypes and across growth stages (P = 0.012). Emmer had the greatest R_d pre-anthesis whereas spelt Oberkulmer had the greatest, post-anthesis (10.26 and 25.63 µmol m^{-2} s^{-1}, respectively). Xi19 had the lowest R_d both pre and post anthesis (5.05 and 4.11 µmol m^{-2} s^{-1}, respectively).

The maximum rate of carboxylation ranged from 186 to 342 µmol m^{-2} s^{-1} (pre-anthesis) and 130 to 291 µmol m^{-2} s^{-1} post-anthesis. Rate of electron transport (J_{max}) did not show any statistical significance, which parallels that observed in the

previous set of carbon response data. No significant differences were observed although results were also standardised for leaf temperature using the curve-fitting tool devised by Sharkey *et al.,* (2007).

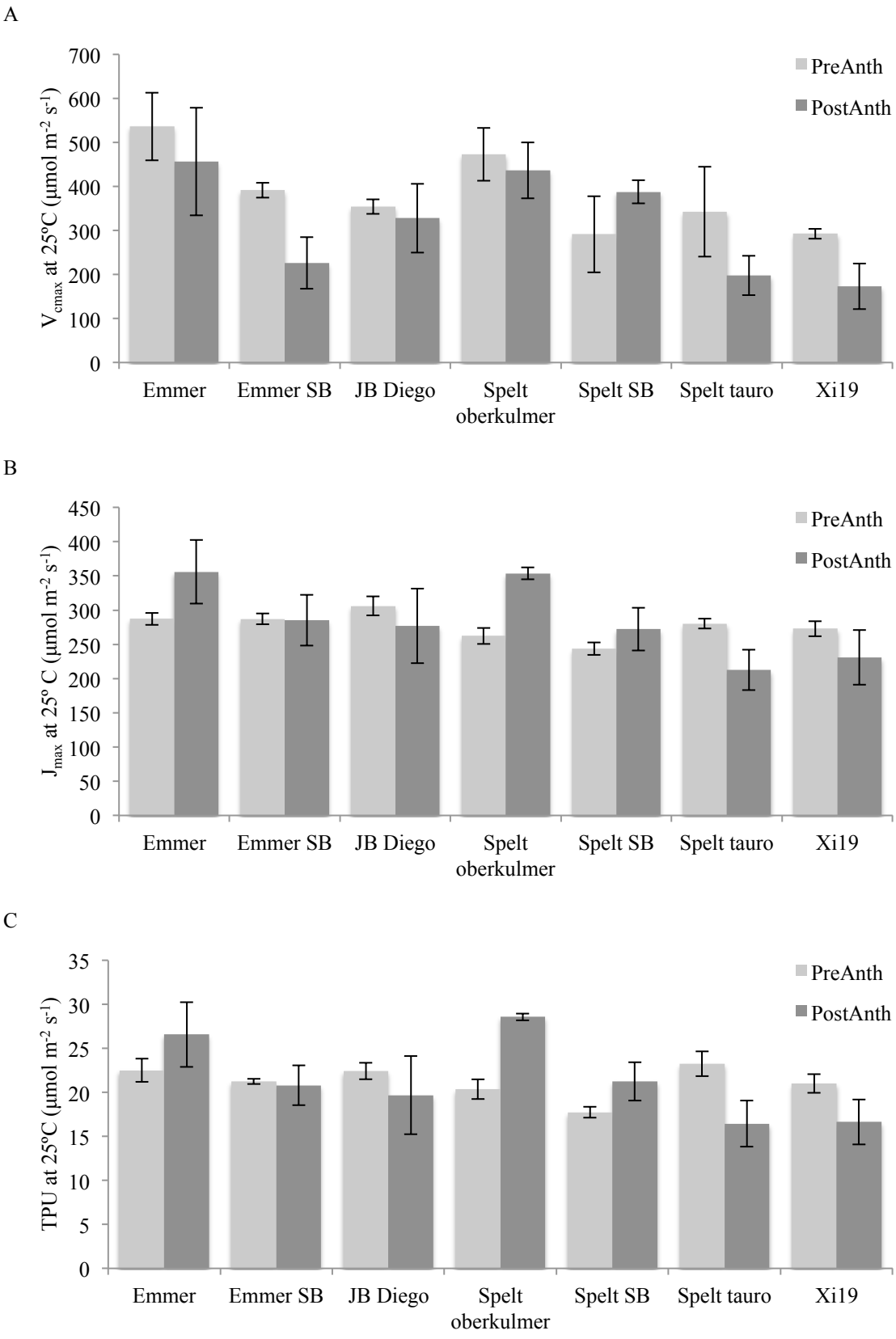


Figure 4.2 *i*: Values determined from fitted A/C_i curves, with a normalised leaf temperature (25°C). A shows the maximum rate of carboxylation (V_{cmax}), B) the rate of electron transport (J_{max}) and C) the triose phosphate utilisation (TPU) limitation of each of the investigated genotypes. The bars represent the standard error of the mean (where n = 4).

D

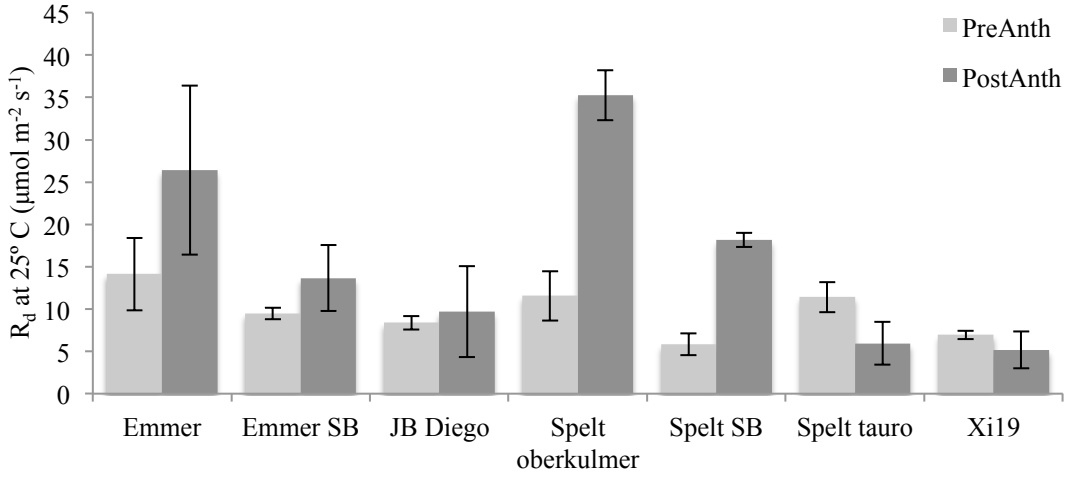


Figure 4.2 *ii*: Values determined from fitted A/C_i curves, with a normalised leaf temperature (25°C). D) shows the determined respiration (R_d) of each of the investigated genotypes. The bars represent the standard error of the mean (where n = 4).

When standardised for temperature, results were very similar in terms of ranking, indicating that leaf temperature variations may not have affected the results (Figure 4.2). Once again, the analysis showed that the only two parameters that showed significant differences between genotypes were TPU (P = 0.021) and R_d (P = 0.011). TPU was highest in emmer, emmer SB, spelt Tauro and JB Diego indicating that pre anthesis, these genotypes had a lesser limitation to increasing atmospheric CO_2, compared to other genotypes. This was also the case for spelt Oberkulmer and emmer, post-anthesis, which indicates that TPU is not necessarily consistent through the life of the flag leaf.

Once again, differences between genotypes for maximum catalytic rate were not significant although the general trend shows that V_{cmax} reduced with flag leaf age in all cultivars except spelt SB. J_{max} was not significantly different, as in the previous results analysis (Chapter Three, Section 3.3.2).

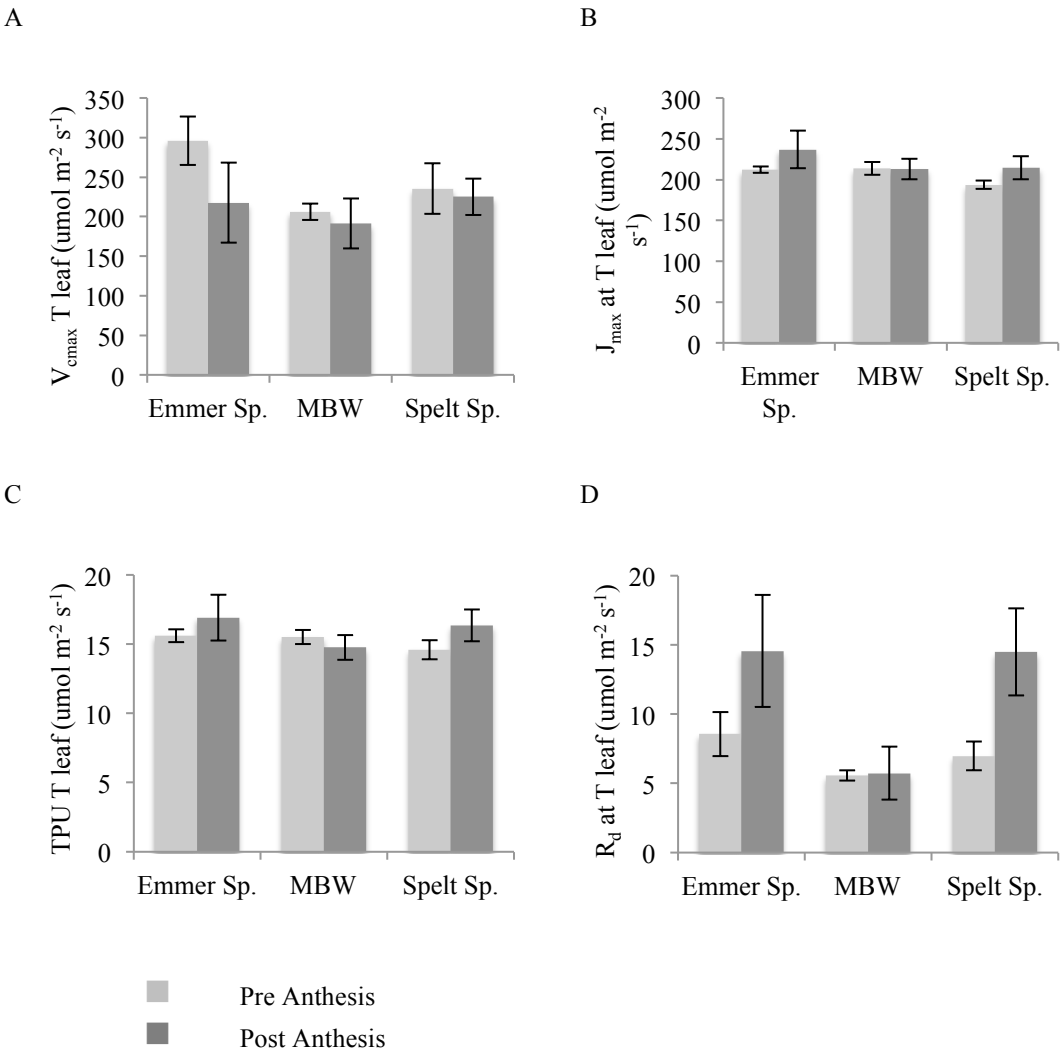


Figure 4.3: Values determined from fitted A/C_i curves, performed at T leaf. A) shows the maximum rate of carboxylation (V_{cmax}), B) the rate of electron transport (J_{max}), C) the triose phosphate utilisation (TPU) and D) the determined respiration rates (R_d) of each of the investigated species. The bars represent the standard error of the mean.

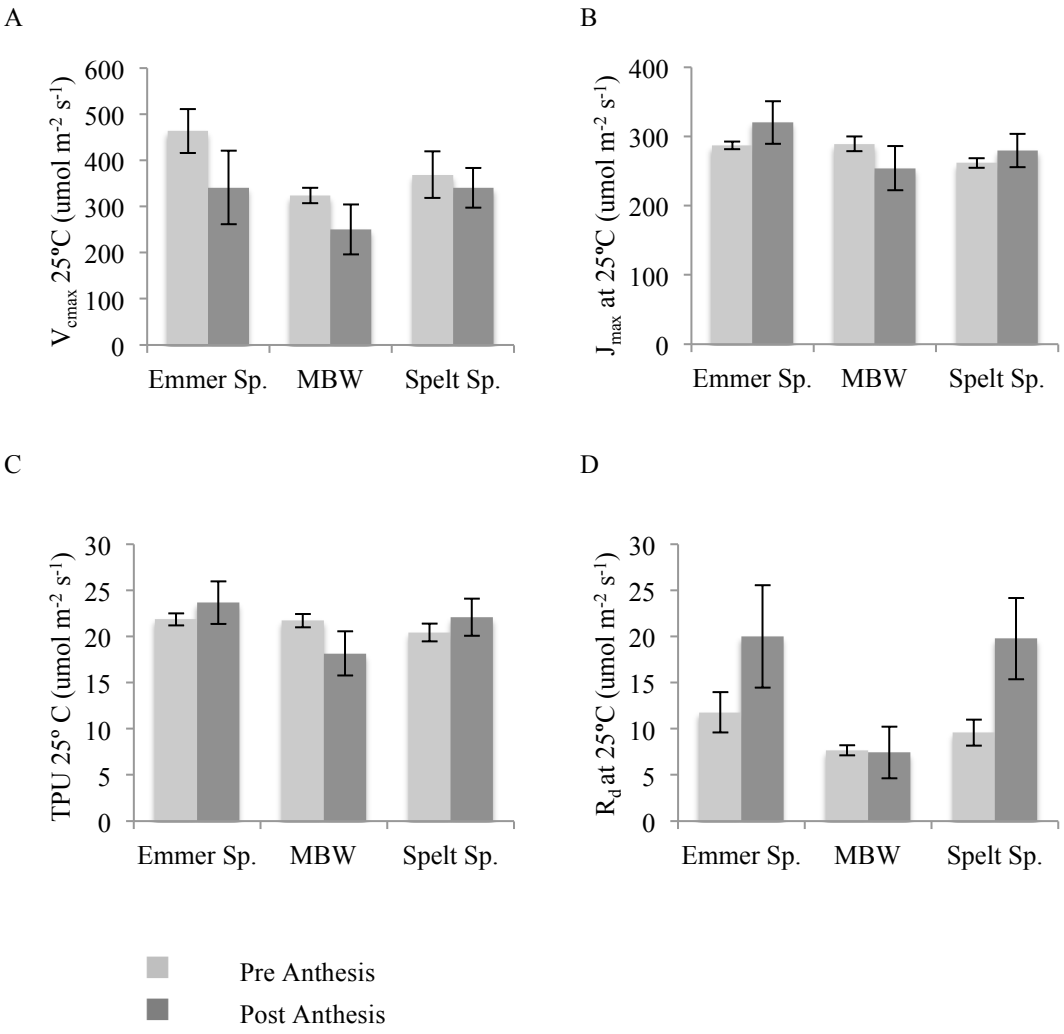


Figure 4.4: Values determined from fitted A/C_i response, with a normalised leaf temperature of 25ºC. A) shows the maximum rate of carboxylation (V_{cmax}), B) the rate of electron transport (J_{max}), C) the triose phosphate utilisation (TPU) and D), the determined respiration rates (R_d) of each of the investigated species. The bars represent the standard error of the mean.

There were no significant differences when data were analysed by species at T leaf (Figure 4.3). Once again however, TPU was highest for emmer, both pre and post anthesis (as also observed in glasshouse II although this was not significant). Results were also adjusted for 25ºC leaf temperatures, however this analysis also did not show statistical significance (Figure 4.4).

4.3.2 Water Use Efficiency

Instantaneous transpiration measurements were performed over the experimental period, from emergence of the flag leaf until flag leaf senescence. In this experiment the flag leaf was used as a representative to gauge the photosynthetic activity of each of the genotypes. Figure 4.5 shows results for the genotypic assessments, whereas Figure 4.6 shows the assessment by species.

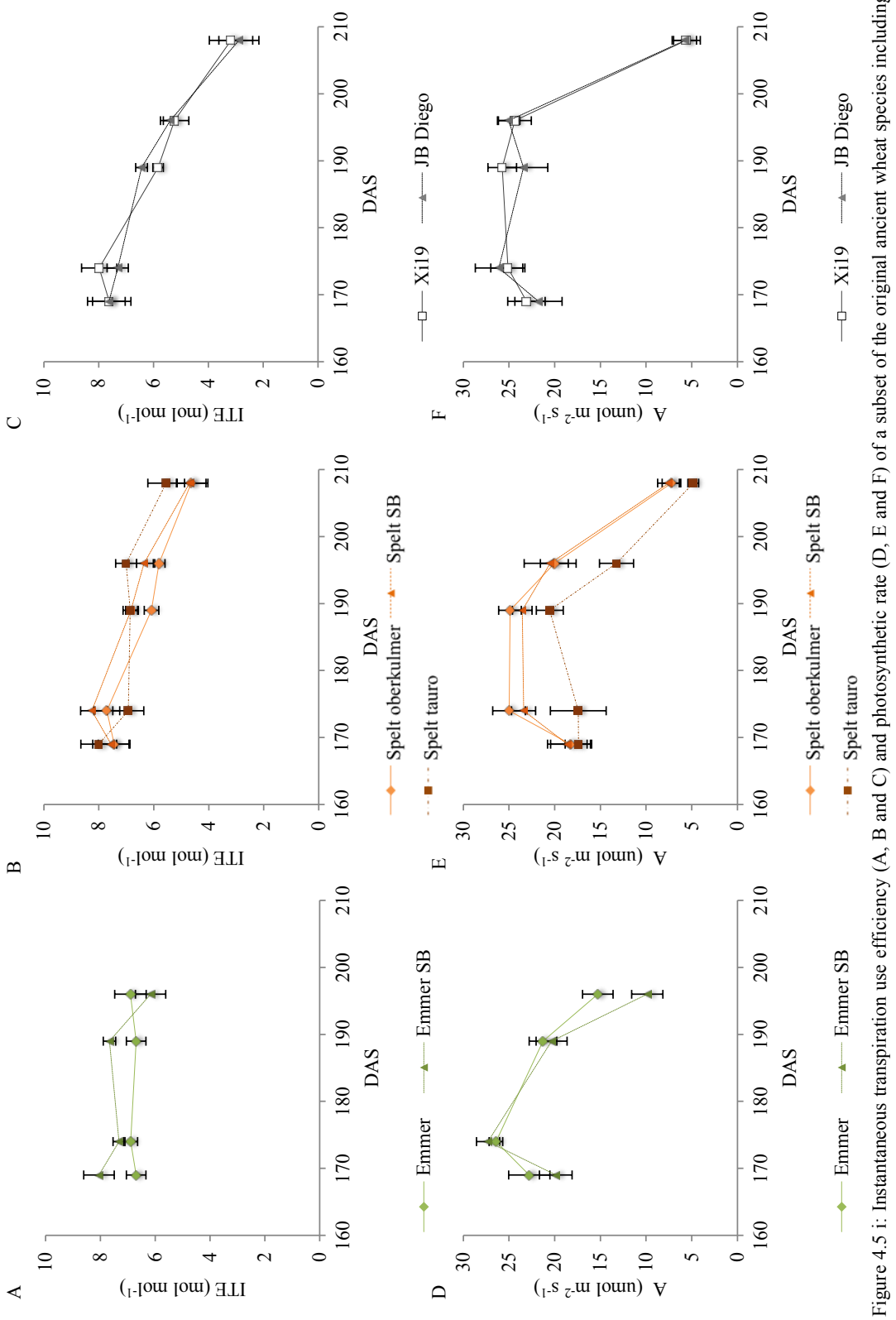


Figure 4.5 i: Instantaneous transpiration use efficiency (A, B and C) and photosynthetic rate (D, E and F) of a subset of the original ancient wheat species including all emmer (Aand D) and spelt species (B and E) as well as modern bread wheat (C and F) for comparison from growth stage 31 onwards (error bars denote SEM).

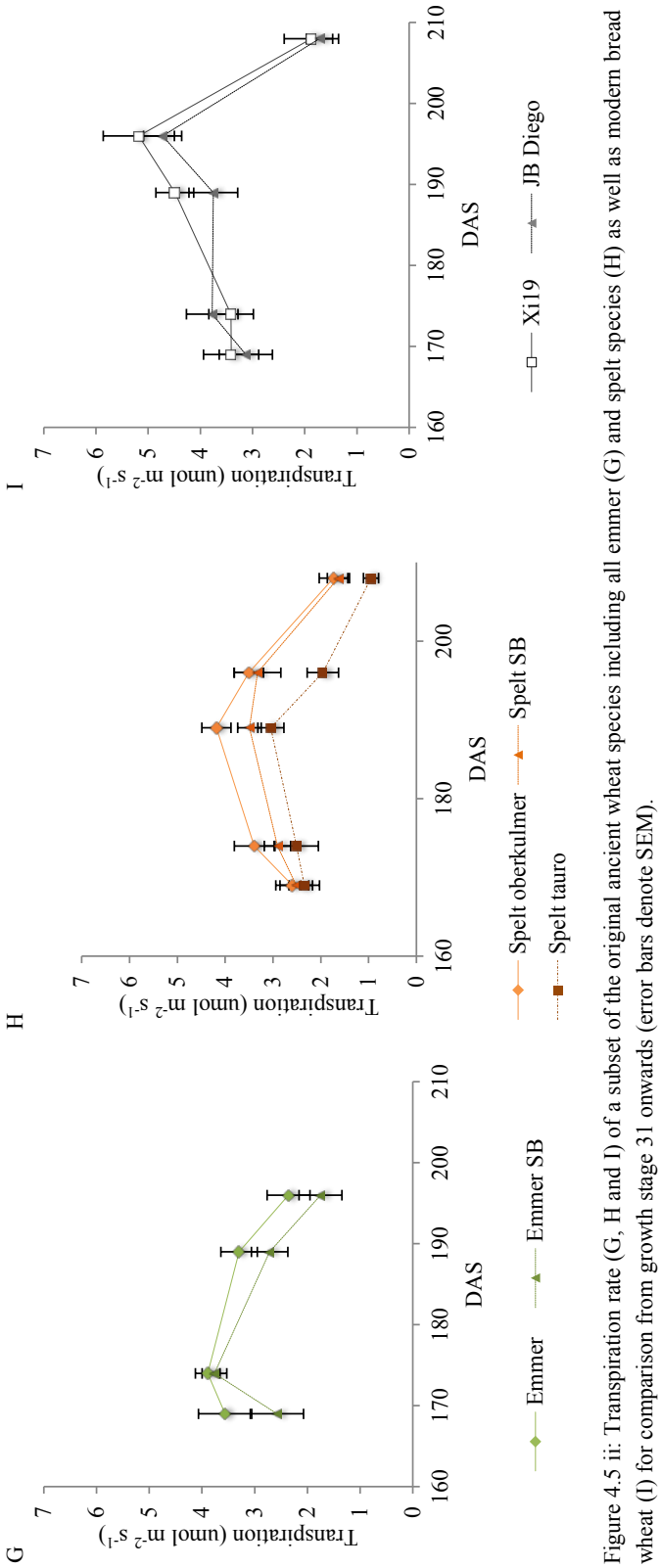


Figure 4.5 ii: Transpiration rate (G, H and I) of a subset of the original ancient wheat species including all emmer (G) and spelt species (H) as well as modern bread wheat (I) for comparison from growth stage 31 onwards (error bars denote SEM).

4.3.2.1 ITE Measurements

Sampling began at 169 DAS where the average ITE for all genotypes was 7.58 mol mol^{-1} (Figure 4.6). Emmer SB and spelt Tauro were observed to have significantly greater ITE than other genotypes. Spelt Oberkulmer, spelt SB and both modern bread cultivars however, were also shown to be efficient in terms of leaf water use. Emmer had the lowest transpiration efficiency (6.83 mol mol^{-1}) on 169 DAS but did not decline to the same extent as JB Diego or Xi19 (2.88 and 3.17 mol mol^{-1}), consistent with findings from glasshouse experiment II, ITE decreased over time from, 7.59 (169 DAS) to 4.23 (DAS) as would be expected of aging flag leaves. Figure 4.5 shows that generally, ancient wheat species (emmer and to a lesser degree, spelt species) remain quite consistent for ITE throughout the life of the flag leaf however, modern bread wheat genotypes tended to decline quite rapidly from 196 to 208 DAS. Differences in ITE were highly significant between genotypes ($P < 0.001$), sampling dates ($P < 0.001$). The interaction between the two was also highly significant ($P < 0.006$).

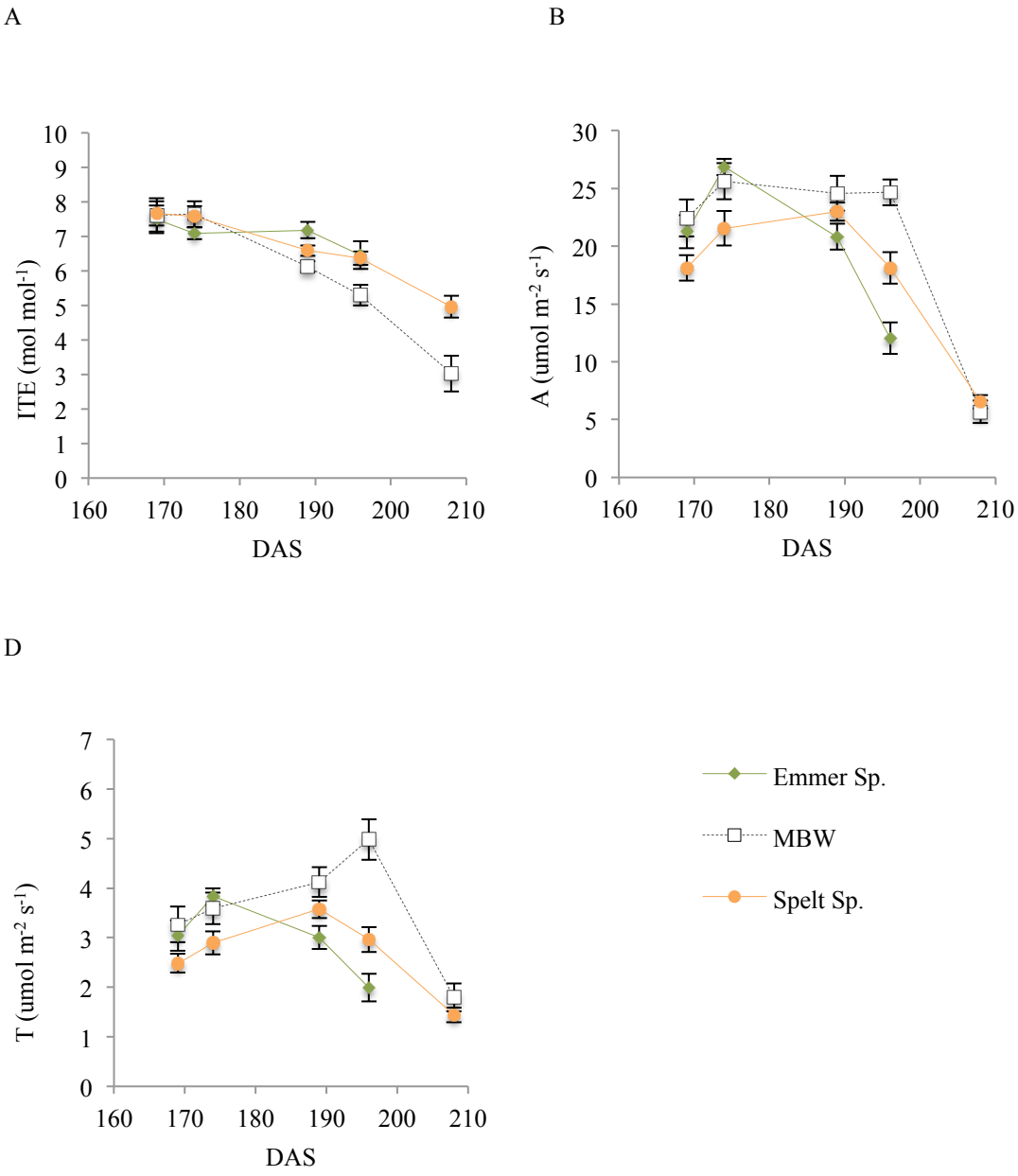


Figure 4.6: A, Instantaneous transpiration efficiency, B, photosynthetic rate and C, transpiration rate of a subset of the original ancient wheat collated by species including all emmer and spelt species as well as modern bread wheat for comparison from growth stage 39 onwards.

ITE was significantly different between species across sampling dates ($P < 0.001$) (Figure 4.6). Generally, all species reduced for instantaneous transpiration efficiency over the sampling period, as leaves became older. Modern bread wheat declined more rapidly after 174 DAS whereas emmer and spelt had the greatest ITE,

indicating that these were the most efficient throughout the sampling period ($P < 0.001$).

4.3.2.2 Photosynthesis

Photosynthetic rates averaged 20.27 μmol m^{-2} s^{-1} at 169 DAS to 5.77 at 208 DAS (Figure 4.5). Emmer showed greater than average photosynthetic rate (22.83 μmol m^{-2} s^{-1}) while spelt genotypes had significantly lower photosynthetic rates ranging from 18.27 to 17.4 μmol m^{-2} s^{-1} at 169 DAS. All genotypes peaked for photosynthetic activity in 174 DAS, particularly for emmer and emmer SB (26.48 and 17.41 μmol m^{-2} s^{-1}), indicating that emmer can maintain consistent (emmer) or high ITE (emmer SB) as a result of high photosynthetic rates (and comparatively lower transpiration rates) as was also observed in glasshouse experiment II (Chapter Three, section 3.3.5.1). However, photosynthetic rates declines after 174 DAS for emmer and leaves senesced before the final measurement date (Figure 4.6); on these sampling days modern bread wheat cultivars had the highest photosynthetic rates observed. Differences were significant between by genotype ($P < 0.001$), sampling date ($P < 0.001$), as well as the interaction between the two ($P < 0.001$).

4.3.2.3 Transpiration rates

Transpiration was lower than average in all spelt cultivars (2.87 μmol m^{-2} s^{-1}) at 169 and 174 DAS (Figure 4.5). Emmer, Xi19 and JB Diego had above average transpiration rates (169 DAS). Differences between genotype and sampling date were highly significant ($P < 0.001$). Transpiration rates were also significantly different between species over the sampling period ($P < 0.001$), with modern wheat having the highest transpiration rate on 196 and 208 DAS (Figure 4.6). Spelt species had consistently lower transpiration rates on all measurement dates, similar with that observed in glasshouse experiment II.

4.3.2.4 Internal stomatal CO_2 concentrations

Differences between C_i were highly significant between genotypes and sampling date (where P <0.001) however, were not significant by a margin for the interaction (P = 0.06) (Figure 4.7). As with previous result sets, internal carbon dioxide concentrations were highest in those genotypes that displayed greater photosynthetic rates, such as emmer and emmer SB, particularly on 169 and 174 DAS. When analysed by species, modern bread wheat had a comparatively high C_i, followed by spelt and emmer (P <0.001), which reflects the higher photosynthetic rates of modern bread wheat (Figure 4.8).

4.3.2.5 Stomatal conductance

Spelt genotypes had the lowest conductance on 169 and 174 DAS. Spelt Tauro and spelt SB had low stomatal conductance (G_s) (Figure 4.7). However, all other genotypes had greater than average G_s. Differences between genotype and sampling date were significant (P <0.001). Results show that conductance consistently declined from the first sampling date to 208 DAS (0.178 to 0.0952) for all genotypes. Generally conductance was highest in those genotypes that displayed greater photosynthetic rates such as emmer and emmer SB on 196 and 174 DAS. The highest conductance rates were observed in modern bread wheat species (P <0.001) (Figure 4.8).

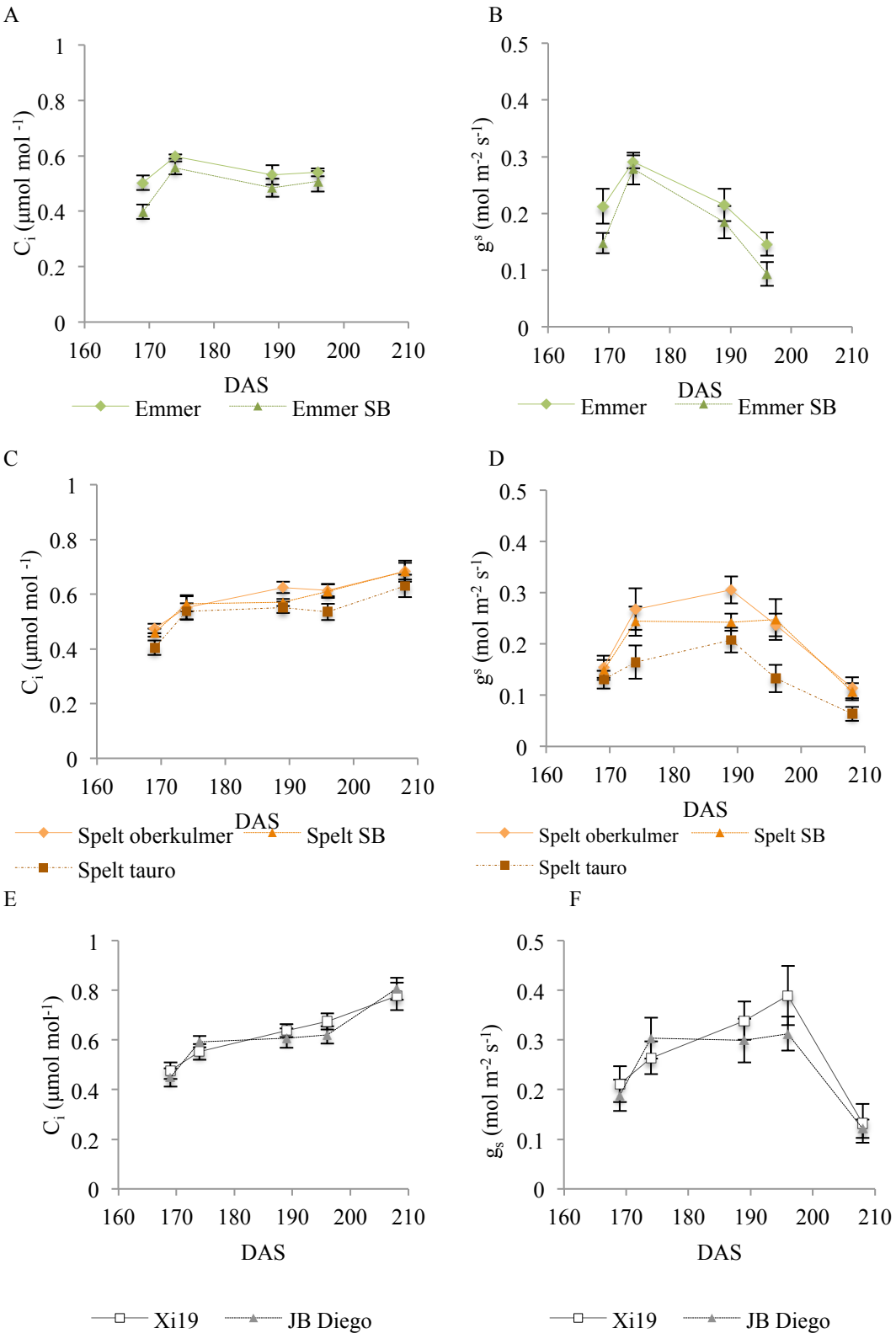


Figure 4.7: Internal stomatal CO_2 concentrations and stomatal conductance during ITE measurements of five ancient wheat and two modern bread wheat cultivars both pre and post anthesis. Figure includes internal-stomatal CO_2 concentrations (A, C and D for emmer, spelt and MBW genotypes, respectively) and stomatal conductance (G_s) B, D and F for emmer, spelt and MBW genotypes, respectively) against DAS.

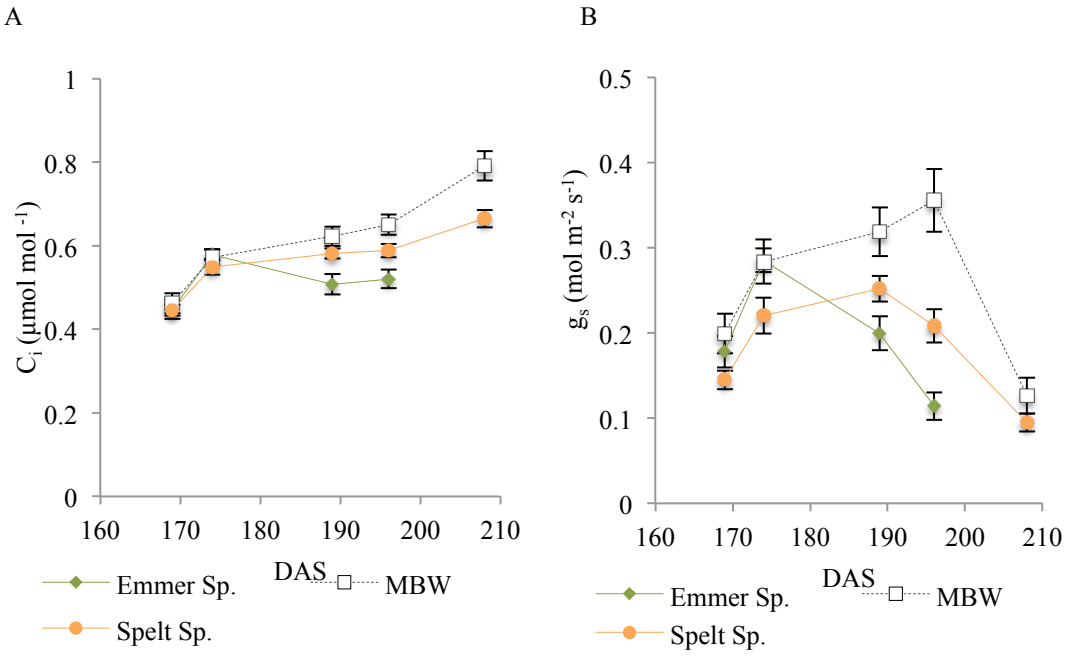


Figure 4.8: Stomatal responses simultaneously measured during ITE measurements of three species both pre and post anthesis. A) shows sub-stomatal CO_2 concentrations and B) shows stomatal conductance (G_s) against DAS.

4.3.3 Specific Flag Leaf Area

Specific flag leaf area (SLA) was significantly different between genotypes (P = 0.025), (Figure 4.9). It would be expected that lower SLA would imply a greater *in situ* rate of photosynthesis, as observed by Poorter & Evans *et al.* (1998); SLA was greater for emmer and emmer SB, observed to have high photosynthetic rates on 169 and 174 DAS. It was thought that increased leaf thickness would be associated with high photosynthetic rates where greater leaf machinery, per unit area may originate from extra layers or longer palisade cells, leading to increased chloroplast numbers and photosynthetic enzymes per unit leaf thus increasing photosynthetic capacity (Evans & Poorter, 2001). Results however showed that genotypes observed to have greater photosynthetic rates, in fact had greater SLA, inferring that they also had thinner leaves. Spelt Oberkulmer, Tauro and SB also had high SLA, indicating thinner leaves. Cornelissen *et al.* (2003) states that lower SLA values tend to

correspond with high investments in leaf 'defenses' particularly structural defenses, associated with increased leaf lifespan (Cornelisson *et al*., 2003), potentially indicative of the 'stay green' trait observed in spelt cultivars in field experiments. Modern bread wheat had comparatively low SLA compared to several ancient species, indicating thicker leaves.

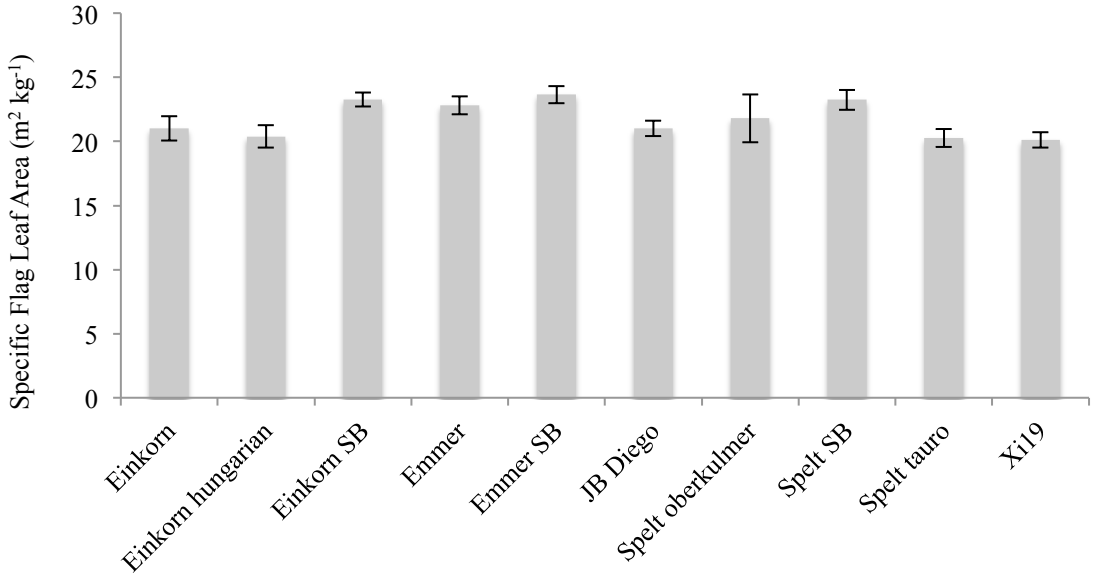


Figure 4.9: Specific flag leaf area for five ancient wheat cultivars and two modern bread wheat cultivars measured in gashouse experiment III (error bars denote SEM).

SLA by species was also significantly different (P = 0.043) (Figure 4.10) where emmer had the greatest SLA, followed by spelt then modern bread wheat (23.24, 21.92 and 20.56 m^2 kg^{-1}, respectively) indicating that overall, ancient species had thinner leaves. This could be the underlying trait that confers the consistently high photosynthetic rates and increased ITE observed in previous experiments (although this was not necessarily the case in the current glasshouse experiment results since emmer and emmer SB only had increased photosynthetic rates on the first two sampling dates). Reich *et al*. (1998) state that thinner leaves, which presumably have

smaller quantities of nitrogen per unit, would allow better access for CO^2 to catalytic sites, thus increasing the efficiency of Rubisco activity.

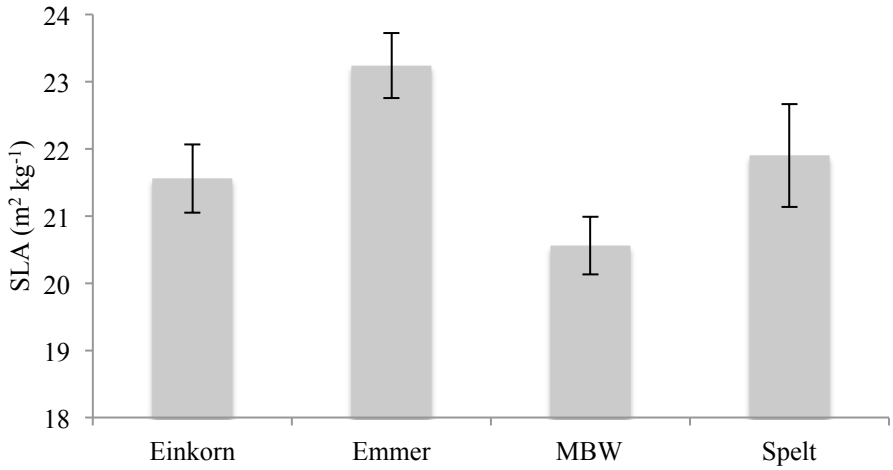


Figure 4.10: Specific flag leaf area (m^2 kg^{-1}) for five ancient wheat cultivars and two modern bread wheat cultivars measured in glasshouse experiment III. Error bars denote SED.

4.3.4 Assessment of WUE using carbon isotope discrimination

The grain harvested from glasshouse III was analysed using carbon isotope discrimination. Carbon isotope discrimination has been widely used as a means to assess WUE and generally the lower the carbon isotope discrimination, the higher the water use efficiency. The grain content is therefore used as a measure of WUE throughout the rain filling period (Figure 4.11).

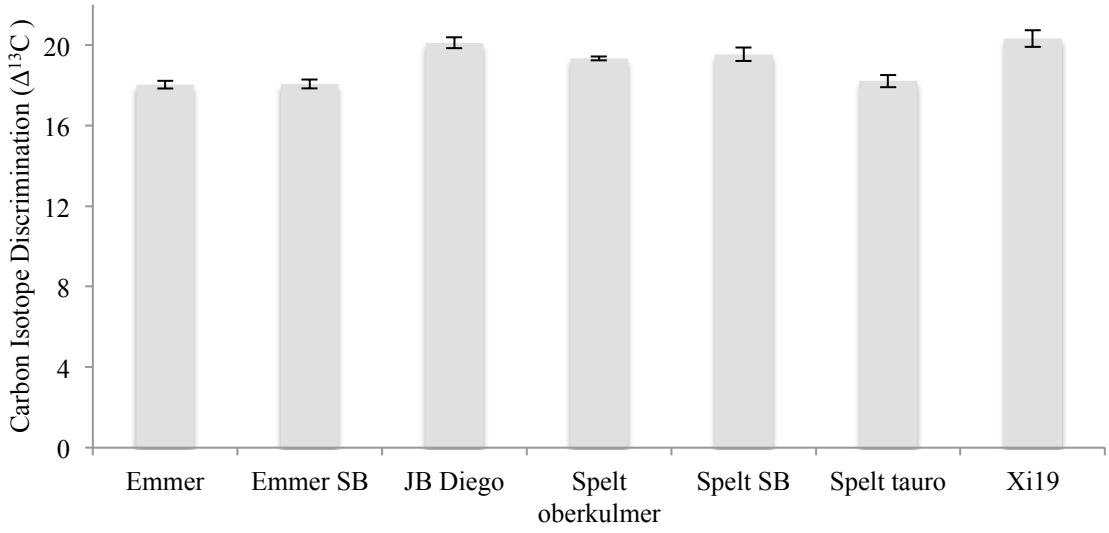


Figure 4.11: Carbon isotope discrimination for five ancient wheat cultivars and two modern bread wheat cultivars measured in glasshouse experiment III (error bars represent SEM).

Emmer, emmer SB and spelt Tauro had significantly lower $\Delta^{13}C$ ($P < 0.001$) (Figure 4.11). JB Diego and Xi19 displayed the highest (20.1 and 20.32, respectively). This was consistent with ITE results of the flag leaf over time. Also indicated was that modern bread wheat, shown to have consistently lower water use efficiency throughout the entire life of the leaf in ITE results, which is also indicated in Figure 4.6. These consistencies indicate that higher ITE observed for both ancient wheat species may have had a bearing on the $\Delta^{13}C$ grain content.

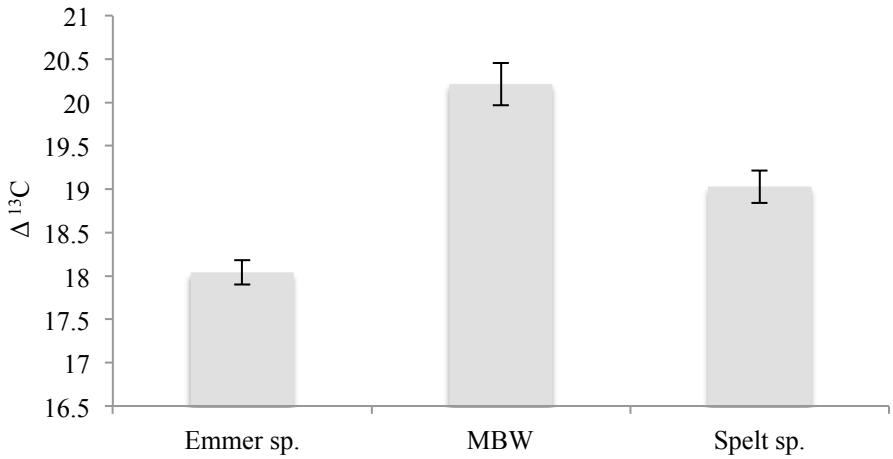


Figure 4.12: Carbon isotope discrimination for three wheat species measured from grain in glasshouse experiment III (error bars show SEM).

When analysed by species, $\Delta^{13}C$ was significantly different ($P < 0.001$) indicating that WUE, during the grain filling differed depending on species, furthermore species were ranked similarly with ITE results. $\Delta^{13}C$ was highest among modern bread wheat (20.21) species, and lowest for emmer (18.04) (Figure 4.12).

4.3.5 GH III biomass accumulation

In glasshouse experiment III the total amount of biomass produced (m^{-2}) was calculated (Table 4.2), as well as the grain yield and harvest indices of each genotype. Surprisingly, einkorn SB produced the greatest amount of biomass (g m^{-2}) whereas Xi19 produced the least (P <0.001). Einkorn SB also produced the greatest harvest however, much of this could be chaff and rachis as the two were very difficult to separate from grain without damage to grain occurring. Spelt SB, emmer SB and JB Diego also produced a comparably large amount of grain per m^2 (853.2, 707.5 and 1076.1g m^2). Differences among species were highly significant (P <0.001) although HI was significant (P <0.001).

Table 4.2: Grain yield, biomass and the deduced harvest index from glasshouse experiment III.

Genotype	Grain (m^2)	Biomass (g m^{-2})	Harvest Index
Einkorn	970.6	2350	0.42
Einkorn Hungarian	918.1	2304	0.39
Einkorn SB	1544.9	3484	0.44
Emmer	761.0	2440	0.31
Emmer SB	707.5	2160	0.33
JB Diego	1076.1	2126	0.50
Spelt Oberkulmer	777.7	2003	0.39
Spelt SB	853.2	2247	0.38
Spelt Tauro	651.9	2001	0.32
Xi19	729.8	1882	0.40
P	<0.001	<0.001	<0.001
SED (76 DF)	152.9	269.9	0.04

4.3.6 Green area persistence

Green area persistence was monitored in glasshouse experiment III from 154 DAS until 208 DAS, by which point all flag leaves had undergone full senescence. All genotypes followed the same general trend where flag leaf chlorophyll content,

indicated by SPAD readings, were initially high at the beginning of sampling, which corresponded to flag leaf emergence (58.32 and 49.48 for Xi19 and JB Diego, respectively). This point corresponded to flag leaf emergence. SPAD readings were significantly different by genotypes and sampling day ($P < 0.001$) (Figure 4.13). As observed in previous chapters, MBW generally had the greatest SPAD at the start of season. After approximately 191 DAS, all genotypes declined from leaf 'greenness'. MBW, JB Diego and Xi19 generally had the greatest SPAD readings throughout sampling although spelt genotypes generally had greater SPAD scores when compared to all einkorn and emmer cultivars. On the final sampling day (208 DAS) einkorn, einkorn SB, spelt SB, Tauro and Oberkulmer however had the greatest SPAD readings although it was clear that the flag leaves were no longer viable.

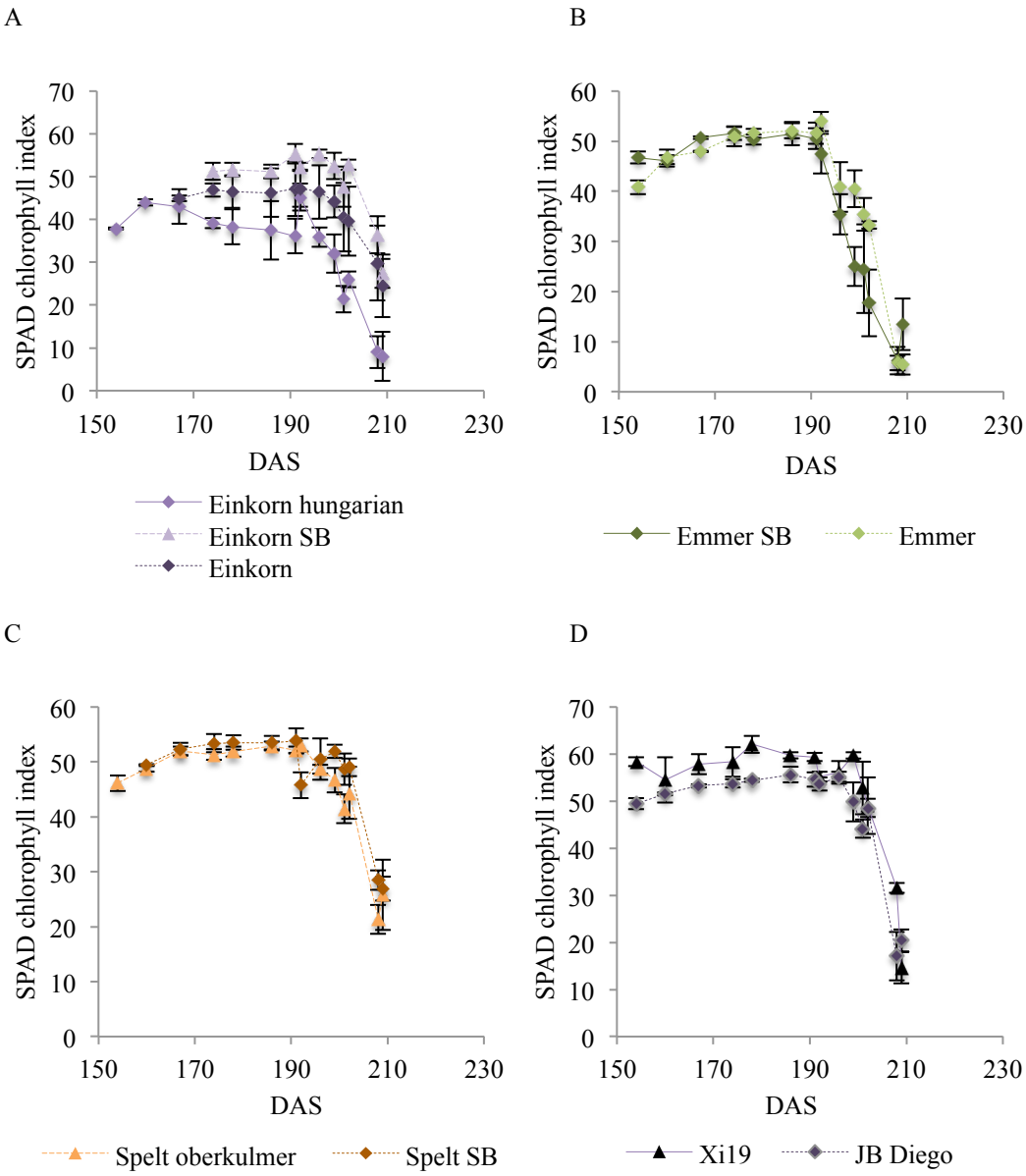


Figure 4.13: SPAD chlorophyll index of seven ancient species and two modern bread wheat species throughout glasshouse experiment III (from 154 to 208 DAS). (P <0.001, 261 DF, SED = 4.123) (error bars denote SEM by species).

When analysed by species, there were significant differences between species and by sampling day (P <0.001) (Figure 4.14). Modern bread wheat tended to have greater SPAD values early in the season and these were maintained throughout sampling. Einkorn species had the lowest leaf 'greenness' from 154 DAS to 191 (where values ranges from 37.88 to 46.66) however from 191 to 208 DAS emmer species showed the lowest SPAD values and therefore declined in terms of chlorophyll content of the

flag leaf at a faster rate when compared to other genotypes. These results did not show the presence of green area persistence trait for spelt species, although spelt did perform similarly to modern bread wheat.

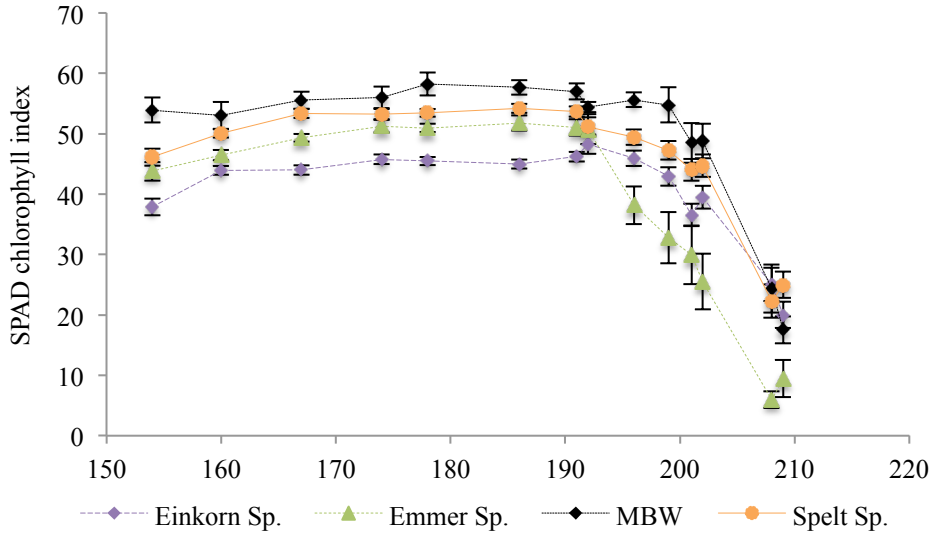


Figure 4.14: SPAD reading of four wheat species throughout glasshouse experiment III (from 154 to 208 DAS) (P <0.001, 338 DF, SED = 3.662) (bars represent SEM by species).

4.4 Discussion

4.4.1 Glasshouse experiment III

Previous chapters have assessed a range of traits both in the glasshouse and in the field. Field results (Chapter Two) indicated that there are differences, particularly for resource use efficiency and partitioning of acquired assimilates. In particular, einkorn, einkorn SB, spelt Tauro and SB showed high RUE although the true origins of these were not discernable. Measurements were therefore scaled down to the leaf level in two glasshouse experiments. The first focused on the full range of ancient wheat species, taking IRGA measurements within which plants were exposed to incremental atmospheric CO_2 concentrations in order to investigate biochemical properties the leaf. A small amount of variance was observed only for triose phosphate limitation. The study was, however, widened in the subsequent experiment (glasshouse experiment II) to include photosynthetic responses to light, which allowed assumptions to be made about the efficiency of genotypes at varying light exposures. There was significant variation observed for maximum photosynthetic rates and instantaneous transpiration efficiency also differed. Differences between genotypes observed for the mechanisms by which ITE was maintained; emmer increased photosynthesis and had high stomatal conductance, whereas spelt species achieved significantly higher ITE through reduced transpiration coupled with moderate photosynthetic rates and low conductance.

4.4.2 Biochemical parameters from A/C_i responses

In light of results from previous chapters, a sub-set of genotypes, which primarily include emmer and spelt cultivars, was established for glasshouse experiment III in which the biochemical properties at the flag leaf level were investigated. Although einkorn did show an intermediate mechanism for ITE (between that described for emmer and spelt), it was omitted. This was primarily due to poor emergence and the much slower developmental rates. Assessment of einkorn therefore would have been impractical, especially in light of equipment availability and time constraints for experiment III. Variance for V_{cmax} could be due to a number of factors including amounts of Rubisco within the leaf, specificity for CO_2 or affinity for oxygen. ANOVA of the subset of genotypes showed that there was no variation for V_{cmax} which corroborates those results reported previously in glasshouse experiment I. This indicates the investigated genotypes did not differ significantly in respect to Rubisco concentrations or O_2 affinity, indicating that the kinetic properties of Rubisco have been preserved among these ancient and modern genotypes (Wullschleger, 1993).

Triose phosphate utilisation limitation (TPU) was highest for emmer, emmer SB, spelt Tauro and MBW, Xi19, emmer and spelt Oberkulmer, reducing the limitation to carbon accumulation of chloroplast products such as triose phosphate (Sharkey *et al*., 2007). High pre-anthesis TPU displayed by emmer and emmer SB, high TPU pre-anthesis TPU are consistent with maximum rates of photosynthesis observed in glasshouse II. TPU was only consistently high between pre and post-anthesis for emmer indicating that these genotypes showed some proficiency to utilse the products of photosynthesis supplied by chloroplasts at a faster rate when compared

to other investigated genotypes. No ancient wheat genotypes showed significant variation for J_{max}, which supports previous results observed in glasshouse II.

4.4.3 Instantaneous Transpiration Efficiency

Condon *et al*., (2004) states increments in both carbon gained and water transpired to be instrumental for the enhancement of WUE. Assessment of ITE in glasshouse experiment III focused on a subset of genotypes to further investigate the mechanism observed in glasshouse experiment II, from which it was hypothesised that emmer had high photosynthetic rates corresponding with high conductance, and spelt had reduced transpiration rates corresponding with low conductance (Chapter Three, section 3.3.5.3). ITE, photosynthesis and transpiration measurements were measured on four separate occasions between 169 and 200 DAS. At 169 DAS, emmer SB was observed to have high ITE although emmer, previously seen to have high ITE in GH II, had the lowest ITE when compared to all other genotypes on this sampling date. At 169 DAS, ITE results were higher than those observed in glasshouse experiment II. This may be due to flag leaf age as the flag leaves assessed in glasshouse experiment II were considerably younger. Although emmer did not have high ITE at the start of the experiment, this genotype does maintain ITE over the course of the measurements. ITE in MBW, Xi19 and JB Diego declined at a faster rate. Additionally spelt Tauro and SB had high ITE throughout, and spelt Oberkulmer also maintained a relatively consistent ITE only reducing on the final sampling date. This was also observed on a species basis; modern bread wheat, spelt and emmer had similar ITE on 169 DAS, after which modern bread wheat declined. Spelt and emmer species continued to have consistently higher ITE until the close of measurements (although emmer species flag leaves had senesced by the final

measurement date, therefore there were only four sampling days for emmer but five for spelt and modern bread wheat. At 208 DAS, ITE for spelt species was significantly greater than modern bread wheat.

Genotypes were also described for photosynthetic rates and transpiration rates which, due to stomatal regulation, are intricately linked and therefore form the basis of ITE. Emmer had higher than average photosynthetic rates on 169 and 174 DAS, corroborating results from Chapter Three. On the following sampling dates however, high photosynthetic rates were not observed for emmer or emmer SB. Additionally, transpiration rates were highest for emmer, which is in contrast to that observed in GHII. Furthermore, MBW genotypes had high transpiration rates. The previous experiment discusses fundamental differences for ITE regulation either through reducing transpiration or increasing photosynthesis. This was reflected in species averages showing that modern bread wheat had greater transpiration compared to both spelt and emmer species towards the end of sampling.

C_i is a measure of CO_2 concentrations within the stomatal cavity, and therefore provides an indication of the quantity of substrate that is present for photosynthesis. Measurement of C_i allows assumptions to be made regarding the limitations on photosynthesis relating to biochemical and diffusion factors (Farquhar & Sharkey, 1982). C_i was greatest in those genotypes where photosynthetic rates were highest, namely modern bread wheat cultivars Xi19 and JB Diego. This was also reflected when data was analysed by species. As well as C_i, conductance plays a major role in photosynthesis as it provides information about the diffusivity of gases into and out of the leaf. Spelt genotypes displayed the lowest mesophyll conductance. Modern bread wheat had high mesophyll conductance, which consequently increased C_i,

therefore increasing photosynthetic rates. Furthermore, increased stomatal conductance may indicate differences in leaf physiology. These could be caused by increased stomatal aperture density, which are also likely to increase the amount of the primary substrate for photosynthesis (CO_2) that diffuses into the leaf.

The contrasting mechanisms previously observed for emmer and spelt genotypes for ITE were not observed in glasshouse experiment III, which may be due to the difference in water regime. The current experiment aimed to assess genotypes without resource constraint however all previous work had grown genotypes in water-limited conditions. Therefore, it is possible that these genotypes employ these mechanisms only when under drought stress.

4.4.4 WUE through $\Delta^{13}C$ of the grain

In glasshouse experiment III, WUE was assessed on two scales; flag leaf instantaneous transpiration use efficiency using IRGA, and the $\Delta^{13}C$ of grain which infers the WUE of the plant during the grain filling period. It was observed that spelt Tauro, emmer and emmer SB, genotypes previously observed to have high WUE through ITE measurements, had low $\Delta^{13}C$, indicating high WUE throughout the grain filling period. Although this was not necessarily the case at individual points, when the data was observed over the course of the five measurement dates, findings here are consistent with ITE results from GHIII and also corroborate the findings of GHII where cultivar emmer, and spelt genotypes showed an enhanced ITE. Similar rankings of ITE and $\Delta^{13}C$ indicate that WUE may well differ between genotypes, and species analysis showed the same trend where emmer and spelt species had greater $\Delta^{13}C$ than modern bread wheat which supports previous findings that wild

and cultivated emmer genotypes have the potential for superior WUE (Peleg *et al*., 2005; Al-Hakimi, 1998).

4.4.5 Specific Leaf Area

Specific leaf area relates to the leaf mass per unit leaf therefore greater SLA equates to thinner leaves (Westoby *et al*., 2002). It was expected therefore that, with increasing SLA, photosynthetic machinery within the leaf reduce also, potentially reducing photosynthetic capability. In glasshouse experiment III however, SLA was greatest for emmer and emmer SB, both of which were observed to have increased photosynthetic rates on the first two sampling dates. It is thought however, that these results may derive from lower leaf nitrogen content, leading to differences in the structural arrangement of photosynthetic components, which allowed greater access for CO_2 to catalytic sites within the leaf. Reich *et al*. (1998) state that for Rubisco to operate efficiently, the photosynthetic machinery needs to be spread thinly across the surface of the cell wall. Emmer and emmer SB were also observed to have high A_{sat} in glasshouse II, which supports these findings. Further investigation would require leaf physiological analyses, beyond the scope of the current project.

4.4.6 Biomass production

In glasshouse experiment III, the greatest amounts of biomass were produced by einkorn SB. Once again, MBW cultivars, Xi19 and JB Diego produced the least biomass. As observed in glasshouse experiment II, although ancient wheat species, particularly emmer, emmer SB and spelt SB produced a large biological yield, this was not necessarily reflected in in the harvestable product. Einkorn, einkorn SB and einkorn hungarian all produced the greatest quantities of biomass however, this was thought to be due to chaff and awns being present in the final grain weight as

einkorn ears were difficult to thresh without damaging individual grains, therefore a certain degree of compromise was needed. However, the high biological and harvestable yield observed for einkorn SB may also be instructive of high RUE observed in Chapter Two and the findings for high einkorn SB A_{sat} during investigation of light response in Chapter Three. Generally, total biological yield reflected harvestable yield as where large amounts of biomass were produced, so too were large harvestable yields.

In glasshouse experiment III, emmer and emmer SB displayed much lower transpiration and photosynthetic rates, particularly on 189, and 196 DAS than other genotypes. This may have reduced the amounts of total biomass and harvestable yields produced when compared to genotypes such as einkorn and einkorn SB as well as spelt SB. Furthermore, photosynthetic rates were lower for spelt Tauro which was also the genotype that produced the least total biomass and yield. Modern bread wheat, Xi19 and JB Diego produced the greatest yields; these genotypes also displayed the greatest C_i and stomatal conductance.

HI was significantly different and was greatest for einkorn and einkorn SB (potentially a result of high amounts of chaff and awns content in the final yield). HI was also high for JB Diego and Xi19. These results for MBW corroborate what was observed in Chapter Two although HI was much greater in the current experiment than GHII; this was a result of normal development for all spelt plants. Spelt Oberkulmer and SB had comparable harvest indices to MBW, Xi19 and JB Diego. Once again, results indicate that ancient wheat genotypes, particularly einkorn species, do have an ability to produce biomass. Generally results have indicated that ancient species do not partition assimilate to economic yield. The findings of

glasshouse experiment III however, contradict this, therefore the viability of these ancient wheat for agricultural purposes remains unclear.

Although results showed that SPAD readings significantly differed between genotypes and by species, glasshouse experiment III did not indicate the presence of a stay green trait, contradicting that already observed within previous experiments in the current project. It is possible that this was due to non-limiting irrigation which may have not been the case in the field trials of 2010 and 2011 where the trait was first observed since these were both rain-fed. Furthermore, the green area persistence trait was observed to be particularly severe in glasshouse experiment II where plants were purposefully exposed to post-anthesis drought (although this might also be an artifact, caused by abnormal development). It might however, be the case that this trait is a protection mechanism. Lawson *et al*. (2012) states that prolonged survival of green area may be a result of an enhanced ability to react to reactive oxygen species (ROS), which could be expressed within stressful environments or alternatively may be caused by an adaption in the chlorophyll catabolic pathway (Thomas *et al*., 2001). This absence of 'stay green' in glasshouse experiment III was particularly unfortunate; since the 'stay green' trait in GHIII could not be confirmed, it was not possible confirm whether green area was photosynthetically active, although Chapter Two does indicate that spelt genotypes continue to accumulate biomass between anthesis and harvest which indicates that further investigation is warranted. Additionally, it would also be interesting to investigate the effects that green area persistence has on nitrogen re-mobilisation.

4.5 Conclusions

This component of the experiment was a means to explore the selected genotypes without water limitation. Data gained here did show some consistencies, for instance investigation of biochemical properties of the leaf showed very little variation for carboxylation rates or electron transport which are traits that are considered to be highly conserved within crop species (Wullschleger, 1993), thus the variation between these ancient wheat and modern genotypes proved insufficient to provide such differences. Additionally, genotypes that displayed high RUE in Chapter Two were also observed to possess a high maximum rate of photosynthesis perhaps indicating an enhanced ability to accumulate biomass at the leaf level. Furthermore, genotypes with potential green area persistence traits displayed slower reductions in photosynthetic rates over sampling dates when compared to MBW.

Results from glasshouse experiment III showed that ancient species produced quantities of biomass comparable to MBW, however these were not translated to yields (as was also observed in glasshouse experiment II). HI therefore, was much greater for modern wheat genotypes than for the ancient species. This implies that the introduction of traits from ancient wheat species is likely to derive from a proficiency to produce biomass rather than ability for yield production. Furthermore, as the HI threshold for modern wheat cultivars approaches, biomass production may hold the key for yield enhancement. Chapter Three indicated that ancient wheat had leaf level mechanisms that conferred a more conservative use of water through greater ITE, as did $\Delta^{13}C$ analysis in GH III. These mechanisms however, were observed to a lesser extent in the current chapter, as was also the case for green area longevity. It is thought that this occurred because the experiment was maintained

without water limitation, indicating that the traits thought to impact high RUE observed in Chapter Two such as ‘stay green’ and increased ITE (observed in glasshouse experiment II) may be an adaptation to limited irrigation, and therefore only arise when plants are maintained under drought. Results are therefore by no means conclusive, but consistencies throughout data show that a degree of variation does exist between these ancient wheat genotypes and modern bread wheat cultivars that may be useful to introduce wider resource use traits for the improvement of modern bread wheat.

Chapter Five:

General discussion and conclusions

5.1 Introduction

Physiological and yield potential data for ancient wheat species is relatively sparse although spelt and emmer have been reported to performed well within low input conditions (Troccoli and Codianni, 2005). Other research indicates that old cereal cultivars have higher radiation use efficiency than their modern counterparts (Muurinen & Peltonen-Sainio, 2005). This project aimed to characterise the traits of ancient wheat species and compare them with the characteristic traits of modern bread wheat. In the first phase of the experiment, detailed analysis of the above ground partitioning, yield and morphology were studied for the eight ancient wheat species (Chapter Two), six were found to be of interest for resource use efficiency or had been indicated to have favorable characters such as WUE (Reported by Isaaks, 2009 and Sparkes, 2010). In Chapter Three, further analyses assessed the biochemical properties of genotypes, after which a sub-set of five genotypes were selected. Chapter Four analyses were scaled down to physiologically characterise leaves. This chapter aims to integrate the main findings of the project, regarding the initial hypothesis and relevant findings previously reported in the literature.

Biological yield may be enhanced through several avenues; 1) the duration of the crop may be increased, 2) the fraction of solar radiation intercepted may be enhanced, or alternatively 3) the efficiencies at which individual plant metabolisms can convert resources into plant dry matter may be enhanced (Murchie *et al*., 2008). These factors culminate to determine the proficiency at which a species will translate resources into biological yield. There are a number of variables thought to influence RUE; the variation for some of these has been discussed in the current work.

5.2 Plant growth, development and canopy architecture

Morphological character traits, ultimately affect the amounts of Photosynthetically Active Radiation (PAR) intercepted by a crop canopy, and therefore have a large bearing on biological yields. A vast number of elements will affect morphology; these include development rates, tiller economy, and leaf biomass partitioning (Azam-Ali & Squire, 2002).

Miralles & Slafer (1997) state that genetic reductions in the height of wheat canopies would not adversely affect light interception within optimal conditions. Field experiments outlined in Chapter Two highlighted that, at key growth stages modern bread wheat, although observed to generally have reduced height throughout the season, showed increased height at growth stage 31. The faster developmental rates of MBW was theorised to confer early vigour, allowing increased rate of canopy expansion. This limited weed competition and allowed a larger proportion of the low incident light conditions during the initial weeks of the UK winter wheat season, to be utilised. Canopy architecture is influential in resource capture; Muurinen & Peltonen-Sainio (2006) state that canopy height influences radiation spread within the canopy; height influenced the fraction of light intercepted, radiation use efficiencies as well as the biomass accumulation, in turn impacting GAI. Modern bread wheat intercepted the largest fraction of light per unit height, therefore intercepting more light within the uppermost layers of the canopy, allowing flag leaves, which are the main contributors to carbon assimilation, the greatest proportions of incident light. This was thought to be a more ‘economical’ use of radiation within environments such as those within the UK, where incident irradiance is often the limiting factor.

Tiller production was variable across years with ancient species, especially einkorn, producing more tillers than modern bread wheat cultivars in 2010, as was hypothesised at the outset of the project. The increased tiller production for ancient species in 2010, agrees with Critchley (2001), who stated that increased vegetative phase (due to slow development) increased the time frame where tiller production could occur. Furthermore, Sparkes *et al*., (2006) state that plant population affects tiller initiation therefore, this tiller production was probably influenced by large differences in population densities (due to the variable emergence). The extent of the differences for tiller production were not conclusive since ancient wheat species had greater tiller production compared to MBW in 2010, whereas the converse was true in 2011. Additionally, GAI was also influenced by population density and tillering; GAI developed until anthesis after which it declined. Increments in GAI observed from flag leaf emergence to anthesis in einkorn and einkorn SB however, were enhanced through increased shoot production. Reynolds and Trethowan (2007) state that high tiller production is a mechanism whereby ground cover can be increased. The proliferation of tiller numbers in einkorn and einkorn SB also corresponded with increased fractional interception (*F*). The conclusions made from this component of the experiment are subject to the variation imposed by the differential emergence rates, which naturally, had an impact on plant population, tiller production and survival and therefore, also influenced light interception. It is therefore not possible to accept H_2, which stated that modern bread wheat, would produce fewer tillers, results did indicate however, that modern bread wheat did partition fewer assimilates towards tillers indicated by smaller proportions of biomass being directed to leaf and straw material, when compared to ancient wheat species.

5.3 Biomass production and RUE

In field experiments, bread wheat produced more biological yield when compared to ancient wheat species. Despite low emergence, spelt species generally produced more biomass (g m^{-2}) compared to einkorn and emmer. Furthermore, spelt displayed increments in biomass from anthesis through to pre-harvest, although this was observed to a lesser degree in 2011. These trends were consistent with the extended GAI observed in spelt species. Therefore, despite low plant densities, spelt indicated proficiency for biomass production, which was similar to that of modern bread wheat across both seasons. This was further supported by high RUE, particularly for spelt Oberkulmer and Tauro, both at pre- and post- anthesis in 2011 when compared to all modern bread wheat cultivars, as was hypothesised. High RUE was not consistent for these genotypes in 2010 therefore H_5, stating that spelt germplasm would have greater RUE cannot be accepted. Einkorn and einkorn SB also displayed high RUE across both experimental years, which was thought to be due to profuse tillers production because of low plant density. Einkorn species were also observed to produce reasonable yields in 2011 where ear indices were comparable to those of MBW. However, in 2010, spelt species directed the largest proportions of biomass towards the ear of the ancient species. These findings imply that the shorter culm length of modern bread wheat did not confer greater RUE as Toyota *et al*. (2010) suggested.

In glasshouse experiment II, spelt Oberkulmer produced the greatest biomass, although this did not translate through to yield, which could have been a reflection of poor development observed for spelt genotypes. Low yields may also be indicative of the lower photosynthetic rates observed for these cultivars. Therefore, it is thought that this advantage for biomass production was a function of increased green area

duration, rather than photosynthetic capability, indicating a green area persistence trait. Einkorn cultivars were also observed to produce comparable amounts of biomass however this was thought to be a result of poor establishment and consequently, profuse tillerring. These results support the hypothesis (H_1) stating that ancient wheat biomass production, particularly that of einkorn and spelt would be comparable to modern bread wheat.

Investigation of canopy structure combined with assimilate partitioning data, indicated that the shorter stature of modern bread wheat, and greater GAI, allowed for greater harvest indices and larger quantities of assimilates to be partitioned towards the ear. However, the taller ancient wheat species, partitioned greater quantities of biomass towards tiller production. Further assessment of biomass partitioned to the ear in 2010, show emmer species to direct the largest proportion of biomass toward ear components although this was not necessarily instructive of greater yield, since JB Diego, achieved the highest harvest index (HI). This therefore supports H_4, suggesting that modern bread wheat partitioned more carbon towards the ear when compared with ancient species, and therefore had greater harvest indices. This implies that the structure (corroborated by high GAI and *F*) of JB Diego and modern bread wheat in general, to be preferable to that of emmer and ancient species. It is important to note therefore that, although the economic yield of modern bread wheat was greater, a small proportion of this derives from the ability to produce biomass, but instead, originates from HI which has been selectively bred into germplasm (Shearman *et al*., 2005). This can be illustrated by einkorn, which had the lowest tiller survival rate, however despite this, still produced reasonable yields compared to other genotypes. It is therefore the ability to produce greater biological yields, rather than yield production in ancient wheat species that could

provide the necessary genetic gains (Shearman *et al*., 2005). The investigations performed in 2010 and 2011 could not identify a clear trend in dry biomass partitioning by genotypes or by species, however Takahasi & Nakaseno (1990) suggested that biomass partitioning typically influences the fraction of irradiance that the canopy is able to intercept and thus will indirectly impact the amounts of biomass accumulated.

5.4 Photosynthetic radiation capture and conversion

It could be the case that enhanced RUE may stem from enhancements to the photosynthetic machinery or processes. Chapter Three shows that there were positive associations between maximum rates of photosynthesis and RUE, indicating the importance of leaf level traits to overall productivity. Chapter Four followed on from this, by describing some of the factors which impose limitations to productivity at the leaf level.

5.4.1 Biochemical aspects of leaf physiology

An increase in carboxylation rates could be fundamental to superior RUE. It has been reported that variation in A_{sat} (GH II), should also reflect similar variation in related parameters such as maximum rates of carboxylation (V_{cmax}) (Reich *et al*., 1998). Einkorn and spelt Tauro, which both had high RUE in field trials (where only pre-anthesis RUE differed in 2011) had relatively high V_{cmax} also. Differences between genotypes for V_{cmax} however, were not significant; in fact little variation was observed for biochemical parameters, which was also the case in GH III. This corroborates Wullschleger (1993), who found no differences in the biochemical reactions that regulated gas exchange between crop species.

In both glasshouse experiment I and III however, there were significant differences found for R_d and TPU. The former represents the CO_2 lost through respiration, resulting in assimilate losses. Respiration is an essential process which is affected by the efficiency of photosynthesis as well as the irradiance capture (Azam-Ali & Squire, 2004). The latter therefore, infers that respiration will be influenced by canopy architecture. In GH I, emmer and spelt SB had the greatest R_d whereas emmer and spelt Oberkulmer were observed to have high R_d in GH III. Consistently however, modern bread wheat showed reduced R_d when compared to ancient species (both pre and post-anthesis for glasshouse experiment III), indicating that MBW had consistently lower respiration rates. This is pertinent since respiration can account for up to 30% of the rate of photosynthesis (Rawsthorne, 1992). The lower respiration rates of modern bread wheat therefore imply an increased efficiency. Furthermore, MBW maintained R_d from pre to post anthesis in glasshouse experiment III, whereas emmer and spelt showed large increases after anthesis, indicating that R_d increased with leaf age. TPU in spelt Tauro and einkorn SB, displaying high RUE in previous field trials, indicating lower limitation imposed by the products of photosynthesis (such as triose phosphate). Stomatal conductance (G_s) affects the diffusion of CO_2 across the cell wall and is therefore a major limitation for photosynthesis (Terashima *et al*., 2011). In glasshouse experiment I, G_s did differ between species, being much lower in einkorn and MBW. This would provide a particular advantage because of the low catalytic rate of Rubisco (Terashima *et al*., 2011).

5.4.2 Photosynthetic capacity

In Chapter One, it was hypothesised that ancient wheat genotypes and modern bread wheat cultivars would have comparable photosynthetic rates. Results suggested that

this was not the case where in glasshouse experiment II pre-anthesis emmer and einkorn SB, had greater photosynthetic rates. In the same experiment, A_{sat}, defined as the maximal rate of photosynthesis under light saturated conditions, was generally seen to reduce with time (from pre to post-anthesis), indicating that the photosynthetic capabilities of the flag leaf reduced with age in all genotypes except for Spelt SB, spelt Tauro and Xi19. Spelt Oberkulmer also displayed conserved A_{sat} photosynthetic rates from pre to post anthesis. Emmer, also displayed high pre and post anthesis photosynthetic rates during ITE measurements (GH II). These genotypes therefore had an enhanced ability to assimilate carbon, which may derive from increased Rubisco concentrations per unit leaf area (Terashima *et al.*, 2011). Reich *et al*. (1998) state that variation for photosynthetic assimilation (A_{sat}) is primarily due to differences in biochemistry rather than differences in CO_2 supply. It was also these genotypes that had a greater ability to assimilate carbon in light limited conditions, indicated from high quantum yields. Therefore photosynthetic rates of emmer and einkorn SB are comparable to those of the MBW cultivar investigated. This supports H_6, which stated that the photosynthetic rates of modern bread wheat and ancient wheat species would not differ, relative to einkorn SB (pre-anthesis only) and emmer, however must be rejected when considering the other investigated genotypes. A_{sat} results also suggest that spelt genotypes may contribute to carbon accumulation to a greater degree, post-anthesis, which could also be linked to the 'stay green' leaf traits observed in spelt all genotypes. Furthermore, this carbon accumulation may also be related to the generally lower SPAD values observed for spelt genotypes pre-anthesis, which were seemingly 'conserved' throughout the life of the flag leaf.

It is possible that this variation derives from the intrinsic physiology of the leaf, which may be caused by 1) differential Rubisco limitations 2) Rubisco concentrations or 3) physiological variation in leaf structure. Although 1) and 2) were not investigated in the current work, investigation of SLA, thought to represent the variation due to environmental adaptation (Reich *et al*., 1997), indicated that some variation may exist for leaf structure between these genotypes. SLA relates to the leaf area per unit mass invested, and therefore indicates efficient light capture and photosynthetic capacity (Reich *et al*., 1997). MBW had significantly thicker leaves, compared to ancient species, which Reich *et al*. (1998) infers reduced A_{sat} per unit nitrogen (N). Emmer had the thinnest leaves as well as high A_{sat} in GH II, which also supports this hypothesis.

Leaves are highly complex structures containing photosynthetic machinery however, the packaging and orientation of the various components is highly dynamic among species (Morison & Lawson, 2007). Photosynthesising cells and chloroplasts are arranged some distance from stomatal openings, thus in different species, the diffusion pathway for CO_2 differs. The relevance of this may be considered since it describes that pathway by CO_2 diffusion pathway (Morison & Lawson, 2007). It is therefore likely that the structural differences between the two epidermal layers are indicative of the variation; leaf thickness (SLA), may be used to indirectly infer structural differences between genotypes. Results indicate that emmer had reduced leaf thickness compared to MBW, inferring that Rubsico was spread more thinly across the cell wall, allowing CO_2 to diffuse to catabolic sites with greater ease (Reich *et al*., 1997) whereas the thicker, more dense leaves, within MBW may have caused leaf shading which could have limited light reaching the chloroplast, consequently reducing CO_2 access to active sites (Reich *et al*., 1997). Further

assumptions can also be made from SLA; Reich *et al*. (1997) state that plants with high SLA, high A_{sat} and short leaf life spans (as observed for modern bread wheat species) commonly have high relative growth rates.

The increased A_{sat} of einkorn SB may also be linked with high RUE observed in both field trials. Despite being low, the A_{sat} for spelt genotypes were fairly consistent from pre to post anthesis and actually increased with leaf age for spelt SB and Tauro. This stability for carbon accumulation could indicate that the stay green trait suggested by SPAD measurements and visual scoring (Chapter Two) was 'functional', i.e. was still photosynthetically active, and therefore contributing to carbon assimilation. Thus, although other genotypes may well have an enhanced ability to assimilate carbon at limited and saturating light intensities, spelt Tauro and SB may maintain A_{sat} for a longer duration, providing a basis for the high RUE previously reported. As well as spelt SB and Tauro, Xi19 showed increased A_{sat} from pre to post-anthesis. Overall, the data combined is not clear cut however, there are inferences of greater carbon assimilation for some of the genotypes, one in particular being that of the 'stay green' trait in spelt. The exact causes of the variation for photosynthetic ability are not known, however results indicate that increased life-span and instantaneous productivity, indicated by A_{sat}, confer some advantage for RUE and biomass production. Further work could be carried out investigating the content and re-allocation of nitrogen to various photosynthetic pools, which may help to undercover the basis of the observed variation.

5.5 Water Use Efficiency

There is a requirement to identify plants which harbour underlying mechanisms for improved WUE (McAusland *et al*., 2013). As discussed in Chapter One, water use

efficiency can be defined through 1) instantaneous transpiration use efficiency (A/T), 2) ratios of biomass to water uptake or 3) carbon isotope discrimination ($\Delta^{13}C$). It was hypothesised that since the ancient varieties included in the current study would have originated from the dry, rain-fed Fertile Crescent, they would possess traits that confer an adaption to limited water supply and therefore, be more efficient in water use. Similar rankings using all three methods indicate that WUE differs between genotypes and species where emmer and spelt species had greater $\Delta^{13}C$ than modern bread wheat. All glasshouse experiments indicate enhanced WUE in ancient wheat species, except for glasshouse experiment III, where enhanced ITE was not observed, potentially because drought conditions were not imposed. Even so, although ITE was not consistently high after the first sampling date, a trend was observed where ancient wheat species maintained ITE over time. Results support previous findings that wild and cultivated emmer genotypes have the potential for superior WUE (Peleg *et al*., 2005; Al-Hakimi, 1998). High ITE in wheat is usually associated with lower stomatal conductance and photosynthetic rates (Fischer, 2011). All spelt cultivars displayed low stomatal conductance (pre and post-anthesis), which may be the origin of the low photosynthetic rates observed in spelt genotypes, therefore increasing ITE. Spelt genotypes, particularly spelt Oberkulmer, consistently displayed low transpiration rates, coupled with moderate photosynthetic rates. The large quantities of biomass produced however, suggest that the trade off for lower photosynthetic rate and transpiration rate, leading to high ITE did not allow them to produce large economic yields however, paid dividends in terms of biological yield production. In contrast, emmer genotypes indicated that ITE was enhanced by increased photosynthetic rates. Furthermore, einkorn had high photosynthetic rates pre-anthesis for high ITE and low transpiration post-anthesis

and therefore seemingly used both mechanisms to conserve ITE. Stomatal conductance for einkorn was also intermediate of those of emmer and spelt cultivars. This suggests that these ancient wheat genotypes, originating from the dry rain-fed Fertile Crescent, were more conservative in their use of water, supporting H_7. Additionally, results indicated that the WUE observed in ancient species derived from low transpiration and conductance in spelt species only. The contrasting mechanisms observed for emmer and spelt genotypes in glasshouse II were not observed in glasshouse experiment III, thought to be a result of the different water regimes used; glasshouse experiment III aimed to assess genotypes without resource constraint however all previous work had grown genotypes in water-limited conditions. Therefore, it is possible that these genotypes employ these mechanisms only when under drought stress. It might, therefore, be the case that this trait is a protection mechanism. Lawson *et al*. (2012) states that prolonged survival of green area may be a result of an enhanced ability to react to reactive oxygen species (ROS) which, could be expressed within stressful environments or alternatively may be caused by an adaption in the chlorophyll catabolic pathway (Thomas *et al*., 2001). There is some debate as to the environmental conditions under which this trait is useful. Christopher *et al*. (2008) reported that, in wheat, stay green was only useful when water was available post-anthesis, while Borrell & Hammer (2000) found that stay green in sorghum is associated with post-flowering drought resistance. Results corroborate the observation that spelt has greater canopy persistence (Sparkes, 2010). Larbi & Mekliche (2004) state that genotypes reported to have functional green area persistence during grain filling may be the key to securing wheat yields in semi-arid regions.

5.6 Green area persistence

The final aspect of the project related to the 'stay green' trait. It was thought that spelt cultivars would display green area persistence particularly, post-anthesis when compared to all other genotypes. Christopher *et al*. (2008) states that increased flag leaf duration may afford plant the propensity to resist drought in certain environmental conditions. It could therefore be purported that spelt species, particularly spelt Oberkulmer, were able to maintain a high WUE (indicated through ITE measurements and biomass/water uptake ratios) as a result of the 'stay green' trait, particularly under drought. The extent to which spelt species stayed 'green' in glasshouse experiment II surpassed that observed in any of the previous experiments and could be purported to be a result of the drought conditions imposed which might may have lead to the expression of these tolerance traits (Lawson *et al*., 2012). The results of GH III demonstrated that ancient wheat species, particularly emmer species, had significantly greater specific leaf area, indicating reduced leaf thickness. Reich *et al*. (1998) report that increased nitrogen per unit area leaf follows from increased leaf thickness, associated with increased chloroplasts width, reducing the activity of Rubisco by reducing the diffusion of CO_2 to catalytic sites (Reich *et al*., 1998). Conellison *et al*. (2003) also state that low SLA tends to correspond with structural investments in leaf 'defenses'. Spelt species had a high SLA and was also observed to 'stay green' post-anthesis. MBW however, had thicker leaves, which generally senesced earlier; Reich *et al*. (1997) suggest that this may be due to the overall cost where A_{sat} and respiration are dependent on the abundance of photosynthetic enzymes, pigments and other compounds. The high provision of these may provide high net CO_2 exchange, but ultimately, this will limit the longevity of the leaf (Reich *et al.*, 2007). Additionally, environmental conditions

also influence SLA, where species grown within resource rich environments tend to display higher SLA overall (Cornellison *et al*., 2003); thus the non-limiting conditions in which plants were maintained may be a confounding factor which meant that emmer, which did not display green area persistence, had higher SLA than with spelt species. Results indicate that spelt species display the 'stay green' trait through increased green area longevity compared to the other species assessed, supporting H_3. Further analyses should assess this 'stay green' trait under non-limited water and drought conditions, and investigate the extent to which photosynthetic area is maintained and functional in the two environments. Increasing photosynthesis is a promising avenue through which productivity may be enhanced. Clearly, the maximum leaf photosynthetic rate is the main theoretical variable that influences RUE (Sinclair & Muchow, 1999) however, the current work also suggests that duration could enhance photosynthetic assimilation.

5.7 Further Work

This project, for the most part, explored selected genotypes without water limitation. Data gained here did show some consistencies, however it might be useful to characterise these genotypes under severe drought, as this seems to be the environment in which the 'stay green' trait and WUE (through the ITE mechanism), has been most apparent. These may allow RUE and WUE to be related as Caviglia & Sadras (2001) state they are. The project aimed to be as comprehensive as possible however, with the benefit of hindsight, all glasshouse experiments would use soil columns and include additional investigation of root biomass. It was clear that plant emergence continued to be a constraining factor, particularly in field experiments, which limited identification of interception traits. Avenues to circumvent this would be to treat seed in order to increase viability or alternatively increase seed rates, and

then thin plants to the equivalent population densities. Canopy traits were measured as comprehensively as possible however, the analyses could further be enhanced by placing sensors in the field and recording continuous data even between growth stages.

The scope for developing the current project is expansive. With the prospect of techniques that allow greater throughput as well as a higher resolution of traits, WUE in these species could be explored to provide much firmer conclusions. The techniques used all have specific drawbacks, for instance $\Delta^{13}C$ are destructive measurements that are based on cumulative seasonal conditions, and therefore may mask specific phenotypic traits (McAusland *et al*., 2013); the use of a range of methods allows WUE to be investigated at different scales which can indicate consistencies in the data; these have proved to be useful in the current work. However, Lawson & Morison (2006) and McAusland *et al*. (2013) report techniques whereby leaf diffusion can be visualised in order to screen genotypes for gas exchange. This would allow spatial patterns of CO_2 concentrations, which factor in the dynamics between A and g_s, to be characterised, allowing a more comprehensive understanding of WUE (McAusland *et al*., 2013). Such results could elucidate the variation for diffusion of gases into and out of the leaf. Structural analyses, such as microtome sectioning would also be valuable. This type of study would be useful for genotypes such as emmer and spelt, which have shown high photosynthetic ability and tolerance to water deficit.

Additionally, given the apparent differences for water uptake between genotypes, water use could be investigated in relation to root traits. An example of which observed synthetic wheat derivatives which had genes from the diploid wild species

T. tauschii (DD genome), showed that plants had similar dry weight to control cultivars however, roots were distributed more deeply into the soil profile (Reynolds *et al*., 2007). Additionally, root screening techniques, such as WinRhizo (Regent instruments Inc., Quebec, Canada) could be utilised as these are less time consuming and provide a more informative analyses than biomass growth analyses (McAusland *et al*., 2013).

5.8 Conclusions

The current work investigated several morphological and physiological parameters of ancient and modern bread wheat cultivars, some of which appear to influence the efficiency and assimilation of carbon and water. The current work shows sufficient variation to that suggest that survival and duration may be the priority in ancient wheat rather than productivity, with some genotypes indicating increased WUE and leaf longevity. In field trials high RUE was observed for several of the ancient wheat species. Although during this particular experiment, there were confounding factors, which made the origin of this efficiency unclear, further research did highlight potential factors that may have contributed to these findings. The most prominent were 1) green area longevity and 2) enhanced WUE, both of which contributed to a proficiency to produce biological yields comparable to those of MBW.

Spelt species consistently displayed green area longevity, essentially lengthening the growing season and therefore leading to greater biomass accumulation, therefore taking advantage of high incident radiation within the UK winter wheat growing season. The green area longevity observed in spelt appeared to be conserved throughout the species, presenting in all genotypes investigated however, it emerged that there may be some plasticity for this trait which was indicated by the lack of ‘stay green’ where plants were watered without limitation. These findings do

however highlight a successful adaptation within drought prone environments, which could prove to be of value to future modern wheat breeding. Additionally, investigation of leaf level water use highlighted variation between species for the mechanism by which ITE was maintained, traits which could be utilised in order to produce novel wheat varieties with adaptations to specific environmental conditions. An example of which is the production of the Australian varieties, Drysdale and Rees, where backcrossing techniques allowed ITE to be enhanced whilst maintaining traits that afforded the varieties protection against biotic stresses (Condon *et al.*, 2004). Enhanced WUE and green area longevity traits could provide promising adaptations to plants within resource-limited environments. Therefore they highlight avenues through which the biological yield per unit resource may be boosted in the production of modern wheat cultivars. Such traits may prove to be useful to supplement the variation for resource use in modern bread wheat.

Despite a broad analysis of these genotypes, further clarification of the mechanisms responsible for these adaptive traits are required therefore, this research provides a foundation for the development of quantitative trait investigations that should be performed within controlled environments. Close collaboration of molecular physiology and cell biology would also be an advantage with the potential to use genetic microsatellites with a range of metabolic and structural capabilities that may be altered through gene expression. The array of genomic data available, and the availability of genetic markers could allow genetic trait mapping, which further increases the feasibility of marker assisted breeding (Lawson *et al*., 2012). The current project provides indications that ancient wheat genotypes may prove useful in supplementing genetic variation in modern bread wheat in order to enhance productivity for more efficient crop systems.

References

Aggarwal P & Sinha S (1983a) Relationship between mother shoot and tillers as a criterion of selection for wide or specific adaptability to drought in wheat. *Neurology* **152:** 310-320.

Aggarwal P & Sinha S (1983b) Water stress and water-use efficiency in field grown wheat: A comparison of its efficiency with that of C4 plants. *Agricultural Meteorology* **29:** 159-167.

Al-Hakimi A (1997) Primitive tetraploid wheat species to improve drought tolerance in durum wheat. In *Triticeae III*. *Proceedings of the Third International Triticeae Symposium*, pp 4-8.

Araus J, Slafer G, Reynolds M & Royo C (2002) Plant breeding and drought in C3 cereals: what should we breed for? *Annals of Botany* **89:** 925-940.

Austin R, Bingham J, Blackwell R, Evans L, Ford M, Morgan C & Taylor M (1980) Genetic improvements in winter wheat yields since 1900 and associated physiological changes. *The Journal of Agricultural Science* **94:** 675-689.

Azam-Ali SN & Squire GR (2002) *Principles of tropical agronomy*: CABI.

Beadle C & Long S (1985) Photosynthesis—is it limiting to biomass production? *Biomass* **8:** 119-168.

Bertin P, Gregoire D, Massart S & De Froidmont D (2001) Genetic diversity among European cultivated spelt revealed by microsatellites. *Theoretical and Applied Genetics* **102:** 148-156.

Bognár Z, Láng L & Bedő Z (2007) Effect of environment on the plant height of wheat germplasm. *Cereal Research Communications* **35:** 281-284.

Borrell AK & Hammer GL (2000) Nitrogen dynamics and the physiological basis of stay-green in sorghum. *Crop Science* **40:** 1295-1307.

Boyer JS (1982) Plant productivity and environment. *Science* **218:** 443-448.

Burgos MS, Messmer M, Stamp P & Schmid J (2001) Flooding tolerance of spelt (*Triticum* spelta L.) compared to wheat (*Triticum aestivum* L.)–A physiological and genetic approach. *Euphytica* **122:** 287-295.

Calderini DF & Slafer GA (1998) Changes in yield and yield stability in wheat during the 20th century. *Field Crops Research* **57:** 335-347.

Campbell KG (1997) Spelt: agronomy, genetics, and breeding. *Plant Breeding Reviews* **15:** 187-214.

Campbell NA and Reece JB (2002) Biology (Sixth Edition). Benjamin Cummings.

Carver BF & Nevo E (1990) Genetic diversity of photosynthetic characters in native populations of *Triticum dicoccoides*. *Photosynth Res* **25:** 119-128.

Cassman KG (1999) Ecological intensification of cereal production systems: yield potential, soil quality, and precision agriculture. *Proc Natl Acad Sci U S A* **96:** 5952-5959.

Caviglia OP & Sadras VO (2001) Effect of nitrogen supply on crop conductance, water- and radiation-use efficiency of wheat. *Field Crops Research* ***69:*** *259-266*.

Chaves M & Oliveira M (2004) Mechanisms underlying plant resilience to water deficits: prospects for water-saving agriculture. *Journal of Experimental Botany* **55:** 2365-2384.

Chaves MM, Pereira JS, Maroco J, Rodrigues M, Ricardo CPP, Osorio M, Carvalho I, Faria T & Pinheiro C (2002) How plants cope with water stress in the field? Photosynthesis and growth. *Annals of Botany* **89:** 907-916.

Christopher J, Manschadi A, Hammer G & Borrell A (2008) Developmental and physiological traits associated with high yield and stay-green phenotype in wheat. *Crop and Pasture Science* **59:** 354-364.

Clark B, Cockerell V & Thomas J (2004) Wheat seed health & seed-bornediseases – a guide. *HGCA*.

Condon A, Richards R & Farquhar G (1993) Relationships between carbon isotope discrimination, water use efficiency and transpiration efficiency for dryland wheat. *Crop and Pasture Science* **44:** 1693-1711.

Condon A, Richards R, Rebetzke G & Farquhar G (2002) Improving intrinsic water-use efficiency and crop yield. *Crop Science* **42:** 122-131.

Condon AG, Richards RA, Rebetzke GJ & Farquhar GD (2004) Breeding for high water-use efficiency. *J Exp Bot* **55:** 2447-2460.

Cornelissen J, Lavorel S, Garnier E, Diaz S, Buchmann N, Gurvich D, Reich P, Ter Steege H, Morgan H & Van Der Heijden M (2003) A handbook of protocols for standardised and easy measurement of plant functional traits worldwide. *Australian Journal of Botany* **51:** 335-380.

Critchley CS (2001) A physiological explanation for the canopy nitrogen requirement of winter wheat. PhD Thesis. The University of Nottingham.

Davies B, Baulcombe D, Crute I, Dunwell J, Gale M, Jones J, Pretty J, Sutherland W & Toulmin C (2009) *Reaping the Benefits: Science and the sustainable intensification of global agriculture*: Royal Society.

Dempster S (2013) The physiological basis of genetic variation in radiation-use efficiency and biomass in wheat. PhD Thesis. The University of Nottingham.

Diaz-Alves AT (2008) Resource capture characteristics of ancient wheat species. MSc Thesis. The University of Nottingham.

Ehleringer J & Pearcy RW (1983) Variation in quantum yield for CO2 uptake among C_3 and C_4 plants. *Plant physiology* **73:** 555-559.

Ehrlinger J & Björkman O (1977) Quantum yields of CO2 uptake in C_3 and C_4 plants; dependence on temperature, CO2, and O2 concentration. *Plant physiology* **59:** 86-90.

Evans JR (1996) Developmental constraints on photosynthesis: effects of light and nutrition. In *Photosynthesis and the Environment*, pp 281-304. Springer.

Ewert F & Pleijel H (1999) Phenological development, leaf emergence, tillering and leaf area index, and duration of spring wheat across Europe in response to CO_2 and ozone. *European journal of Agronomy* **10:** 171-184.

Falqueto AR, Cassol D, Magalhães Júnior AMd, Oliveira ACd & Bacarin MA (2009) Physiological analysis of leaf senescence of two rice cultivars with different yield potential. *Pesquisa Agropecuária Brasileira* **44:** 695-700.

Farquhar GD, von Caemmerer S & Berry JA (1980) A biochemical model of photosynthetic CO_2 assimilation in leaves of C_3 species. *Planta* **149**: 78-90.

Farquhar GD & Richards R (1984) Isotopic composition of plant carbon correlates with water-use efficiency of wheat genotypes. *Functional Plant Biology* **11:** 539-552.

Farquhar GD, Ehleringer JR & Hubick KT (1989) Carbon isotope discrimination and photosynthesis. *Annual review of plant biology* **40:** 503-537.

Farquhar GD, O'leary M & Berry J (1982) On the relationship between carbon isotope discrimination and the intercellular carbon dioxide concentration in leaves. *Functional Plant Biology* **9:** 121-137.

Farquhar GD & Sharkey TD (1982) Stomatal conductance and photosynthesis. *Annual review of plant physiology* **33:** 317-345.

Fischer R (2011) Wheat physiology: a review of recent developments. *Crop and Pasture Science* **62:** 95-114.

Fischer R & Edmeades GO (2010) Breeding and cereal yield progress. *Crop Science* **50:** S-85-S-98.

Foulkes M, Hawkesford M, Barraclough P, Holdsworth M, Kerr S, Kightley S & Shewry P (2009) Identifying traits to improve the nitrogen economy of wheat: recent advances and future prospects. *Field Crops Research* **114:** 329-342.

Frederick JR & Bauer PJ (1999) Physiological and numerical components of wheat yield. *Wheat: Ecology and Physiology of Yield Determination***:** 45-65.

Gelang J, Pleijel H, Sild E, Danielsson H, Younis S & Selldén G (2000) Rate and duration of grain filling in relation to flag leaf senescence and grain yield in spring wheat (*Triticum aestivum*) exposed to different concentrations of ozone. *Physiologia Plantarum* **110:** 366-375.

Gororo N, Eagles HA, Eastwood R, Nicolas M & Flood R (2002) Use of Triticum tauschii to improve yield of wheat in low-yielding environments. *Euphytica* **123:** 241-254.

Goyne P, Milroy S, Lilley J & Hare J (1993) Radiation interception, radiation use efficiency and growth of barley cultivars. *Crop and Pasture Science* **44:** 1351-1366.

Gregersen P, Holm P & Krupinska K (2008) Leaf senescence and nutrient remobilisation in barley and wheat. *Plant Biology* **10:** 37-49.

Gupta P (1993) Seed vigour testing. *Handbook of seed testing***:** 242-249.

Haefele S, Siopongco J, Boling A, Bouman B & Tuong T (2009) Transpiration efficiency of rice (*Oryza sativa* L.). *Field Crops Research* **111:** 1-10.

Hafsi M, Akhter J & Monneveux P (2007) Leaf senescence and carbon isotope discrimination in durum wheat (*Triticum durum* Desf.) under severe drought conditions. *Cereal Research Communications* **35:** 71-80.

Han H, Li Z, Ning T, Zhang X, Shan Y & Bai M (2008) Radiation use efficiency and yield of winter wheat under deficit irrigation in North China. *Plant Soil Environ* **54:** 313-319.

Hancock JF (2012) *Plant evolution and the origin of crop species*: CABI.

Hardin LS (2008) Meetings that changed the world: Bellagio 1969: The green revolution. *Nature* **455:** 470-471.

Hay RK & Porter JR (2006) *The physiology of crop yield*: Blackwell Publishing.

Hedden P (2003) The genes of the Green Revolution. *Trends Genet* **19:** 5-9.

Hibberd JM, Sheehy JE & Langdale JA (2008) Using C_4 photosynthesis to increase the yield of rice-rationale and feasibility. *Curr Opin Plant Biol* **11:** 228-231.

Hirasawa T & Hsiao TC (1999) Some characteristics of reduced leaf photosynthesis at midday in maize growing in the field. *Field Crops Research* **62:** 53-62.

Hoisington D, Khairallah M, Reeves T, Ribaut JM, Skovmand B, Taba S & Warburton M (1999) Plant genetic resources: what can they contribute toward increased crop productivity? *Proc Natl Acad Sci U S A* **96:** 5937-5943.

Issack MA (2009) Resource capture characteristics of ancient wheat species. MSc Thesis. The University of Nottingham.

Jamieson P, Brooking I, Semenov M & Porter J (1998) Making sense of wheat development: a critique of methodology. *Field Crops Research* **55:** 117-127.

Jianlin W, Guirui Y, Quanxiao F, Defeng J, Hua Q & Qiufeng W (2008) Responses of water use efficiency of 9 plant species to light and CO_2 and their modeling. *Acta Ecologica Sinica* **28:** 525-533.

Kanton R & Dennett M (2008) Radiation capture and use as affected by morphologically contrasting maize/pea in sole and intercropping. *West African journal of applied ecology* **13:** 55-66.

Karimi M & Siddique K (1991) Crop growth and relative growth rates of old and modern wheat cultivars. *Crop and Pasture Science* **42:** 13-20.

Kiniry J, Jones C, O'toole J, Blanchet R, Cabelguenne M & Spanel D (1989) Radiation-use efficiency in biomass accumulation prior to grain-filling for five grain-crop species. *Field Crops Research* **20:** 51-64.

Kramer P & Turner N (1980) Drought, stress, and the origin of adaptations. *Adaptation of plants to water and high temperature stress***:** 7-20.

Kramer PJ & Boyer JS (1995) *Water relations of plants and soils*: Academic press.

Langdale JA, Zelitch I, Miller E & Nelson T (1988) Cell position and light influence C_4 versus C_3 patterns of photosynthetic gene expression in maize. *EMBO J* **7:** 3643-3651.

Larbi A & Mekliche A (2004) Relative water content (RWC) and leaf senescence as screening tools for drought tolerance in wheat. *Options Méditerranéennes Série A, Séminaires Méditerranéens* **60:** 193-196.

Larcher W (2003) *Physiological plant ecology: ecophysiology and stress physiology of functional groups*: Springer.

Lawson T (2009) Guard cell photosynthesis and stomatal function. *New Phytol* **181:** 13-34.

Lawson T & Blatt M (2014) Stomatal size, speed and responsiveness impact on photosynthesis and water use efficiency. *Plant Physiol* (Epub ahead of print).

Lawson T, Kramer DM & Raines CA (2012) Improving yield by exploiting mechanisms underlying natural variation of photosynthesis. *Curr Opin Biotechnol* **23:** 215-220.

Lawson T & Morison J (2006) Visualising patterns of CO_2 diffusion in leaves. *New Phytol* **169:** 641-643.

Leverenz J & Jarvis P (1979) Photosynthesis in Sitka spruce. VIII. The effects of light flux density and direction on the rate of net photosynthesis and the stomatal conductance of needles. *Journal of Applied Ecology***:** 919-932.

Leverenz JW (1994) Factors determining the nature of the light dosage response curve of leaves. *Photoinhibition of photosynthesis: from molecular mechanisms to the field***:** 221-251.

Li Q, Liu M, Zhang J, Dong B & Bai Q (2009) Biomass accumulation and radiation use efficiency of winter wheat under deficit irrigation regimes. *Plant Soil Environ* **55:** 85-91.

Long SP & Bernacchi CJ (2003) Gas exchange measurements, what can they tell us about the underlying limitations to photosynthesis? Procedures and sources of error. *J Exp Bot* **54:** 2393-2401.

Lunagaria M & Shekh A (2006) Radiation interception, light extinction coefficient and leaf area index of wheat (Triticum aestivum L.) crop as influenced by row orientation and row spacing. *J Agric Sci* **2:** 43-54.

Lunagaria M & Shekh A (2007) Radiation use efficiency of wheat (*Triticum aestivum* L.) crop as influenced by date of sowing, row spacing and row orientation. *Journal of Agrometeorology* **9:** 282-285.

Lutz W, Sanderson W & Scherbov S (2001) The end of world population growth. *Nature* **412:** 543-545.

Mashhadi HR & Zand E (2004) Canopy profile distribution of leaf area, light and nitrogen in some Iranian winter wheat cultivars released during the last 50 years. In *Proceedings of the 4th International Crop Science Congress, Brisbane, Australia, 26th September to 1st October*.

McAusland L, Davey P, Kanwal N, Baker N & Lawson T (2013) A novel system for spatial and temporal imaging of intrinsic plant water use efficiency. *Journal of Experimental Botany* **64:** 4993-5007.

Miao Z, Xu M, Lathrop RG & Wang Y (2009) Comparison of the A–Cc curve fitting methods in determining maximum ribulose 1· 5 bisphosphate carboxylase/oxygenase carboxylation rate, potential light saturated electron transport rate and leaf dark respiration. *Plant, Cell & Environment* **32:** 109-122.

Miralles D & Richards R (2000) Responses of leaf and tiller emergence and primordium initiation in wheat and barley to interchanged photoperiod. *Annals of Botany* **85:** 655-663.

Miralles DJ & Slafer GA (1997) Radiation interception and radiation use efficiency of near-isogenic wheat lines with different height. *Euphytica* **97:** 201-208.

Mitchell PL & Sheehy JE (2006) *Supercharging rice photosynthesis to increase yield*: New Phytol. 2006;171(4):688-93.

Monteith J (1965) Evaporation and environment. In *Symp*. *Soc*. *Exp*. *Biol*, Vol. 19, p 4.

Monteith J (1981) Climatic variation and the growth of crops. *Quarterly Journal of the Royal Meteorological Society* **107:** 749-774.

Monteith J & Moss C (1977) Climate and the efficiency of crop production in Britain [and discussion]. *Philosophical Transactions of the Royal Society of London B, Biological Sciences* **281:** 277-294.

Morison J I L & Lawson T (2007). Does lateral gas diffuson in leaves matter? *Plant, Cell and Environment* **30:** 1072-1085.

Murchie E, Pinto M & Horton P (2009) Agriculture and the new challenges for photosynthesis research. *New Phytologist* **181:** 532-552.

Muurinen S & Peltonen-Sainio P (2006) Radiation-use efficiency of modern and old spring cereal cultivars and its response to nitrogen in northern growing conditions. *Field Crops Research* **96:** 363-373.

Mwale S, Azam-Ali S & Massawe F (2007) Growth and development of bambara groundnut (*Vigna subterranea*) in response to soil moisture: 1. Dry matter and yield. *European journal of Agronomy* **26:** 345-353.

Nevo E, Carver BF & Beiles A (1991) Photosynthetic performance in wild emmer wheat, *Triticum dicoccoides*: ecological and genetic predictability. *Theor Appl Genet* **81:** 445-460.

Ngyuen C (2014) Identification of radiation use efficiency traits in a wheat x spelt population. PhD Thesis (under review). The University of Nottingham.

Nilson SE & Assmann SM (2007) The control of transpiration. Insights from Arabidopsis. *Plant physiology* **143:** 19-27.

O'Connell M, O'Leary G, Whitfield D & Connor D (2004) Interception of photosynthetically active radiation and radiation-use efficiency of wheat, field pea and mustard in a semi-arid environment. *Field Crops Research* **85:** 111-124.

Ortiz R, Sayre KD, Govaerts B, Gupta R, Subbarao G, Ban T, Hodson D, Dixon JM, Iván Ortiz-Monasterio J & Reynolds M (2008) Climate change: Can wheat beat the heat? *Agriculture, Ecosystems & Environment* **126:** 46-58.

Pagnotta MA, Mondini L & Atallah MF (2005) Morphological and molecular characterization of Italian emmer wheat accessions. *Euphytica* **146:** 29-37.

Parsons R, Weyers J, Lawson T & Godber I (1998) Rapid and straightforward estimates of photosynthetic characteristics using a portable gas exchange system. *Photosynthetica* **34:** 265-279.

Passioura J (1977) Grain yield, harvest index, and water use of wheat. *Journal of the Australian Institute of Agricultural Science* **43:** 117-121.

Paveley N, Lockley D, Vaughan T, Thomas J & Schmidt K (2000) Predicting effective fungicide doses through observation of leaf emergence. *Plant Pathology* **49:** 748-766.

Pearcy RW, Ehleringer JR, Mooney HA & Rundel PW (1989) *Plant physiological ecology: field methods and instrumentation*: Chapman and Hall Ltd.

Peleg Z, Fahima T, Abbo S, Krugman T, Nevo E, Yakir D & Saranga Y (2005) Genetic diversity for drought resistance in wild emmer wheat and its ecogeographical associations. *Plant, Cell & Environment* **28:** 176-191.

Peng J, Korol AB, Fahima T, Roder MS, Ronin YI, Li YC & Nevo E (2000) Molecular genetic maps in wild emmer wheat, *Triticum dicoccoides*: genome-wide coverage, massive negative interference, and putative quasi-linkage. *Genome Res* **10:** 1509-1531.

Peng J, Richards DE, Hartley NM, Murphy GP, Devos KM, Flintham JE, Beales J, Fish LJ, Worland AJ, Pelica F, Sudhakar D, Christou P, Snape JW, Gale MD & Harberd NP (1999) 'Green revolution' genes encode mutant gibberellin response modulators. *Nature* **400:** 256-261.

Poorter H & Evans JR (1998) Photosynthetic nitrogen-use efficiency of species that differ inherently in specific leaf area. *Oecologia* **116:** 26-37.

Rajbhandari BP (2004) Eco-Physiological Aspects of Common Buckwheat. *Advances in Buckwheat Research***:** 101.

Rawsthorne S (1992) C3–C4 intermediate photosynthesis: linking physiology to gene expression. *The Plant Journal* **2:** 267-274.

Reich PB, Walters MB & Ellsworth DS (1997) From tropics to tundra: global convergence in plant functioning. *Proceedings of the National Academy of Sciences* **94:** 13730-13734.

Reif JC, Zhang P, Dreisigacker S, Warburton ML, van Ginkel M, Hoisington D, Bohn M & Melchinger AE (2005) Wheat genetic diversity trends during domestication and breeding. *Theor Appl Genet* **110:** 859-864.

Reich PB, Walters MB, Ellsworth DS, Vose JM, Volin JC, Gresham C & Bowman WD (1998) Relationships of leaf dark respiration to leaf nitrogen, specific leaf area and leaf life-span: a test across biomes and functional groups. *Oecologia* **114:** 471-482.

Reynolds M, Calderini D, Condon A & Rajaram S (2001) Physiological basis of yield gains in wheat associated with the LR19 translocation from Agropyron elongatum. In *Wheat in a Global Environment*, pp 345-351. Springer.

Reynolds M & Trethowan R (2007) Physiological interventions in breeding for adaptation to abiotic stress. *Frontis* **21:** 127-144.

Reynolds MP, Van Ginkel M & Ribaut JM (2000) Avenues for genetic modification of radiation use efficiency in wheat. *Journal of Experimental Botany* **51:** 459-473.

Sage RF (2002) Variation in the kcat of Rubisco in C3 and C4 plants and some implications for photosynthetic performance at high and low temperature. *Journal of Experimental Botany* **53:** 609-620.

Salamini F, Ozkan H, Brandolini A, Schafer-Pregl R & Martin W (2002) Genetics and geography of wild cereal domestication in the near east. *Nat Rev Genet* **3:** 429-441.

Sharkey TD, Bernacchi CJ, Farquhar GD & Singsaas EL (2007) Fitting photosynthetic carbon dioxide response curves for C_3 leaves. *Plant, Cell & Environment* **30:** 1035-1040.

Siddique K, Belford R, Perry M & Tennant D (1989) Growth, development and light interception of old and modern wheat cultivars in a Mediterranean-type environment. *Crop and Pasture Science* **40:** 473-487.

Sinclair T & Horie T (1989) Leaf nitrogen, photosynthesis, and crop radiation use efficiency: a review. *Crop Science* **29:** 90-98.

Sinclair TR & Muchow RC (1999) Radiation use efficiency. *Advances in Agronomy* **65:** 5-265.

Singels A & Smit M (2002) The effect of row spacing on an irrigated plant crop of sugarcane variety NCo376. In *Proc S Afr Sug Technol Ass*, Vol. 76, pp 94-105.

Singels A, Smit M, Redshaw K & Donaldson R (2005) The effect of crop start date, crop class and cultivar on sugarcane canopy development and radiation interception. *Field Crops Research* **92:** 249-260.

Skovmand B, Reynolds M & Delacy I (2001) Searching genetic resources for physiological traits with potential for increasing yield. *Application of physiology in wheat breeding***:** 17-28.

Smale M (1997) The green revolution and wheat genetic diversity: some unfounded assumptions. *World Development* **25:** 1257-1269.

Snaydon R (1991) productivity of C3 and C4 plants: a reassessment. *Functional ecology* **5:** 321-330.

Sparkes D (2010) Are'ancient wheat species' more adapted to hostile environments than modern bread wheat?: short communication. *South African Journal of Plant and Soil* **27:** 331-333.

Sparkes D, Holme S & Gaju O (2006) Does light quality initiate tiller death in wheat? *European journal of Agronomy* **24:** 212-217.

Srivalli S & Khanna-Chopra R (2009) Delayed wheat flag leaf senescence due to removal of spikelets is associated with increased activities of leaf antioxidant enzymes, reduced glutathione/oxidized glutathione ratio and oxidative damage to mitochondrial proteins. *Plant Physiology and Biochemistry* **47:** 663-670.

Steduto P & Albrizio R (2005) Resource use efficiency of field-grown sunflower, sorghum, wheat and chickpea: II. Water use efficiency and comparison with radiation use efficiency. *Agricultural and forest meteorology* **130:** 269-281.

Takahashi T & Nakaseko K (1990) Seasonal change of photosynthetically active radiation intercepted by a spring wheat canopy and its relation to dry matter production. *Japanese Journal of Crop Science* **59:** 778-784.

Terashima I, Hanba YT, Tholen D & Niinemets Ü (2011) Leaf functional anatomy in relation to photosynthesis. *Plant physiology* **155:** 108-116.

Thomas H, Ougham H, Canter P & Donnison I (2002) What stay- green mutants tell us about nitrogen remobilization in leaf senescence. *Journal of Experimental Botany* **53:** 801-808.

Toyota M, Shiotsu F, JiaBin B, Morokuma M & Kusutani A (2010) Effects of reduction in plant height induced by chlormequat on radiation interception and radiation-use efficiency in wheat in southwest Japan. *Plant Production Science* **13:** 67-73.

Trethowan R & Mujeeb-Kazi A (2008) Novel germplasm resources for improving environmental stress tolerance of hexaploid wheat. *Crop Science* **48:** 1255-1265.

Troccoli A & Codianni P (2005) Appropriate seeding rate for einkorn, emmer, and spelt grown under rainfed condition in southern Italy. *European journal of Agronomy* **22:** 293-300.

van der Veen M & Palmer C (1997) Environmental factors and the yield potential of ancient wheat crops. *Journal of archaeological science* **24:** 163-182.

Verma V, Foulkes M, Worland A, Sylvester-Bradley R, Caligari P & Snape J (2004) Mapping quantitative trait loci for flag leaf senescence as a yield determinant in winter wheat under optimal and drought-stressed environments. *Euphytica* **135:** 255-263.

Wang E & Engel T (1998) Simulation of phenological development of wheat crops. *Agricultural Systems* **58:** 1-24.

Watson D (1952) The physiological basis of variation in yield. *Adv Agron* **4:** 101-145.

Weir A & Barraclough P (1986) The effect of drought on the root growth of winter wheat and on its water uptake from a deep loam. *Soil use and management* **2:** 91-96.

Westoby M, Falster DS, Moles AT, Vesk PA & Wright IJ (2002) Plant ecological strategies: some leading dimensions of variation between species. *Annual review of ecology and systematics* **33:** 125-159.

Whaley J, Sparkes D, Foulkes M, Spink J, Semere T & Scott R (2000) The physiological response of winter wheat to reductions in plant density. *Annals of Applied Biology* **137:** 165-177.

Winzeler H, Schmid J & Winzeler M (1993) Analysis of the yield potential and yield components of F1 and F2 hybrids of crosses between wheat (*Triticum aestivum* L.) and spelt (Triticum spelta L.). *Euphytica* **74:** 211-218.

Wullschleger SD (1993) Biochemical limitations to carbon assimilation in C3 plants—a retrospective analysis of the A/Ci curves from 109 species. *Journal of Experimental Botany* **44:** 907-920.

Xu W, Subudhi PK, Crasta OR, Rosenow DT, Mullet JE & Nguyen HT (2000) Molecular mapping of QTLs conferring stay-green in grain sorghum (Sorghum bicolor L. Moench). *Genome* **43:** 461-469.

Zamir D (2001) Improving plant breeding with exotic genetic libraries. *Nat Rev Genet* **2:** 983-989.

Zhang H, Oweis TY, Garabet S & Pala M (1998) Water-use efficiency and transpiration efficiency of wheat under rain-fed conditions and supplemental irrigation in a Mediterranean-type environment. *Plant and Soil* **201:** 295-305.

Zhu G & Spreitzer RJ (1996) Directed mutagenesis of chloroplast ribulose-1, 5-bisphosphate carboxylase/oxygenase Loop 6 substitutions complement for structural stability but decrease catalytic efficiency. *Journal of Biological Chemistry* **271:** 18494-18498.

Appendices

Appendix One: Field trial layout and husbandry (2010)

Figure A1.1: Experimental design and layout of field experiment (2010). Discard was MBW, Claire.

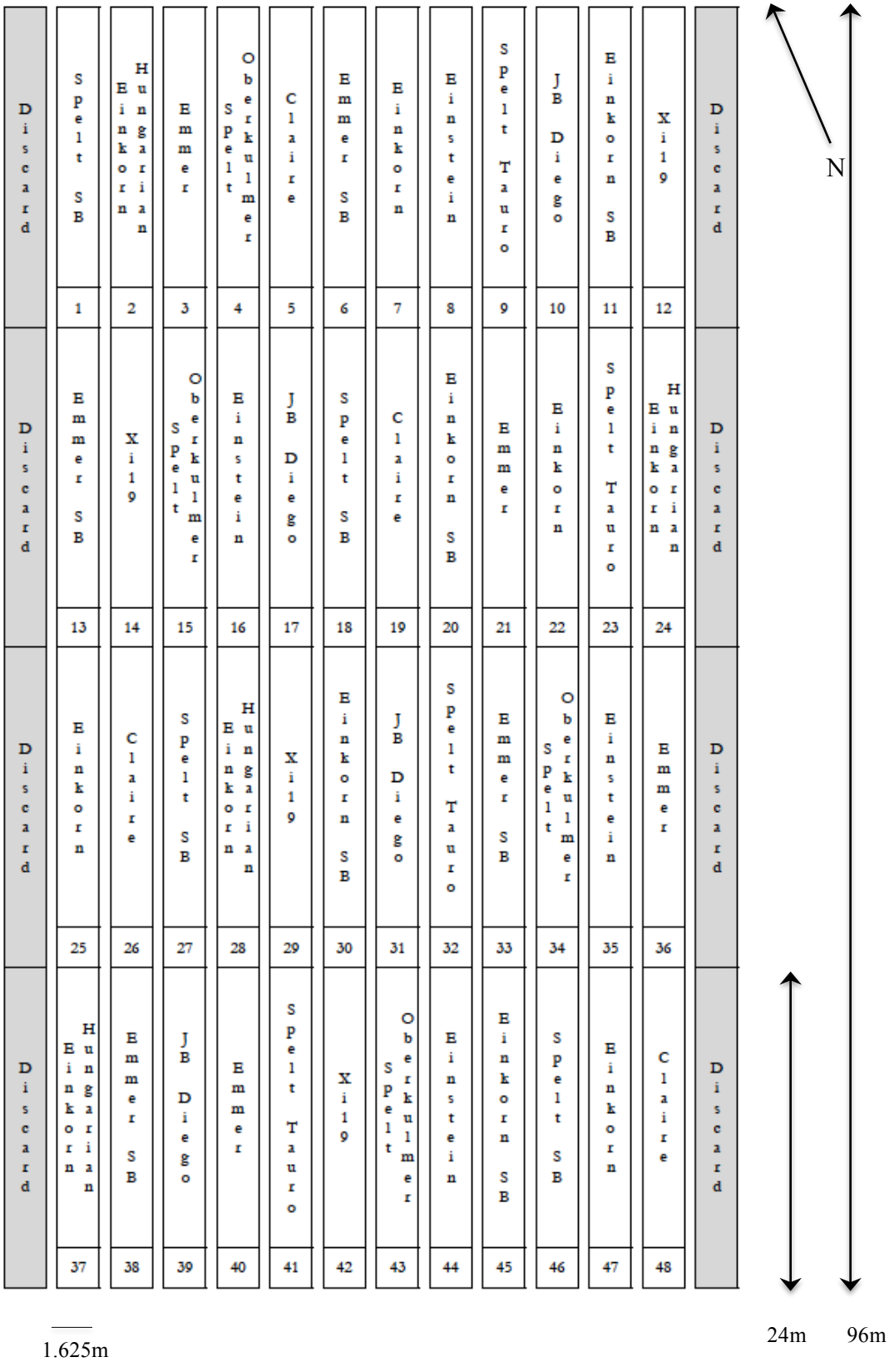


Table A1.1: Site details for the 2010 field experiment.

Field details	
Field	S02
Previous crop	Winter Oats
SNS N Index (12/11/2009)	174.1 kg/ha, SNS Index 5
Soil Indices	P:3, K:3, Mg:4, pH:6.9

Table A1.2: Sowing information for field experiment, 2010.

Soil cultivation	Date
Plough	14/09/2009
Powerharrow	15/09/2009
Roll after drilling	28/10/009

Table A1.3: Details of soil cultivation for field experiment 2010.

Sowing detail	
Seed rate (m^{-2})	$250m^2$
Drill type	Wintersteiger
Row width (cm)	12.5
Plot length (m)	12
Plot width (m)	1.625

Table A1.4 Details of Plant Growth Regulator (PGR) applications in the 2010 field experiment.

PGR	Rate	Date
Chlormequat	1.0 l/ha	20/11/2009
Chlormequat & Moddus	0.75 l/ha & 0.2 l/ha	20/11/2009

Table A1.5 Details of fertiliser applications in the 2010 field experiment.

Fertiliser	Rate	Date
Manganese Jett	1.0 l/ha	20/11/2009
27N, 9 SO_3	148 kg/ha & 40kg/ha N, 13.3 kg/ha	03/03/2010
Human Extra	1 l/ha	08/04/2010
Nitram	145 kg/ha N (50kg/ha N)	08/04/2010
Human extra	1l /ha	28/04/2010
Nitram	116 kg/ha 34.5% (40 kg/ha N)	14/05/2010
Magnor	1.23 l/ha	27/05/2010

Table A1.6 Details of herbicide applications in the 2010 field experiment.

Herbicide	Rate	Date
Picona SC	3.0 l/ha	20/11/2019
Hatra & Biopower	1.2 l/ha & 1 l/ha	28/04/2010
Starene XL	1.23 l\ha	27/05/2010

Table A1.7 Details of fungicide applications in the 2010 field experiment.

Fungicide	Rate	Date
Alto Elite	0.75 l/ha	08/04/2010
Proline & Amristar Opti	0.65 l/ha & 0.75 l/ha	28/04/2010
Brutus, Amistar Opti &Corbel	1.23 l/ha, 1.0 l/ha &0.5 l/ha	27/05/2010
Folicur, Corbel & Justice	0.75 l /ha, 0.5 l/ha & 0.15 l/ha	09/07/2010

Table A1.8 Details of insecticide applications in the 2010 field experiment.

Insecticide	Rate	Date
Permasect C	0.25 l /ha	20/11/2009
Aphox	0.25/ha	09/07/2010

Appendix Two: Field trial layout and husbandry (2011)

Figure A2.1: Experimental design and layout of field experiment (2011). Discard was MBW, Duxford.

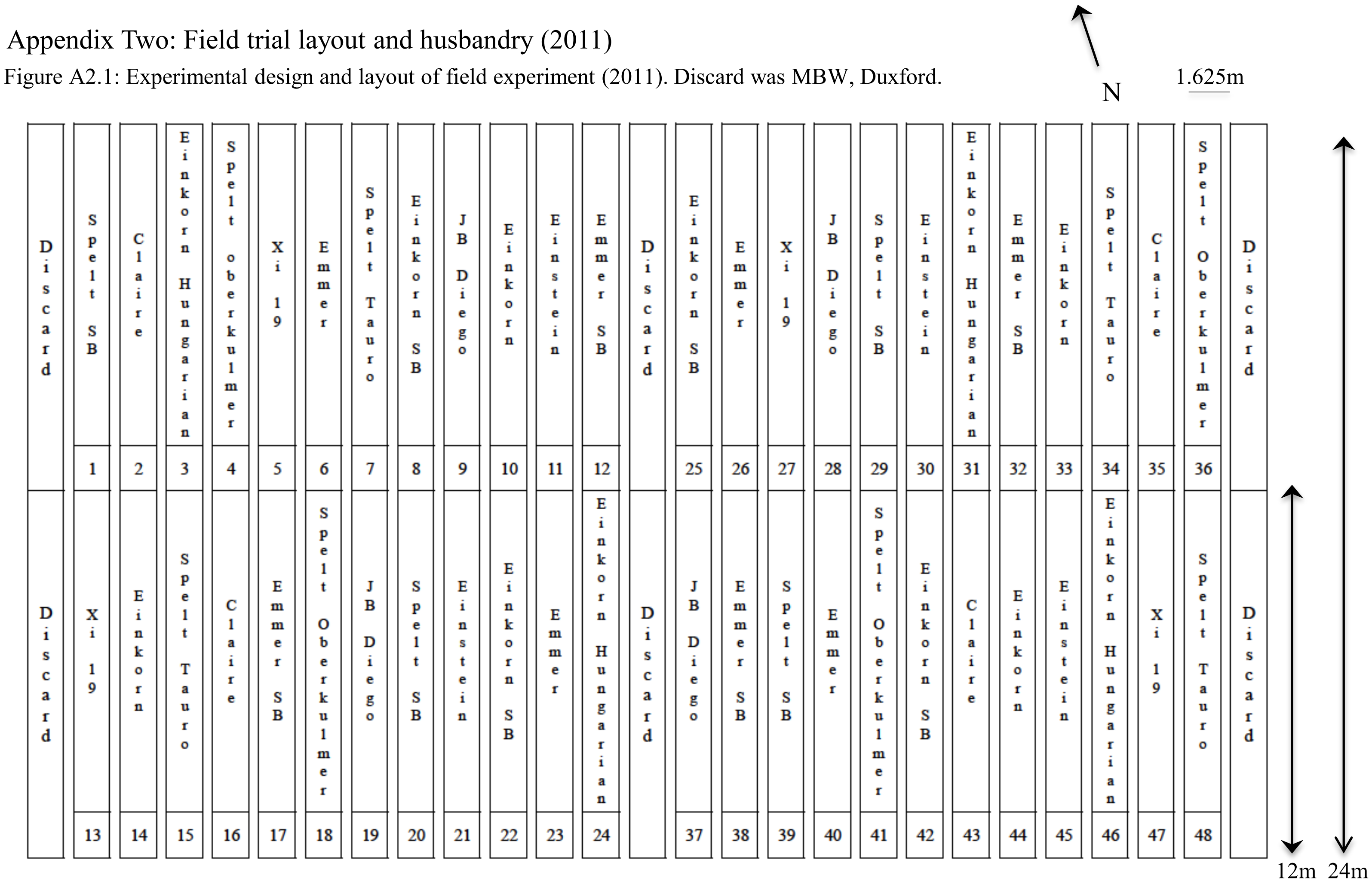


Table A2.1: Site details for experiment 2011.

Field Detail	
Field	S10
Previous crop	Winter Oats
SNS N Index (09/09/2010)	32.9 kg/ha, SNS Index O
Soil Indices	P:4, K:3, Mg:4, pH:7.2

Table A2.2: Sowing information for field experiment, 2011.

Sowing details	
Sowing	13/10/2010
Seed rate (m^{-2})	300 seeds m^2
Drill type	Wintersteiger
Row width (cm)	12.5
Plot length (m)	12
Plot width (m)	1.625

Table A2.3: Details of soil cultivation for field experiment 2011.

Soil cultivation	Date
Plough	16/09/2010
Powerharrow	11/10/2010
Roll after drilling	14/10/2010

Table A2.4 Details of Plant Growth Regulator (PGR) applications in the 2011 field experiment.

PGR	Rate	Date
Adjust	1.0 l/ha	25/03/2011
Adjust	0.8 l/ha	20/04/2011

Table A2.5 Details of fertiliser applications in the 2011 field experiment.

Fertiliser	Rate	Date
Nitram	30 kg/ha N	08/03/2011
Human extra	1l/ha	08/03/2011
Human extra	1 l/ha	25/03/2011
Nitram	80 kg/ha N	06/04/2011
Human extra	1l /ha	20/04/2011
Mitram	60 kg/ha N	06/05/2011
Magnor	1.0 l/ha	24/05/2011

Table A2.6 Details of herbicide applications in the 2011 field experiment.

Herbicide	Rate	Date
Hatra, Picona & Biopower	1l/ha, 1.7ha & 1l/ha	08/03/2011
Spitfire	1.0 l/ha	24/05/2011

Table A2.7 Details of Fungicide applications in the 2011 field experiment.

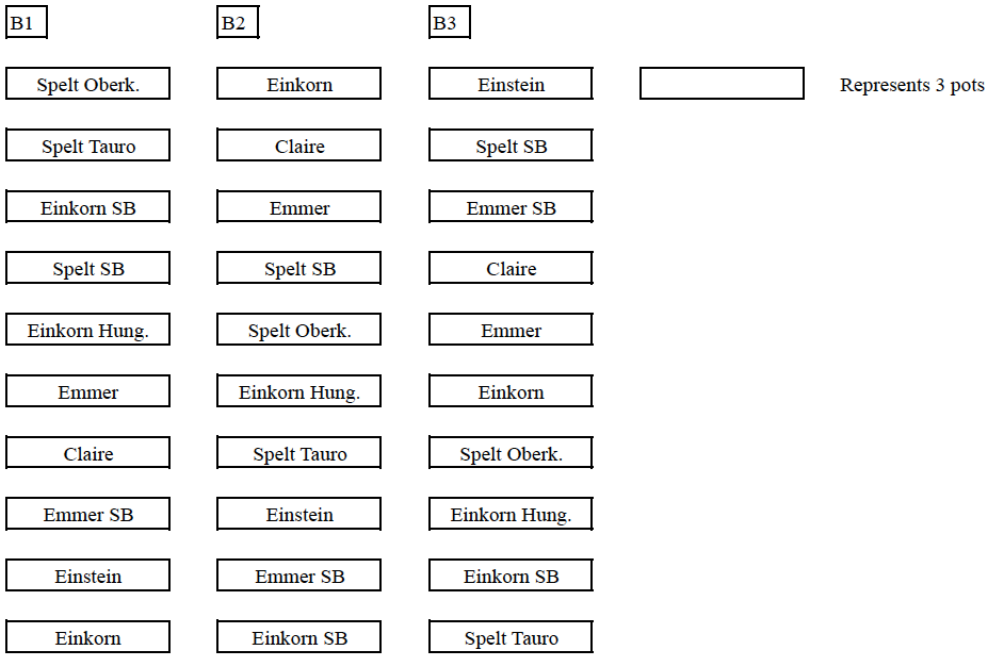
Fungicide	Rate	Date
Alto Elite CTL & Vegas	0.75 l/ha, & 0.15 l/ha	25/03/2011
Proline & Alto Elite	0.5 l/ha & 0.5 l/ha	20/04/2011
Comet, Justic & Prolinee	0.5 l/ha, 0.1 l/ha & 0.5 l/ha	24/05/2011
Caramba	0.75 l /ha	15/06/2011

Table A2.8 Details of insecticide applications in the 2011 field experiment.

Insecticide	Rate	Date
Permasect	0.25 l /ha	08/03/2011
Aphox	0.25/ha	15/06/2011

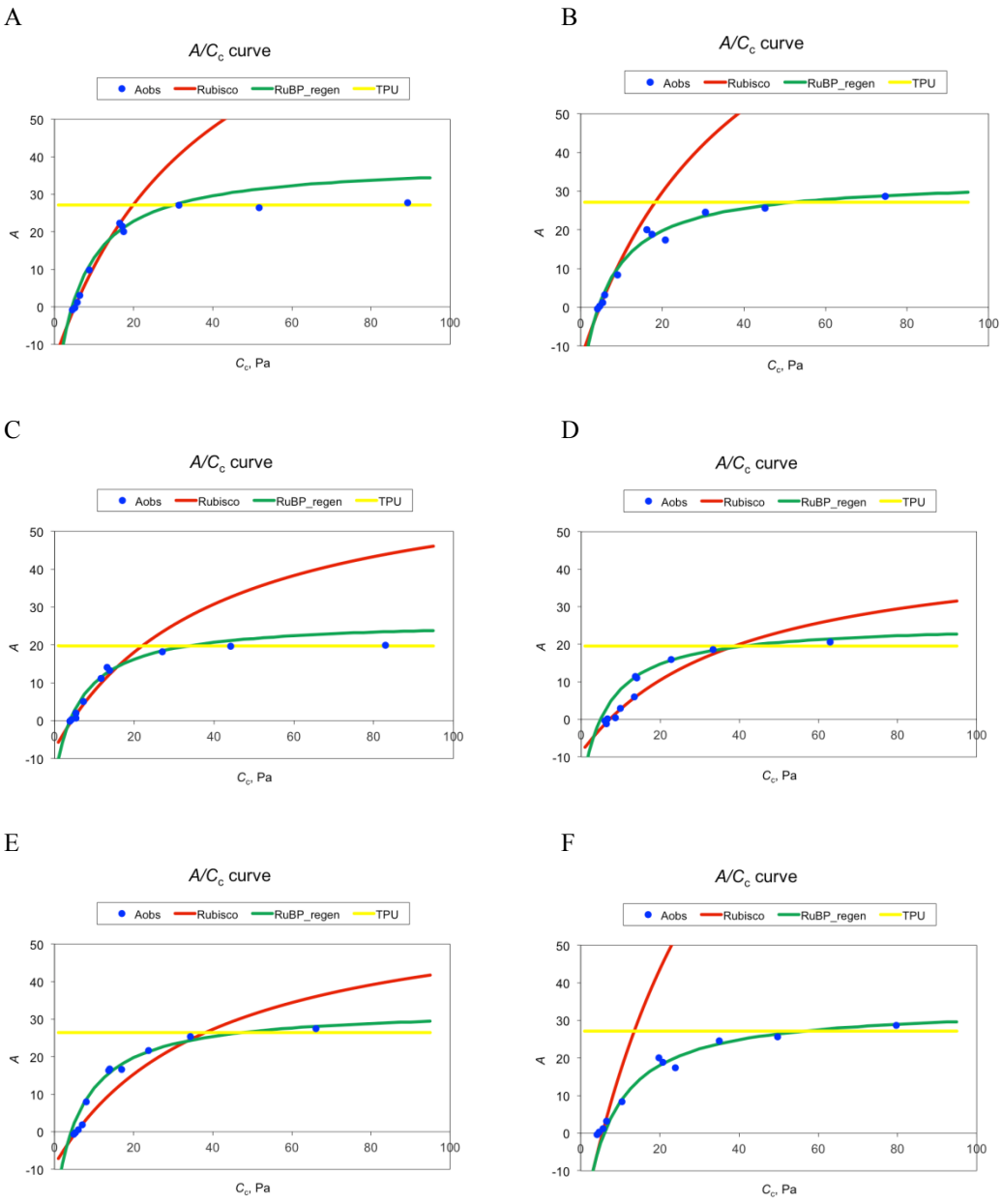
Appendix Three: Glasshouse experiment I layout

Figure A3.1: Experimental design and layout of glasshouse experiment I.



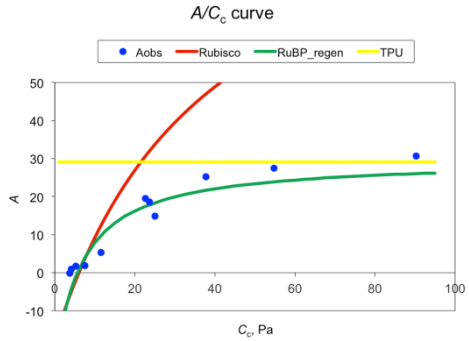
Appendix Four: GH experiment I sample output

Figure A4.1: Examples of A/C_i output using the model constructed by Sharkey *et al.* (2007).

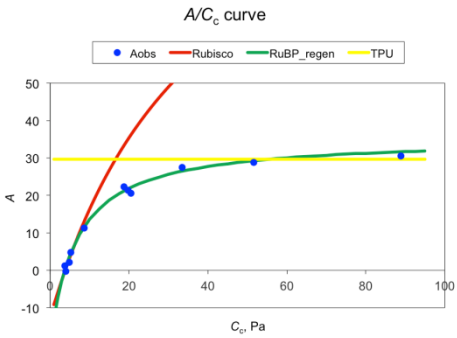


Figuare A4.1 *a*: Example genotypic responses showing photosynthetic response to varying carbon dioxide concentrations. Using the model constructed by Sharkey *et al.* (2007), C_i was converted into C_c (Chloroplast CO_2) and plotted against the net photosynthesis for 6 wheat genotypes; A, Claire B, einkorn; C, einkorn Hungarian; D, einkorn SB; E, Einstein F, emmer. In the figures, blue circles (Aobs) denote the observed photosynthetic rate at known C_c. The red line represents the part of the photosynthetic CO_2 response that is limited by Rubisco. The green line corresponds to the RuBP-regeneration state and the yellow boundary symbolises the TPU state.

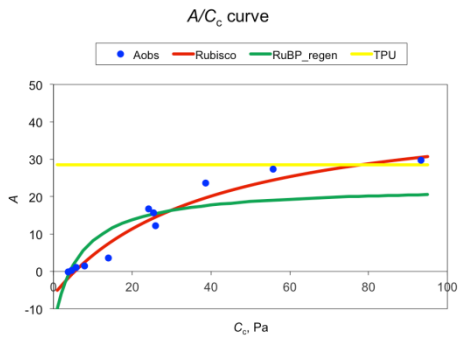
G



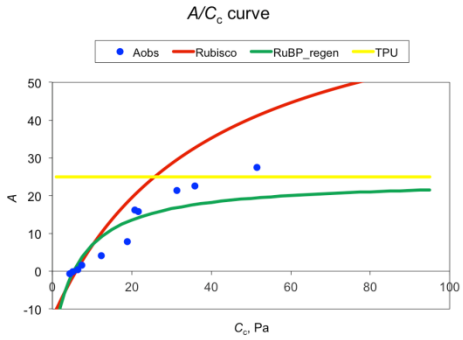
H



I



J



K

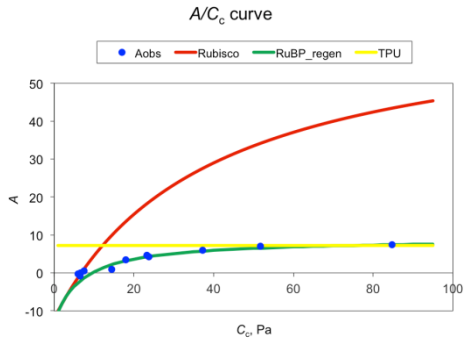


Figure A4.1 *b*: Example genotypic responses showing photosynthetic response to varying carbon dioxide concentrations. Using the model constructed by Sharkey *et al.* (2007), C_i was converted into C_c (Chloroplast CO_2) and plotted against the net photosynthesis for 5 wheat genotypes; G, emmer SB; H, JB Diego I, spelt oberkulmer; J, spelt SB; K, spelt tauro. In the figures, blue circles (Aobs) denote the observed photosynthetic rate at known C_c. The red line represents the part of the photosynthetic CO_2 response that is limited by Rubisco. The green line corresponds to the RuBP-regeneration state and the yellow boundary symbolises the TPU state.

Appendix Five: Glasshouse experiment II layout

Figure A5.1: Experimental design and layout of glasshouse experiment II.

Emmer SB	Spelt SB	Einkorn SB	Spelt Tauro	Emmer	Spelt Oberkulmer	Einkorn	Xi19
1	2	3	4	5	6	7	8
Spelt SB	Emmer SB	Einkorn	Xi 19	Spelt Tauro	Emmer	Spelt Oberkulmer	Einkorn SB
9	10	11	12	13	14	15	16
Xi 19	Spelt Tauro	Emmer SB	Emmer	Spelt SB	Spelt Oberkulmer	Einkorn SB	Einkorn
17	18	19	20	21	22	23	24

Appendix Six: Glasshouse experiment III layout

Figure A6.1: Experimental design and layout of glasshouse experiment III.



Appendix Seven: Glasshouse experiment chemical application information

Table A7.1: Components of Hortimix standard 15-7-30 (fertiliser) (Hortifeeds, UK).

Composition information/ingredients	Analysis (w/w)
Total water soluble Nitrogen	15.00%
Total Nitrate Nitrogen (NO_3-N)	8.50%
Total Ammoniacal Nitrogen	1.40%
Total Ureic Nitrogen	5.10%
Total Phosphorus Pentoxide soluble in water (P_2O_5)	7.00%
Total Potassium Oxide soluble in water (K_2O)	30.00%
Total Magnesium Oxide (MgO)	1.60%
Iron chelated by EDTA (Fe)	1533 mg/kg
Manganese (Mn)	1000 mg/kg
Boron (B)	300 mg/kg
Zinc (Z)	270 mg/kg
Copper (Cu)	200 mg/kg
Molybdenum (Mo)	120 mg/kg

Table A7.2: Corbel information (fungicide) (BASF, UK).

Composition information/ingredients	Content (w/w)
Fenproplmorph	79.8%
Cyclohexanone	<20%
Calcium alkyl benzene sulfonate in Isobutanol	<5%
pH value	8-9 (water, 1% (m), 20°C)

Table A7.3: Decis information (insecticide) (Bayer UK).

Composition information/ingredients	Concentration
Deltamethrin	2.81
Tetrapropylene benzene sulfonate, calcium salt	>10.00 - <5.00
2 Methylpropan-1-ol	>1.00- <5.00
2, 6-Di-tert-butyl-4-methylphenol	>0.10-<0.25
Solvent Naphtha (petroleum), light aromatic	>25.00